



University  
of Glasgow

Garrett, Alice Catherine (2021) *Development of a point-of-care molecular diagnostic tool for malaria and schistosomiasis in low-resource settings*. PhD thesis.

<https://theses.gla.ac.uk/82700/>

Copyright and moral rights for this work are retained by the author

A copy can be downloaded for personal non-commercial research or study, without prior permission or charge

This work cannot be reproduced or quoted extensively from without first obtaining permission in writing from the author

The content must not be changed in any way or sold commercially in any format or medium without the formal permission of the author

When referring to this work, full bibliographic details including the author, title, awarding institution and date of the thesis must be given

Enlighten: Theses

<https://theses.gla.ac.uk/>  
[research-enlighten@glasgow.ac.uk](mailto:research-enlighten@glasgow.ac.uk)



Development of a point-of-care  
molecular diagnostic tool for malaria  
and schistosomiasis in low-resource  
settings

Alice Catherine Garrett  
BSc (Hons) Physics

Submitted in fulfilment of the requirements for the  
Degree of Doctor of Philosophy

Division of Biomedical Engineering

School of Engineering

College of Science and Engineering

University of Glasgow

October 2021

## **Abstract**

There is an imminent need for more sensitive and low-cost point-of-care diagnostics for low-resource settings. Molecular diagnostics are becoming increasingly relevant in global efforts for disease elimination, although, healthcare workers face practical and logistical problems in the implementation of such tests in low-resource laboratories and environments. This has propelled the development of tailored point-of-care (POC) molecular diagnostic tests, however, to date there is lack of investigations into POC molecular tests trialled in low-resource settings.

The World Health Organization (WHO) have highlighted the importance of the elimination of malaria and schistosomiasis in the 2030 roadmap to achieve sustainable development goals. Work previously conducted within the Biomedical Research Division at The University of Glasgow resulted in the development of a low-cost POC molecular diagnostic platform for malaria. The technique is reliant on loop-mediated isothermal amplification (LAMP). This thesis describes the adaptation of the technique to aid the diagnosis of schistosomiasis. Furthermore, field-trials were undertaken in collaboration with the Vector Control Division in Uganda, to assess the logistics and feasibility of POC LAMP to detect *plasmodium* and schistosome DNA in rural low-resource-settings.

Molecular detection of malaria and schistosomiasis has the potential to provide more sensitive diagnostic tests which will benefit current surveillance programs and epidemiological studies. Additionally, the assessment of field trials will assist those developing POC molecular tests for use in low-resource environments out-with clinical and laboratory settings. Due to the malleability of the technique, this could further benefit additional POC testing and disease surveillance studies in-the-field, thus, contributing to the development of future work in these areas.

# Contents

Abstract .....	i
List of Figures .....	xii
Acknowledgements .....	xxix
Authors Declaration .....	xxx
List of publications and conferences.....	xxxii
List of commonly used abbreviations .....	xxxiii
Chapter 1: Introduction .....	1
1.1 Malaria.....	2
1.1.1 Transmission .....	2
1.1.2 Clinical manifestations.....	3
1.1.3 Prevention .....	4
1.2 Schistosomiasis .....	5
1.2.1 Transmission .....	6
1.2.2 Clinical manifestations.....	7
1.2.2.1 Intestinal schistosomiasis.....	8
1.2.2.2 Urogenital schistosomiasis .....	8
1.2.3 Prevention .....	8
1.3 Treatment.....	9
1.3.1 Malaria .....	9
1.3.2 Schistosomiasis .....	9
1.3.3 Mass drug administration.....	10
1.4 Diagnosis .....	11
1.4.1 The diagnostic gold standard .....	11
1.4.2 Sensitivity and specificity .....	11
1.4.3 Microscopy.....	13

1.4.3.1	Malaria gold standard: blood smear.....	13
1.4.3.2	S. mansoni gold standard: Kato-Katz method .....	15
1.4.4	Immunological diagnosis .....	16
1.4.4.1	Antibody tests .....	16
1.4.4.2	Antigen tests .....	16
1.5	Molecular diagnosis .....	18
1.5.1	Introduction to PCR .....	18
1.5.1.1	Monitoring PCR amplification .....	19
1.5.2	Introduction to loop-mediated amplification .....	21
1.5.2.1	LAMP primers .....	21
1.5.2.2	Principles of LAMP .....	23
1.5.3	Molecular diagnosis of malaria and schistosomiasis .....	25
1.6	Point of care testing .....	26
1.6.1	Current diagnostic approaches at the point of care .....	26
1.6.2	Rapid POC antigen tests .....	27
1.6.2.1	Malaria: POC RDT .....	27
1.6.2.2	S. mansoni: POC-CCA .....	28
1.6.3	Limitations of current POC tests.....	29
1.7	Advances in POC testing .....	30
1.7.1	Molecular diagnostics for use at the POC.....	31
1.7.2	Challenges to consider for application of POC tests in LMICs .....	33
1.7.3	Considerations for a POC molecular diagnostic platform .....	34
1.7.4	Paper for POC Molecular Diagnostics.....	35
1.7.4.1	Paper-based DNA processing .....	36
1.7.4.2	POC detection of molecular amplicons .....	37
1.7.4.3	Limitations of current POC NAAT studies .....	38
1.7.4.4	The POC Paper Device .....	39

1.8	Aims & Objectives .....	40
Chapter 2:	Materials, Methods & Development .....	41
2.1	Standard procedures for DNA extraction, amplification and quantification .....	41
2.1.1	Sample preparation and DNA extraction .....	41
2.1.1.1	Promega MagaZorb® Protocol for DNA extraction from blood.....	42
2.1.1.2	Modified (Scale-down) DNA Extraction from blood for use on the Paper Device	44
2.1.1.3	DNA Extraction from Blood Stored on FTA® cards.....	44
2.1.2	DNA quantification.....	45
2.1.3	DNA Amplification & Molecular Detection .....	45
2.1.3.1	Interpreting qPCR fluorescence data .....	46
2.1.3.2	TaqMan™ qPCR.....	48
2.1.3.3	Calibration data for detection of plasmodium DNA by qPCR.....	51
2.1.3.4	Confirmatory qPCR on field-collected samples .....	52
2.1.3.5	LAMP .....	54
2.1.4	Confirmation of SYBR™ Green amplification of PCR and LAMP products	59
2.2	The Paper Device .....	61
2.2.1	Overview of Diagnostic Method.....	61
2.2.2	Sample Processing & DNA Extraction .....	62
2.2.3	Amplification & Molecular Detection in the Diagnostic Cassette.....	65
2.2.4	Interpretation of Lateral Flow Strip Results .....	66
2.2.5	Dilution of Amplicons on LF strips .....	67
2.2.6	Interpreting results in the Diagnostic Cassette.....	68
2.2.7	Fabrication of the diagnostic cassette .....	70
2.2.7.1	Paper based microfluidics.....	70
2.2.7.2	Plastic cassette .....	71
2.2.8	Device Assembly.....	74

2.2.9	Device Assembly for the Field Trials .....	77
2.2.10	Heating .....	79
2.3	Statistical Analysis .....	82
2.4	Summary of the Method Development .....	83
Chapter 3:	Development of the <i>S. mansoni</i> assay .....	84
3.1	Introduction .....	84
3.1.1	Molecular Assays .....	84
3.1.2	Target specimen .....	85
3.2	Chapter Aims & Objectives.....	87
3.3	Materials and Methods .....	88
3.3.1	<i>S. mansoni</i> Gene Targets .....	88
3.3.1.1	mtDNA target gBlock.....	88
3.3.1.2	gDNA target gBlock .....	89
3.3.2	Stool Substitute .....	89
3.3.3	Egg Flotation Cassette .....	90
3.3.4	<i>S. mansoni</i> DNA extraction.....	91
3.3.4.1	Schistosome genomic DNA.....	91
3.3.4.2	DNA extraction from <i>S. mansoni</i> ova.....	92
3.3.4.3	DNA extraction from cercariae stored on FTA® cards.....	92
3.3.4.4	Extraction of <i>S. mansoni</i> DNA from stool .....	93
3.3.5	Molecular reagents .....	95
3.3.5.1	<i>S. mansoni</i> Primers .....	95
3.3.5.2	Isothermal Mastermix .....	99
3.4	Results .....	100
3.4.1	qPCR .....	100
3.4.2	Detection of <i>S. mansoni</i> DNA by LAMP .....	102
3.4.2.1	SM: mtDNA target sequence.....	102

3.4.2.2	Development of the SMchrom: gDNA target sequence .....	104
3.4.2.3	Development of the SMchromL & SM primer sets.....	106
3.4.3	Detection of <i>S. mansoni</i> DNA on LF strips .....	107
3.4.4	Investigation into tagged primer sets .....	108
3.5	Discussion .....	111
3.5.1	Biotin and FITC tagged LAMP primers .....	111
3.5.2	Detection of <i>S. mansoni</i> DNA on LF strips .....	111
3.6	Conclusion.....	113
3.7	Future Work.....	113
3.8	Take home points .....	114
Chapter 4:	Field studies .....	115
4.1	Introduction .....	115
4.2	Chapter Aims & Objectives.....	116
4.3	Ethics & Logistics .....	117
4.4	Study Settings.....	118
4.5	Materials, Methods & Development .....	120
4.5.1	Fieldwork preparation .....	120
4.5.1.1	Diagnostic Devices .....	120
4.5.1.2	Equipment.....	120
4.5.1.3	Reagent organisation.....	121
4.5.2	Workflow.....	121
4.5.2.1	Enrolment.....	122
4.5.2.2	Sample collection.....	122
4.5.2.3	Sample Processing .....	123
4.5.3	Molecular Diagnostic Workflow .....	124
4.5.4	Reference diagnostics.....	125
4.5.4.1	Malaria Gold Standard: Microscopic examination of a blood smear ...	125



4.5.4.2	Bilharzia gold standard: Kato-Katz examination.....	126
4.5.4.3	Malaria RDT .....	125
4.5.4.4	Bilharzia RDT (POC-CCA).....	127
4.5.4.5	Hatching.....	127
4.5.5	Heating for LAMP .....	129
4.5.6	An overview of the field trials .....	130
4.6	Results .....	131
4.6.1	Preliminary assessment of the field environment .....	131
4.6.1.1	Multiplex malaria cassette .....	131
4.6.1.2	Singleplex <i>S. mansoni</i> cassette .....	131
4.6.1.3	Factors effecting the Paper Device in-the-field .....	133
4.6.1.4	Considerations for future trials .....	133
4.6.2	Multiplex cassette and frugal heating .....	134
4.6.2.1	Multiplex malaria and schistosomiasis cassette.....	135
4.6.2.2	Factors effecting the malaria and schistosome Paper Device in-the-field 136	
4.6.2.3	Considerations for future trials .....	137
4.6.3	Integration of controls into the multiplex malaria and <i>S. mansoni</i> cassette.137	
4.6.3.1	Multiplex malaria and <i>S. mansoni</i> cassette.....	138
4.6.3.2	Mini-LAMP .....	139
4.6.3.3	MiniPCR™ .....	140
4.6.3.4	Factors effecting the multiplex malaria and <i>S. mansoni</i> Paper Device in- the-field 143	
4.7	Discussion .....	144
4.7.1	Logistical problems .....	144
4.7.1.1	Consent .....	145
4.7.1.2	Variation of samples.....	145
4.7.1.3	Heating.....	145

4.7.1.4	Molecular controls .....	146
4.7.2	Reference diagnostics.....	147
4.7.2.1	Microscopy .....	147
4.7.2.2	Malaria RDT .....	148
4.7.2.3	S. mansoni RDT.....	148
4.7.2.4	S. mansoni Hatching Tests.....	149
4.7.3	Development of the Paper Device in-the-field.....	150
4.7.3.1	Selection of Participants .....	150
4.7.3.2	Comparative Diagnostics .....	150
4.7.3.3	Additional Resources .....	151
4.7.3.4	Study Site Selection .....	152
4.7.3.5	Study Impact .....	152
4.8	Conclusion.....	153
4.9	Take home points .....	155
Chapter 5:	Storage of molecular reagents .....	156
5.1	Introduction .....	156
5.1.1	Storage of molecular reagents .....	156
5.1.2	Lyophilisation of molecular reagents for storage.....	157
5.2	Chapter Aims & Objectives.....	158
5.3	Materials and Methods .....	159
5.3.1	LAMP reagents .....	159
5.3.1.1	Primers .....	159
5.3.1.2	Mastermix .....	160
5.3.2	Storage of molecular reagents .....	161
5.3.2.1	Molecular reagents stored in-the-field.....	161
5.3.2.2	Imitating field storage conditions .....	161
5.3.2.3	Freeze-drying molecular reagents.....	162

5.3.3	An overview of experiments .....	163
5.4	Results .....	164
5.4.1	Calibration of the detection of <i>plasmodium</i> DNA by LAMP .....	164
5.4.2	Storage of reagents to mimic storage in-the-field .....	165
5.4.2.1	Liquid primer storage.....	165
5.4.2.2	LAMP reagent storage .....	168
5.4.3	Storage of molecular reagents in-the-field.....	170
5.4.3.1	Molecular reagents returned from the field .....	170
5.4.3.2	Primer mix returned from the field.....	172
5.4.3.3	Isothermal Mastermix returned from the field.....	174
5.4.4	Freeze-drying of LAMP reagents.....	175
5.5	Discussion .....	177
5.6	Conclusions .....	179
5.7	Take home points.....	179
Chapter 6:	Conclusions and Future work .....	180
6.1	The <i>S. mansoni</i> singleplex cassette .....	180
6.2	The multiplex malaria and schistosome cassette with frugal heating .....	181
6.3	The multiplexed malaria and <i>S. mansoni</i> cassette with integrated controls .....	182
6.4	Overall assessment of the field trials.....	182
6.5	Storage of molecular reagents .....	185
6.6	Future work .....	185
Chapter 7:	Appendices .....	187
7.1	Description of Mastermix.....	187
7.2	DNA conversion table .....	188
7.3	ABI fluorescence data .....	189
7.3.1	Code to plot the LAMP data .....	189
7.3.2	ABI filter spectrum .....	191

7.4	Melt temperature data.....	192
7.5	DNA extraction trials .....	193
7.6	The development of SM Primers.....	197
7.6.1	SM qPCR data.....	197
7.6.2	SM LAMP primers.....	198
7.7	Reference Diagnostic test methods .....	200
7.7.1	Blood smear for microscopic diagnosis of malaria.....	200
7.7.2	Malaria HRP2/pLDH (Pf/pan) RDT .....	202
7.7.3	The Kato-Katz method for detection of intestinal helminths.....	203
7.7.4	POC-CCA to detect <i>S. mansoni</i> .....	204
7.7.5	The <i>S. mansoni</i> hatching test.....	206
7.8	The multiplex malaria preliminary field trial .....	207
	Bibliography.....	208

## List of Tables

Table 2-1: Primer names and sequences used for qPCR amplification of plasmodium and <i>S. mansoni</i> DNA. Sources of the assays are referenced in the table.....	49
Table 2-2 : Primer names and sequences used for LAMP amplification of plasmodium; <i>S. mansoni</i> mitochondrial; and BRCA1 and <i>S. haematobium</i> DNA (used as controls during field trials and developed by Dr Gaolian Xu for use on the Paper Device).....	55
Table 2-3: Symbols for statistical analysis. Ranges of p values, statistical significance and associated symbols for graphical representation.....	82
Table 3-1: <i>S. mansoni</i> LAMP primer sequences. Sources for respective primer sets are included as references within the table. Where modifications were made to the sequence, the change has been highlighted. ....	96
Table 4-1: An overview of the field trials described in this chapter. The details of the cassette iteration; LAMP assay and sample specimen; and comparative tests, carried out in each trial are stated.....	130
Table 4-2: Table of the basic equipment and consumables used for PCR, LAMP and POC-LAMP in the field. Y= used, -= not in use, Y/N = used where appropriate. ....	141
Table 5-1: Primer concentrations and volumes (per reaction) used to make up plasmodium (PPAN) and 5X pan Primer Mix for LAMP amplification.....	160
Table 5-2: An overview of the experiments carried out in this chapter, a description of the experiment and LAMP reagent storage conditions; the reagents used for the comparative reaction, as a reference control for each experiment; and the target for the assay. ....	163
Table 7-1: The names, manufacturers and descriptions of Mastermix used for isothermal amplification (LAMP), PCR and qPCR throughout the scope of this project. ....	187
Table 7-2: The DNA conversion table. The conversions from ng/ $\mu$ L of DNA used in the NAATs to copies per reaction. The qPCR and LAMP reactions comprise of 2 $\mu$ L and 5 $\mu$ L of target DNA respectively.....	188
Table 7-3: The theoretical and experimental melt temperatures for the respective target samples. The experimental values display the range of melt temperatures returned from three separate LAMP runs.....	192

## List of Figures

Figure 1-1: The plasmodium life cycle. Figure obtained from the CDC website, <https://www.cdc.gov/malaria/about/biology/index.html>. ① during a blood meal, an infected mosquito inoculates the human host with plasmodium sporozoites. ②-④ The human liver stage. The sporozoites infect the liver cells where they mature into schizonts. The infected liver cells eventually rupture, releasing merozoites into the blood stream. ⑤-⑦ The human blood stages. Rupturing of the liver cells initiates the human blood stages. Here there are two scenarios, 1: ⑤&⑥ the parasites undergo asexual reproduction within the erythrocytes. This continues the erythrocytic cycle. 2:⑤&⑦ the parasites differentiate into gametocytes (sexual erythrocytic stages). ⑧ The gametocytes which are ingested by an Anopheles mosquito during a blood meal, initiating the sporogonic cycle, where the parasite undergo sexual reproduction within the mosquito ⑨-⑫.....3

Figure 1-2: The schistosome life cycle. Figure obtained from the CDC website, <https://www.cdc.gov/parasites/schistosomiasis/biology.html>. ① The eggs excreted by an individual with a schistosome infection enter the water source (snail habitat). ②-③ The ova hatch, releasing miracidia into the water, which locate and infect respective snails host. ④-⑥ The sporocysts reproduce asexually within the snail and develop into free-swimming cercariae, which are released from the snail into the water, where they can penetrate the skin of the human host, initiating the human cycle of the disease. ⑦-⑨ The cercariae lose their tail during penetration of the human skin, becoming a schistosomulae, and migrate in the blood to the liver, where they mature into adult worms. ⑩ The mature worms pair in the portal vein in the liver and migrate towards the mesenteric venules of the intestine (*S. mansoni* and *S. japonicum*) or venous plexus of the bladder (*S. haematobium*). The worms reproduce sexually and lay eggs, which migrate into the intestine or bladder and shed in the stool/ urine.....7

Figure 1-3: Blood smear Images. (a) Preparation of blood smears on microscopy slides in-the-field. (b) Blood smear from a patient with malaria; microscopic examination shows

Plasmodium falciparum parasites (located by the arrows) infecting some of the patient's red blood cells (CDC photo). (c) Malaria gold standard, microscopy. MoH VCD technicians conducting microscopic examination for plasmodium parasites on site in-the-field.....14

Figure 1-4: Images of *S. mansoni* ova as seen through microscope during KK examination. The malachite green stain causes *S. mansoni* ova to appear with a pink hue, enabling eggs to be distinguished from the slide and stool debris. (a) *S. mansoni* ova observed at 4X magnification. (b) *S. mansoni* ova observed at 10X magnification. Images of KK slides provided by Oliver Higgins.....15

Figure 1-5: The PCR process. PCR amplification is achieved by a process of thermal cycling. The denaturation step (at 95°C) is required to break the hydrogen bonds, and separate the target sequence into single strands of DNA. Then the temperature is lowered to enable annealing of the primers to their complimentary regions of single stranded DNA. And to allow synthesis of the complimentary sequence during the elongation step. This process is repeated, resulting in exponential amplification of the target DNA sequence. ....19

Figure 1-6: LAMP primer design. The design of LAMP primers is based on six regions of the target sequence; F3, F2, F1, B1, B2, and B3. LAMP requires four core primers (F3, B3, FIP and BIP), and two optional additional Loop primers (LPF and LPR). F3 and B3 are designed at opposing ends of the target sequence. The FIP and BIP primer design spans the target sequence and complimentary strand. The additional Loop primers (LPRF and LPR, which are included in this study) are designed using the complimentary strand corresponding the region between F1 and F2, and B1 and B2 respectively.....22

Figure 1-7: LAMP schematic illustration – source NEB (<https://www.neb-online.de/en/pcr-and-dna-amplification/isothermal-amplification/>). Amplification initiates from strand invasion from one of the inner primers (FIP or BIP) and synthesizes the complimentary strand. The strand-displacement activity of the LAMP DNA polymerase displaces the Internal Primer complimentary strand, which in turn acts as a template for the alternate Internal Primer. Both the synthesized Internal Primer strands consist of F1, B1 and their complimentary sequences (F1c and B1c, respectively), which form self-hybridising loops and result in the signature LAMP dumbbell structure. The LAMP dumbbell structure, contains multiple primer binding sites, and as a result, acts as the template for cyclic amplification. ....24

Figure 1-8: Examples of current POC diagnostic tests. (a) A diagram of the basic structure of a rapid POC LF test (<https://www.sigmaldrich.com/technical-documents/articles/ivd->

immunoassay/lateral-flow/getting-started-with-ivd-lateral-flow.html). (b) A diagram to show the function of a LF strip. (c) The Alere™ Malaria P.f POC RDT, image obtained from the Abbott product documents (<https://www.globalpointofcare.abbott/en/product-details/alere-malaria-ag-pf.html>). (c) The POC FLOTAC equipment, the Fill-FLOTAC used for stool sample preparation and the Mini-FLOTAC disk to facilitate direct observation of helminth ovum (Cringoli et al., 2017).....27

Figure 1-9: RDTs for malaria and *S. mansoni*. (a) The CareStart™ Malaria HRP2/pLDH (Pf/pan) Combo Test. (b) The POC-CCA® lateral flow test - Rapid Medical Diagnostics, Pretoria (South Africa).....28

Figure 1-10: Examples of mobile phone platforms for the direct observation of parasites for the diagnosis of schistosomiasis. (a) A photo of the mobile phone microscope for diagnosis of schistosomiasis described by Bogoch, et al. The slide is inserted into the sample tray which enables X-Z scanning (b) The Newton Nm1-600 XY – a portable and commercially available field microscope, the device is attached to a tripod during observation. (c) The reversed-lens CellScope attached to an iPhone 5s, which is manually held over the sample and moved to scan the slide – both trialled in-the-field as described by Coulibaly, et al....31

Figure 1-11: Examples of commercially available molecular diagnostic systems. (a) GeneXpert® rapid test platform, the extracted sample is added to the cartridge which contains the necessary molecular component. The benchtop set-up requires a computer or laptop for diagnostic read-out. (b) The TB-LAMP system, Figure manipulated from <https://www.human.de/products/molecular-dx/tb-lamp/>, sample preparation is facilitated using the heaters on top of the machine and LAMP diagnosis is determined visually using a UV light source built into the tube heating compartment. ....32

Figure 1-12: Molecular methods for point-of-care scenarios. (a) RNA extraction in-the-field in Kenya for viral genome sequencing. (b) The microfluidic device for POC molecular amplification described by Xu et al., the microfluidic component is used for sample amplification and is coupled with mobile phone technology to enable result analysis. (c) Molecular amplification conducted in a droplet utilising surface acoustic waves for sample lysis and amplification. ....33

Figure 1-13: Examples of paper DNA processing. (a) A FTA® Whatman® card used in-the-field to collect blood samples for analysis on return to the laboratory in the U.K. (b) The “Paper Machine” described by Connelly, Rolland and Whitesides. Sample preparation and amplification is conducted on paper disks within the plastic sliding cassette, following



amplification, the diagnostic read-out is conducted visually by sliding the disk to the detection window and exposing it to UV light. (c) The paper origami device described by Yang et al., sample processing is conducted on the paper origami piece, then DNA is eluted into the plastic cassette for amplification and visual read-out using a UV light. (d) The paperfluidic molecular diagnostic chip described by Rodriguez et al., whereby the sample processing and amplification is conducted on the chip made from paper and adhesive film. The result read-out is conducted by visual analysis of the LF strip.....37

Figure 1-14: An Example of the POC Paper Device. The printed paper fluidic for sample processing is attached to the back of the laser cut PMMA cassette using double sided tape. The LF strips are inserted within the cassette sealed with adhesive film. Iterations of the Paper Device designs will be further discussed in Chapter 2. ....39

Figure 2-1: Schematic of the MagaZorb® DNA Mini-Prep Kit Protocol for blood samples. The blood sample was lysed ①-③, to release DNA prior to binding. The Binding Buffer and MZ was added to the solution ④, mixed and left for 10 minutes at room temperature, mixing at 2 minute intervals. The tube was placed on the magnetic rack, sedimenting MZ beads, and supernatant was removed ⑤. The Wash buffer was added to the tube, the solution was mixed to free MZ beads from contaminants ⑥ & ⑦ before sedimenting the MZ beads and removing supernatant ⑧. The Wash step was repeated twice. The DNA was retrieved from the MZ beads using the Elution Buffer ⑨-⑪: Elution buffer was added to the tube; the solution was mixed to free the bound DNA from MZ beads; the solution was heated for 10 minutes to aid elution; and finally the tube was placed on the magnetic rack to sediment MZ beads. The supernatant containing extracted DNA was transferred into a new tube for storage ⑫.....43

Figure 2-2: qPCR linear amplification curve. The  $\Delta$  normalised reporter value ( $\Delta R_n$ ); fluorescent signal minus the baseline value, is plotted against the cycle number. A typical amplification curve resembles a sigmoidal curve. Amplification is measured by the Ct value, the cycle number which corresponds to the fluorescence reaching a determined threshold value. ....46

Figure 2-3: Melt curve data. The fluorescence data is recorded as the temperature is increased. (a) The normalized melt curve. The normalized reporter ( $R_n$ ) is plotted against

temperature. The melt temperature is determined at the 50% of the drop in fluorescent intensity. (b) The derivative melt curve. The derivative of the Rn is plotted against temperature to visualise the melt peak. ....47

Figure 2-4: Schematic of (a) plasmodium pan qPCR primer set (PANchrom) targeting pan-plasmodium gDNA. (b) *S. mansoni* qPCR primer set (SMchrom), targeting *S. mansoni* gDNA. The arrows depict the direction of polymerisation for each primer sequence. ....50

Figure 2-5: qPCR calibration data for plasmodium DNA. (a) Fluorescence data collected from ABI machine for TaqMan qPCR amplification of serially diluted plasmodium gDNA. Data plotted in brown, pink, dark blue, blue, purple and green are 20, 10, 10<sup>-1</sup>, 10<sup>-2</sup>, 10<sup>-3</sup> ng/μL gDNA samples and dH<sub>2</sub>O respectively. (b) Average qPCR Ct Values for serially diluted DNA templates; synthetic gBlock DNA template in orange and plasmodium genomic DNA (gDNA) in blue. The error bars are the standard deviation for the Ct values obtained for the respective DNA concentrations. ....52

Figure 2-6: qPCR amplification of FTA<sup>®</sup> extracted samples. An example of an amplification curve from a confirmatory qPCR run. The graph shows the amplification curve of: the positive control DNA (+ Control gDNA); a DNA sample containing plasmodium DNA, extracted from blood stored on FTA<sup>®</sup> card returned from the field (+FTA<sup>®</sup> Extract); and the negative control (NC). ....53

Figure 2-7: Cycle threshold (Ct) and time to cycle threshold (Ctt). The Ct values (orange) reports the cycle number at which the sample fluorescence passes crosses the determined threshold. The Ctt (green) reports the time at which the sample fluorescence crosses the same threshold and also takes into account the time where the ABI machine was heating and stabilising at 65°C before the initiation of the ‘temperature cycling’ program; taking such measures into account resulted in more reproducible and comparable data. ....58

Figure 2-8: Gel electrophoresis of PPAN qPCR amplicons. Image captured depicts bands of amplified qPCR product from samples containing serial dilutions (10 to 10<sup>-3</sup> ng/μL) of plasmodium falciparum genomic DNA (gDNA). Size of amplified product is determined against the reference DNA ladder (first lane), ‘-’ denotes the negative control, whilst ‘p’ denotes positive control (10<sup>-2</sup> ng/μL gBlock DNA). ....60

Figure 2-9: Example of the diagnostic cassette. The labels highlight key components of the cassette: 1- The finger pumps, the buffer chambers which produce fluid flow when pushed; 2- amplification chambers, where molecular reagents and DNA are inserted for

amplification; 3- valves, included to hold reagents in their respective chambers until fluid flow is initiated; 4- LF strips for visual read out of amplification results.....61

Figure 2-10: Preparation of finger drop blood sample for processing on the Paper Device. Unless otherwise stated the reagents for sample preparation were obtained from the Promega MagaZorb® Kit. First the Blood sample was lysed ①-③. The DNA was bound to MZ using the Binding Buffer④ and left for 5 minutes at room temperature, mixing at 2 minute intervals. The tube was placed on the magnetic rack and supernatant was removed ⑤. The first wash was conducted in the tube ⑥ - ⑦ before transferring the DNA bound to MZ to the paper microfluidic device for downstream processing ⑧-⑩ (Figure continues on the following page). Wash Buffer was pipetted on top of the MZ beads on the sample spot to complete washing⑪. The paper was folded into the elution position and the Elution Buffer was pipetted on top of the MZ beads; eluted DNA was captured by the paper tabs ⑫-⑭. Molecular reagents were pipetted into the amplification wells and covered with adhesive film, before placing the cassette in the custom heat block to conduct LAMP ⑮-⑰. ....63

Figure 2-11: The LF strips detect presence of FITC and biotin complex, molecules incorporated into the double stranded DNA LAMP amplicons. The biotin in the amplified product binds to the streptavidin coated gold nanoparticles embedded in the conjugation pad. The FITC binds to the anti-FITC embedded in the Test line. Incorporation of both FITC and biotin in the LAMP amplicons result in gold nanoparticles being captured at the Test line (producing a red band). The remaining gold nanoparticles continue to flow down the LF strip and are captured at the Control line. ....65

Figure 2-12: Interpretation of the amplification result using a LF strip. A red line at the test line and control line indicates a positive result. A red line at the control line and absence of a test line indicates a negative result. In absence of the control line (regardless of the presence of a band in the test line), the test is invalid.....66

Figure 2-13: Effect of dilution of LAMP amplicons on LF read-out. LAMP was conducted using the qPCR machine, the amplified samples were serially diluted and added to the LF strips with two drops of Wash Buffer (supplied with the strips). The LF strips are marked with their respective sample, Water (-), LAMP negative control (H<sub>2</sub>O), serially diluted

amplified samples: 100,000X dilution (-5), 10,000X (-4), 1,000X (-3), 100X (-2), 10X (-1) and A is the original amplified solution. ....67

Figure 2-14: To determine the results from the Diagnostic Cassette, the results of the test PC and NC strips (marked P & - on the cassette respectively) must be acknowledged with the test result (marked 1 on the cassette). A positive result is depicted in the first diagram ①, NC= negative, PC= positive, 1= positive, overall: positive. A negative result is shown in ②, NC= negative, PC= positive, 1= negative, overall: negative. Diagnostic cassettes (③-⑥) show examples of invalid tests, the faults are circled in blue. ....69

Figure 2-15: Paper based microfluidic device: (a) used to test x4 targets (b) used to test x3 targets on the diagnostic cassette. Each design includes: a wash panel; a sample spot for, application of the sample; elution channels, to guide fluid flow from the sample spot to the amplification chamber; a placement pad, to simplify attachment to the diagnostic cassette. ....70

Figure 2-16: The progression of cassette design. (a) Examples of the diagnostic cassette designed and used in successive field trials. (b) The finalised design for manufacturing within the laboratory. The design required two sides of adhesive film for cassette assembly. (c) Finalised design for field trials, incorporates PMMA backing, with inlet holes cut from the amplification chambers. ....73

Figure 2-17: Making the Parafilm® valves using the custom valve mould plate. The tweezers were used to push the Parafilm® globules into the circular wells (mimicking valves) in the plastic valve mould. The scalpel was used to slice the excess Parafilm® from the top of the well. The globules were then removed from the mould and inserted into the diagnostic cassette. ....75

Figure 2-18: Assembly of the diagnostic cassette; diagram modified from materials used for training purposes. Steps ①&② describe fabrication of the cassette front, the adhesive film was prepared and kept aside until needed. Steps ③&④ describe fabrication of the cassette backing (this step is omitted from assembly of field devices). ⑤&⑥ Describes creation of Parafilm valves and insertion of LF strips. ⑦The cassette is closed using the prepared backing film; ⑧&⑨The wash chambers were filled with 80µL nuclease free water and

closed using excess adhesive film (omitted from field devices). Step ⑨ shows the finished cassette, an extra piece of adhesive film is needed to close the amplification chamber after processing.....76

Figure 2-19: Device assembly. (a) The printed paper origami devices exposure to UV in preparation for use in the field. (b) Set-up in preparation for manufacturing of the paper Device for field trials. The cleaned diagnostic cassettes were arranged alongside the pre-cut adhesive film with pre-punched inlets, prepared valves and paper tabs (filter paper). The Diagnostic cassettes were manufactured inside a flow hood to allow exposure of all equipment to UV before use and ensure a clean environment during preparation to decrease risk of contamination from external DNA. ....77

Figure 2-20: The custom heat block to house the diagnostic cassettes for heating inside the dry heat bath; fabricated by Thomas Dickson and Stephen Monaghan in the school of Engineering Mechanical Engineering Workshop.(a) The custom heat block, placement of diagnostic cassette is demonstrated. (b)Assembly of the heat block. The aluminium plates were fabricated to be assembled and fixed together with bolts. The design enables the block to be disassembled, facilitating disinfection after use.....79

Figure 2-21: Design figure of the custom heat block manufactured to heat the Paper Device diagnostic cassette. (a) 3D design rendered on SOLIDWORKS, the design depicts a diagnostic cassette placed in the heat block. (b) Top view of the heat block design with dimensions. (c) Side cut view of the heat block design with dimensions.....80

Figure 2-22: The laboratory set up to observe heating of the paper diagnostic cassette. (a) Thermal data collected from the thermocouple placed inside the diagnostic cassette (green line); the optimum temperature required for LAMP (blue horizontal line); time to reach optimum temperature (purple dotted line), 2 min 33 s. (b) The diagnostic cassette was modified to incorporate a thermocouple into the amplification well. Thermal data was collected by the PicoLog6 Thermocouple Data Logger. The box was placed over the heating set up to mimic working set-up in the field. ....81

Figure 3-1: Sequence of *S. mansoni* 202 bp gBlocks Gene Fragment to act as a positive control target for SM primer mix, targeting mtDNA, mitochondrial minisatellite region (GenBank Accession No. L27240). ....88

Figure 3-2: Sequence of *S. mansoni* 125 bp gBlocks for SMchrom positive control target, targeting *S. mansoni* gDNA tandem repeat unit, sm1-7(GenBank Accession No. M61098.1). ....89

Figure 3-3: Stool substitute. A recipe for faecal substitute was modified from that acquired from NHS virology department, Glasgow. The stool substitute was spiked with beads and *S. mansoni* ova to conduct preliminary extraction trials. ....89

Figure 3-4: Egg flotation cassette design. The cassette was designed on Solidworks to imitate the function of a mini-FLOTAC device. The open design was created to enable floating debris in the flotation well (1) to be transferred to the collection well (2) by sliding motion of the lid. The concentrated solution was then able to be transferred from the collection well for downstream processing. (a) The cassette base, with sample wells and alignment track. (b) The cassette lid with alignment rods to facilitate sliding motion. (c) Design of the assembled cassette.....91

Figure 3-5: The sample preparation for extraction of DNA from stool. Steps 1-4 follow the Mini-FLOTAC technique, homogenisation of the faecal sample in the flotation solution – the Figure is adapted from that published by Maurelli, Rinaldi and Cringoli. Steps 5 & 6 describe the modified flotation technique using the flotation cassette. ....94

Figure 3-6: Schematics of *S. mansoni* primers within target sequence. (a) SM primer set targeting *S. mansoni* mtDNA. (b) SMchrom primer set targeting *S. mansoni* gDNA sequence, attempts to tag the internal primers (BIP & FIP) with FITC and Biotin were made to enable read-out on the LF strips. (c) SMchromL primer set, to incorporate loop primers into the SMchrom target sequence. ....98

Figure 3-7: (a) The fluorescence curves obtained from conducting qPCR on a range of *S. mansoni* target DNA, serially diluted gBlocks -  $10^{-1}$  &  $10^{-2}$  ng/ $\mu$ L (red & navy blue); and extracted cercariae (green), egg (blue) and adult worm (black) DNA. There was no amplification observed from the NC (pink). (b) The mean Ct values (N=5) obtained from conducting qPCR following the methods in Section 2.1.3.2 on a range of *S. mansoni* DNA targets. The error bars are the standard deviation of Ct values obtained for each target. ...100

Figure 3-8: Gel electrophoresis of SMchrom qPCR samples. DNA from a variety of *S. mansoni* target DNA samples (egg, cercariae, gBlock) sources were amplified by qPCR and gel electrophoresis was carried out to validate amplification. The intensity of the fluorescent band is proportional to the amount of product in the well. The relative intensity of bands between the gBlock and gDNA samples suggest higher concentration of DNA in the gBlock sample, this corresponds with respective Ct values.....101

Figure 3-9: LAMP calibration data for SM gBlock dilution series. The gBlock was serially diluted and LAMP was carried out using SM primer mix. (a) & (b) The fluorescence results

collected by the ABI machine monitoring real-time LAMP. The dilution concentrations  $10^{-1}$ ,  $10^{-3}$ ,  $10^{-4}$ ,  $10^{-5}$ ,  $10^{-6}$ ,  $10^{-7}$ ,  $10^{-8}$  ng/ $\mu$ L are labelled 1-7 respectively. LAMP was not successful for all sample dilutions 6 & 7, hence the results were not included in the calibration curve. (c) Graphical representation of the average Ctt value for each DNA concentration, the error bars show the standard deviation of the Ctt values obtained for the respective gBlock DNA concentration. The increase of Ctt with decreasing DNA concentration is as expected. ....103

Figure 3-10: The development of SMchrom LAMP assay. (a) Primary LAMP development was undertaken using the qPCR SMchromF3 & SMchromB3 oligo sequences with published internal primer sequences. However, this lead to false amplification of no target negative controls ‘NC’. (b) The false amplification of NC samples ‘NC#2’ was confirmed by gel electrophoresis. (c) Further development was carried out using a modified B3 oligo (SMchromB3\_2), this lead to successful LAMP results, amplification was observed for control target DNA ‘PC’ and was not present for NC. (d) Integration of FITC and biotin molecules into the SMchrom assay. LAMP carried out with FITC and biotin tagged FIP & BIP primer sets did not produce visible amplification result. (e) The samples were run on LF strips and positive LF read out was determined for both PC & NC. ....105

Figure 3-11: Gel electrophoresis for confirmation of isothermal amplification of cercariae (C), egg (EGG) and gBlock DNA sequence (gB) for both SM and SMchromL (SMC) primer sets. Bright bands signify presence of amplified DNA in the sample. The SM and SMchromL bands appear in line with the 200bp and 100bp reference ladder respectively, suggesting correct amplification. No bands were present for the no template control (SM NC), where both SM and SMchromL (SMC) no template controls reactions were combined in the final well of the gel. ....106

Figure 3-12: Summary of the results of amplification using the mtDNA & gDNA targeting primer sets. SM and SMchromL was able to amplify all extracted DNA samples, however no amplification was achieved using SMchrom primers, suggesting that tagging the internal primers inhibits LAMP. ....107

Figure 3-13: Detection of amplified product on LF strips (a) SM amplified *S. mansoni* samples run on the LF strip. Positive results confirmed by presence of two lines within the result observation window, for *S. mansoni* cercariae (C), egg (EGG) and gBlock (gBlock) DNA. (b) SMchromL amplified *S. mansoni* samples run on the LF strip. No positive results suggest failure of one or both of the Loop primers during amplification. ....108

Figure 3-14: Melt curve analysis of FITC and biotin modified primer sets exported directly from ABI software. Melt curve analysis of LAMP carried out using: (a) SM tagged primer set and the developed SMchromL tagged primer set; (b) PPAN tagged primer set; and PPAN untagged primer set. The melt peak is marked with a blue arrow. The ‘dipped shoulder’ observed for tagged primer sets is marked in red. This is not observed in the tagged SMchromL melt curve, which resembles the profile of the PPAN untagged melt curve (both yellow). (c) The ‘dipped shoulder’ was confirmed to be caused by FITC primer by analysing melt curves produced by LAMP carried out using tagged PPAN primers with: isothermal Mastermix containing dsDNA binding dye (ISO-004); and isothermal Mastermix which does not include dsDNA binding dye (ISO-004ND). The normalised melt curve data shows the increase in fluorescence (boxed in red) which results in the ‘dipped shoulder’ observed in the derivative reporter graphical data.....110

Figure 4-1: The field site. (a) The classroom used to conduct the second field study in Apache, Apac District, Uganda. (b) The study set-up in the classroom. The participants were registered at the desk by the entrance to the room. The desks in the centre of the room were used as a waiting area. Sampling and comparative diagnostics were conducted at the front of the room. (c) Molecular diagnostic work stations were set-up at the back of the room. Work was conducted linearly across the room: DNA extraction; addition of molecular reagents; heating (LAMP); and diagnostic read-out. ....118

Figure 4-2: Transportation of equipment. (a) Fieldwork equipment and personal luggage being loaded into the 4x4 in VCD, Kampala. (b) Equipment and luggage packed in and secured on top of the car. ....121

Figure 4-3: Schematic for the sample collection and processing for diagnosis of schistosomiasis and malaria in the field. FTA® storage refers to the storage of a finger prick of blood on an FTA® card. FTA® was used for safe transportation of the sample to the UK for downstream qPCR testing in the laboratory. ....122

Figure 4-4: Molecular diagnostic workflow in the laboratory as compared to the field site room. Molecular diagnostic work flow was set-up linearly. DNA extraction from blood samples was conducted in Laboratory 1 (on the DNA extraction bench). Extracted DNA samples were transferred to Laboratory 2 (on the DNA bench) for addition of molecular reagents before being moved to the final location to conduct DNA amplification. In-the-field, this process was mimicked by creating a linear work-flow from sampling to DNA amplification, where team members at each bench, avoid moving between sample processing stages conducted on separate benches.....124



Figure 4-5: KK examination. (a) Equipment to conduct KK test. (b) A small section of the faecal sample being pushed through the fine sieve. (c) The sieved sample collected and transferred into the KK template on top of the microscope slide. After removal of the KK template, a stool pellet remains on the slide. (d) Pre-soaked malachite cellophane strips applied on top of the stool pellet for staining to aid microscopic examination. ....126

Figure 4-6: Preparation for the hatching test. (a) A diagram of the ‘hatching set’ made from two nylon nets. The inner mesh (200 µm) and outer mesh (41 µm), fitted with a bottle cap to catch ‘s.mansoni egg sized debris’. (b) The sample preparation for hatching s.mansoni ova from collected stool samples. The faecal sample was prepared: the stool shook in the sample container to break up the sample; sieved through the fine mesh sieve with a toothbrush; and passed through the ‘hatching set’. Debris expelled from the hatching set was collected in the dirty wash bucket. After collection of ‘egg sized debris’ in sample containers, the hatching set was washed in the ‘clean wash buckets’ to be re-used. ....128

Figure 4-7: Heating set-up to conduct point-of-care LAMP during the preliminary field trials. The paper diagnostic cassettes were balanced on a standard 1.5 ml tube heat block within the dry heat bath. A plastic box was placed over the heater in attempt to retain heat and deter insects. ....129

Figure 4-8: Summary of the results obtained for processing stool samples to detect S. mansoni DNA using the Paper Device in-the-field. POC LAMP results were analysed against comparative diagnostics in the field (Kato-Katz and hatching tests). The preliminary trial resulted in 8 confirmed true-positive results; 2 confirmed true-negative results; and a single false-positive reported by the Paper Device \* one of the negative KK results was a false-negative, the sample was determined as positive in the confirmatory hatching test. 132

Figure 4-9: Frugal testing using a local cooking stove. (a) LAMP amplification conducted in a saucepan on a gas heater purchased in the field. A thermometer was used to control the temperature visually around 63°C ± 4°C. (b) Set-up of gas heater used for amplification. Microscope boxes were used to shield the heater from wind to limit heat fluctuation. ....134

Figure 4-10: A summary of the result obtained for the multiplex malaria and schistosome cassette. The detection of plasmodium and S. mansoni DNA in a 5 µL whole blood sample in-the-field. Amplification was carried out using a portable gas stove. Point-of-care LAMP results were analysed against comparative diagnostics in the field (blood smear or Kato-Katz) and malaria results were analysed against comparative qPCR conducted in the laboratory on return to the U.K. ....136

Figure 4-11: A summary of the result obtained for the multiplex malaria and *S. mansoni* cassette. The detection of plasmodium and *S. mansoni* DNA in a 5  $\mu$ L whole blood sample in-the-field. Point-of-care LAMP results were analysed against comparative diagnostics in the field (blood smear or Kato-Katz) and malaria results were analysed against comparative qPCR conducted in the laboratory on return to the U.K. ....139

Figure 4-12: miniPCR™ and gel electrophoresis in the field. (a) PCR was carried out using the miniPCR™ thermal cycler in the field. The miniPCR™ was powered by a rechargeable battery pack and temperature cycling was monitored on the laptop. (b) Elías Kabbas-Piñango capturing an image of the gel electrophoresis bands using the BlueGel™ electrophoresis system. (c) Image of the bands produced from Amplified PCR product from control DNA templates and a whole blood sample following DNA extraction. The bands highlighted in the image 6-9 (~150 bp) are amplified PCR product from the positive control DNA template and PPAN and BRCA1 DNA in the whole blood sample. ....142

Figure 5-1: Schematic of the plasmodium PAN LAMP primer sequences targeting 220 bp of pan species plasmodium mitochondrial DNA. The arrows depict the direction of polymerisation for each primer sequence. ....159

Figure 5-2: Plasmodium PAN LAMP calibration data. (a) Fluorescence data collected from ABI machine for LAMP amplification of serially diluted plasmodium gBlock DNA. Data plotted in red, pink, purple, blue and green are  $10^{-3}$ ,  $10^{-4}$ ,  $10^{-6}$ ,  $10^{-8}$  ng/ $\mu$ L gBlock samples and negative control (dH<sub>2</sub>O) respectively. A single  $10^{-8}$  ng/ $\mu$ L gBlock sample amplified, hence, LOD was determined as  $10^{-6}$  ng/  $\mu$ L. (b) Average C<sub>tt</sub> Values from LAMP amplification of diluted gDNA (blue) and gBlock DNA (orange). Use of gBlock DNA allows amplification of samples 1000X diluted as compared to gDNA. At concentration of  $10^{-3}$  ng/  $\mu$ L, gBlock DNA (C<sub>tt</sub>=6.5) amplifies 10.6 cycles faster than the corresponding gDNA sample (C<sub>tt</sub> =17.1). ....165

Figure 5-3: Primer Stability. Primer mix was stored in a 37°C incubator (1-5), at room temperature (grey) and as a control at -20°C (black) for 7 days. LAMP amplification of target gBlock DNA ( $10^{-6}$  ng/ $\mu$ L) was conducted in triplicate each day on the ABI machine, C<sub>tt</sub> was recorded for each sample. LAMP amplification was carried out over a 5 day period to simulate field work structure. There was no significant difference found between C<sub>tt</sub> values of control (C) and room temperature (RT) samples, the results were compiled into a single bar. The experiment was repeated twice. C<sub>tt</sub> results were compiled to calculate the mean (15.8, 15.9, 17.0, 19.0, 16.2, 20.9) and standard deviation (0.8, 1.1, 1.4, 1.6, 1.5, 0.2) of amplification times for C, RT and samples stored in the incubator days 1-5 respectively. For

each sample, a no template negative control was conducted in triplicate. Statistical analysis: ns represents no statistical significance ( $p \geq 0.05$ );  $0.01 > p \geq 0.001$  is represented by \*\*; and  $p < 0.0001$  is represented by \*\*\*\*. ....167

Figure 5-4: Reagent stability. Both Primer mix and re-suspended Mastermix (ISO-DR004) were stored at laboratory room temperature and in a 37°C incubator for 24 hours. LAMP amplification ( $10^{-5}$  ng/ $\mu$ L gBlock DNA) was carried out using the ABI machine after 6 and 24 hours of reagent storage. Control reagents were stored at -20°C. C, RT & 37 refer to results from reagents stored at -20°C, laboratory room temperature and 37°C respectively. Additionally, at 24 hours LAMP was conducted using the Mastermix stored in the incubator with control primer mix (24\*). No amplification was present for no target negative controls. Statistical analysis: ns represents no statistical significance ( $p \geq 0.05$ );  $0.05 > p \geq 0.01$  is represented by \*;  $0.001 > p \geq 0.0001$  is represented by \*\*\*;  $p < 0.0001$  is represented by \*\*\*\* .....169

Figure 5-5: Molecular reagents field storage. A bottle of freeze-dried Mastermix (ISO-DR004) and an Eppendorf of primer mix was taken to Uganda and stored in field conditions for 10 days. On return to the U.K, the Mastermix was re-suspended following manufacturers recommendations. (a) LAMP amplification of  $10^{-6}$  ng/ $\mu$ L gBlock DNA was conducted on the ABI machine using field stored reagents and control reagents (Mastermix stored following manufacturers recommendations and primer mix stored at -20°C): (1) Control Mastermix and primer mix; (2) Field stored Mastermix and control primer mix; and (3) Both field stored Mastermix and primer mix. No template negative controls were run in triplicate for each sample. (b) Amplified samples were run on LF strips for confirmation. Statistical analysis:  $p \geq 0.05$  is represented by ns; ns\* where F test was significant.....171

Figure 5-6: Field storage conditions. Primer mix was taken to Uganda and stored in field conditions for 10 days. On return to the U.K, LAMP amplification of  $10^{-6}$  ng/ $\mu$ L gBlock DNA was carried out on the ABI machine using field stored primers and Mastermix stored in the laboratory (-20°C). The Ctt values obtained for amplification of field stored primer mix (Uganda) are plotted alongside Ctt values obtained in earlier primer storage experiments (see Section 5.4.2.1, Figure 5-3); primer mix stored at 37°C (37) and -20°C (C). A no template negative control was run in triplicate, no amplification was observed from the negative sample. Statistical analysis:  $p \geq 0.05$  is represented by ns;  $0.05 > p \geq 0.01$  is represented by \*;  $0.01 \geq p > 0.001$  is represented by \*\*.....173

Figure 5-7: Lyophilised isothermal Mastermix stability. A bottle of freeze-dried master mix (ISO-DR004) that was stored in Uganda for 10 days at room temperature, was brought back

to the lab and re-suspended following manufacturers recommendations. LAMP was conducted after re-suspension (t=0) and after storage at laboratory room temperature (RT) and various elevated temperatures for 24 hours. The results were interpreted by LF strips, a single no template negative control and duplicate target DNA samples (5  $\mu\text{L}$  of  $10^{-5}$  ng/ $\mu\text{L}$  gBlock) was amplified on the ABI machine. (L) Refers to the control reaction, where molecular mix was stored at  $-20^{\circ}\text{C}$ . .....174

Figure 5-8: Lyophilised molecular reagents. Freeze-drying was tested with a few reagent mixes: (a) ISO-004 Mastermix, unsuccessful; (b) LYO-004 Mastermix and original ‘5  $\mu\text{L}$ ’ primer mix; (c) LYO-004 and modified ‘1  $\mu\text{L}$ ’ primer mix. (d) The Freeze dried reagent mix with 1  $\mu\text{L}$  of the primer mix was stored for 7 days within a  $37^{\circ}\text{C}$  incubator and at room temperature. The difference in Ctt between control and lyophilised reagents was statistically significant ( $p < 0.0001$ ), however, the variation in Ctt throughout the week was non-significant.....175

Figure 7-1: The ABI FAST 7500 qPCR machine spectrum filter information as provided by the manufacturer. The dsDNA binding dye and FITC produce emission spectrum  $\sim 520$  nm, thus the fluorescence resulting from LAMP is recorded by Filter 1.....191

Figure 7-2: DNA extraction processed on the Paper Device. (a) DNA extraction from whole blood spiked with plasmodium gBlock DNA to  $10^{-2}$  ng/ $\mu\text{L}$ , whole blood, WB-, was used as a negative control for extraction. (a) Paper tabs were centrifuged to collect eluted DNA for LAMP amplification on the ABI machine. Ctt values for gDNA extraction were 6.7, 7.2, 7.3 cycles (blue star); and associated controls ( $10^{-4}$  &  $10^{-5}$  ng/  $\mu\text{L}$ ) were 10.0 and 12.9 cycles, which coincided with calibration data (red line). There was no amplification from the no target control, NC, or negative whole blood sample, WB-. (b) % recovery of gBlock DNA extracted from whole blood using the Paper Device method, the extraction was repeated three times; % recovery 35.7,23.3,22.8% is displayed for each repeat 1,2,3 respectively. (c) DNA extraction of genomic plasmodium DNA (50 ng), PBS was used as a negative control for extraction. The graph displays the Ctt values for extracted gDNA (red star) as compared to calibration Ctt data (blue line). There was no amplification from the no target control, ‘NC’ or the negative PBS samples.(d) % recovery of gDNA extracted from PBS using the Paper Device method, the extraction was repeated three times; % recovery is displayed 21.0, 24.1 and 19.9% for each repeat 1,2,3 respectively.....194

Figure 7-3: The results from the extraction of plasmodium DNA spiked into whole blood and PBS processed on the Paper Device. The results of amplification were determined by LF read-out. The engravings on the diagnostic cassette ‘2’, ‘1’, ‘P’, ‘-’, where ‘2’ & ‘1’ refer

to the sample result, ‘P’ & ‘-‘ refer to the PC and NC respectively. (a) WB++, cassette depicts a positive result (see Figure 2-14 for details on identification of results), 1 & P were inverted as indicated in black marker on the cassette. (b) WB-, depicts a negative results. (c&d) Results of dDNA extraction from PBS. (c) 50 ng plasmodium gDNA, cassette depicts a positive result. (d) PBS, cassette depicts a negative result. ....195

Figure 7-4: The SMchrom qPCR fluorescence curves. TaqMan qPCR was carried out using gBlock, *S. mansoni* egg DNA and extracted DNA from positive blood samples stored on FTA cards (+FTA Extract). Amplification was conducted for 60 samples, however, no amplification was observed from +FTA Extract.....197

Figure 7-5: Fluorescence data collated for SM LAMP of a variety of target schistosome DNA samples. LAMP was carried out with gDNA (*Schistosoma* DNA provided by SCHISTO\_PERSIST), *S. mansoni* ova and adult worm DNA extracted using the Promega MagaZorb kit. There was no amplification observed from the NC. ....198

Figure 7-6: Fluorescence data collated for SM and SMchromL LAMP of a variety of target schistosome DNA samples. LAMP was carried out with gBlocks, and extracted *S. mansoni* ova and cercariae DNA. Amplification was confirmed by melt curve analysis. There was no amplification observed for NC samples. Amplification of (a) the SM gBlock using the SM primer set. (b) Extracted *S. mansoni* cercariae DNA using the SM primer set. (c) Extracted *S. mansoni* ova DNA using the SM primer set. (d) Extracted *S. mansoni* cercariae DNA using the SMchromL primer set. (e) Extracted *S. mansoni* ova DNA using the SMchromL primer set. (f) Mean C<sub>tt</sub> values obtained for amplification of extracted *S. mansoni* ova and cercariae DNA using the SM (orange) and SMchromL (yellow) primer sets, the SM primer set resulted in quicker amplification as compared to the SMchromL primer set.....199

Figure 7-7: Malaria gold standard, microscopy. (a) FTA® storage cards left to dry alongside the collection of dried blood smears on microscopy slides prior to Giemsa staining. (b) VCD technicians conducting microscopic examination for plasmodium parasites in blood smear. (c) Illustrations of different plasmodium species and life stages as expected to be observed by microscopy. ....201

Figure 7-8: Carestart™ Malaria HRP2/pLDH (Pf/pan) RDT. (a) Instructions for the Malaria RDT test procedure as provided by the manufacturer. (b) Review of the different possible test results. A band must be present in the control window ‘C’ for the test to be valid. All tests which do not present with a band in the control window ‘C’ should be noted as invalid. No bands suggests a negative result. A band present in the ‘T1’ window suggests the patient

does have falciparum malaria (Pf). A band present in the ‘T2’ window suggests that the patient has non-falciparum malaria.....202

Figure 7-9: Bilharzia POC-CCA in the field. (a) The assay procedure, as supplied by the manufacturer. (b) Interpretation of results from the POC CCA cassette as published by the manufacturer (Rapid Medical Diagnostics, Pretoria, RSA). (c) Diagnostic cassettes after addition of urine samples; the cassettes were market with patient unique ID number.....205

Figure 7-10: The results collected from the preliminary field trial for P.PAN reagents (Reboud et al., 2018).....207

## **Acknowledgements**

Firstly thank you to my supervisors Jon Cooper and Julien Reboud who made this project possible and for their continued encouragement and support. Thank you to Andrew Glidle, Rab Wilson, the technical staff within the School of Engineering and the host of post docs and PhD students for technical and practical support over the years. Thank you to the MCCIR and Fiona Allan (Natural History Museum, London) for donating schistosome specimen from their archives, and Lauriane Sollelis (University of Glasgow) for providing plasmodium DNA. Thank you to Edridah Tukahebwa, Moses Adriko, Moses Arinaitwe, Candia Rowell, Aaron Atuhaire and Diana Ajambo from the Vector Control Division Uganda, without whom field work would not have been possible. Thank you to our collaborators within the University of Glasgow, Poppy Lamberton, Christina Faust, Lauren Carruthers and Elías Kabbas-Piñango, who were always there to answer all questions regarding NTDs (no matter how trivial), thank you for all that you have taught me and making field work fun.

Thank you Melanie Jimenez for your constant support and for helping me regain my enthusiasm and love for science when experiments were going particularly poorly. To my lab, office, lunch and gym buddies Xi King, Louise Mason and Laura Charlton, thank you for your friendship and brightening up the grey days in the Rankine.

I would like to thank my family and friends across the globe for their support. To my friends who are always up for an adventure, always making life fun and were always there (in person or on the phone) when I most needed them. Finally, to my parents, John and Cathy Garrett, and my sister Katie, for their unconditional and unending encouragement and love.

## Authors Declaration

I declare that, except where explicit reference is made to the contribution of others, that this dissertation is the result of my own work and has not been submitted for any other degree at the University of Glasgow or any other institution.

Printed Name: ALICE GARRETT

Signature:

A handwritten signature in black ink, appearing to read 'Alice Garrett', written in a cursive style.



## List of publications and conferences

The British Society for Parasitology (BSP) Spring Meeting 2017. University of Dundee. April 2-5, 2017 – Poster Presenter.

McGill Summer Institute in Infectious Diseases and Global Health – Workshop on Global Health Diagnostics. June 12-16, 2017 – Attendee.

One Health, Many Perspectives: Emerging Research from LMICs, Post Graduate & Early Career Researcher symposium. Liverpool School of tropical Medicine. August 30, 2018 – Presenter.

‘Paper-based microfluidics for DNA diagnostics of malaria in low resource underserved rural communities’- PNAS March 12, 2019 116 (11) 4834-4842. Julien Reboud, Gaolian Xu, Alice Garrett, Moses Adriko, Zhugen Yang, Edridah M. Tukahebwa, Candia Rowell, and Jonathan M. Cooper.

‘Demonstrating the Use of Optical Fibres in Biomedical Sensing: A Collaborative Approach for Engagement and Education’- Sensors 2020, 20(2), 402. Katjana Ehrlich, Helen E. Parker, Duncan K. McNicholl, Peter Reid, Mark Reynolds, Vincent Bussiere, Graham Crawford, Angela Deighan, Alice Garrett, András Kufcsák, Dominic R. Norberg, Giulia Spennati, Gregor Steele, Helen Szoor-McElhinney and Melanie Jimenez.

‘Smartphone-based DNA diagnostics for malaria detection using deep learning for local decision support and blockchain technology for security’- Nature Electronics 4, pages615–624 (2021). Xin Guo, Muhammad Arslan Khalid, Ivo Domingos, Anna Lito Michala, Moses Adriko, Candia Rowel, Diana Ajambo, Alice Garrett, Shantimoy Kar, Xiaoxiang Yan, Julien Reboud, Edridah M. Tukahebwa & Jonathan M. Cooper.

## List of commonly used abbreviations

ABI machine - Applied Biosystems Instrumentation FAST 7500 qPCR machine  
bp - Base pair  
CAA - Circulating anodic antigen  
CCA - Circulating cathodic antigen  
Ct - Cycle threshold  
Ctt - Cycle threshold time  
DALYs – Disability-adjusted life years  
DNA - Deoxyribonucleic acid  
dsDNA - Double stranded DNA  
ELISA - Enzyme-linked immunosorbent assay  
EPG - Eggs per gram  
FAM - Fluorescein amidites  
FITC - Fluorescein isothiocyanate  
FS - FLOTAC flotation solution  
gBlock - gBlock Gene Fragment  
gDNA - Genomic DNA  
IDT - Integrated DNA technologies (IDT, Leuven, Belgium)  
LAMP - Loop-mediated isothermal amplification  
LF - Lateral flow  
LMIC - Lower-middle income country  
LOD - Limit of detection  
M – Molar  
MDA - Mass drug administration  
mtDNA - Mitochondrial DNA  
MZ - MagaZorb Reagent  
NAAT - Nucleic acid amplification tests  
NC - Negative no template control  
NDA - non-disclosure agreement  
*P.* - Plasmodium  
PBS - Phosphate buffered saline  
PC – Positive control  
PCR - Polymerase chain reaction  
PK - Proteinase K  
PMMA - Poly(methyl methacrylate)  
POC - Point of Care  
PPAN - Plasmodium pan species  
PVC - Polyvinyl chloride  
qPCR - Quantitative polymerase chain reaction  
RDT - Rapid diagnostic test  
*S.* - Schistosoma  
SEA - Soluble egg antigen  
SH - Schistosoma haematobium  
SM - Schistosoma mansoni  
ssDNA - Single stranded DNA  
TAE - Tris-acetate-EDTA  
TAMRA – Carboxytetramethylrhodamine  
TB – Pulmonary tuberculosis  
TE - Tris-EDTA (Ethylenediaminetetracetic acid)  
UV - Ultraviolet light  
VCD - Vector Control Division  
WB - Whole blood  
WBC - White blood cell (leucocyte)  
WHO - World Health Organization

## Chapter 1: Introduction

The World Health Organization (WHO) highlighted the importance of the elimination of malaria and schistosomiasis in the 2030 roadmap to achieve sustainable development goals (World Health Organization, 2020a). Highly sensitive molecular diagnostics to inform accurate and timely treatment of infectious diseases – such as malaria and schistosomiasis – can benefit populations living in remote rural communities (Peeling and McNerney, 2014). Applications of molecular diagnostics are also becoming increasingly relevant in global efforts for disease elimination, where the testing of asymptomatic patients is an important factor for the identification of disease reservoirs (Peeling and McNerney, 2014) – highlighted during the COVID-19 pandemic (Tang *et al.*, 2020; Udugama *et al.*, 2020). However, healthcare workers face practical and logistical problems in the implementation of molecular tests, which often rely on centralised laboratories, require expensive instrumentation and complex techniques (Pai *et al.*, 2012; Caliendo *et al.*, 2013).

Work previously conducted within the Biomedical Research Division at The University of Glasgow resulted in the development of a low cost, point-of-care molecular diagnostic platform for malaria (Xu, Nolder, *et al.*, 2016). Adaptation of the technique to aid the diagnosis of schistosomiasis could provide more accurate detection of schistosome infections at the point-of-care (Fernández-Soto *et al.*, 2014). Despite treatment and surveillance programs, malaria and schistosomiasis are prevalent throughout Uganda. Molecular detection of malaria and schistosomiasis has the potential to benefit current surveillance programs, as progress is made toward elimination there will be a need for molecular tests to detect infection in low prevalence settings and to monitor progress toward elimination (Peeling and McNerney, 2014). An abundance of reports present molecular tests aimed for use at the point-of-care, however, evidence of trials in low-resource and rural environments are lacking. On-going collaborations with the University of Glasgow, the Ministry of Health (MoH) and the Vector Control Division (VCD) in Uganda has facilitated this study to assess the point-of-care molecular diagnostic tests in rural and limited-resource<sup>1</sup> settings in Uganda.

---

<sup>1</sup> Limited-resource - for the purpose of this work - refers to environments with basic facilities and limited or no access to mains electricity and running water. Additionally it references where communities have extremely limited or no accessible health care providers and facilities, or a health system which cannot deliver optimal levels of care.

## 1.1 Malaria

Malaria is an acute febrile illness, caused by the parasite of the genus *plasmodium* (World Health Organization, 2020b). Nearly half of the world's population lives in areas at risk of malaria (CDC, 2020). Although malaria is a risk throughout tropical areas of the world, over ninety percent of the global burden is located in the African region (World Health Organization, 2018). African countries alone make up over ninety percent of the reported malaria cases (World Health Organization, 2019b). The most vulnerable groups are children under the age of five and individuals who are immunocompromised (Unicef, 2018).

### 1.1.1 Transmission

The *plasmodium* parasite is transmitted to the human host by the parasite vector - an infected female Anopheles mosquito (Ashley et al., 2018). The *plasmodium* parasite has three distinct life stages, which exists between the vector and human host. The *plasmodium* life cycle is depicted in Figure 1-1. During a blood meal, a *plasmodium*-infected mosquito inoculates the human host with *plasmodium* sporozoites<sup>2</sup> (Ashley et al., 2018). In the first stage of infection, the sporozoites travel to the liver of the human host, infecting the liver cells where they mature into schizonts<sup>3</sup>. The infected liver cells eventually rupture, releasing merozoites<sup>4</sup> into the blood stream. The merozoites invade the erythrocytes (red blood cells), initiating the second stage of the malaria cycle. Within the erythrocyte, merozoites form ring structures – an immature trophozoite<sup>5</sup> - which feed on the haemoglobin, at this point in the *plasmodium* life cycle there are two distinct scenarios.

1. The trophozoite mature into schizonts, which undergoes asexual reproduction within erythrocytes to produce merozoites. The new merozoites then rupture the red blood cell, reinitiating the erythrocytic cycle - this cycle is responsible for the clinical manifestations of the disease (CDC, 2019a).
2. Some of the parasites differentiate into gametocytes (sexual erythrocytic stages). The gametocytes are ingested by an anopheles mosquito during a blood meal, which then undergo sexual reproduction within the mosquito (CDC, 2019a). The mosquito conserves the malaria cycle during the next blood meal taken from a human host.

---

<sup>2</sup> Sporozoites: the motile spore-like stage of parasites of the phylum Sporozoa.

<sup>3</sup> Schizonts: a cell that divides by schizogony (asexual reproduction) to form daughter cells

<sup>4</sup> Merozoites: a small sporozoan produced by schizogony, capable of initiating a new development cycle

<sup>5</sup> A trophozoite is the ring stage of the erythrocytic cycle, that feed on haemoglobin and forms a granular pigment called haemozoin.

The cyclical lifecycle of the parasite, which spans across the two hosts, causes a major barrier to elimination of the disease. To achieve and maintain malaria elimination in areas that have already reduced transmission to very low rates, identification of the essential operational changes have to accompany a switch in focus from burden reduction, to interruption of transmission (Moonen *et al.*, 2010).

[Image removed due to copyright restrictions]

The QR code links to the image source.

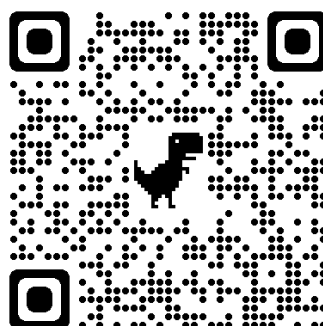


*Figure 1-1: The plasmodium life cycle. Figure obtained from the CDC website, <https://www.cdc.gov/malaria/about/biology/index.html>. ① during a blood meal, an infected mosquito inoculates the human host with plasmodium sporozoites. ②-④ The human liver stage. The sporozoites infect the liver cells where they mature into schizonts. The infected liver cells eventually rupture, releasing merozoites into the blood stream. ⑤-⑦ The human blood stages. Rupturing of the liver cells initiates the human blood stages. Here there are two scenarios, 1: ⑤&⑥ the parasites undergo asexual reproduction within the erythrocytes. This continues the erythrocytic cycle. 2: ⑤&⑦ the parasites differentiate into gametocytes (sexual erythrocytic stages). ⑧ The gametocytes which are ingested by an Anopheles mosquito during a blood meal, initiating the sporogonic cycle, where the parasite undergoes sexual reproduction within the mosquito ⑨-⑫.*

### **1.1.2 Clinical manifestations**

There were an estimated 228 million cases of malaria and 405,000 related deaths in 2018 alone (World Health Organization, 2019b). Malaria presents as a fever that develops

suddenly, an immune response caused by rupture of mature schizonts within the host (Crutcher and Hoffman, 1996). In primary stages of the illness, headaches and chills usually accompany the fever. If malaria is left untreated, these symptoms can progress into severe illness, referred to as ‘severe malaria’ (CDC, 2019a). Severe malaria occurs when illness results in organ failure or blood abnormalities. Severe malaria symptoms range from seizures, behavioural changes and respiratory distress, to abnormalities in blood coagulation and haemoglobinuria (haemoglobin in the urine) (Ashley et al., 2018). The most threatening type of malaria - caused by the parasite *P. falciparum* - develops quickly, if the acute attack is rapidly diagnosed and treated, prognosis is good (Bartoloni, 2012). Unfortunately preliminary stages of malaria present similar symptoms to many other illnesses and diseases, highlighting the importance for diagnostic tests which are able to provide a diagnosis in the early stages of the illness to reduce fatalities.

For those working in remote areas, or clinics with limited resources in endemic<sup>6</sup> regions, symptom-based diagnosis is still common-practice (Bell *et al.*, 2006). However, studies have shown that access to malaria rapid diagnostic tests (RDTs), has resulted in a shift away from the long-standing practice of treating all cases of fever as malaria (Altaras *et al.*, 2016); highlighting the profound implications that RDTs have for fever management and public health in tropical regions (Bell *et al.*, 2006).

### **1.1.3 Prevention**

Blood meals taken by the mosquito fuel the malaria cycle. At present, malaria prevention efforts focus on vector control (to reduce the frequency of bites) and mass drug administration, discussed further in Section 1.3.3 . The main vector control methods include use of bed nets, indoor residual spraying and larval source management (habitat modification and manipulation). Indoor residual spray interventions were once widely adapted, but have been abandoned by some countries due to associated risks to human health and environmental hazards (Tizifa *et al.*, 2018; Tangena *et al.*, 2020). Habitat manipulation includes measures such as drain clearance and application of insecticides to greenery and stagnant water bodies, however, this is less suitable in rural areas (Tizifa *et al.*, 2018). Additionally, there are a number of commercially available spatial repellents, the methods utilised depend upon the location and environment of use (Achee *et al.*, 2012). Travelers visiting malaria-endemic countries are advised to wear long, loose clothing; to use mosquito

---

<sup>6</sup> An area in which there is an ongoing, measurable incidence of malaria infection and mosquito-borne transmission over a succession of years (World Health Organization, 2019a)

repellent frequently; and to sleep under insecticide treated mosquito nets (NHS, 2020). However, the advised measures cannot always be implemented by those living in endemic regions (Tizifa *et al.*, 2018).

Distribution of free insecticide treated nets is a core intervention in national malaria control strategies of all sub-Saharan African countries (Olafeju *et al.*, 2018). Due to an increase in funding available for malaria prevention, bed nets are now available to a much larger portion of households in endemic regions, 28 million nets were distributed throughout sub-Saharan Africa in 2018 alone (World Health Organization, 2019b). However, the success of the bed net intervention for control programs is dependent on sufficient supply per household and correct usage of nets (Olafeju *et al.*, 2018; Njumkeng *et al.*, 2019).

## 1.2 Schistosomiasis

Schistosomiasis (also known as Bilharziasis) is an acute and chronic parasitic disease caused by blood flukes in the genus *Schistosoma* (World Health Organization, 2020c). There are three main species infecting humans, *Schistosoma haematobium* (*S. haematobium*) - the urogenital form of *schistosomiasis*; *S. mansoni* and *S. japonicum* - the intestinal forms of *schistosomiasis* (CDC, 2019b). *S. japonicum* is only prevalent in a few countries in South East Asia, however, the geographical distribution of *S. mansoni* and *S. haematobium* overlap in the African and Middle Eastern regions. *S. mansoni* is also present in the Caribbean, Brazil and Venezuela (CDC, 2019b). The disease is most commonly associated to poor and rural communities, due to lack of adequate sanitation procedures and frequent contact with infected fresh water sources. Estimates show that at least 290 million people required preventative treatment for schistosomiasis in 2018, of whom at least 90% were living in Africa (World Health Organization, 2020c).

Although prevalence of schistosomiasis is high, morbidity reports are low and variable (Gryseels and Strickland, 2013). Schistosomiasis is associated with conditions such as anaemia, chronic pain and undernutrition (Gray *et al.*, 2011). Assessing the burden of schistosomiasis due to morbidity is difficult (Gryseels *et al.*, 2006; World Health Organization, 2020c), hence, meta-analysis estimates the disease burden based on the Disability-Adjusted Life Years (DALYs). The global burden of schistosomiasis as expressed in DALYs takes into account the mortality and disability attributed to the disease (Gryseels *et al.*, 2006). For example, where the global burden estimated 15,000 lives lost due to schistosomiasis, the total number of DALYs due to schistosomiasis was estimated at 1.75-2.0 million (Gryseels and Strickland, 2013).

### 1.2.1 Transmission

Human schistosomiasis is transmitted when larval forms of *Schistosoma* (cercariae<sup>7</sup>), which exist in contaminated fresh water, penetrate human skin (Gryseels *et al.*, 2006). For this reason people are infected whilst completing routine activities such as farming, fishing and washing. The schistosomulae<sup>8</sup> matures into an adult worm and couples with a blood fluke of the opposite sex within the human host. The pair migrate to the mesenteric blood vessels surrounding the large intestine (*S. mansoni*); or venous plexuses around the urinary bladder (*S. haematobium*) (Weerakoon *et al.*, 2015). A matured female worm can lay up to 300 eggs into the capillary walls of the respective organ per day (Cheever and Duvall, 1974; Pellegrino and Coelho, 1978). The eggs then migrate into the intestine/bladder, where some are excreted by the host, which enables diagnosis of schistosomiasis by the identification of the ova in respective stool or urine specimens (Ajibola *et al.*, 2018).

Similarly to malaria, schistosomiasis is reliant on two hosts to complete the life and transmission cycles (CDC, 2019b). The human acts as an intermediate host and the fresh water snails – species belonging to genus *Biomphalaria* and *Bulinus*- are the vector for *S. mansoni* and *S. haematobium* respectively (Weerakoon *et al.*, 2015). The life cycle is re-initiated when ova excreted by the infected human host re-enter the habitat of the fresh water snails. With ambient temperature, water purity and sunlight, the ova (excreted by the human host) hatch and release miracidia<sup>9</sup> into the water (Kassim and Gibertson, 1976). The miracidia infect the respective snail hosts then reproduce asexually and developing within the vector, and once developed the cercariae leaves the snail, re-entering the water source and reinitiating the transmission cycle (Gryseels *et al.*, 2006; CDC, 2019b).

---

<sup>7</sup> A free-swimming larval stage of *Schistosoma* which passes between hosts.

<sup>8</sup> The stage of the life cycle immediately after penetration of the hosts skin, marked by the loss of the larval tail and undergoing physiologic modifications allowing it to survive within the mammalian host.

<sup>9</sup> A free-swimming ciliated larval stage which passes from the egg to the snail host.



[Image removed due to copyright restrictions]

The QR code below links to the image source.

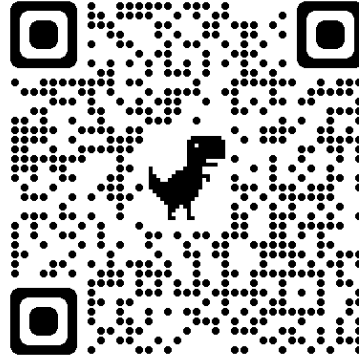


Figure 1-2: The schistosome life cycle. Figure obtained from the CDC website, <https://www.cdc.gov/parasites/schistosomiasis/biology.html>. ① The eggs excreted by an individual with a schistosome infection enter the water source (snail habitat). ②-③ The ova hatch, releasing miracidia into the water, which locate and infect respective snails host. ④-⑥ The sporocysts reproduce asexually within the snail and develop into free-swimming cercariae, which are released from the snail into the water, where they can penetrate the skin of the human host, initiating the human cycle of the disease. ⑦-⑨ The cercariae lose their tail during penetration of the human skin, becoming a schistosomulae, and migrate in the blood to the liver, where they mature into adult worms. ⑩ The mature worms pair in the portal vein in the liver and migrate towards the mesenteric venules of the intestine (*S. mansoni* and *S. japonicum*) or venous plexus of the bladder (*S. haematobium*). The worms reproduce sexually and lay eggs, which migrate into the intestine or bladder and shed in the stool/urine.

### 1.2.2 Clinical manifestations

Schistosome infections present symptoms which are consistent with many other diseases and intestinal/urogenital parasitic infection (Gray *et al.*, 2011). The common symptoms for intestinal and urogenital schistosomiasis are as follows.

### **1.2.2.1 Intestinal schistosomiasis**

Symptoms that present as a result of an *S. mansoni* infection occur due to the human hosts' immune response to the *S. mansoni* ova trapped in the intestinal walls (Gryseels *et al.*, 2006). Mild symptoms of intestinal schistosomiasis can result in abdominal pain, diarrhoea and the presence of blood in stool. More severe cases of the disease (chronic bilharzia), are associated with chronic local inflammatory response to the schistosome eggs trapped in the hosts tissue, resulting in intestinal disease or liver fibrosis - accumulation of fluid and hypertension of the abdominal blood vessels lead to a distinctive enlarged abdomen (Gray *et al.*, 2011). Chronic schistosomiasis can cause delayed growth, anaemia and malnutrition, therefore is particularly detrimental to children. In rare and chronic cases, eggs which migrate to the brain or spinal cord can cause speech disturbances, seizures and paralysis (CDC, 2019b).

### **1.2.2.2 Urogenital schistosomiasis**

Similarly to intestinal schistosomiasis, in cases of urogenital schistosomiasis, the host displays symptoms in response to *S. haematobium* ova trapped in the bladder tissue. The trapped ova may lead to inflammatory or obstructive disease in the urinary tract (Gray *et al.*, 2011). A classic symptom of a *S. haematobium* infection is haematuria (World Health Organization, 2020c). In advanced cases, damage to the kidney and fibrosis of the bladder and ureter can occur (Gray *et al.*, 2011). Other long term consequences associated with *S. haematobium* infection are infertility and bladder cancer (Gryseels *et al.*, 2006; World Health Organization, 2020c). Although mortality rates remain low, the long term consequences of the disease are high (Gryseels *et al.*, 2006).

## **1.2.3 Prevention**

WHO NTD road map to attain sustainable development goals, highlights the push towards the elimination of schistosomiasis by 2030 (World Health Organization, 2020a). Urbanisation, waste control efforts and destruction of snail habitat have influenced a decrease in schistosome infections (Rollinson *et al.*, 2013; Tchuem Tchuente *et al.*, 2017). The Vector Control Division (VCD) use education programs to discourage communities from both drinking and coming in contact with schistosome infected water, and dissuade practicing of open urination and defecation. However, in poorer and rural areas, behavioural changes can be hindered where clean water supplies are limited; toilet infrastructure is

sparse; and a communities livelihood relies heavily on high risk activities such as fishing and farming (Rollinson *et al.*, 2013; Adriko *et al.*, 2018).

Throughout high-risk populations in sub-Saharan Africa, the drug Praziquantel is administered annually for the prevention of long term chronic schistosomiasis (Mutapi *et al.*, 2017; Adriko *et al.*, 2018; Ajibola *et al.*, 2018). However, treatment is still required for those who become infected between successive treatment programs. Due to the unspecific symptoms resulting from both schistosome and *plasmodium* infections, it is crucial that sensitive and specific in-field diagnostics are available to inform appropriate treatment.

### **1.3 Treatment**

For both malaria and schistosomiasis, successful treatment of the respective diseases can prevent disability and the loss of human life. Additionally, treatment interrupts the parasite life cycle and as a result can interrupt disease transmission within communities (Tchuem Tchuente *et al.*, 2017). Prevention methods are successful in decreasing the risk of infection, however, treatment of the diseases is fundamental in reducing long-term health consequences and mortality once an individual has been infected (Rollinson *et al.*, 2013).

#### **1.3.1 Malaria**

Standard treatment protocol for non-complicated *P. falciparum* malaria consists of artemisinin-based combination therapies (ACTs) (World Health Organization, 2015). There are a large array of different ACTs, each is a combination of two or more drugs that work against the *plasmodium* parasite (CDC, 2019c). The aim of ACTs is to cure both blood and liver-stage infections, preventing relapse of infection (World Health Organization, 2015). Malaria caused by other *plasmodium* parasites can be treated by ACTs or Chloroquine (World Health Organization, 2015). Although, high-level resistance of *P. vivax* to Chloroquine has hindered its use for treatment in South-East Asia (World Health Organization, 2015; CDC, 2019c).

#### **1.3.2 Schistosomiasis**

The current approach for the control of schistosomiasis, is based on preventative chemotherapy with Praziquantel (Bergquist *et al.*, 2017). Praziquantel is currently the only drug available to treat schistosomiasis (Lamberton *et al.*, 2010; Cioli *et al.*, 2014). The efficacy, cost and ease of distribution of Praziquantel, facilitates its distribution through mass

drug administration programs. However, due to the lack of efficacy against the parasite in immature stages, it does not eliminate recurring infections (Cioli *et al.*, 2014).

### **1.3.3 Mass drug administration**

Mass drug administration (MDA), for tackling malaria in endemic settings has been used extensively over the past 80 years (World Health Organization, 2015). MDA for bilharzia is in comparatively earlier stages. Uganda was the first country in sub-Saharan Africa to implement a bilharzia MDA program in 2002 (Adriko *et al.*, 2018). The objective of MDA is to provide therapeutics to a large proportion of an endemic population, to cure any asymptomatic individuals and prevent re-infection during the post-treatment prophylaxis (White, 2008).

MDA results in a sharp term decline in prevalence and incidence of the target disease in the recipient communities. If disease transmission is not interrupted following termination of MDA programs, the original prevalence levels within communities will eventually return (Gray *et al.*, 2011; World Health Organization, 2015). Methods to interrupt transmission of malaria by reducing mosquito bite rates were mentioned in Section 1.1.3. Similarly, the methods to prevent the transmission of schistosomiasis and the complications associated with implementing change in endemic communities were discussed in Section 1.2.3.

In addition to reducing bite and infection incidence, in order to maintain low prevalence rates within the communities, continued Praziquantel and antimalarial treatment must be available to individuals who present with schistosomiasis and malaria following MDA (World Health Organization, 2015). Due to growing fears of drug resistant strains of parasites (White, 2008), it is recommended to obtain a malaria diagnosis prior to prescribing treatment, and in endemic areas, to move away from the common practice of primarily treating all febrile cases as malaria (Boyce and O'meara, 2017). There is currently a single drug available for treatment of schistosomiasis – Praziquantel. Any emergences of resistance to Praziquantel would be detrimental to control efforts (Lamberton *et al.*, 2015), which again, highlights the importance of the ability to identify and treat the infected individuals. This is where access to an appropriate diagnostic for surveillance, early diagnosis and case management of the respective diseases are vital (McMorrow *et al.*, 2011). The diagnostic procedures must be sufficient to detect asymptomatic individuals and those with low-level infections (Rollinson *et al.*, 2013).

## **1.4 Diagnosis**

The two prevalent methods for the diagnosis of malaria and schistosomiasis are microscopy and immunological tests (Moody, 2002; Ajibola *et al.*, 2018). Although stains and microscopes have improved, standard microscopy methods have not changed dramatically in more than a century (Caliendo *et al.*, 2013). Although, developments in diagnostic techniques and technologies in the last 20 years have propelled the expansion of new diagnostic tests.

### **1.4.1 The diagnostic gold standard**

The gold standard for diagnostics is defined as '*the test that is best under reasonable conditions*' (Versi, 1992). A hypothetical ideal gold standard can identify all individuals with a disease, as disease positive, and does not falsely identify healthy individuals as disease positive. The following terms are fundamental to understanding the utility of diagnostic tests:

1. True-positive: the patient has the disease and tests positive
2. False-positive: the patient does not have the disease but the test is positive
3. True-negative: the patient does not have the disease and the test is negative
4. False-negative: the patient has the disease and the test is negative.

A hypothetical ideal gold standard test does not have any false-negative or false-positive results, however, in reality the gold standard will be the best performing test available under reasonable conditions (Caliendo *et al.*, 2013). Gold standards are constantly challenged and superseded when appropriate (Versi, 1992). In order to replace the current gold standard test, the new method must be widely accepted; accessible; and improve diagnostic capabilities - for instance, by reducing the proportion of false-negative tests and therefore providing more successful patient management (Pendley and Lindner, 2017). The methods used to analyse the performance of a diagnostic test will be described in the following section.

### **1.4.2 Sensitivity and specificity**

Sensitivity and specificity are statistical measures widely used in medicine, and applied to analyse the performance of diagnostic tests (Lalkhen and McCluskey, 2008). The clinical sensitivity of a test, measures the percentage of positive tests which result from individuals who are disease positive (Pendley and Lindner, 2017), thus describing the proportion of true-positive results identified by a test.

$$\text{Clinical Sensitivity} = \frac{\text{True Positives}}{\text{True Positives} + \text{False Negatives}}$$

On the other hand, the clinical specificity describes the ability of a test to correctly identify disease negative individuals, this is achieved by calculating the proportion of true-negative results identified by a test (Lalkhen and McCluskey, 2008).

$$\text{Clinical Specificity} = \frac{\text{True Negatives}}{\text{True Negatives} + \text{False Positives}}$$

Ideally a test will have both high clinical sensitivity and specificity, but there is a trade-off between the two. The clinical sensitivity is dependent on the tests limit of detection (the analytical sensitivity<sup>10</sup>), which corresponds to the lowest concentration of disease load detectable (Pendley and Lindner, 2017). Tests with high analytical sensitivity increase the likelihood of false-positive results, resulting in lower clinical specificity (Lalkhen and McCluskey, 2008). Similarly, tests with high analytical specificity<sup>11</sup> (reducing instances of cross-reactivity), may result in lower clinical sensitivity. The clinical test performance can also be impacted by many other factors that are independent of the test design, including the disease prevalence (Bujang and Adnan, 2016).

The intended application and environment of use is important when determining the requirements of clinical sensitivity and specificity of a test (Caliendo *et al.*, 2013). For example, newer tests which may require expensive equipment and consumables may not be appropriate to diagnose prevalent diseases in low-resource environments. In lieu of the perfect test, a good alternative is to subject patients who are initially positive to a test with high sensitivity/low specificity, to a second test with low sensitivity/high specificity. In this way, nearly all of the false positives may be correctly identified as disease negative (Lalkhen and McCluskey, 2008). However, in rural and remote clinics in LMICs individuals may need to travel for many hours to seek care, as a result, health practitioners may feel they need to provide treatment due to lack of an alternate diagnosis (Altaras *et al.*, 2016).

---

<sup>10</sup> Analytical sensitivity – also known as limit of detection, the lowest concentration of analyte that the test can detect.

<sup>11</sup> Analytical specificity - or cross-reactivity – describes whether the test will detect other diseases that are not the target disease, which can lead to false positive results.

### 1.4.3 Microscopy

Globally, microscopy remains the gold standard diagnostic for many parasitic diseases (Rougemont *et al.*, 2004); this is true for both malaria and schistosomiasis (Doenhoff *et al.*, 2004; Bell *et al.*, 2006; Tangpukdee *et al.*, 2009; Gray *et al.*, 2011). The microscopy methods rely on the direct observation and detection of the parasites or parasite ovum within patient specimens (Wongsrichanalai *et al.*, 2007; Weerakoon *et al.*, 2015). The specific methods for diagnosing malaria and schistosomiasis microscopically will be further discussed here.

#### 1.4.3.1 Malaria gold standard: blood smear

The gold standard diagnosis for malaria is a blood smear (Rougemont *et al.*, 2004). Microscopy remains the only U.S. Food and Drug Administration (FDA)-approved endpoint for assessing the outcomes of drug and vaccine trials, and for serving as a reference standard in the evaluation of new tools for malaria diagnosis (Wongsrichanalai *et al.*, 2007). The technique - which was developed in 1904 - has been unchanged for over 100 years (Moody, 2002; Fleischer, 2004). In suspected malaria cases, venous blood is drawn or taken from a finger prick, then blood smears are prepared (see Figure 1-3(a)) and examined microscopically for the presence of *plasmodium* parasites as shown in Figure 1-3(b) (Cnops *et al.*, 2011).

Globally, blood smears are conducted in hospitals and laboratories to diagnose cases of malaria (UCLHS NHS, 2020). Where equipment and experienced technicians are available, the technique is able to produce a quantitative diagnosis, by providing an estimate for the quantity of parasites per  $\mu\text{L}$  of blood (World Health Organization, 2010). The limit of detection for microscopic observation of *plasmodium* parasites is reported as 50 parasites/ $\mu\text{L}$  when conducted by an experienced examiner (Moody, 2002). Theoretically the technique is 100% specific, as observing *plasmodium* parasites in a blood smear confirms presence of malaria. In many malaria-endemic regions, microscopic diagnosis has limitations, including a shortage of skilled microscopists, inadequate quality control, and the possibility of misdiagnosis due to low parasitemia or mixed infections, all of which effect the sensitivity of the technique, and may result in a high proportion of false-negative results (Berzosa *et al.*, 2018). By comparison with newer techniques (qPCR, discussed in later sections), the sensitivity and specificity of microscopic diagnosis of malaria has been calculated as 57% and 99% respectively (Mfuh *et al.*, 2019).

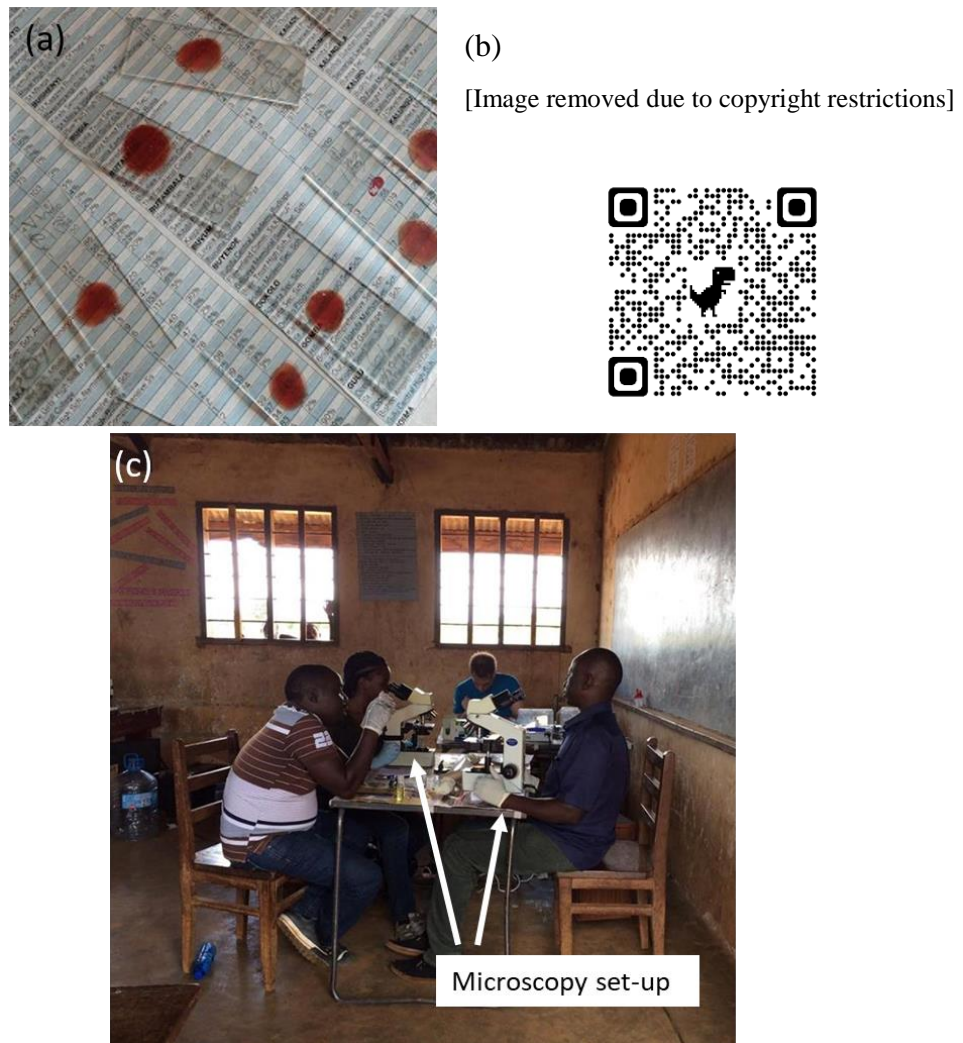


*Figure 1-3: Blood smear Images. (a) Preparation of blood smears on microscopy slides in-the-field. (b) Blood smear from a patient with malaria; microscopic examination shows Plasmodium falciparum parasites (located by the arrows) infecting some of the patient's red blood cells (CDC photo). (c) Malaria gold standard, microscopy. MoH VCD technicians conducting microscopic examination for plasmodium parasites on site in-the-field.*

In Uganda microscopy examinations are usually limited to tier III health facilities<sup>12</sup> (Kirunga Tashobya et al., 2006), however, the Ugandan MoH VCD frequently conduct district surveys using microscopic diagnosis for their national prevalence and treatment records. In such scenarios, the trained technicians travel to test sites throughout Uganda with their equipment to conduct microscopic examinations in settings where they would not usually be available, as shown in Figure 1-3(c) (Kabaterine *et al.*, 2011).

<sup>12</sup> Uganda's healthcare system is divided into national and district-based levels. The district –based health system is divided into tiers. The lowest being tier I, which consists of village health teams (VHTs) -community health workers who deliver health education, preventative and simple curative services. Tier II is an out-patient health centre run by a nurse. Tier III is a health centre which includes the services provided at tier II, and in addition, provides in-patient, simple diagnostic and maternal health services. Tier IV includes services provided at tier III, and additional blood transfusion services and emergency obstetric care (World Health Organization, 2017; Nampala, 2018).



#### 1.4.3.2 *S. mansoni* gold standard: Kato-Katz method

Microscopy for parasitological examination is included in the WHO Essential In Vitro Diagnostics list (World Health Organization, 2018a). The gold standard for diagnosing bilharzia is the Kato-Katz (KK) method. The KK technique, developed in 1972, relies on microscopic examination of *S. mansoni* ova within a small stool specimen (approximately 41.7 mg) (Doenhoff et al., 2004; Genchi *et al.*, 2019). Images of *S. mansoni* eggs as seen during microscopic examination are shown in Figure 1-4 and described in more detail in the Appendices, Section 7.7.3. During regional parasitological surveys, trained MoH VCD healthcare workers routinely conduct KK examinations for diagnosis of helminth infections (Kabatereine *et al.*, 2011). In Uganda, the health sector structure limits microscopic diagnosis to sub-county health facilities, where laboratory services are available (Kirunga Tashobya et al., 2006).

As the gold standard, analysis of the sensitivity and specificity of KK is not widely assessed. Theoretically, the technique is 100% specific as the identification of *S. mansoni* eggs results in a true positive. However, some studies have reported lower specificities of 83.2 and 91.1% (Shane *et al.*, 2011; Foo *et al.*, 2015). Standard protocol entails conducting a double KK examination, where two slides prepared from the stool specimen are examined. Repeat reading increase sensitivity of the technique, however, also increases the cost of examination (Lamberton *et al.*, 2014).

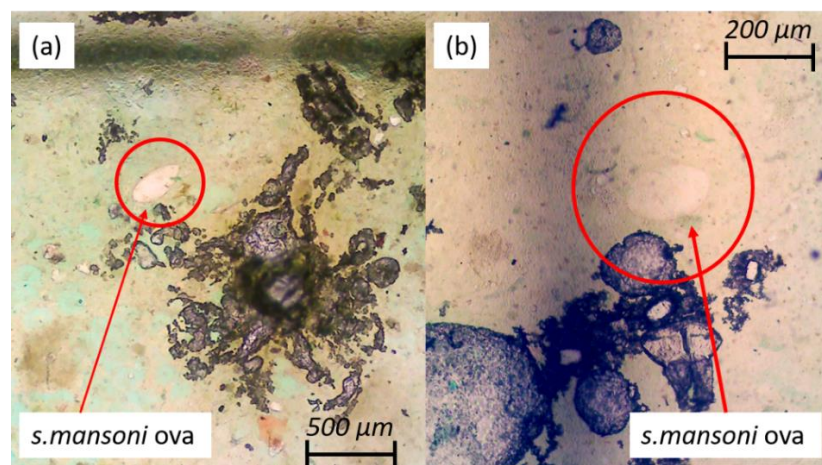


Figure 1-4: Images of *S. mansoni* ova as seen through microscope during KK examination. The malachite green stain causes *S. mansoni* ova to appear with a pink hue, enabling eggs to be distinguished from the slide and stool debris. (a) *S. mansoni* ova observed at 4X magnification. (b) *S. mansoni* ova observed at 10X magnification. Images of KK slides provided by Oliver Higgins.

#### 1.4.4 Immunological diagnosis

Alternative methods to microscopy have come available in the past 50 years (Wongsrichanalai *et al.*, 2007). Immunological tests for infectious disease include tests which detect antigens<sup>13</sup> produced by a pathogen, or antibodies<sup>14</sup> released by the host in response to an infection (Caliendo *et al.*, 2013). Examples of immunological diagnostics for malaria and *S. mansoni*, include tests that detect circulating parasite antigens or anti-schistosomal and *plasmodium* antibodies in plasma, serum or urine (Spencer *et al.*, 1979; Nausch *et al.*, 2014; Kato-Hayashi *et al.*, 2015).

##### 1.4.4.1 Antibody tests

Antibody levels are not related to the intensity of infection and cannot be used to differentiate between past and active infections (van Lieshout *et al.*, 1997). As a result, antibody detection has lower diagnostic value in endemic settings (Utzinger *et al.*, 2015), but remains a useful technique for laboratories in countries typically without transmission of malaria or schistosomiasis (NHS Greater Glasgow and Clyde, 2019; UCLHS NHS, 2020). For this reason, immunological diagnosis in endemic regions focuses on antigen detection tests.

##### 1.4.4.2 Antigen tests

Antigens produced by parasites are secreted into the human hosts' bloodstream during active infection, as a result, this can be used to inform a diagnosis in disease prevalent areas (Weerakoon *et al.*, 2015). There are a large array of antigens that can be detected to confirm the presence of malaria and schistosome infections respectively (Wongsrichanalai *et al.*, 2007; Corstjens *et al.*, 2014). The levels of antigens expressed in human specimens determine the feasibility for their detection to aid diagnosis (Moody, 2002). For malaria, the most prominent antigens used to aid immunological diagnosis are the histidine-rich protein II (HRP-II) and parasite lactate dehydrogenase (pLDH). HRP-II and pLDH are produced by plasmodium trophozoite and gametocyte stages respectively, and both are abundant in peripheral blood specimens (Moody, 2002). The pLDH antigen can be used to distinguish *falciparum* and *non-falciparum plasmodium* infections, however, as a result of higher levels

---

<sup>13</sup> A toxin or other foreign substance which induces an immune response in the body, especially the production of antibodies.

<sup>14</sup> A blood protein produced in response to and counteracting a specific antigen. Antibodies combine chemically with substances which the body recognizes as alien, such as bacteria, viruses, and foreign substances in the blood.

of HRP-II produced by *P.falciparum*, the presence of HRP-II is commonly used to diagnose *P.falciparum* infections (Sulzer and Wilson, 1969; Spencer *et al.*, 1979; CDC, 2016).

Examples of the antigens targeted for the detection of schistosome infections include the soluble egg antigen (SEA), circulating anodic antigen (CAA) and circulating cathodic antigen (CCA)<sup>15</sup> (Weerakoon *et al.*, 2015). Quantification of the schistosome adult worm antigens CAA and CCA in serum and urine has been reported as an alternative diagnosis of active schistosomiasis since the late 1980's (van Lieshout *et al.*, 1997). Unlike malaria, detection of these schistosome antigens cannot provide a species specific diagnosis (van Lieshout *et al.*, 1997). However, due to low levels of CCA present as a result of *S. haematobium* infections, the detection of CCA to determine *S. haematobium* infections is not advised (Stothard *et al.*, 2006).

Antigen detection is possible due to parasite secretions, alternatively, pathogen DNA can be detected to determine presence of infection (Wooden *et al.*, 1993; Pontes *et al.*, 2002). The *plasmodium* and *S. mansoni* parasites reside within the human host, as a result, detection of parasite DNA has been achieved from a range of human specimen (Mharakurwa *et al.*, 2006; Wichmann *et al.*, 2009; Johannes Enk *et al.*, 2012; Sandeu *et al.*, 2012).

---

<sup>15</sup> These glycoproteins are produced in the gut of schistosome worms (genus specific) and secreted into the host bloodstream during active schistosome infection (Weerakoon *et al.*, 2015)

## 1.5 Molecular diagnosis

Molecular diagnosis refers to the process of identifying a disease by studying molecules, such as proteins and nucleic acids (DNA or RNA), in a tissue or fluid specimen (<https://www.cancer.gov/publications/dictionaries/cancer-terms/def/molecular-diagnosis>).

Developments in molecular biology technologies have generated new diagnostic strategies, the most notable is the polymerase chain reaction (PCR) – discovered in 1985 (Saiki *et al.*, 1985; Mullis and Faloona, 1987). PCR is a method to rapidly generate copies of a specific DNA sequence (Patrinos *et al.*, 2017). PCR-based techniques are a recent development for the diagnosis of malaria, and have proven to be one of the most specific and sensitive diagnostic methods, particularly in cases with low parasitemia or mixed infection (Morassin *et al.*, 2002).

### 1.5.1 Introduction to PCR

PCR has proved an extremely useful diagnostic tool in clinical laboratories (Public Health England, 2018) – highlighted throughout the COVID-19 pandemic (Tang *et al.*, 2020; Zhai *et al.*, 2020). PCR is more sensitive than the previously described diagnostic methods (Mfuh *et al.*, 2019). Exponential amplification of small amounts of specific DNA sequences, enables detection and diagnosis of diseases from relatively small sample volumes (Public Health England, 2018). Prior to PCR, sample preparation includes DNA extraction and purification from the clinical specimen, this concentrates the target DNA, and removes inhibitory substances present in clinical samples (such as whole blood), to improve amplification outcomes (Becker *et al.*, 2004). Extraction of DNA from the test specimen (further discussed in Section 2.1.1), involves lysis of the specimen to isolate and purify sample DNA. The purity of recovered DNA impacts the outcome of a PCR, often the extraction process is lengthy (> 30 minutes per sample if completed manually), and therefore sample preparation is often a limiting factor in PCR diagnostics (Becker *et al.*, 2004).

The two main reagents of PCR are the oligonucleotides (oligo), otherwise known as primers, and the DNA polymerase. The target DNA sequence is determined by the choice of PCR primers. The primers - short, single-stranded DNA sequences; are complementary to the target DNA region. The DNA polymerase is an enzyme which synthesizes DNA molecules, facilitating amplification of the target DNA sequence by creating two identical DNA strands from a single original template (Carter and Shieh, 2010). PCR amplification is achieved by a process of thermal cycling. The cycling process usually proceeds a defined denaturation step at 95°C in order to break hydrogen bonds between double-stranded DNA (dsDNA) and

form single-strands of DNA (ssDNA). A typical PCR cycle includes three steps (see Figure 1-5): denaturation at 95°C; annealing (around 60°C), to allow primers to recombine to the ssDNA; and extension (or elongation), enabling formation of the new replicate dsDNA sequence (Biassoni and Raso, 2020). The cycle is repeated resulting in exponential amplification of the target DNA sequence, a schematic of the PCR process is shown in Figure 1-5.

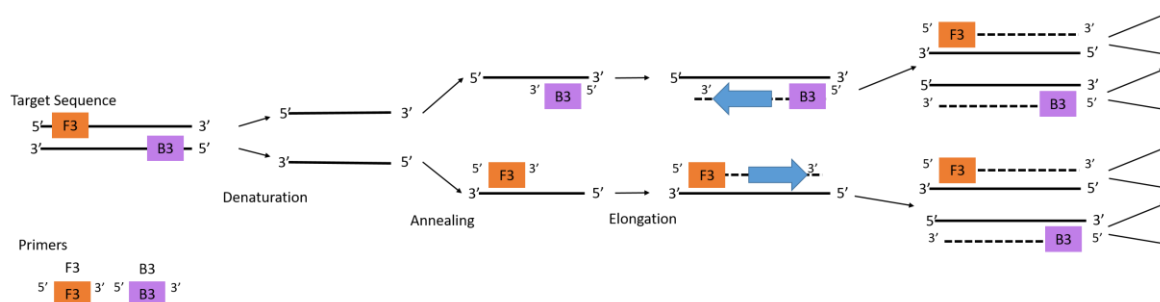


*Figure 1-5: The PCR process. PCR amplification is achieved by a process of thermal cycling. The denaturation step (at 95°C) is required to break the hydrogen bonds, and separate the target sequence into single strands of DNA. Then the temperature is lowered to enable annealing of the primers to their complimentary regions of single stranded DNA. And to allow synthesis of the complimentary sequence during the elongation step. This process is repeated, resulting in exponential amplification of the target DNA sequence.*

### **1.5.1.1 Monitoring PCR amplification**

Real-time PCR (qPCR) is a technique which allows amplification progression to be monitored by observing changes in fluorescent signal (Spiess et al., 2008). An advantage of qPCR is that the intensity of infection can be assessed from the amplification data, resulting in a quantitative diagnostic technique which can better inform treatment needs. Two popular methods of monitoring qPCR amplification are by use of SYBR™ Green dye and TaqMan reagents (Applied Biosystems, 2010).

#### **1.5.1.1.1 SYBR™ Green detection**

SYBR™ Green dye is a dsDNA binding dye, which exhibits fluorescence during illumination when bound to dsDNA (Biassoni and Raso, 2020). As the qPCR cycles progress, DNA amplification results in an exponential increase in fluorescent signal, which is detected by the light sensor of the qPCR machine (Biassoni and Raso, 2020). SYBR™ Green dye is economical, however, as the dye binds non-specifically to all double-stranded DNA sequences, additional tests must be conducted to verify qPCR amplification data (Applied Biosystems, 2010). Melt curve or gel analysis -which will be discussed in Section 2.1.3.1.2

& 2.1.4, should be conducted following qPCR amplification to rule out non-specific product formation.

#### **1.5.1.1.2 *TaqMan reagents***

Similarly to a primer, TaqMan probes are designed to hybridize to a short sequence within the target DNA sequence (Heid *et al.*, 1996). The 5' end of the probe is tagged with a fluorescent dye, for example, Fluorescein amidites (FAM) whilst the 3' end is tagged with a fluorescence quencher molecule, Carboxytetramethylrhodamine (TAMRA) is commonly used (Heid *et al.*, 1996; Biassoni and Raso, 2020). Whilst the fluorophore and quencher are in close proximity and excited by the qPCR machine light source, fluorescence from the fluorophore is not observed as a result of quenching by the quencher molecule (Heid *et al.*, 1996; Carter and Shieh, 2010). During the annealing phase of the qPCR cycle, the TaqMan probe anneals to the target ssDNA region (Heid *et al.*, 1996; Carter and Shieh, 2010). In the extension phase, the *Taq* polymerase (within the master mix) extends the primer, synthesizing the DNA sequence towards the probe (Heid *et al.*, 1996; Biassoni and Raso, 2020). 5' prime nuclease activity of the *Taq* polymerase degrades the TaqMan probe and as a result cleaves the fluorophore from the quencher molecule (Heid *et al.*, 1996; Carter and Shieh, 2010). Once released from the quencher, the fluorescence emitted from the fluorophore can be detected by the light sensor. This results in an observed increase in fluorescent signal which is specific to amplification of the desired target DNA sequence (Heid *et al.*, 1996; Carter and Shieh, 2010).

In many reference laboratories, PCR-based amplification remains the gold standard nucleic acid amplification test (NAAT), although the requirement for efficient thermal cycling and trained staff hinders application in low resource environments (Alemayehu *et al.*, 2013). A major limitation of PCR and qPCR is the requirement for thermal cycling which relies on expensive (and often large) machines to efficiently heat samples. Isothermal amplification methods have more recently emerged as an alternative NAAT to PCR (Hopkins *et al.*, 2013; Najafabadi *et al.*, 2014; Tanner and Evans, 2014). Elimination of thermal cycling from the NAAT method has enabled NAAT-based diagnosis to be conducted closer to patients (at the point-of-care) and in rural communities, by reducing reliance on expensive thermal cycling equipment (Sandeu *et al.*, 2012; Hopkins *et al.*, 2013). For development of tests in Sub-Saharan Africa, the test amplification conditions should be higher than standard room temperature, consequently leading the focus to loop-mediated amplification – which is conducted around 65°C.

## **1.5.2 Introduction to loop-mediated amplification**

Loop-mediated isothermal amplification (LAMP) is an isothermal amplification technique. Amplification at a single temperature diminishes the necessity for expensive thermocycling equipment and results in cheaper and faster DNA amplification (World Health Organization, 2016); making the technique desirable for point-of-care applications (Hopkins *et al.*, 2013). Unlike PCR, LAMP requires up to 6 primers to conduct amplification; 4 core and 2 loop primers (Tanner and Evans, 2014). Progression of amplification can be monitored in real time by use of dsDNA binding dyes, such as SYBR™ Green and target specific probes (Li *et al.*, 2016). As with qPCR, successful LAMP reactions can be confirmed by visual inspection of change in fluorescence, changes in colour or gel electrophoresis (Salant *et al.*, 2012; Gadkar *et al.*, 2018). Additionally, incorporation of 5'-end labelled primers enables outcomes of amplification to be determined on lateral flow devices (Zhang *et al.*, 2019), further discussed in Section 1.7.3 and 2.2.3.

### **1.5.2.1 LAMP primers**

The design of LAMP primers is based on six distinct regions of the target sequence, F3, F2, F1, B1, B2 and B3 (these are displayed in Figure 1-6). Similar to PCR, LAMP has a forward and reverse primer set (F3 & B3) designated at opposing and complimentary ends of the target sequence. The additional primers (not necessary for PCR) are the two core primers; the Forward Inner Primer (FIP) and the Backward Inner Primer (BIP); and the Forward and Backward Loop Primer, LPF and LPR respectively (PrimerExplorer, 2019). The FIP consists of the F2 sequence (at its 3' end) that is complementary to the F2c region, and the same sequence as F1c region at its 5' end. Similarly, the BIP consists of the B2 sequence (at its 3' end) that is complementary to the B2c region, and the same sequence as the B1c region at its 5' end. The Loop primers are designed using the complementary strand corresponding to the sequence between F1 and F2, and B1 and B2 for LPF and LPR respectively (PrimerExplorer, 2019).

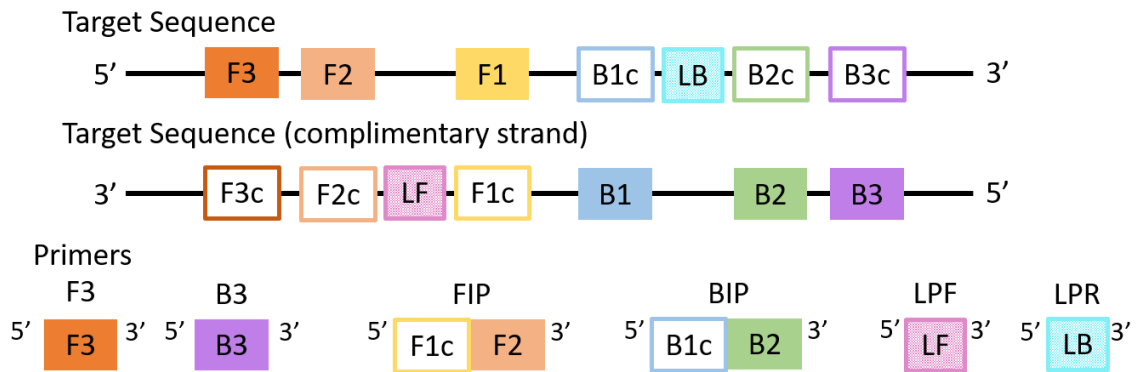


*Figure 1-6: LAMP primer design. The design of LAMP primers is based on six regions of the target sequence; F3, F2, F1, B1, B2, and B3. LAMP requires four core primers (F3, B3, FIP and BIP), and two optional additional Loop primers (LPF and LPR). F3 and B3 are designed at opposing ends of the target sequence. The FIP and BIP primer design spans the target sequence and complimentary strand. The additional Loop primers (LPRF and LPR, which are included in this study) are designed using the complimentary strand corresponding the region between F1 and F2, and B1 and B2 respectively.*

There are five key factors in LAMP primer design; primer melt temperature ( $T_m$ ); the stability at the end of each primer, which corresponds to the change in free energy associated with each primer; the GC content, which should be 40% to 65%; avoiding secondary structures by ensuring primers are not designed in complimentary sequences; and the distance between primers, all of which pose limitations on the target sequence length (PrimerExplorer, 2019). Detailed guidance on primer design is available in the PrimerExplorer guide to LAMP primer design, the number of factors and primers required in LAMP assay design result in a very complicated design process, as a result the online programs, such as the PrimerExplorer software (PrimerExplorer V4/V5, <http://primerexplorer.jp/elamp4.0.0/index.html>) are commonly used for LAMP primer design. LAMP primer design is a very complicated procedure, as a result, this study will focus on the development of published assays to translate into use on the POC LAMP test.



### ***1.5.2.2 Principles of LAMP***

LAMP is achieved using the LAMP primers (described above) and GspSSD or Bst LAMP DNA polymerase (Tanner and Evans, 2014). Unlike PCR DNA polymerase (which requires thermal cycling for DNA strand-displacement), the LAMP DNA polymerase consists of an enzyme that has both heat-resistant properties and a strand-displacement type DNA polymerase activity, this enables synthesis of a new DNA strand whilst dissociating the hydrogen bond of the double stranded template (Li *et al.*, 2017). LAMP is a much more complicated mechanism than PCR, the LAMP amplification process is split into two principle phases and is displayed in Figure 1-7. In the initial phase, the F2 of the FIP hybridises to F2c of the target DNA strand, this guides the synthesis of the complementary DNA strand. The F3 primer anneals to the F3c region of the DNA template (outside of the FIP). The strand-displacement activity of the LAMP DNA polymerase releases the FIP hybridised complimentary strand, allowing double stranded DNA to be synthesized from the F3 primer and template DNA strand. The displaced FIP synthesized strand contains both the F1 and complementary F1c sequence, this forms a self-hybridising loop structure at the 5' end of the strand. This loop strand also acts as the template strand for the corresponding BIP and B3 primers, which carry out a similar process to the corresponding FIP and F3 primers, this results in a dissociated strand which has looped 5' and 3' ends (resembling a dumbbell structure), which acts as the template for cycle amplification in phase two of the LAMP mechanism.

The LAMP dumbbell structure contains multiple sites for primer binding (see the illustration in Figure 1-7); the sequence ends, which are F3 and B3 binding sites; and the loop structures, which are annealing sites for the FIP, BIP and Loop primers. The rapid synthesis of double stranded DNA leads to an abundance of LAMP dumbbell structured DNA, resulting in exponential amplification.

[Image removed due to copyright restrictions]

The QR code below links to the image source.

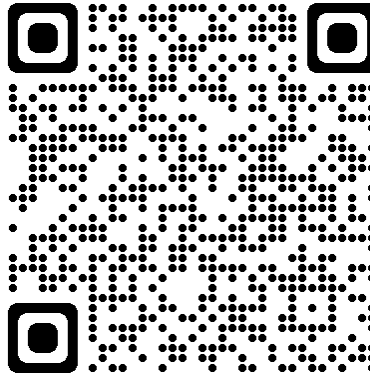


*Figure 1-7: LAMP schematic illustration – source NEB (<https://www.neb-online.de/en/pcr-and-dna-amplification/isothermal-amplification/>). Amplification initiates from strand invasion from one of the inner primers (FIP or BIP) and synthesizes the complimentary strand. The strand-displacement activity of the LAMP DNA polymerase displaces the Internal Primer complimentary strand, which in turn acts as a template for the alternate Internal Primer. Both the synthesized Internal Primer strands consist of F1, B1 and their complimentary sequences (F1c and B1c, respectively), which form self-hybridising loops and result in the signature LAMP dumbbell structure. The LAMP dumbbell structure, contains multiple primer binding sites, and as a result, acts as the template for cyclic amplification.*

### 1.5.3 Molecular diagnosis of malaria and schistosomiasis

Both PCR and LAMP methods have been previously explored to diagnose malaria and *S. mansoni* infections (Hopkins *et al.*, 2013; Fernández-Soto *et al.*, 2014; Cook *et al.*, 2015). The ability to amplify specific DNA regions enables species specific diagnosis, which can be essential for targeting treatment effectively (Rougemont *et al.*, 2004). Amplification of schistosome DNA has been achieved from a range of specimen (Lodh *et al.*, 2013; Fernández-Soto *et al.*, 2014; Song *et al.*, 2015), suggesting developments to current specimen and sample processing methods can be pursued. PCR has enabled diagnosis of malaria with low-parasitemia, demonstrating improved sensitivity against current diagnostic methods (Rougemont *et al.*, 2004; Sandeu *et al.*, 2012; Mfuh *et al.*, 2019). Developments in NAAT such as LAMP kits, have brought molecular diagnosis closer to clinics and field-based laboratories (Hopkins *et al.*, 2013; Magro *et al.*, 2017a). Although, the NAAT kits described by Hopkins and Magro do not appear fit for use in low-resource settings, due to the requirement for an abundance of laboratory equipment and consumables. Point-of-care tests with lower reliance on laboratory equipment are favoured when working in low-resource and rural environments (Pai *et al.*, 2012). LAMP does not require thermal cycling, and as a result can be carried out using cheaper, simpler and smaller heating equipment, which is more appropriate for use in low-resource environments (Sharma *et al.*, 2015). Access to trialled and published LAMP assays to detect *plasmodium* and *S. mansoni* DNA can facilitate the transfer of the molecular tests onto point-of-care platforms. Prior to this study, there was little evidence to suggest that point-of-care NAATs had been carried out in rural and remote communities. Further developments in LAMP diagnostic cassettes or cartridges able to provide a more sensitive diagnosis at the site of patient care could be critical to elimination programs, not only for malaria and schistosomiasis, but for other infectious diseases given that NAATs can detect low levels of asymptomatic infections which may act as reservoirs for future disease emergence (Reboud *et al.*, 2018).

## 1.6 Point of care testing

Point-of-care (POC) diagnostics is a broad term which applies to a diagnostic device or test utilized at or near the site of patient care (Drain *et al.*, 2014). These tests offer rapid results, allowing for timely initiation of appropriate therapy, and/or facilitation of linkages to care and referral. Most importantly, POC tests can be simple enough to be used at the primary care level and in remote settings with no laboratory infrastructure (Pai *et al.*, 2012). The need to make healthcare more patient centred is a global trend based on the premise that healthcare should be more centred on the patient than the provider (St John and Price, 2014). This term includes an array of technologies, a few examples are, a portable ultra-sound, which can be taken to the bedside of a hospitalised patient (GE Healthcare, 2019); glucose monitoring systems, which can be used both clinically or by a patient / non-professional; and an at home lateral flow pregnancy test (St John and Price, 2014). POC testing is a necessary component of affordable worldwide healthcare (Sharma *et al.*, 2015). Where there are limited-resources or where it is very hard to physically access relevant healthcare facilities, POC approaches can save hundreds of thousands of lives every year (Peeling and Mabey, 2010). For the purpose of this study, focus is brought to POC technologies currently used outside of clinical settings to diagnose malaria and *S. mansoni* infections.

### 1.6.1 Current diagnostic approaches at the point of care

The current principles of diagnosis for malaria and *S. mansoni* at the POC remain the same as clinical settings, however, developments have enabled improved methods for parasite observation in low-resource areas and the adaptation of clinical immunological tests into simple and easy-to-use lateral flow (LF) assays (Mfuh *et al.*, 2019). The POC immunological tests – otherwise known as POC rapid diagnostic tests (RDTs) - are often used to detect infection at a community level and in lower-tier health facilities without laboratories, increasing availability of immunological tests at the point-of-need (Altaras *et al.*, 2016). Examples of LF tests are shown in Figure 1-8(a-c).

The gold-standard microscopy methods are described in Section 4.5.4 . Microscopy based advances in sample processing and observational techniques, such as the Mini-FLOTAC technique, simplify direct parasite observation to perform surveys in laboratories with limited-resources (Barda *et al.*, 2013a; Nikolay *et al.*, 2014). The Mini-FLOTAC technique eliminates sieving, centrifugation and staining steps by use of the Fill-FLOTAC and provides a clean sample within the Mini-FLOTAC reading disk to facilitate direct observation and quantification of helminth eggs (Cringoli *et al.*, 2017), see Figure 1-8(d).

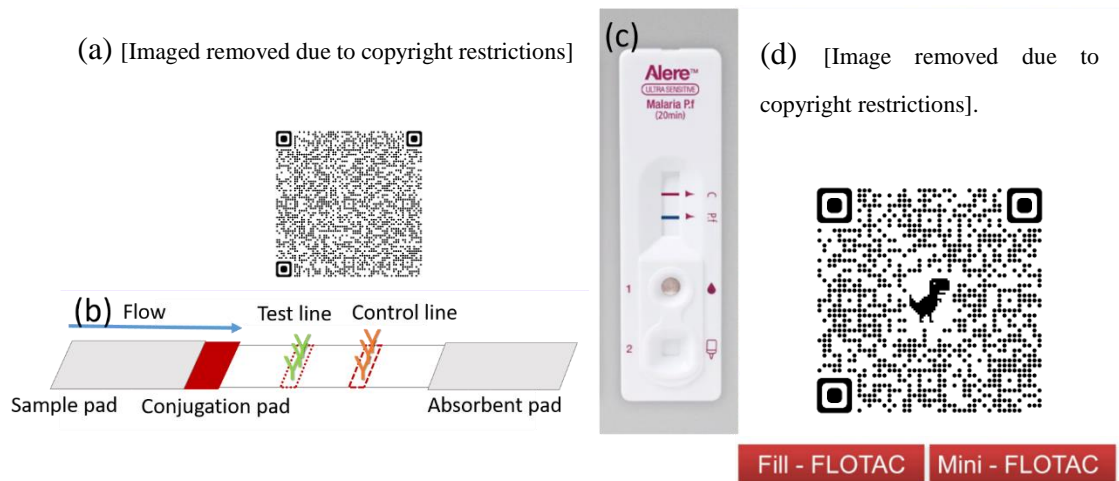


Figure 1-8: Examples of current POC diagnostic tests. (a) A diagram of the basic structure of a rapid POC LF test (<https://www.sigmaldrich.com/technical-documents/articles/ivd-immunoassay/lateral-flow/getting-started-with-ivd-lateral-flow.html>). (b) A diagram to show the function of a LF strip. (c) The Alere™ Malaria P.f POC RDT, image obtained from the Abbott product documents (<https://www.globalpointofcare.abbott/en/product-details/alere-malaria-ag-pf.html>). (d) The POC FLOTAC equipment, the Fill-FLOTAC used for stool sample preparation and the Mini-FLOTAC disk to facilitate direct observation of *helminth ovum* (Cringoli *et al.*, 2017).

### 1.6.2 Rapid POC antigen tests

The introduction of POC RDTs for malaria and schistosomiasis has aided diagnosis of malaria and schistosomiasis in communities and lower tier health facilities throughout sub-Saharan Africa (Altaras *et al.*, 2016). Ease of use and quick LF feed-back result in high adherence to RDT diagnosis in low resource settings (Ndyomugenyeni *et al.*, 2016). The most notable advantage of POC RDTs is that there is less reliance on an experienced healthcare technician or expensive equipment, resulting in far-reaching diagnostic availability (Tseroni *et al.*, 2015). POC RDTs have proved useful in both mass screening and individual diagnosis (Tseroni *et al.*, 2015) where quick sample preparation, and simple LF read-out after 20 minutes is much more time efficient than microscopy (McMorrow *et al.*, 2011).

#### 1.6.2.1 Malaria: POC RDT

The CareStart™ Malaria HRP2/pLDH (Pf/pan) Combo Test used during field trials conducted in Uganda (see Figure 1-9 (a)) is a commercially available test, which enables a species specific LF diagnosis to be made by detecting *plasmodium* parasite antigens. RDTs are reported to be thought of as “fundamental in diagnoses” by healthcare workers in remote areas (Kimani *et al.*, 2017). Where prevalence of malaria within a community is greater than fifty percent, RDTs are reported to be much more cost effective than microscopy and ‘clinical symptom based treatment’ (Uzochukwu *et al.*, 2009). For providers working in remote areas

with limited means, the introduction of RDTs has denoted a major shift from the long-standing practice of treating all fevers presumptively as malaria (Altaras *et al.*, 2016; Ndyomugenyi *et al.*, 2016). The manufacturers report sensitivity and specificity as > 95% and 99% respectively (Alere, 2016), although the performance has been reported to decrease below 100 parasites per  $\mu\text{L}$  of blood (Berzosa *et al.*, 2018).



Figure 1-9: RDTs for malaria and *S. mansoni*. (a) The CareStart™ Malaria HRP2/pLDH (Pf/pan) Combo Test. (b) The POC-CCA® lateral flow test - Rapid Medical Diagnostics, Pretoria (South Africa).

#### 1.6.2.2 *S. mansoni*: POC-CCA

The POC-CCA lateral flow test is available from Rapid Medical Diagnostics, Pretoria (South Africa) – see Figure 1-9(b). The LF strip for *Bilharzia* identifies presence of the schistosome circulating cathodic antigen (CCA) in the patients' urine (non-species specific diagnosis). The POC-CCA test method - described further in Section 4.5.4.4 - requires much less time and expertise than microscopy. The POC-CCA RDT provide diagnosis in low resource settings, where microscopy is not available (Foo *et al.*, 2015). The POC-CCA is an important surveillance tool, with reports of improved sensitivity as compared to KK examination in-the-field (Adriko *et al.*, 2014). Manufacturers report that in heavy (> 400 EPG) and low infection (<100 EPG), the sensitivity is reported as 100% and 70% respectively, and the reported specificity is 95% (Rapid Medical Diagnostics, 2018).

### 1.6.3 Limitations of current POC tests

Microscopy is still used for diagnosis of malaria and schistosomiasis at the POC in clinics with sufficient resources. The main limitation of direct parasite observation in-the-field is the necessity for trained technicians and equipment. For the diagnosis of schistosomiasis, the variation of schistosome egg excretion, the dispersal of ova in stool samples, and the quantity of slides examined per specimen, can all affect the tests sensitivity (Lodh *et al.*, 2013; Lamberton *et al.*, 2014; Weerakoon *et al.*, 2015). Additionally, the analytical sensitivity of microscopic examinations is reported to be lower when conducted under field conditions (Payne, 1988; Morassin *et al.*, 2002; Berzosa *et al.*, 2018). The accuracy of microscopic diagnosis is heavily dependent on the intensity of infections and the training and experience of the individual conducting the examination (Lamberton *et al.*, 2014; Ajibola *et al.*, 2018; Berzosa *et al.*, 2018). In order to accurately diagnose individuals with low parasitemia, it is clear that there is a need for a diagnostic technique which is more sensitive and with a lower dependence on the individual conducting the test. Furthermore, providing a diagnosis in low resource settings also favours tests which are rapid, require less specialised equipment, and lower running costs (Pai *et al.*, 2012).

POC RDTs require less equipment, time and result in lower running costs than traditional microscopic examinations (Uzochukwu *et al.*, 2009). The current methods are relatively simple and easily explained by manufacturers' instructions through simple diagrams (Rapid Medical Diagnostics, 2018; ACCESSBIO, 2020). The accuracy and application of RDTs remain heavily reliant on factors such as correct storage and end user performance (Moonasar *et al.*, 2007). Under manufacturer's instructions, ambient storage temperature of the RDT kits should be maintained (Rapid Medical Diagnostics, 2018). Temperatures throughout sub-Saharan Africa are generally higher and fluctuate significantly throughout the day. Therefore in the absence of temperature controlled storage conditions, the tests performance may be compromised (Moonasar *et al.*, 2007).

Improved performance of malaria RDTs as compared to microscopy has been confirmed by numerous investigators (Tseroni *et al.*, 2015; Boyce and O'meara, 2017), however, there are some doubts as to whether the RDTs will perform adequately in elimination settings (McMorrow *et al.*, 2011), where tests will be required to detect low-level infections in asymptomatic individuals, who may act as reservoirs for future disease emergence (Reboud *et al.*, 2018). Manufacturers report on product performance based on analysis of use in controlled laboratory environments, conditions which cannot be maintained in-the-field

(Moonasar *et al.*, 2007). Both the working environment, infection levels and population prevalence will subsequently effect the test performance (Adriko *et al.*, 2014). This further highlights the importance of conducting trials in-the-field to assess current and novel diagnostic platforms in real world conditions (Foo *et al.*, 2015; Fuss *et al.*, 2018), which is generally overlooked by test developers (Engel *et al.*, 2016).

## **1.7 Advances in POC testing**

Advances in technology and manufacturing methods has led to the simplification of diagnostic processing and continual miniaturisation of electronics, driving the translation of traditional laboratory diagnostic techniques into POC testing platforms (St John and Price, 2014).

Advances in optical techniques have enabled mobile phones (see Figure 1-10) to be used in place of microscopes for the diagnosis of malaria and schistosomiasis at the POC (Coulibaly *et al.*, 2016a; Coulibaly *et al.*, 2016b; Bogoch *et al.*, 2017; Rajchgot *et al.*, 2017). Mobile phones have also been suggested for the detection and reporting of parasitic disease in remote settings (Coulibaly *et al.*, 2016a). Teixeira *et al.* and other investigators highlight that when conducting investigations in-the-field, the images could easily be sent to a trained technician in a centralized laboratory or clinic for diagnosis (Teixeira *et al.*, 2007; Favero *et al.*, 2017; Lindholz *et al.*, 2018).

The separation of *S. mansoni* ova from stool samples has been achieved using magnetic beads (Teixeira *et al.*, 2007). Integration of magnetic particles into sample processing can remove the need for centrifugation steps, hence, reducing the volume of equipment necessary in sample preparation methods, resulting in testing methods which are more desirable for use at the POC. Magnetic bead-capture has also been used in antibody conjugation and DNA extraction and purification methods (Berensmeier, 2006; Noh *et al.*, 2019). These newer POC tests may not be as cheap and equipment-free as currently used RDTs and dipstick tests, but may prove to be impactful and cost-effective in the right settings (Pai *et al.*, 2012).



(a)[Image removed due to copyright restrictions]



(b&c) [Image removed due to copyright restrictions]



*Figure 1-10: Examples of mobile phone platforms for the direct observation of parasites for the diagnosis of schistosomiasis. (a) A photo of the mobile phone microscope for diagnosis of schistosomiasis described by Bogoch, et al. The slide is inserted into the sample tray which enables X-Z scanning (b) The Newton Nm1-600 XY – a portable and commercially available field microscope, the device is attached to a tripod during observation. (c) The reversed-lens CellScope attached to an iPhone 5s, which is manually held over the sample and moved to scan the slide – both trialled in-the-field as described by Coulibaly, et al.*

### **1.7.1 Molecular diagnostics for use at the POC**

Increasing popularity of molecular diagnosis has resulted in the development of smaller and portable extraction and amplification systems (Ahrberg *et al.*, 2016; González-González *et al.*, 2019; Lim *et al.*, 2019). Spurred by the COVID-19 pandemic, NAATs are now conducted in diagnostic laboratories across the globe (Udugama *et al.*, 2020). Prior to the pandemic, investigators reported the use of molecular tests to diagnose pulmonary tuberculosis (TB). The commercially available TB GeneXpert® (Figure 1-11(a)) and TB-LAMP systems (Figure 1-11(b)) have been deployed in hospitals in Asia and Africa (St John and Price, 2014; World Health Organization, 2016), however, the use of the TB GeneXpert® in remote clinics, resulted in the test being deployed in settings that do not match its intended settings of use (Engel *et al.*, 2016). The GeneXpert® was developed for use in primary care centres, emergency departments and hospital laboratories, to facilitate patient management closer to sites of patient care. The GeneXpert® platform requires a computer; a constant electricity supply; and ambient temperatures (2 to 28°C), all of which cannot be guaranteed

in low-resource and field environments; the challenges of working in low-resource environments will be discussed further in subsequent sections.

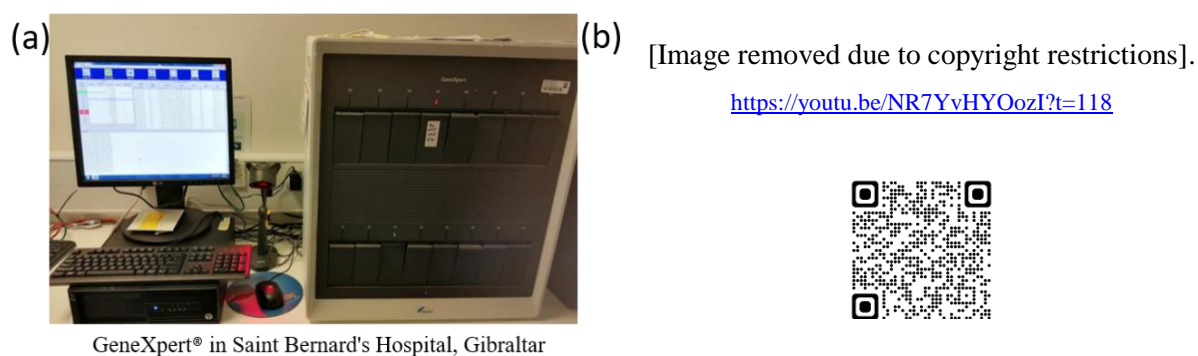


*Figure 1-11: Examples of commercially available molecular diagnostic systems. (a) GeneXpert® rapid test platform, the extracted sample is added to the cartridge which contains the necessary molecular component. The benchtop set-up requires a computer or laptop for diagnostic read-out. (b) The TB-LAMP system, Figure manipulated from <https://www.human.de/products/molecular-dx/tb-lamp/>, sample preparation is facilitated using the heaters on top of the machine and LAMP diagnosis is determined visually using a UV light source built into the tube heating compartment.*

Investigators have explored the ‘lab-in-a-suitcase’ approach for remote molecular testing – as seen in Figure 1-12(a), (Brunker *et al.*, 2020), however, there remains a lack of commercial incentive to develop POC molecular testing platforms for neglected diseases, which is mainly undertaken in the not-for-profit and academic sectors (Peeling and McNerney, 2014). Although NAATs can be carried out on crude samples, specimen preparation and DNA extraction enhanced NAAT outcomes by removing interfering and inhibitory substances from the clinical samples (Becker *et al.*, 2004). Manual sample preparation and DNA extraction methods (described further in Chapter 2), are generally lengthy, labour intensive and require an abundance of consumables. POC molecular platforms in development include portable, or hand-held specimen preparation platforms, which incorporate channels or microfluidic systems for DNA extraction and purification steps (Mohamad Azimi *et al.*, 2011; Xu *et al.*, 2020) reducing reliance on consumables and manual pipetting processes (see Figure 1-12(b)).

PCR and isothermal amplification have also been reported using a range of hand-held systems. Surface acoustic waves have been used to instigate thermal cycling to conduct PCR in a droplet – see Figure 1-12(c) - (Reboud *et al.*, 2012), and microfluidic chips have been deployed to conduct ‘pocket’ isothermal amplification (Xu *et al.*, 2020). Although literature searches reveal that there are an array of POC molecular devices in development aimed for use in low-resource environments (Govindarajan *et al.*, 2012; Singleton *et al.*, 2014; Mauk

*et al.*, 2015; Rodriguez *et al.*, 2016; Xu *et al.*, 2020), evidence of trials conducted at the intended point-of-use are lacking. This is not limited to POC molecular testing, test developers often do not know much about the settings they are developing tests for, and only more recently have some developers begun testing their prototypes in low-resource settings (Engel *et al.*, 2016).

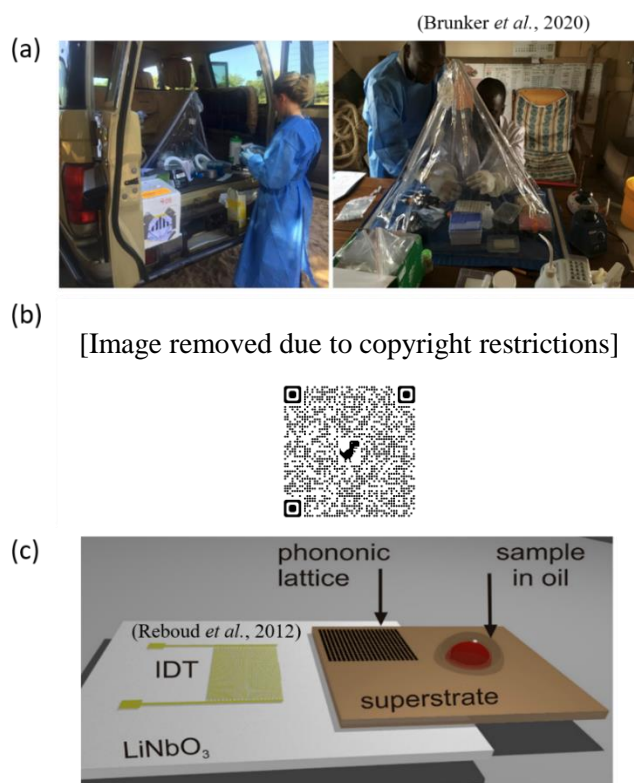


*Figure 1-12: Molecular methods for point-of-care scenarios. (a) RNA extraction in-the-field in Kenya for viral genome sequencing. (b) The microfluidic device for POC molecular amplification described by Xu et al., the microfluidic component is used for sample amplification and is coupled with mobile phone technology to enable result analysis. (c) Molecular amplification conducted in a droplet utilising surface acoustic waves for sample lysis and amplification.*

### 1.7.2 Challenges to consider for application of POC tests in LMICs

The emergence of more sensitive and accurate POC tests have the potential to dramatically enhance the quality of diagnosis available to patients' in LMICs (Pai *et al.*, 2012). However, there are additional challenges that limit implementation of new techniques which impact diagnosis and treatment at the POC in LMICs, not all of which are technological, but are constraints inherent in the health care system (Peeling *et al.*, 2017). Barriers for use include lack of access to reliable electricity and running water; the expense and availability of equipment and consumables; access to technical support and repairs; the cost and breadth of training needed to ensure that tests are conducted correctly; the theft of equipment; and

finally, the settings that the test is deployed in, does not match a manufacturer's testing environment (Engel *et al.*, 2016). These are all factors that need to be considered during the development of POC tests. For example, commercially available PCR and LAMP kits often use tailored reaction tubes and heating systems, which would rely on consistent supply chains for consumables, and in the case of equipment failure, access to technical support which would likely be limited in low-resource clinics.

In this project focus is drawn to a NAAT platform which does not require specialist facilities to manufacture, therefore making it easy to produce; and a cassette which is made from readily available materials. LAMP NAATs eliminate requirements for thermal cycling, resulting in simpler heating platforms which make it a favourable NAAT method for use in POC settings. LAMP assays for the detection of *plasmodium* and *S. mansoni* DNA are readily accessible, which facilitates development and translation of validated assays onto the POC platform. The POC NAAT method will be developed using basic laboratory equipment, fit for use in field environments, and later transferred into the field to assess the performance in real-world settings. More specific considerations for the proposed POC NAAT are discussed in the following section.

### **1.7.3 Considerations for a POC molecular diagnostic platform**

The simplicity of the LAMP procedure relative to other NAATs and the decreased infrastructure costs associated with isothermal amplification, open an array of opportunities by bringing molecular-level parasite detection within reach of national vector control programs (Hopkins *et al.*, 2013). A device which enables highly sensitive molecular diagnosis at the POC can prove extremely useful in specific applications such as screening and elimination programs (Peeling *et al.*, 2017). The POC devices described in Section 1.7.1, are practical solutions for providing a prompt diagnosis at the site of patient care. However, digital and microfluidic methods require specialist manufacturing facilities – such as clean-room facilities - and skilled professionals to manufacture and assemble the diagnostic devices resulting in expensive manufacturing processes. Implementing an application specific assay on a microfluidic chip is still a very complex and cumbersome task bearing technical risks and with it also financial risks (Mark *et al.*, 2010). In sub-Saharan Africa, access to certain materials, specialist facilities and equipment is limited. Here we aim to develop a simpler diagnostic assembly, in the aim to reduce costs and reliance on specialist facilities. A simple standardised diagnostic platform with the capacity to evolve for local needs has the potential to become a diagnostic solution that is provided in the region or

country of need, and this is the direction that molecular diagnostics need to take in order to be useful in tropical and low-resource settings.

Manufacturing fluidic cassettes by laser cutting is a simple and affordable alternative to 3D printing and fabrication of microfluidic cassettes using lithography (Walsh *et al.*, 2017). The relatively cheap and easy-to-use laser cutting machines are more accessible and do not require specialist facilities, such as a well-equipped laboratory or clean room facilities (Walsh *et al.*, 2017). Additionally, materials such as PMMA are readily available; affordable and durable; and can be easily laser cut to produce a diagnostic cassette. As such, PMMA and laser cutting was incorporated into the POC cassette design during this study.

The necessity for complicated optical systems to provide results for NAAT can be eliminated by integration of paper LF strips into the diagnostic method. LF strips are currently used in POC RDT applications, the familiarity of the diagnostic read-out has potential to increase the acceptance of a POC NAATs in resource-limited settings. For this reason, LF strip read-out was encompassed into the POC cassette procedure. Fully integrated systems which combine the components of sample preparation and analyte detection remain a challenge for technology transfer (Sin *et al.*, 2014). Paper has far reaching applications in POC diagnosis, in addition to analyte detection and result read-out – achieved using LF strips, the development of paper-based DNA processing techniques are a promising alternative for more affordable NAAT sample processing (St John and Price, 2014; Connelly *et al.*, 2015).

#### **1.7.4 Paper for POC Molecular Diagnostics**

Paper is integral in POC diagnostics, the most notable application being the at home pregnancy test (O'Farrell, 2009; Li and Steckl, 2019). Paper is cheap, easily disposable and versatile, all factors which appeal to point-of-care diagnostics (Li and Steckl, 2019). Since the 1980's, there has been a significant increase in the use of LF based diagnostics (St John and Price, 2014). Not only has paper been implemented for diagnostic read-out, it is also paramount in 'field-appropriate' DNA storage (Smith and Burgoyne, 2004). POC paper diagnostics have been presented by a number of investigators. The described "paper machines" or "paper origami" for sample processing and DNA extraction are promising techniques for application at the POC (Connelly *et al.*, 2015; Xu, Nolder, *et al.*, 2016; Magro *et al.*, 2017a; Yang *et al.*, 2018).

#### ***1.7.4.1 Paper-based DNA processing***

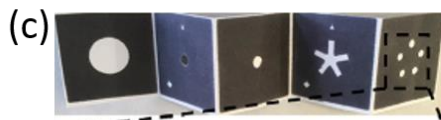
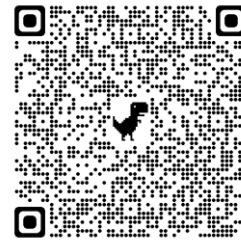
The most notable paper based DNA storage and extraction has been achieved by use of FTA<sup>®</sup> Whatman<sup>®</sup> cards – see Figure 1-13(a) (Ali *et al.*, 2017). The treated cellulose matrix enables long term storage and extraction of DNA from an array of samples (Ahmed *et al.*, 2011; Barbosa *et al.*, 2015). The simplicity of sample lysis on FTA<sup>®</sup> cards has facilitated their integration into POC molecular diagnostic cassettes to enable DNA lysis and purification from raw specimens – see Figure 1-13(b) - (Connelly *et al.*, 2015; Choi *et al.*, 2016). Additionally, “paper origami” has been referenced as a fluidic platform to enable DNA extraction and sample preparation for POC molecular diagnostic – see Figure 1-13(c&d) - (Connelly *et al.*, 2015; Rodriguez *et al.*, 2016; Xu, Nolder, *et al.*, 2016; Magro *et al.*, 2017b; Yang *et al.*, 2018). Printing a hydrophobic pattern - as shown in Figure 1-13(c) - allows a paper channel to be created for fluid flow (Xu, Nolder, *et al.*, 2016; Yang *et al.*, 2018). When the paper is folded it creates a physical boundary or path, acting as a valve or channel between sample preparation steps. The paper fluidic platform is very cheap, easily disposable and can be produced without specialist facilities (such as a clean room, which is required for traditional microfluidic devices). The paper valves and paths direct fluid flow, reducing manual pipetting steps and lower the reliance on traditional laboratory consumables such as centrifuges, all of which make the paper sample preparation platform favourable for the development of a low-cost POC NAAT.



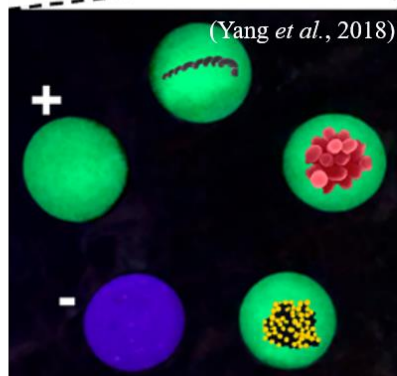
(a)

[Image removed due to copyright restrictions].

The QR code links to the image source.



(c)



(Yang et al., 2018)

(d)

[Image removed due to copyright restrictions]



Figure 1-13: Examples of paper DNA processing. (a) A FTA® Whatman® card used in-the-field to collect blood samples for analysis on return to the laboratory in the U.K. (b) The “Paper Machine” described by Connelly, Rolland and Whitesides. Sample preparation and amplification is conducted on paper disks within the plastic sliding cassette, following amplification, the diagnostic read-out is conducted visually by sliding the disk to the detection window and exposing it to UV light. (c) The paper origami device described by Yang et al., sample processing is conducted on the paper origami piece, then DNA is eluted into the plastic cassette for amplification and visual read-out using a UV light. (d) The paperfluidic molecular diagnostic chip described by Rodriguez et al., whereby the sample processing and amplification is conducted on the chip made from paper and adhesive film. The result read-out is conducted by visual analysis of the LF strip.

#### 1.7.4.2 POC detection of molecular amplicons

Isothermal amplification carried out using DNA eluted on paper has already been achieved within plastic cassettes (Connelly et al., 2015; Xu, Nolder, et al., 2016; Yang et al., 2018), whereby confirmation of LAMP results were determined by observation of UV excited fluorescence (refer to Figure 1-13(b & c) above). Fluorescence read-out requires portable UV lamps or readers to be incorporated into the test protocol, which introduces additional resources into the test procedure. Alternatively, colorimetric tests have been developed which do not require additional equipment, however, changes in ambient light conditions have been reported to affect both fluorescent and colorimetric read-out. As a result, the use

of fluorescence and colorimetric changes for determination of LAMP results may however, be unfavourable in low resource POC settings (Magro et al., 2017b).

LF strips have been widely accepted for interpretation of results in POC diagnostics (Sin *et al.*, 2014), and are integrated into RDTs commonly used throughout sub-Saharan Africa (Mfuh *et al.*, 2019), which suggests that LF strip read-out would be an appropriate development for POC NAATs. Developments in POC NAATs have been made by conducting amplification of DNA on a paper platform wrapped in polyvinyl chloride (PVC), with incorporated LF strip read-out – see Figure 1-13(d) (Choi *et al.*, 2016). Fluorescein isothiocyanate (FITC) and Biotin complexes as novel targets are recognized by standardized strips (Meng *et al.*, 2018). Incorporation of 5'-end FITC and Biotin labelled primers which integrate into complimentary strands of the amplified target DNA, enables amplification outcomes to be assessed qualitatively on the LF strips (Magro et al., 2017b). Commercialisation of the mentioned LF strips has led to an increase in development of LF strip LAMP tests (Cui *et al.*, 2012; Singleton *et al.*, 2014; Rodriguez *et al.*, 2016; Magro et al., 2017b; Zhang *et al.*, 2019). In the development of the POC LAMP platform in this study, we make use of commercially available LF strips to provide LAMP result read out.

#### ***1.7.4.3 Limitations of current POC NAAT studies***

In the POC NAAT methods referenced above, the determination of amplification results often required the investigators to open the chambers or vessels which house the molecular reagents following amplification. Processing in this manner would likely increase the risk of downstream contamination caused by LAMP amplicons (Public Health England, 2018). Further developments in this study, pursue a closed cassette approach in order to minimise risk of amplicon contamination events.

Previous studies highlight the applicability of the respective POC NAAT devices in low-resource or rural environments, however, the studies lack evidence of trials conducted using the devices in the intended settings. There are only a limited number of papers that describe field experiments, where the samples were tested in an established field-based laboratory or clinic (Hopkins *et al.*, 2013; Magro et al., 2017a). The temperature controlled field-based laboratory settings described by Magro *et al.*, is not a direct representation of field conditions in LMICs low-resource and rural environments. Trials in the target environment are a crucial part of test development (Pai *et al.*, 2012; Drain *et al.*, 2014), field-trials would enable the applicability of molecular POC testing to be assessed in real-world conditions (Sin *et al.*, 2014).



#### 1.7.4.4 The POC Paper Device

The POC Paper Device was designed to incorporate aspects of POC NAATs described in Section 1.7, to develop a cheap and easily producible POC device for use in low-resource settings. Due to limited resources in field environments, LAMP was chosen as the favourable NAAT, as it eliminates requirements for thermocycling equipment, enabling tests to be carried out on less expensive and standard heating platforms. The proposed POC Paper Device (an example shown in Figure 1-14), will be developed from the “paper origami device” design by Dr Gaolian Xu (Xu, Nolder, *et al.*, 2016), it will incorporate paper fluidic aspects for sample preparation and DNA purification; as well as LAMP carried out in a closed cassette with LAMP result read-out on LF strips. The *plasmodium* assay was developed by Dr Gaolian Xu, and in this study, published LAMP assays for *S. mansoni* will be developed to enable LF read-out for incorporation into the POC Paper Device.

Despite the abundance of publications presenting POC tests developed for use in low-resource environments, there are very limited reports of tests trialled in the intended settings of use. In this work, the *S. mansoni* assay will be developed for incorporation into the POC Paper Device, to couple the detection of *S. mansoni* and malaria (both are endemic in Uganda). The POC Paper Device will be developed, and trials will be carried out in-the-field in rural Uganda. The outcomes from the field trials will be assessed to pinpoint and resolve obstacles in testing, and assess areas for future development.

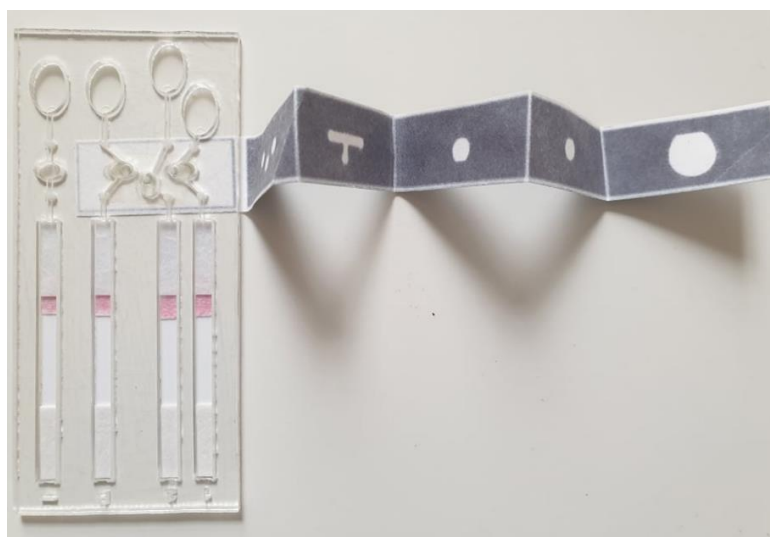


Figure 1-14: An Example of the POC Paper Device. The printed paper fluidic for sample processing is attached to the back of the laser cut PMMA cassette using double sided tape. The LF strips are inserted within the cassette sealed with adhesive film. Iterations of the Paper Device designs will be further discussed in Chapter 2.

## 1.8 Aims & Objectives

The aims of this work were to translate standard laboratory LAMP diagnostics onto a POC platform; to expand the current Paper Device molecular diagnostic platform to detect *S. mansoni* DNA; and assess the use of the POC Paper Device platform to detect *plasmodium* and *schistosome* DNA in rural communities within low resource environments in Uganda, which to date has been largely overlooked.

1. Develop the *S. mansoni* LAMP assay to allow integration of the diagnosis of schistosomiasis into the POC NAAT platform to facilitate expansion of capabilities of the Paper Device. Addressed in the first experimental chapter, this requires published LAMP assays to be assessed for development and translation into the POC Paper Device. The selected assay is required to carry out amplification from a variety of *S. mansoni* specimen, to demonstrate the potential for detection of target DNA within an array of samples.
2. Explore the use of the POC Paper Device in-the-field in low resource and rural environments. Addressed in the second experimental chapter, the POC Paper Device platform is required to identify presence of *plasmodium* and *S. mansoni* DNA within clinical samples collected in rural Uganda, and compared against standard field diagnostics. The developed *S. mansoni* assay will be used to identify presence of schistosome DNA in stool; and both the malaria and *S. mansoni* assay will be used to identify presence of target DNA within a finger-prick of blood. A gained understanding of the study environment is required to revise processes and develop a field-appropriate workflow. The outcomes from the field studies will be used to identify key areas for the development of the Paper Device.
3. Investigate the effects of field storage on the LAMP reagents. Addressed in the third experimental chapter, LAMP outcomes of field stored reagents will be analysed to determine possible effects of field storage on the Paper Device outcomes in-the-field and a field appropriate storage solution for LAMP reagents will be investigated.

## **Chapter 2: Materials, Methods & Development**

Chapter 2 describes the materials and methods used throughout this project. Within this chapter, focus is brought to the sample preparation and methods of detection; the method of DNA extraction; qPCR and LAMP both by fluorescence and on paper. The methods for the design and fabrication of the Paper Device are also described. Further chapters will contain additional materials and methods, when specific to the experiments recorded in the individual chapters. Unless otherwise stated, chemical reagents not provided in kits were obtained from Sigma (Dorset, UK).

### **2.1 Standard procedures for DNA extraction, amplification and quantification**

Section 2.1 describes the methods and materials used for DNA extraction and quantification. DNA extraction was conducted from industry standard synthesized DNA fragments (gBlocks) spiked in buffer; plasmodium parasite DNA and DNA extracted from *S. mansoni* parasite larval stages and ova (gDNA). Further to this, methods of DNA amplification and detection using ABI Fast 7500 qPCR machine (ABI machine) are discussed.

#### **2.1.1 Sample preparation and DNA extraction**

Clinical samples contain materials which pose a risk of inhibition to DNA amplification, inhibition can be caused by a number of materials within raw samples, such as high salt concentrations, haemoglobin and cell debris (Al-Soud and Rådström, 2001). For this reason, DNA extraction and purification is often incorporated into sample processing for NAATs. There are numerous methods for DNA extraction, and processes are categorized into chemical or mechanical extraction (Ali *et al.*, 2017). The primary step of DNA extraction is sample lysis, which is required to break open the cells to release DNA. Sample lysis is followed by a binding step, which involves sequestering DNA for purification. The discovery that silicates have high binding affinity for DNA revolutionised extraction procedures (Vogelstein and Gillespie, 1979; Ali *et al.*, 2017), leading to many commercial products that use spin columns to capture and separate DNA from the target sample. Although spin columns are an effective and quick DNA capturing and purification technique, the requirement for a centrifuge makes the method unfavourable for the settings where the Paper Device is aimed to be used. The following work describes a process in which magnetic

beads are integrated within the DNA extraction method, to remove the need for centrifuges in-the-field. Using the MagaZorb® DNA Mini-Prep Kit (Promega, Southampton, UK), the principles of DNA extraction remain the same as spin column extraction; however, in this case, the DNA is bound to magnetic beads. In the MagaZorb® method, the only additional equipment required was a magnetic rack and heater. The MagaZorb® protocol is described in the following sections.

#### ***2.1.1.1 Promega MagaZorb® Protocol for DNA extraction from blood***

The MagaZorb® protocol is illustrated in Figure 2-1. Unless otherwise stated, reagents for extraction were provided in the MagaZorb® DNA Mini-Prep Kit. The manufacturers' protocol for isolation of DNA from blood begins by ① pipetting 20 µL of proteinase K (PK) solution to the bottom of a 1.7 mL microcentrifuge tube (Axygen™ MaxyClear Snaplock Microtubes, Fisher). 200 µL of whole blood was added to the PK, gently swirling the tube to mix the sample. Following this, 200 µL of Lysis Buffer is added to the solution (lysis buffer and PK are used to free DNA and dissolve cellular proteins); ② mixing by pulse-vortexing until a homogenous mixture was obtained. ③ The tube was then incubated at 56°C in a tight-fitted heat block for 10 minutes. A colour change from red to olive green is expected, indicating complete lysis of whole blood. The second stage of DNA extraction is the binding step: ④ 500 µL of Binding Buffer was pipetted into the solution and mixed by pulse vortexing; followed by 20 µL of MagaZorb® Reagent 'the magnetic beads' (MZ beads). The sample was incubated at room temperature for 10 minutes, manually mixing every 2 minutes. ⑤ Placing the tubes in the magnetic rack (MagRack™ 6, GE Healthcare), the DNA bound to MZ beads were drawn towards the magnet, inverting the magnetic rack a couple of times ensured MZ beads were rinsed from the tube cap. After 2 minutes, the supernatant was removed by aspiration. ⑥ To commence the wash step: 1 mL of Wash Buffer was added to the tube; ⑦ removing the tube from the magnetic rack, inverting the tube several times to disperse the MZ beads and release any waste material; ⑧ sedimenting the DNA bound to MZ beads once again on the magnetic rack and removing the supernatant. The wash step was repeated twice. After the final wash the supernatant should be clear; ensure all liquid is removed from the tube after the final wash, including any liquid trapped in the tube cap. ⑨ To complete the DNA purification, 50 µL of Elution Buffer was pipetted into the tube and ⑩ heat at 56°C for 10 minutes; manually mixing every 2 minutes to release the DNA which was bound to the MZ beads. Finally, ⑪ the MZ beads were deposited as a sediment; ⑫ the supernatant containing the eluted DNA was transferred into a new tube. Isolated DNA was stored at -20°C until needed for analysis.

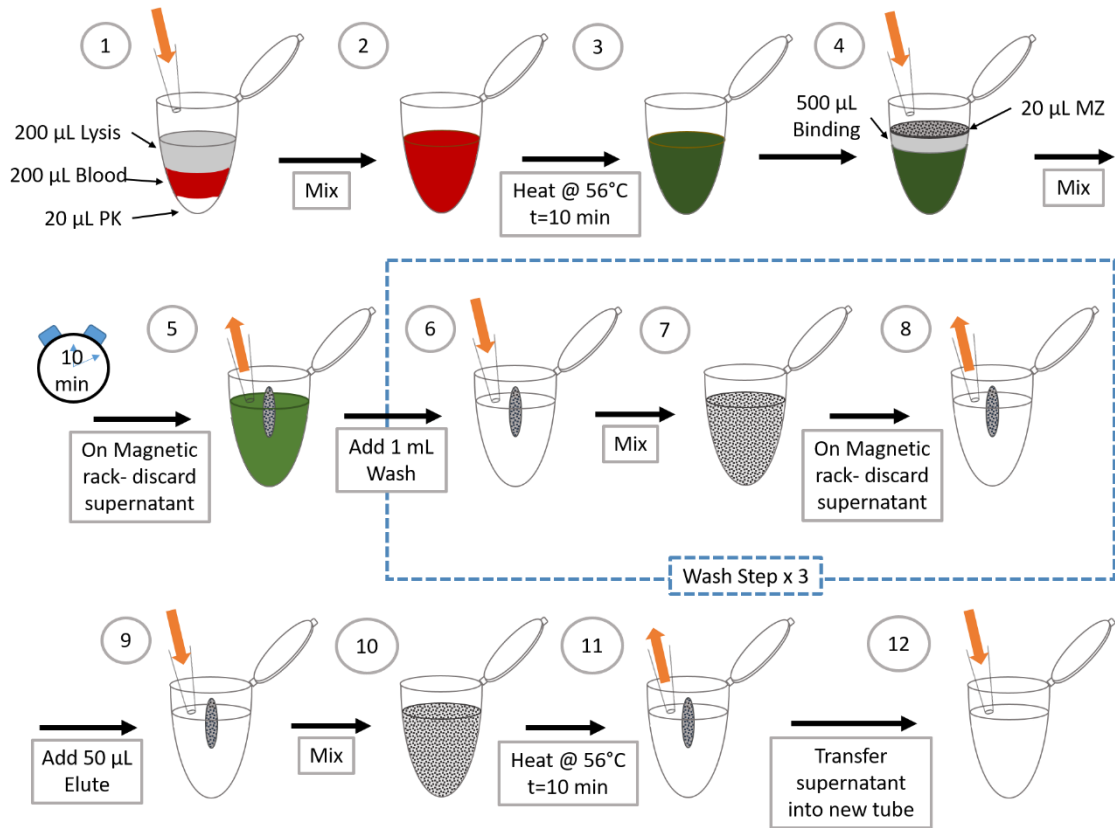


*Figure 2-1: Schematic of the MagaZorb® DNA Mini-Prep Kit Protocol for blood samples. The blood sample was lysed (1)-(3), to release DNA prior to binding. The Binding Buffer and MZ was added to the solution (4), mixed and left for 10 minutes at room temperature, mixing at 2 minute intervals. The tube was placed on the magnetic rack, sedimenting MZ beads, and supernatant was removed (5). The Wash buffer was added to the tube, the solution was mixed to free MZ beads from contaminants (6) & (7) before sedimenting the MZ beads and removing supernatant (8). The Wash step was repeated twice. The DNA was retrieved from the MZ beads using the Elution Buffer (9)-(11): Elution buffer was added to the tube; the solution was mixed to free the bound DNA from MZ beads; the solution was heated for 10 minutes to aid elution; and finally the tube was placed on the magnetic rack to sediment MZ beads. The supernatant containing extracted DNA was transferred into a new tube for storage (12).*

### **2.1.1.2 Modified (Scale-down) DNA Extraction from blood for use on the Paper Device**

Current microscopic and RDT diagnosis for malaria require a finger prick sample of blood, as such, the Paper Device protocol was tailored for a volume of blood obtainable from a finger prick sample. The goal to provide a diagnosis from a finger prick of blood, required the MagaZorb® protocol to be scaled down. *Plasmodium* parasites exist within the erythrocytes of an infected individual, as such, a whole blood sample is an appropriate target to detect *plasmodium* DNA (Xu, Nolder, *et al.*, 2016). Generally, a finger stick collector provides 5-10 µL of blood for RDTs (Luchavez *et al.*, 2007), as a result, the protocol was tailored to work with 5 µL of whole blood.

First 2 µL of PK was added to the bottom of a 1.7 mL microcentrifuge tube, followed by 5 µL of whole blood and 5 µL of Lysis Buffer. This was vortexed by gently flicking the bottom of the tube to obtain a homogeneous mixture. The tube was incubated at 65°C for 10 minutes, after which, 10 µL of Binding Buffer was added to the solution. The solution was mixed by gently flicking the bottom of the tube. 2 µL of MZ reagent was added to the bottom of the tube, the solution was mixed before leaving at room temperature for 5 minutes, mixing at 2 minute intervals. The tube was placed in the magnetic rack and left for a minute to allow beads to coagulate, before removing the supernatant and discarding with waste. 40 µL of Wash Buffer was added to the tube, flicking the bottom of the Eppendorf to disperse the beads. Placing the tube back on the magnetic rack to sediment the beads once again and remove the supernatant. The wash step was repeated twice, ensuring a clear solution was obtained. After the final wash step, 30 µL of Elution Buffer was added to the tube, flicking the bottom of the tube gently to disperse the beads and release the DNA into the eluate. The beads were then sediment using the magnet, and the eluate was transferred into a new tube for processing. Unless needed presently, isolated DNA was stored at -20°C until the time of use.

The modifications to the DNA extraction protocol for integration into the Paper Device method will be further discussed in Section 2.2.2.

### **2.1.1.3 DNA Extraction from Blood Stored on FTA® cards**

FTA® Whatman® cards enable the isolation, purification and storage of nucleic acids for long periods of time at room temperature (Ahmed *et al.*, 2011). The FTA® cards are useful for preserving DNA from a variety of samples: plants, blood, urine, parasite larvae (Ahmed *et al.*, 2011; Gower *et al.*, 2013). Throughout the duration of this project, FTA® cards were

used for preservation of DNA during transportation of blood collected during field studies. Extraction of the preserved DNA from the FTA<sup>®</sup> card was conducted using MagaZorb<sup>®</sup> reagents and Tris-EDTA (TE buffer), pH 8.0 (Sigma, Dorset, UK) with the following method.

A 2 mm diameter biopsy punch was used (6X punches) to remove the blood sample (blood spots) from the FTA<sup>®</sup> card. The blood spots were transferred into a 1.7mL Eppendorf tube before adding 300  $\mu$ L of TE buffer (PH 8.0), and the sample was incubated at room temperature for half an hour. After the incubation period, 20  $\mu$ L of P.K and 200  $\mu$ L Lysis buffer was added to the tube, mixed by pulse vortexing and incubated at 56°C for 20 minutes. The solution was transferred into a new tube, the liquid was squeezed from the pieces of FTA<sup>®</sup> card and transferred with a pipette into the new tube. The Binding, Wash and Elution steps follow the method described in Section 2.1.1.1. The extracted DNA samples were marked with the ID number and date then stored on ice (if used that day) or frozen until the time of use.

### **2.1.2 DNA quantification**

DNA concentration was quantified using the NanoDrop<sup>™</sup> Lite Spectrophotometer (ThermoFisher, UK). To quantify DNA concentration and purity, 2  $\mu$ L of the DNA sample was pipetted directly onto the optical measurement surface. Measurements were repeated three times for three replicate samples to determine the concentration of the DNA sample. The Absorbance (A) of UV light at a wavelength of 260 and 280 nm measured by the NanoDrop<sup>™</sup>, enables the DNA concentration and purity to be determined (Thermo Scientific, 2012). The purity of the sample – determined by the  $A_{260}/A_{280}$  ratio - was recorded. Samples with  $A_{260}/A_{280}$  ratio  $\sim 1.8$  – the characteristic value of pure DNA (Koetsier, Cantor and New England BioLabs, 2019) - were stored at -20°C until time of use, samples with  $A_{260}/A_{280}$  ratios  $< 1.77$  were discarded.

### **2.1.3 DNA Amplification & Molecular Detection**

Molecular amplification using both qPCR and LAMP were carried out within this study. The specific primers used for LAMP will be listed in subsequent chapters. In the following sections, ‘primer mix’ refers to the molecular assay for each target sequence (disease). Both qPCR and LAMP were conducted using the ABI machine and unless otherwise stated, molecular reagents were obtained from Eurofins Genomics (Ebersberg, Germany).

### 2.1.3.1 Interpreting qPCR fluorescence data

#### 2.1.3.1.1 Amplification data

As described in the Introduction, as the qPCR cycles progress, successful amplification results in an exponential increase in fluorescent signal, detected by the qPCR light sensor (Applied Biosystems, 2010). The relative normalised fluorescence data ( $\Delta Rn^{16}$ ) is plotted against the cycle number (Applied Biosystems, 2011). A typical qPCR amplification curve resembles a sigmoidal curve (Spiess et al., 2008), where the initiation of amplification is characterised by the cycle threshold (Ct) number (Biassoni and Raso, 2020). The Ct corresponds to the cycle number at which a samples fluorescent signal crosses the determined threshold value, see Figure 2-2 (Applied Biosystems, 2011). The time to amplification is inversely proportional to the concentration of target DNA in the tested sample (Higuchi *et al.*, 1993; Applied Biosystems, 2010). Higher concentrations of target DNA in a sample result in faster amplification, hence, a lower Ct value. For the purpose of this study we conducted presence/absence qPCR runs, quantitative PCR was not assessed, however, standard curves were conducted to pin-point limitations of the molecular assays. Both probe (TaqMan™) and SYBR™ Green detection were used during this study. SYBR™ Green binds non-specifically to dsDNA, hence, amplification observed using SYBR™ Green dye should be validated by melt curve or gel electrophoresis to distinguish amplification products (Ririe, Rasmussen and Wittwer, 1997) - discussed in the following sections.

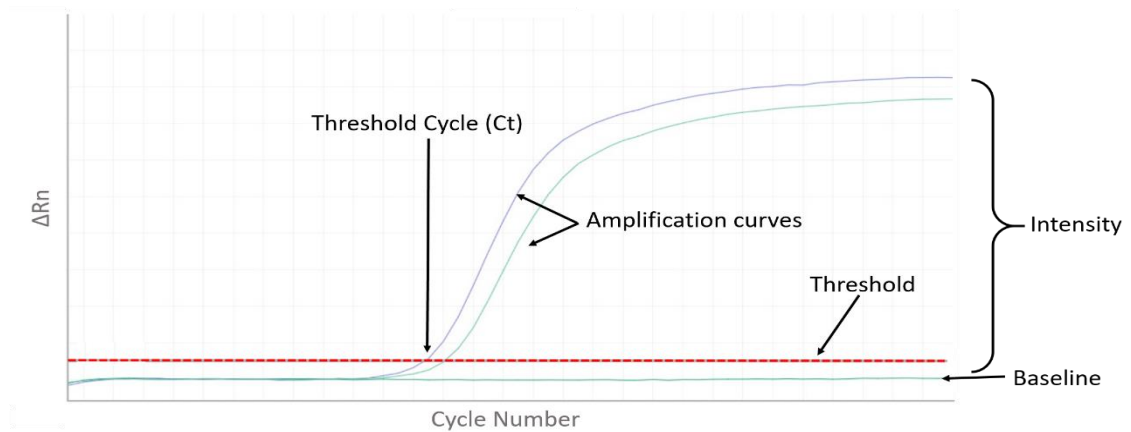


Figure 2-2: qPCR linear amplification curve. The  $\Delta$  normalised reporter value ( $\Delta Rn$ ); fluorescent signal minus the baseline value, is plotted against the cycle number. A typical amplification curve resembles a sigmoidal curve. Amplification is measured by the Ct value, the cycle number which corresponds to the fluorescence reaching a determined threshold value.

<sup>16</sup> Rn is the reporter signal normalized to the fluorescence signal of the reference dye,  $\Delta Rn$  is Rn minus the baseline



### 2.1.3.1.2 Melt Curve Analysis

DNA melting occurs when dsDNA separates into ssDNA (Farrar and Wittwer, 2017). Peaks in melt curve data indicate the melting temperature ( $T_m$ ) of the amplified product (Applied Biosystems, 2010).  $T_m$  for dsDNA is dependent on the sequences GC content (Ririe, Rasmussen and Wittwer, 1997). DNA melting is analysed by observing changes in fluorescent signal from dsDNA binding dyes (such as SYBR™ Green). The fluorescence is observed as the temperature is increased. The fluorescent signal slowly decreases with increasing temperature, refer to Figure 2-3 (a), denaturation of the PCR product is indicated by a sudden drop in fluorescence (Farrar and Wittwer, 2017). The  $T_m$  coincides with the drop in fluorescent signal, it is the temperature at which 50% of the DNA is dissociated into ssDNA (Applied Biosystems, 2010). The  $T_m$  is identified by the peak in the plot of derivative reporter (derivative of the fluorescent signal) vs. temperature data, refer to Figure 2-3 (b). When the  $T_m$  of the desired target sequence is known, a melt curve can aid in identifying non-specific amplification (Ruiz-Villalba *et al.*, 2017). A peak in the melt curve fluorescence data at the expected  $T_m$  suggests amplification of the desired target. Non-specific amplification is typically determined by peaks at differing  $T_m$  or presence of multiple peaks in the melt data (Ruiz-Villalba *et al.*, 2017). For the purpose of this study, theoretical  $T_m$  for the target sequences were obtained using uMelt software (Wittwer Lab), calculated by nearest neighbour model (Dwight, Palais and Wittwer, 2011).

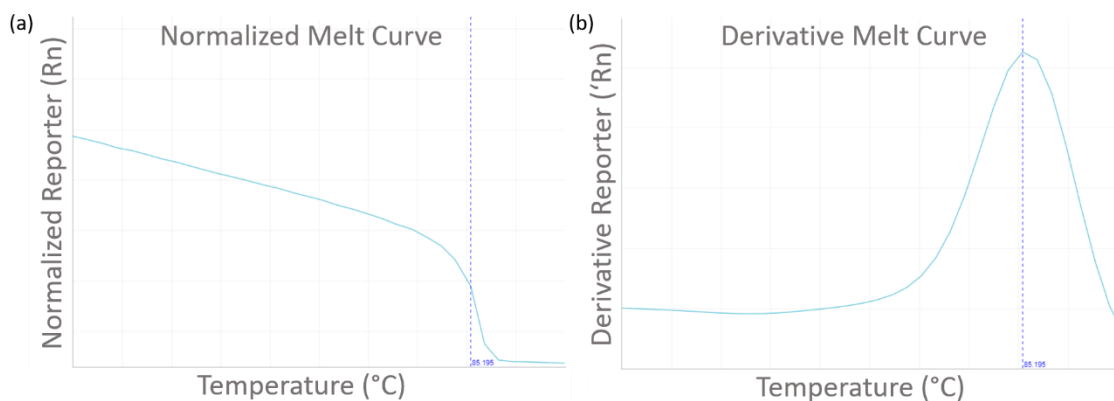


Figure 2-3: Melt curve data. The fluorescence data is recorded as the temperature is increased. (a) The normalized melt curve. The normalized reporter ( $R_n$ ) is plotted against temperature. The melt temperature is determined at the 50% of the drop in fluorescent intensity. (b) The derivative melt curve. The derivative of the  $R_n$  is plotted against temperature to visualise the melt peak.

### **2.1.3.2 *TaqMan*<sup>TM</sup> qPCR**

Probe based qPCR was used for confirmatory testing of blood samples returned to Glasgow from-the-field, to reduce workload by eliminating the need for additional melt curve and gel electrophoresis analysis on all field-collected samples. The molecular ‘Taq probes’ used to perform TaqMan<sup>TM</sup> qPCR amplification were obtained from Integrated DNA technologies, IDT Inc.(Leuven, Belgium). Primer sequences for both pan-plasmodium (PANchrom) and schistosomiasis mansoni (SMchrom) are listed in Table 2-1 . Schematic of the sequences are shown in Figure 2-4. The TaqMan<sup>TM</sup> amplification reagents were made up to a total volume of 20 µL. Amplification was conducted by adding 7 µL of the primer mix and 10 µL of Brilliant Multiplex QPCR Master Mix (Agilent, Stockport, UK) into tube strips (ABI MicroAmp<sup>TM</sup> Fast-8 Tube Strip, Fisher, UK), before adding 2 µL of target DNA and 1 µL of nuclease free water. Both targets (PAN & SM) follow the same amplification process, commencing with a 10-minute melt period, followed by the cycle of: melt, annealing and extension steps, at 95°C (15 seconds), 59°C and 72°C (30 seconds) respectively. In order to amplify DNA extracted from FTA<sup>®</sup> cards, 70 cycles were completed on the ABI machine.

Incorporation of TaqMan probe enables detection of the specific PCR product as it accumulates during PCR cycling. The threshold cycle (Ct) corresponds to the qPCR cycle number at which the probe fluorescence meets the determined threshold value in the amplification plot (Applied Biosystems, 2010). Where appropriate the threshold was determined automatically by the ABI machine. In cases where the automatic threshold or baselines were too low, the threshold was set manually to ensure the threshold was within the exponential growth region of the data set (Applied Biosystems, 2010).

Table 2-1: Primer names and sequences used for qPCR amplification of plasmodium and *S. mansoni* DNA. Sources of the assays are referenced in the table.

Gene Target	Amplicon size & Tm	Primer Name	Sequence (5'-3')	Primer length & Tm	Concentration per reaction (µM)	Reference
18s	157 bp 81°C	PANchromF3	GTT AAG GGA GTG AAG ACG ATC AGA	24 bp 67.5°C	0.2	(Rougemont <i>et al.</i> , 2004)
		PANchromB3	AAC CCA AAG ACT TTG ATT TCT CAT AA	26 bp 64.5°C	0.2	
		PlasProbe	[FAM]-ACC GTC GTA ATC TTA ACC ATA AAC TAT GCC GAC TAG- [TAMRA]	36 bp 75.5°C	0.3	
121-tandem repeat unit, sm1-7  GenBank Accession # M61098.1	110 bp 86°C	SMchromF3	GAT CTG AAT CCG ACC AAC CG	20 bp 67.0°C	0.5	(Enk, Oliveira e Silva and Rodrigues, 2012)
		SMchromB3	ATA TTA ACG CCC ACG CTC TC	19 bp 68.5°C	0.5	
		SMProbe	[FAM]-TCC GAA ACC ACT GGA CGG ATT TTT ATG AT-[TAMRA]	29 bp 73.0°C	0.3	(Wichmann <i>et al.</i> , 2009)

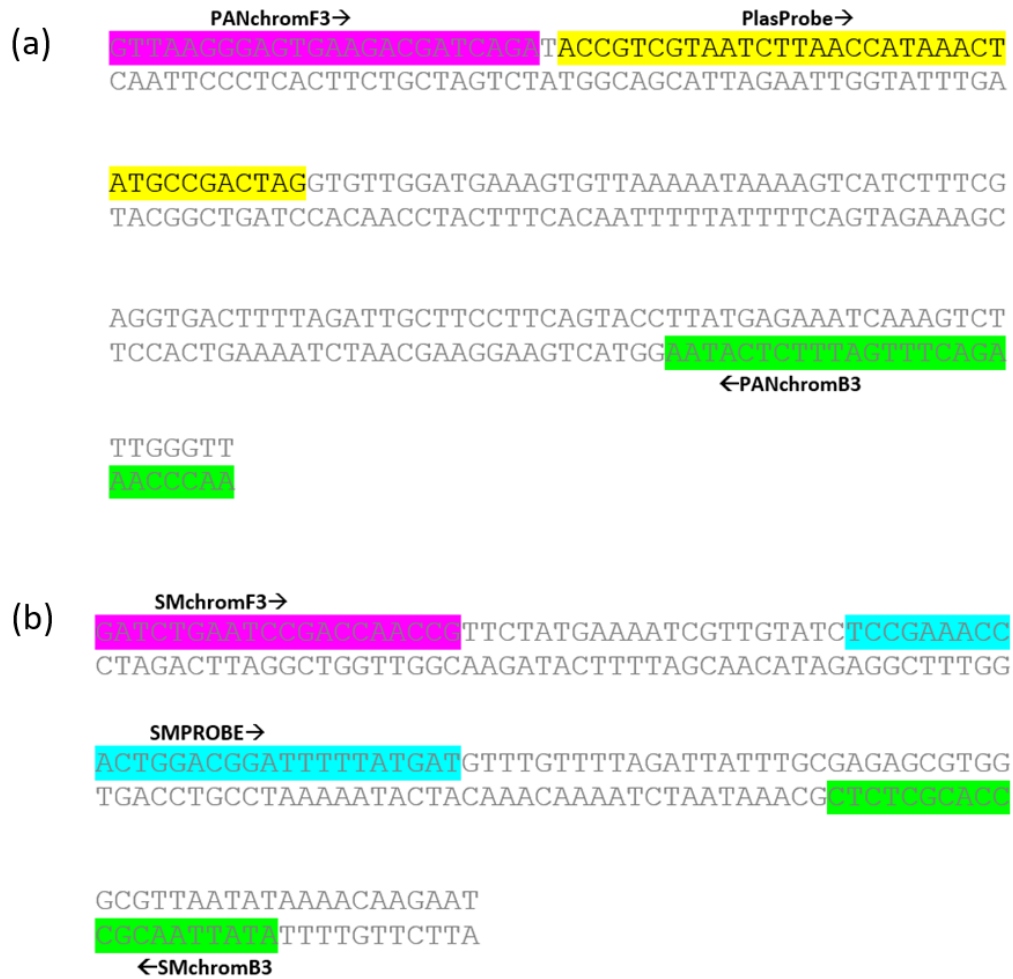


Figure 2-4: Schematic of (a) plasmodium pan qPCR primer set (PANchrom) targeting pan-plasmodium gDNA. (b) S. mansoni qPCR primer set (SMchrom), targeting S. mansoni gDNA. The arrows depict the direction of polymerisation for each primer sequence.

### 2.1.3.3 Calibration data for detection of plasmodium DNA by qPCR

Real time PCR was conducted on the ABI machine using gBlock (IDT, Leuven, Belgium) and genomic *plasmodium* DNA to determine limit of detection of PANchrom molecular reagents following the method described in Section 2.1.3.2. Figure 2-5(a) shows the fluorescence data collected for amplification of genomic and gBlock DNA. The parasite DNA obtained from collaborators and the gBlock DNA was measured on the NanoDrop (quantified in ng/ $\mu$ L), as a result, the DNA used in NAATs throughout this study was reported in ng/ $\mu$ L. The gBlock DNA detected weight can be converted to the corresponding copy number per reaction using Equation 1 in Section 7.2, and the corresponding copy numbers calculated for the *S. mansoni* and *plasmodium* target DNA in NAAT reactions are reported in Table 7-2, from herein the target DNA is reported in ng/ $\mu$ L. Data plotted in purple, dark blue, light blue, green, teal and navy (no amplification) are 20, 10,  $10^{-1}$ ,  $10^{-2}$ ,  $10^{-3}$  ng/ $\mu$ L gDNA samples and negative control (dH<sub>2</sub>O) respectively. Data plotted in black, brown, red, pink and violet are amplification curves for  $10^{-1}$ ,  $10^{-2}$ ,  $10^{-3}$ ,  $10^{-4}$ ,  $10^{-5}$  ng/ $\mu$ L gBlock samples respectively; this corresponds to  $10^9$  to  $10^5$  copies per reaction, a conversion table can be found in Table 7-2 in the Appendices. The mean amplification time (Ct value) for dilutions of gBlock (orange) and genomic DNA (blue) is depicted in Figure 2-5(b). Ct values were determined from fluorescence data at 100,000 RFU. Ct values for genomic DNA dilutions: 20, 10, 0.1, 0.01 ng/ $\mu$ L were 22.0, 25.4, 33.9 and 39.5 respectively. The gBlock DNA target displayed faster amplification times, Ct values corresponded to: 31.8, 35.8, 38.5 and 42.6 concentrations of 0.1 to  $10^{-4}$  ng/ $\mu$ L respectively. The error bars represent standard deviation of the Ct values collated for each DNA concentration. No amplification was observed for DNA concentrations below  $10^{-2}$  &  $10^{-5}$  ng/ $\mu$ L of DNA for genomic and gBlock targets respectively. Figure 2-5 presents the raw data extracted from the ABI machine. The ABI software was unable to combine data from multiple runs, where required, the raw data was compiled and plotted on MATLAB<sup>®</sup> using the code in Section 7.3.1 in the Appendices. The MATLAB<sup>®</sup> code retrieves the raw data extracted from the ABI machine and by use of a user determined baseline, normalises the raw data curves, thus, allowing multiple qPCR data sets to be compiled into a single plot.

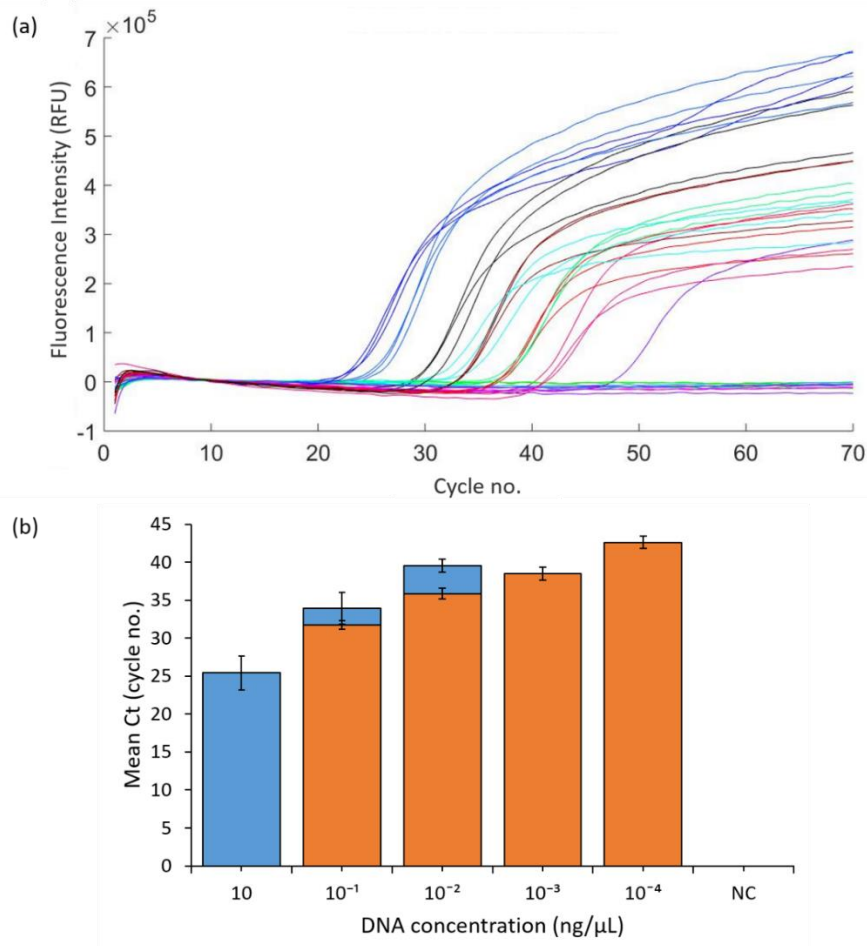


Figure 2-5: qPCR calibration data for plasmodium DNA. (a) Fluorescence data collected from ABI machine for TaqMan qPCR amplification of serially diluted plasmodium gDNA. Data plotted in brown, pink, dark blue, blue, purple and green are 20, 10,  $10^{-1}$ ,  $10^{-2}$ ,  $10^{-3}$  ng/ $\mu$ L gDNA samples and dH<sub>2</sub>O respectively. (b) Average qPCR Ct Values for serially diluted DNA templates; synthetic gBlock DNA template in orange and plasmodium genomic DNA (gDNA) in blue. The error bars are the standard deviation for the Ct values obtained for the respective DNA concentrations.

#### 2.1.3.4 Confirmatory qPCR on field-collected samples

For the purpose of confirmatory TaqMan™ qPCR from blood samples stored on FTA® cards collected in the field, the qPCR set-up was subject to double blinding. The DNA was extracted from blood spots stored on FTA® cards by a first operator, following the protocol referenced in Section 2.1.1.3. Utilising a random number generator function, the extracted samples were allocated new blind ID numbers by a second operator and an additional 10 negative control samples were mixed into the sample cohort.. The qPCR method remains consistent with the method described in Section 2.1.3.2. The blinded DNA samples were dispensed in triplicate into a 96-well plate along with positive and negative no template controls for amplification. The data presented in Figure 2-6 was exported directly from the ABI machine.

## Amplification Plot PPAN qPCR

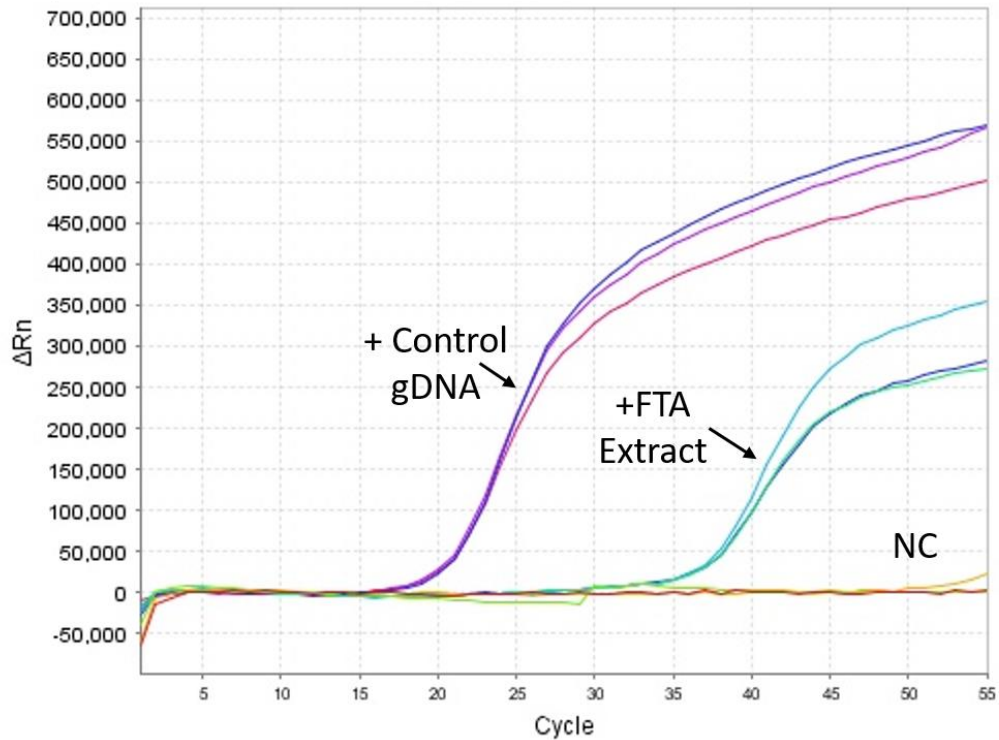


Figure 2-6: qPCR amplification of FTA<sup>®</sup> extracted samples. An example of an amplification curve from a confirmatory qPCR run. The graph shows the amplification curve of: the positive control DNA (+ Control gDNA); a DNA sample containing plasmodium DNA, extracted from blood stored on FTA<sup>®</sup> card returned from the field (+FTA<sup>®</sup> Extract); and the negative control (NC).

After the qPCR results were determined, the blind ID numbers were reassigned to the sample ID for comparison to field results by the second operator. The Ct values associated with each sample were entered into the results spread sheet. The Ct cut-off value was set at 45 cycles. A positive qPCR result, was allocated to a sample ID with resultant amplification, of at least one of the triplicate samples. A positive or negative qPCR result was assigned a value of 1 or 0 respectively, the same was true for microscopy, RDT and the Paper Device results collected in the field. Utilising binary data records, allowed computational formulas to compare the respective data sets, to minimise the possibility of investigator bias.

### **2.1.3.5 LAMP**

LAMP sequences to detect plasmodium and *S. mansoni* DNA have already been designed and published by other investigators (Polley *et al.*, 2010; Fernández-Soto *et al.*, 2014). Here, the LAMP sequences, method and analysis will be further explained.

#### **2.1.3.5.1 Interpreting LAMP fluorescence data**

Progression of LAMP can be monitored similarly to qPCR (see Section 2.1.3.1 for more details). LAMP has been monitored in real-time using: dsDNA intercalating dyes, such as SYBR™ Green; self-quenching and de-quenching probes; and by visible colour changes (Li *et al.*, 2016; Gadkar *et al.*, 2018; Fernández-Soto *et al.*, 2019). Generally the change in fluorescent signal is reported against time (Abdulmawjood *et al.*, 2014; Gadkar *et al.*, 2018), however some investigators maintain analysis of amplification against the cycle number (Li *et al.*, 2016). The methods for establishing time to amplification for LAMP will be further discussed in Section 2.1.3.5.4.

#### **2.1.3.5.2 LAMP assays**

LAMP assays that were used during field trials are listed with their respective references in Table 2-2. The information provided includes gene target, target amplicon size and expected melt temperature (T<sub>m</sub>), calculated using uMelt – described further in the Appendix Section 7.4; the oligo sequences, primer lengths and T<sub>m</sub>; the concentration of the respective oligos within the LAMP reaction; and the reference for the LAMP assays.



Table 2-2 : Primer names and sequences used for LAMP amplification of plasmodium; *S. mansoni* mitochondrial; and BRCA1 and *S. haematobium* DNA (used as controls during field trials and developed by Dr Gaolian Xu for use on the Paper Device).

Gene Target	Amplicon size & Tm	Primer Name	Sequence (5'-3')	Primer length & Tm	Concentration per rn (μM)	Reference
PgMt19	220 bp 85.5°C	PANF3	TCG CTT CTA ACG GTG AAC	18 bp, 63.0°C	0.1	(Polley <i>et al.</i> , 2010)
		PANB3	AAT TGA TAG TAT CAG CTA TCC ATA G	25 bp, 61.5°C	0.1	
		PANFIP	GGT GGA ACA CAT TGT TTC ATT TGA -TCT CAT TCC AAT GGA ACC TTG	45 bp, 75.0°C	0.8	
		PANBIP	GTT TGC TTC TAA CAT TCC ACT TGC -CCG TTT TGA CCG GTC ATT	42 bp, 79.5°C	0.8	
		PANLPR5F	[FITC]- CAC TAT ACC TTA CCA ATC TAT TTG AAC TTG	30 bp, 65.5°C	0.6	
		PANLPR5B	[BIOTIN]- TGG ACG TAA CCT CCA GGC	18 bp, 65.5°C	0.6	
mtDNA minisatellite sequence GenBank Accession #L27240	202 bp 84.5°C	SMF3	TCG TCT ATA GTA CGG TAG G	19 bp, 61.0°C	0.1	(Fernández-Soto <i>et al.</i> , 2014)
		SMB3	TTA TAC TTT AAC CCC CAC C	19 bp, 60.0°C	0.1	
		SMFIP	TGC CAA GTA GAG ACT ACA AAC ATC T - TG GGT AAG GTA GAA AAT GTT	45 bp, 75.5°C	0.8	
		SMBIP	AGA AGT GTT TAA CTT GAT GAA GGG G- AAA CAA AAC CGA AAC CA	42 bp, 75.5°C	0.8	
		SMLPR5F	[FITC]-GTC CTC TTG TTT TTG AAT	18 bp, <60°C	0.6	Dr Gaolian Xu (Unpublished sequence).
		SMLPR5B	[BIOTIN]-CTG CAC GAA ATA CAG AAT C	19 bp, <60°C	0.6	

Gene Target	Amplicon size & Tm	Primer Name	Sequence (5'-3')	Primer length & Tm	Concentration per rn (μM)	Reference
Homo sapiens DNA, chromosome 17 GenBank Accession #AP023477.1	210 bp 87°C	BRCA1F3	TCC TTG AAC TTT GGT CTC C	19 bp, 60.5°C	0.16	(Tanner and Evans, 2014)
		BRCA1B3	CAG TTC ATA AAG GAA TTG ATA GC	23 bp, <60°C	0.16	
		BRCA1FIP	ATC CCC AGT CTG TGA AAT TGG GCA AAA ATG CTG GGA TTA TAG ATG T	46 bp, 77.5°C	0.64	
		BRCA1BIP	GCA GCA GAA AGA TTA TTA ACT TGG G – CAG TTG GTA AGT AAA TGG AAG A	47 bp, 75.5°C	0.64	
		BRCA1LPR5F	[FITC]- GCA GAT AGG CTT AGA CTC AA	20 bp, 61.5°C	0.8	
		BRCA1LPF5B	[BIOTIN]- AGA ACC AGA GGC CAG GCG	18 bp, 68.5°C	0.8	
Schistosoma haematobium isolate sh1 cytochrome c oxidase subunit I (COX1)	215 bp 80°C	SHF3	ATG AAC ATT GTA TCC TCC	18 bp, <60°C	0.1	Dr. Gaolian Xu – Unpublished sequence
		SHB3	CTA AAA CTG GTA ATG AAA GC	20 bp, <60°C	0.1	
		SHFIP	ACC AAC TAG TCT AGA TAC ACC CTT ATC CAT ATC TGA GAA TTC	42 bp, 73.0°C	0.8	
		SHBIP	ACG ATT ATT AGT CGT GTC GAT TAA TAG AAG TAA ACA AAT ACG	23 bp, 71.0°C	0.8	
		SHLPR5F	AGA CTT CTA TAA TAA TAT	18 bp, <60°C	0.6	
		SHLPF5B	AAT AAT CTC ACC TAA AC	17 bp, <60°C	0.6	

#### **2.1.3.5.3 LAMP method**

LAMP was conducted using sequences listed in Table 2-2. 5  $\mu$ L of the primer mix (recipes are stated in subsequent chapters) was added to 15  $\mu$ L of ISO-004 Isothermal Mastermix (OptiGene, Horsham, UK), before adding 5  $\mu$ L of target DNA, to make up the final volume of 25  $\mu$ L per reaction, as recommended by the manufacturer. Nuclease free water was used as a no template negative control sample (NC). The tubes were centrifuged to remove bubbles before amplification. To perform amplification, the samples were heated at 65°C for 35 cycles (35 minutes), with fluorescence quantified each minute. The Isothermal Mastermix contains an unspecified dsDNA binding dye. Following manufacturers' recommendations, the fluorescence was quantified using the FAM/ SYBR™ green detection channel (filter 1 on the ABI machine). The dsDNA binding dye binds non-specifically to all double stranded DNA, detecting presence of LAMP amplified product as the reaction progresses. Following amplification, a melt curve was performed from 45 to 95°C at 2% ramp rate, to rule out potential nonspecific product formation.

#### **2.1.3.5.4 LAMP analysis**

To assess LAMP amplification time, the cycle threshold method applied to qPCR analysis was modified to enable the time to amplification to be calculated (Xu, Zhao, *et al.*, 2016). The LAMP cycle was determined as 65°C (1 minute); therefore the cycle number corresponds to time (minutes) throughout the reaction progression. Unlike qPCR, LAMP is conducted at a single temperature and does not require a 'hot start' or denaturation step. The ABI machine records the amplification progression at the end of each defined cycle, after temperature stabilisation at 65°C. The ABI software required pre-cycle and cycling conditions to be entered to conduct a run, as a result the samples were heated at 65°C during the defined pre-cycle period. The ABI Ct is calculated from fluorescence data collected once the determined 'cycling' phase is initiated, and as a result, the ABI determined Ct does not reflect the true time to amplification, as the pre-cycle time is not accounted for within the data. Hence, the time to start the LAMP 'cycle' (found within the software run file) should be taken into account whilst assessing the time to amplification. When repeating LAMP experiments there were large discrepancies between control and experimental data, when repeated in separate runs. There appeared to be an inverse correlation between the time for the ABI machine to stabilise at the required amplification temperature at the beginning of a run, and the reported Ct values. By addition of the stabilisation time onto the reported Ct value, the cycle time threshold results between different runs became more comparable (see

Figure 2-7 below). For this reason the time to amplification for LAMP throughout this work is determined as the cycle threshold time (Ctt); the Ct value, calculated using ABI software; plus pre-cycle time (run dependent), it is unclear whether the pre-cycle time was taken into consideration in the work presented by Xu and Zhao., *et al.*

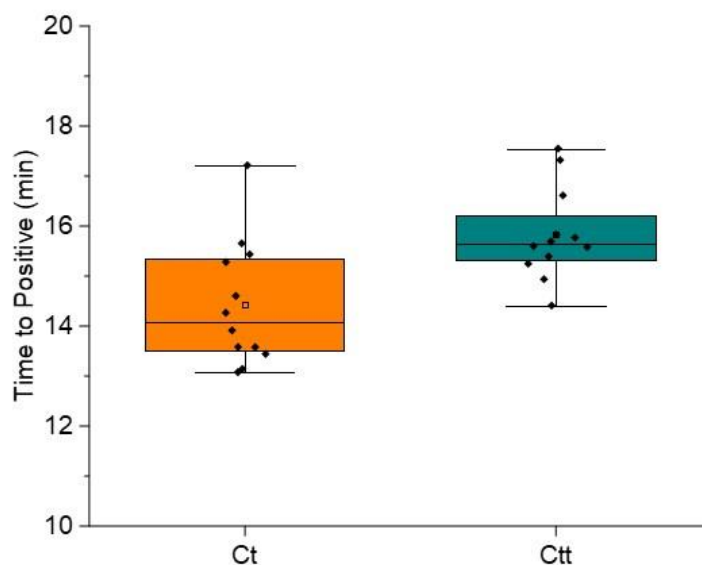


*Figure 2-7: Cycle threshold (Ct) and time to cycle threshold (Ctt). The Ct values (orange) reports the cycle number at which the sample fluorescence passes crosses the determined threshold. The Ctt (green) reports the time at which the sample fluorescence crosses the same threshold and also takes into account the time where the ABI machine was heating and stabilising at 65°C before the initiation of the ‘temperature cycling’ program; taking such measures into account resulted in more reproducible and comparable data*

*The cycle threshold time (Ctt): the Ct value determined by the ABI software plus the pre-cycle time (run-dependent).*

#### 2.1.4 Confirmation of SYBR™ Green amplification of PCR and LAMP products

Gel electrophoresis is used to isolate, identify and characterise properties of DNA fragments (Carter and Shieh, 2010). Gel electrophoresis enables fragments of DNA to be separated by size, allowing verification of PCR product size (Southern, 1975; Ruiz-Villalba *et al.*, 2017) and to confirm presence of LAMP amplification. The DNA is loaded into a well of the gel, immersed in running buffer within the gel dock. Applying a current across the gel causes the negatively charged DNA to migrate towards the cathode (Lee *et al.*, 2012). The mobility of the DNA within the gel is inversely proportional to the length of the DNA fragment (Southern, 1975). A DNA ladder -which contains fragments of known DNA strand lengths, is used to determine the size of the amplified PCR product (Southern, 1975; Wang, Guo and Zhang, 2010). The band resulting from the amplified sample is referenced against the DNA ladder bands to determine the size of the PCR product (Southern, 1975; Lee *et al.*, 2012). A sample band corresponding to the length of the desired PCR product, suggests successful amplification of the desired target DNA (Ruiz-Villalba *et al.*, 2017). A similar outcome is observed when visualising LAMP amplicon, however, LAMP products produce a characteristic ladder pattern – see *Figure 3-11* (Zhang *et al.*, 2010). The bands are not visible to the naked eye. However, by incorporation of an intercalating dye, which fluoresce when bound to DNA and exposed to UV light; the bands can be visualized using gel readers and software such as the Syngene PXi machine and Gensys V.1.5.00 software (SYNGENE, Fisher Scientific, UK).

Positive amplification of DNA can be visualised by gel electrophoresis (Stellwagen, 2009). 500 mL of 1X tris-acetate-EDTA (TAE) Buffer was made up from modified TAE Buffer 50X (Merck, Dorset, UK). 2% agarose gel was made up from 50 mL 1xTAE buffer and 1.00g agarose powder (UltraPure™ Agarose-1000, ThermoFisher, Perth, UK). The solution was brought to boil before adding 5 µL SYBR™ Safe DNA Gel Stain (ThermoFisher, Perth, UK). The liquid solution was poured into the gel cast and the well ‘template’ was added before leaving the gel to set. The gel, was later inserted into the gel dock station and immersed in the remaining 1xTAE buffer. 20 µL of 50 bp DNA step ladder (Merck, Dorset, UK) was pipetted into the first well as the gel control. 3.4 µL of gel loading dye (Purple 6X Gel Loading Dye Purple, New England BioLabs, UK) and 16.6 µL of amplified DNA product were added into each of the respective wells. 80 V was applied across the electrodes for 60 minutes (PowerPac Basic, BIO-RAD, UK).

The gels were visualised using the Syngene PXi machine and Gensys V.1.5.00 software (SYNGENE, Fisher Scientific, UK). For agarose DNA visualisation the respective setting was selected; the gel was inserted into the reader; and the placement was adjusted as necessary to capture an image of the resulting bands. The size of the product was determined relative to the control ladder bands, refer to Figure 2-8. Bands in the size range of the expected product, suggest correct amplification (Lee *et al.*, 2012).

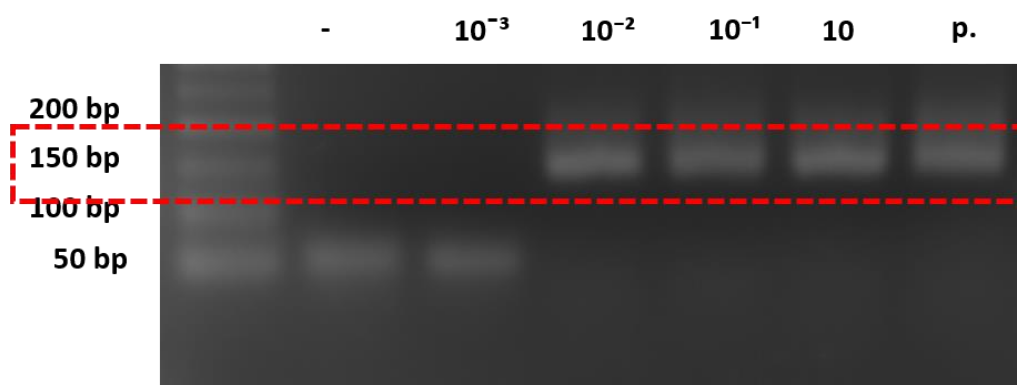


Figure 2-8: Gel electrophoresis of PPAN qPCR amplicons. Image captured depicts bands of amplified qPCR product from samples containing serial dilutions (10 to 10<sup>-3</sup> ng/μL) of plasmodium falciparum genomic DNA (gDNA). Size of amplified product is determined against the reference DNA ladder (first lane), ‘-’ denotes the negative control, whilst ‘p’ denotes positive control (10<sup>-2</sup> ng/μL gBlock DNA).

## 2.2 The Paper Device

The standard methods described in earlier sections were modified to transfer the DNA extraction, LAMP and amplicon detection onto the Paper Device platform. Section 2.2 describes the methods used to conduct detection of *plasmodium* and *schistosoma* DNA using the developed diagnostic tool (the Paper Device). Amplicon detection on the Paper Device is achieved by LF strip read-out, interpretation of results from LF strips are explained in following sections. Design changes made to the diagnostic cassette, in order to accommodate changes in procedure and user feedback are discussed. Furthermore, fabrication and assembly processes used to manufacture the Paper Device are described. Finally, heating systems to conduct LAMP in the diagnostic cassette are highlighted.

### 2.2.1 Overview of Diagnostic Method

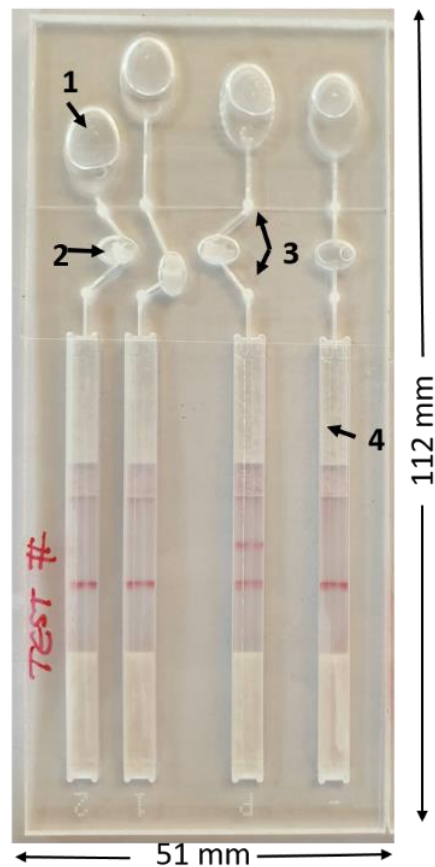


Figure 2-9: Example of the diagnostic cassette. The labels highlight key components of the cassette: 1- The finger pumps, the buffer chambers which produce fluid flow when pushed; 2- amplification chambers, where molecular reagents and DNA are inserted for amplification; 3- valves, included to hold reagents in their respective chambers until fluid flow is initiated; 4- LF strips for visual read out of amplification results.

The Paper Device is a diagnostic tool which enables LAMP to be conducted and results interpreted out with the usual laboratory environment (Reboud *et al.*, 2018), eliminating the need for an expensive qPCR machine. Prior to processing on the printed paper origami device (see Figure 1-14 and Figure 2-10), the sample specimen was lysed and DNA was bound to magnetic beads. The DNA sample is purified and eluted into the diagnostic cassette by use of the paper channels - an example of the diagnostic cassette is shown in Figure 2-9. LAMP was conducted by heating the diagnostic cassette to the appropriate temperature (e.g. 60 °C). Finger pumps (1), were used to push the amplified solution from the amplification chambers (2), towards the LF strips integrated into the plastic cassette (4). Incorporation of tagged molecules in the LAMP primers enables the qualitative result of amplification (positive/negative) to be interpreted from the LF strip in the cassette. The methods associated with this process are discussed further in subsequent sections.

### 2.2.2 Sample Processing & DNA Extraction

The process on paper (illustrated in Figure 2-10) follows the DNA extraction protocol stated in Section 0, from the lysis step ① until completion of the binding step ⑤. Following step 5, the first wash was conducted in the Eppendorf tube by adding 40 µL of Wash Buffer and flicking the bottom of the tube to disperse the magnetic beads (Step ⑥ & ⑦). The tube was then placed on the magnetic rack to sediment the magnetic beads. Removing the tube from the rack, the MZ beads were pipetted from the bottom of the tube and placed onto the sample spot of the wax printed paper origami device (Step ⑧-⑩). The final two washes were completed on the paper origami device by folding the Wash section under the sample spot ⑨ and slowly pipetting 80 µL of Wash Buffer on top of the MZ beads ⑪. By allowing a droplet to form over the MZ beads, the wash buffer and contaminants are pulled through the paper channel to the adsorbent disposable pad below, successive droplets were added until exhausting the 80 µL. Next, the paper origami device was folded into the elution orientation and 30 µL of Elution Buffer was pipetted onto the sample spot (Steps ⑫-⑭). The isolated DNA in elution buffer passes through the Elution Channels to be absorbed by the Paper Tabs in the Amplification Chambers of the plastic cassette. Using a clean pipette tip, the Paper Tabs were pushed into the Amplification Chambers. Downstream processing follows the method in Section 2.1.3.5. The primer mix and Mastermix (ISO-004) were added to the Amplification Chamber ⑮, then sealed with adhesive film ⑯ and the cassette was placed in the custom heat block at 65°C for 30 minutes ⑰. After amplification, the finger pumps were used to transfer the amplified product onto the LF strips for detection. The method of detection and read-out will be further discussed in the following section.



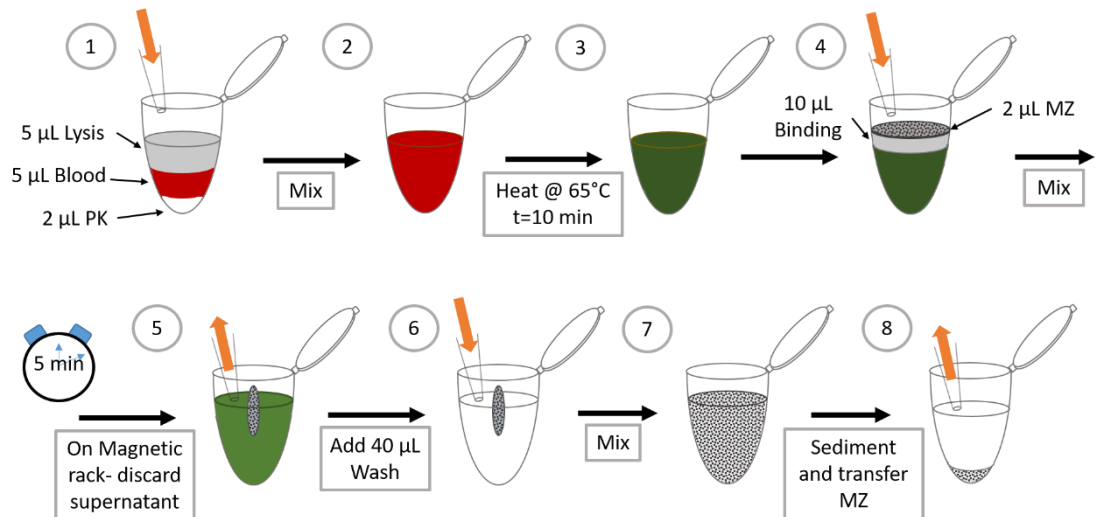
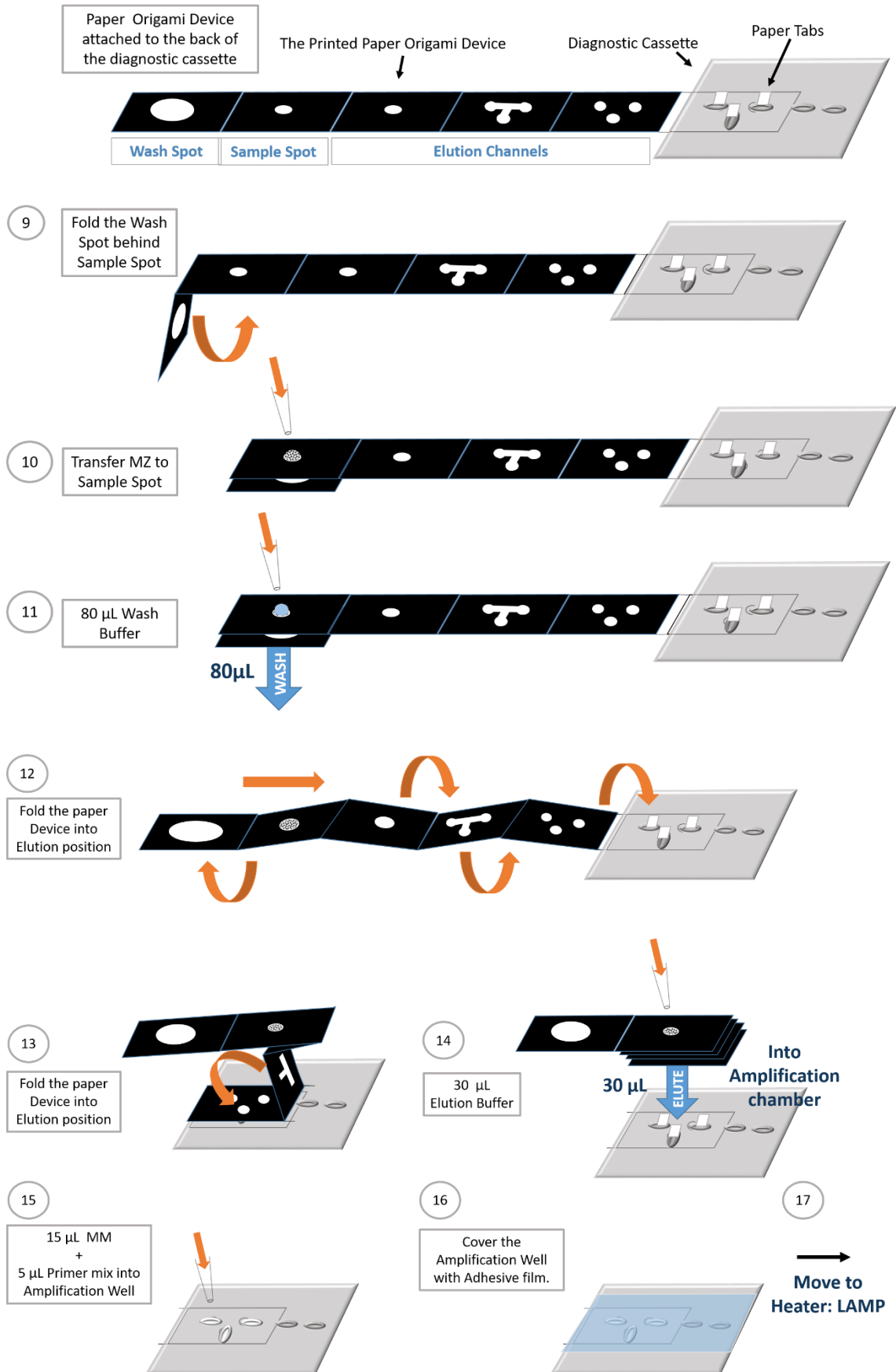


Figure 2-10: Preparation of finger drop blood sample for processing on the Paper Device. Unless otherwise stated the reagents for sample preparation were obtained from the Promega MagaZorb® Kit. First the Blood sample was lysed (1)-(3). The DNA was bound to MZ using the Binding Buffer (4) and left for 5 minutes at room temperature, mixing at 2 minute intervals. The tube was placed on the magnetic rack and supernatant was removed (5). The first wash was conducted in the tube (6) - (7) before transferring the DNA bound to MZ to the paper microfluidic device for downstream processing (8)-(10) (Figure continues on the following page). Wash Buffer was pipetted on top of the MZ beads on the sample spot to complete washing (11). The paper was folded into the elution position and the Elution Buffer was pipetted on top of the MZ beads; eluted DNA was captured by the paper tabs (12)-(14). Molecular reagents were pipetted into the amplification wells and covered with adhesive film, before placing the cassette in the custom heat block to conduct LAMP (15)-(17).



### 2.2.3 Amplification & Molecular Detection in the Diagnostic Cassette

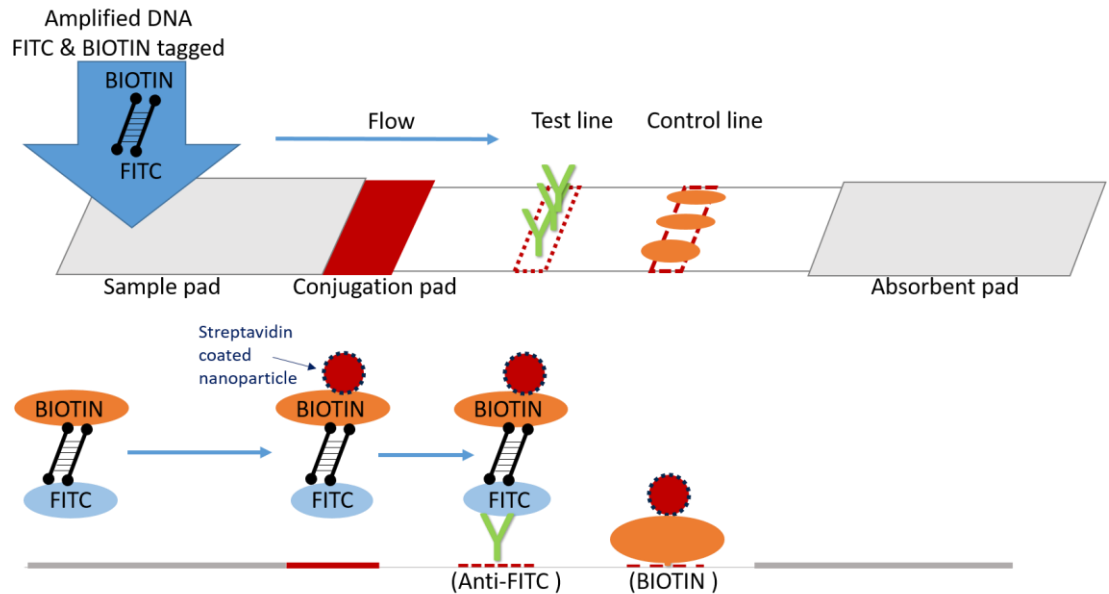


Figure 2-11: The LF strips detect presence of FITC and biotin complex, molecules incorporated into the double stranded DNA LAMP amplicons. The biotin in the amplified product binds to the streptavidin coated gold nanoparticles embedded in the conjugation pad. The FITC binds to the anti-FITC embedded in the Test line. Incorporation of both FITC and biotin in the LAMP amplicons result in gold nanoparticles being captured at the Test line (producing a red band). The remaining gold nanoparticles continue to flow down the LF strip and are captured at the Control line.

LAMP is conducted inside the Amplification Chambers of the diagnostic cassette (see Figure 2-9). The cassette was placed inside a custom designed heat block (shown in Figure 2-20), to enable LAMP to be carried out using a standard dry-heat bath. After amplification, the finger pumps were squeezed to push the amplified sample towards the LF strips. LF strips were purchased from Ustar Biotechnologies (Hangzhou, China). The Loop Primers (LPR5F & LPF5B) are tagged with FITC and biotin molecules, during amplification the molecules are integrated into the double stranded DNA amplicons. The LF strips detect presence of the FITC and biotin complex; created during amplification (Cui *et al.*, 2012). Figure 2-11 illustrates the LF strip method of detection. The amplified product flows from the sample pad, down the LF strip by capillary action (Li and Steckl, 2019). The biotin in the amplified product binds to the streptavidin coated gold nanoparticles embedded in the conjugation pad. The amplified product continues to flow towards the absorbent pad. When passing over the test line (not visible), the FITC, also within the amplicons, binds to anti-FITC doped test line. With the FITC bound to test line and biotin bound to the gold nanoparticles, the test line becomes red in presence of the modified LAMP DNA amplicons. The remaining gold nanoparticles continue to flow down the LF strip and are captured at the immobilized

streptavidin control line, resulting in two red lines. In negative samples, the FITC and biotin molecules will bind to their respective target surface; however in failure to produce amplicons with FITC and biotin complex, no gold nanoparticles will be captured at the test line, resulting in a single red control line (Reboud *et al.*, 2018).

#### 2.2.4 Interpretation of Lateral Flow Strip Results

The interpretation of possible results presented by the LF strip are illustrated in Figure 2-12. A red line at the test line and control line indicates a positive result (amplicons are present). A red line at the control line and absence of a test line indicates a negative result (amplicons are not present). In absence of the control line, regardless of the result in the test line, the LF strip result is invalid.

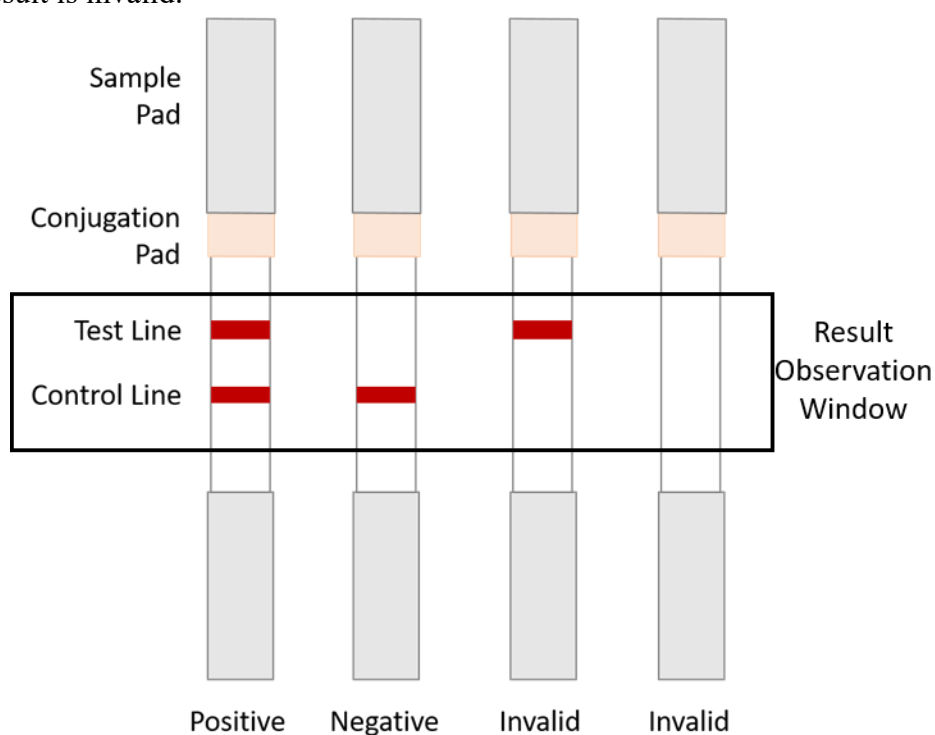


Figure 2-12: Interpretation of the amplification result using a LF strip. A red line at the test line and control line indicates a positive result. A red line at the control line and absence of a test line indicates a negative result. In absence of the control line (regardless of the presence of a band in the test line), the test is invalid.

### 2.2.5 Dilution of Amplicons on LF strips

Finger pumps in the Paper Device containing 80  $\mu\text{L}$  of nuclease free water were used to push the amplified sample toward the LF strip in the cassette. To assess whether dilution of the amplified sample effects the LF results, LAMP was conducted using the ABI machine, and then the amplified samples were serially diluted and added to the LF strips for read out. 0.01 ng/ $\mu\text{L}$  of plasmodium genomic DNA was amplified using protocols stated in Section 2.1.3.5.3 for 40 cycles using the ABI machine. The amplified samples were serially diluted (from the raw amplified sample down to 100,000X dilution of the amplified sample). 10  $\mu\text{L}$  of each sample was pipetted onto the sample pad of the LF strip, followed by two drops of wash buffer (supplied with LF strips). The LF strips were left for 10 minutes before reading (See Figure 2-13). Water was used as a NC for both isothermal amplification and running LF strips.



*Figure 2-13: Effect of dilution of LAMP amplicons on LF read-out. LAMP was conducted using the qPCR machine, the amplified samples were serially diluted and added to the LF strips with two drops of Wash Buffer (supplied with the strips). The LF strips are marked with their respective sample, Water (-), LAMP negative control ( $\text{H}_2\text{O}$ ), serially diluted amplified samples: 100,000X dilution (-5), 10,000X (-4), 1,000X (-3), 100X (-2), 10X (-1) and A is the original amplified solution.*

Both negative control samples (labelled, H<sub>2</sub>O & -); 100,000X (labelled, -5) and 10,000X (labelled, -4) serial dilutions produced results corresponding to a negative result on the LF strips. The 1,000X diluted sample (labelled, -3) produced a faint reading on the test line. The 10X and 100X dilutions (labelled, -2 & -1) did not appear to effect the result interpreted from the LF strip. Up to 100X (-2) dilution of the amplified product should not produce false negative readings on the LF strips. The maximum volume of water available to push the amplified sample from the Amplification Chamber towards the LF strip was 80 µL, which equates to a 4.2X dilution of the reaction volume. Therefore, the dilution is within the detection range and should not affect the Paper Device LF strip results.

### **2.2.6 Interpreting results in the Diagnostic Cassette**

Both negative and positive control reactions were incorporated into the diagnostic cassette for the final field trial (described in detail in Chapter 4). The LF strip results of these controls were involved in determining the result of the diagnostic test. Examples of positive, negative and invalid results obtained from diagnostic cassettes run in the final field trials are illustrated in Figure 2-14. To determine a result for the test, LF strips must show that: the NC (-) = negative; PC (P) = positive; and provide a valid result (positive or negative) for the test sample (1). A diagram depicting the image of the diagnostic cassette run in the field is shown next to the image for ease of interpreting the result in print. The first cassette ① shows a positive result: NC (-) = negative; PC (P) = positive; test = positive; overall = positive. A negative result is shown in the second cassette ②: NC= negative; PC= positive; test= negative; overall = negative. Diagnostic cassettes (③-⑥) show examples of invalid tests, the faults are circled in blue. ③: NC= invalid; PC= invalid; test = positive; overall = invalid. ④: NC= negative; PC= negative; test= negative; overall = invalid. ⑤: NC= invalid; PC= positive; test = positive; overall = invalid. ⑥: NC= positive; PC= positive; test = positive; overall = invalid.

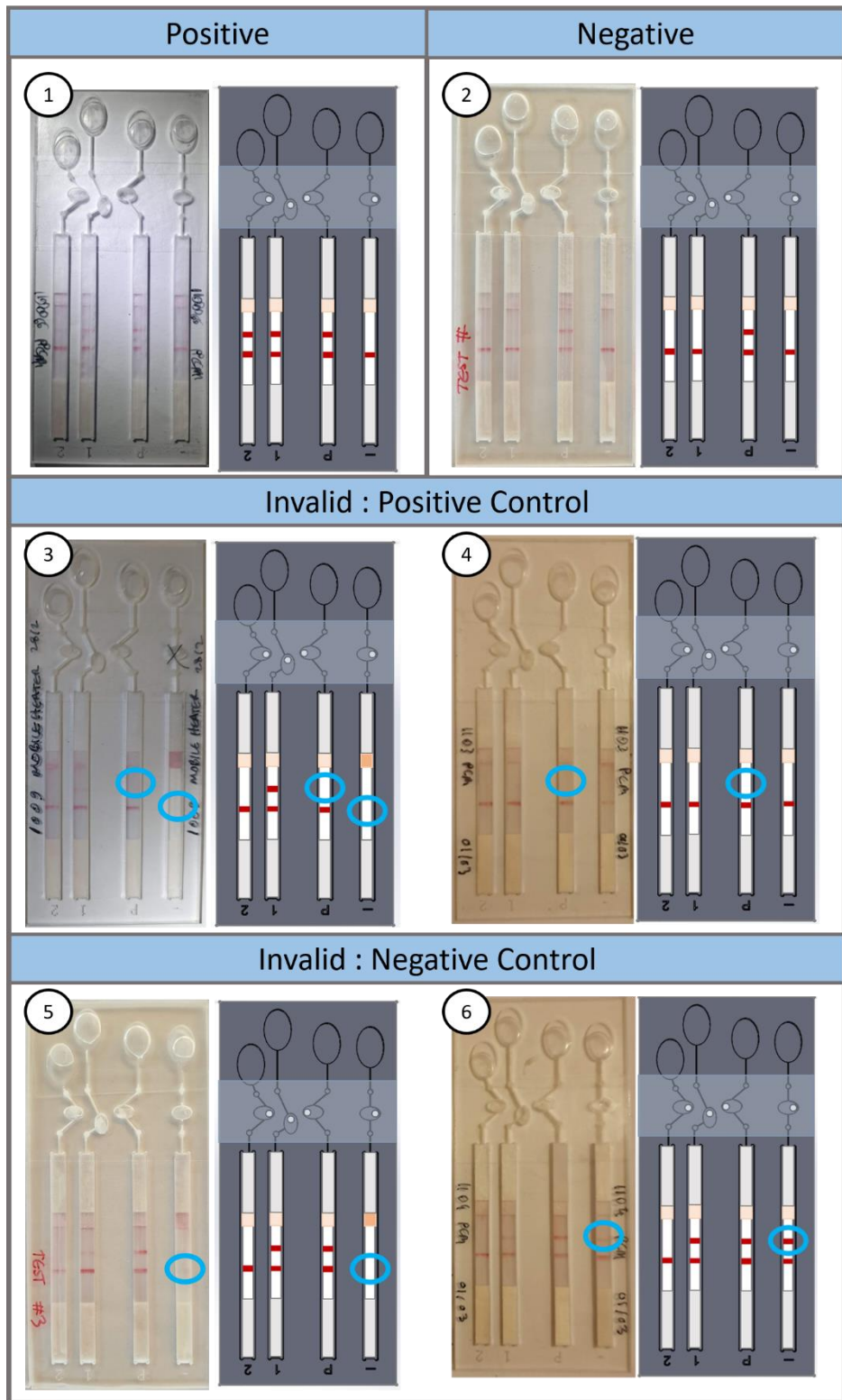


Figure 2-14: To determine the results from the Diagnostic Cassette, the results of the test PC and NC strips (marked P & - on the cassette respectively) must be acknowledged with the test result (marked I on the cassette). A positive result is depicted in the first diagram (1), NC= negative, PC= positive, I= positive, overall: positive. A negative result is shown in (2), NC= negative, PC= positive, I= negative, overall: negative. Diagnostic cassettes ((3)-(6)) show examples of invalid tests, the faults are circled in blue.

## 2.2.7 Fabrication of the diagnostic cassette

The Paper Device consists of three key components: the paper based microfluidic device for sample processing; the plastic cassette, to conduct amplification and provide a closed system; and LF strips to allow visual read-out of results. The paper microfluidic (paper origami device) was produced in the Rankine Building laboratory. The plastic cassette designed was modified from previous devices produced by Dr. Gaolian Xu – for further details refer to Section 2.2.7.2. Devices used in the laboratory were produced by laser cutting (Full Spectrum Laser H-Series Desktop CO<sub>2</sub> Laser).

### 2.2.7.1 Paper based microfluidics

The fabrication of the paper origami device was performed without specialized facilities. Necessary equipment includes: filter paper (GE Healthcare Whatman® Filter paper: Grade 1 Circles, Fisher, UK), a solid ink printer (ColorQube 8570, Xerox) and a standard hot plate. The paper based microfluidic device was designed using CorelDRAW graphics suite. Figure 2-15 shows various geometries, designed to accommodate different diagnostic devices. The geometry was modified to accommodate for the number of tests (targets) to be completed per device and hence the device geometry. Each variant of the paper origami device encompasses a number of panels to complete DNA purification and elution: the wash panel, the sample spot, the elution channels and the placement panel.

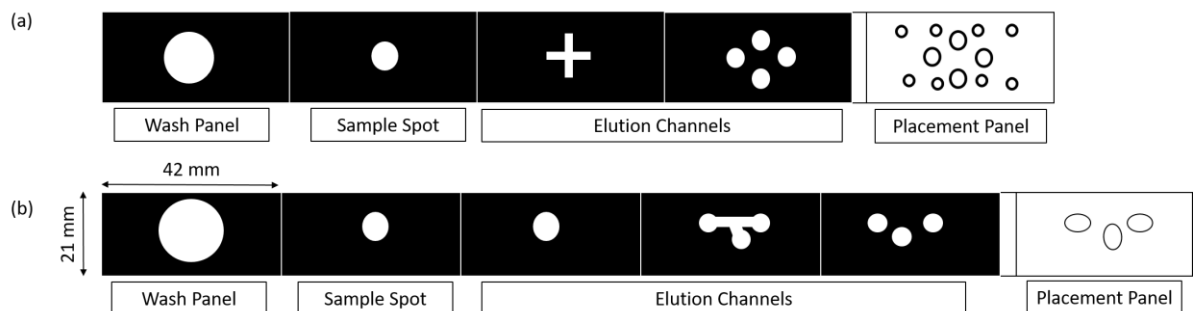


Figure 2-15: Paper based microfluidic device: (a) used to test x4 targets (b) used to test x3 targets on the diagnostic cassette. Each design includes: a wash panel; a sample spot for application of the sample; elution channels, to guide fluid flow from the sample spot to the amplification chamber; a placement pad, to simplify attachment to the diagnostic cassette.



The design was printed onto the filter paper with the solid-ink printer. The wax (ColorQube Ink, Xerox) forms a hydrophobic layer on the filter paper. Placing the paper onto a hot plate at 110°C for 5 minutes, melts the printed wax, diffusing through the paper to produce the hydrophobic pattern through the sheet of filter paper (Yang *et al.*, 2012). When folded appropriately, the ink-free regions of the device come together to form a 3D paper channel. This allows reagents and extracted DNA to flow from the sample spot through the elution channels to the amplification chamber of the diagnostic cassette.

#### **2.2.7.2 Plastic cassette**

The plastic cassette was designed using CorelDraw and Solidworks, Figure 2-16(a) depicts the cassettes used through successive field trials. Multiple field trials were conducted throughout this project (described further in Chapter 4), the Paper Device design was altered to accommodate changes in test procedures, and to modify features to improve usability and test outcomes (discussed further below). The design was imported into (Full Spectrum Laser RetinaEngrave) for laser cutting. The 2 mm poly(methyl methacrylate), PMMA (Stockline Plastic, Glasgow, UK), was laser cut by passing the laser over the design twice at the calibrated power and speed (4.00 and 100.0 respectively). After the preliminary field trial – using cassettes depicted in Figure 2-16(a) ‘SM singleplex’ and ‘Original Malaria multiplex’, a hard plastic backing was added to the design to make the cassette more durable for field use. The design files were sent to Epigem Ltd (Redcar, UK), for manufacturing by computer numerical control machining for use in successive field trials. Using the ‘PPAN & SM integrated controls’ design for reference (See Figure 2-16(b & c)), the geometries remain the same for both device editions; however, the total depth of the field device (c) was increased by 0.5 mm with the addition of the PMMA backing.

The original malaria multiplex cassette (Figure 2-16(a), used in the first field trial) was designed by Dr Gaolian Xu; and the singleplex *S. mansoni* cassette (also used in the first field trial) was modified from the original multiplex design. The cassettes were laser cut from 2mm PMMA and comprised of; 3x7 mm oval finger pumps; 2x2 mm circular amplification wells; and rectangular LF strip wells. Issues with cassette design identified during the first field trial:

- The finger pumps for the multiplex device were too small, pushing the wash solution became painful after processing a few samples;
- The solutions would run towards LF strips when the cassette was dropped. A hard backing was later incorporated to make the cassette more durable for field use;
- The LF strips did not fit in the rectangular wells due to the rounded edges;
- The amplification wells were too small, often the LAMP reagents spilled over the amplification well.
- The singleplex cassette had 5.5x9 mm wash chambers (finger pumps), evading problems with processing.

For the PPAN and schistosomiasis multiplex cassette (used in the second field trial), PMMA backing was incorporated into the design. Wash wells (finger pumps), and the amplification chamber were enlarged (6x9 mm and 3x3 mm respectively), the circular inlet to Wash well was cut from the PMMA backing. The distance between amplification chambers was increased to reduce risk of cross-contamination, and small circular grooves were added to the edges of the rectangular wells to produce tight fit for LF strips. Unfortunately during the secondary field trials, leaks persisted. It was concluded that issues were caused by the valves (Glass microfiber paper and mineral oil) and insufficient contact between adhesive films, most likely due to dust in-the-field.

The PPAN & SM cassette (used in the final field trial), Figure 2-16(b&c), was modified to rectify the challenges faced in the first two field trials. Oval amplification chambers were introduced and the distance between wash and amplification chambers was increased. The valves were manufactured from Parafilm® (see Section 2.2.8 for further details) eliminating leaks. Inlets for the wash and amplification chambers were created at opposing sides of the cassette to avoid overlapping multiple sheets of adhesive film in-the-field.

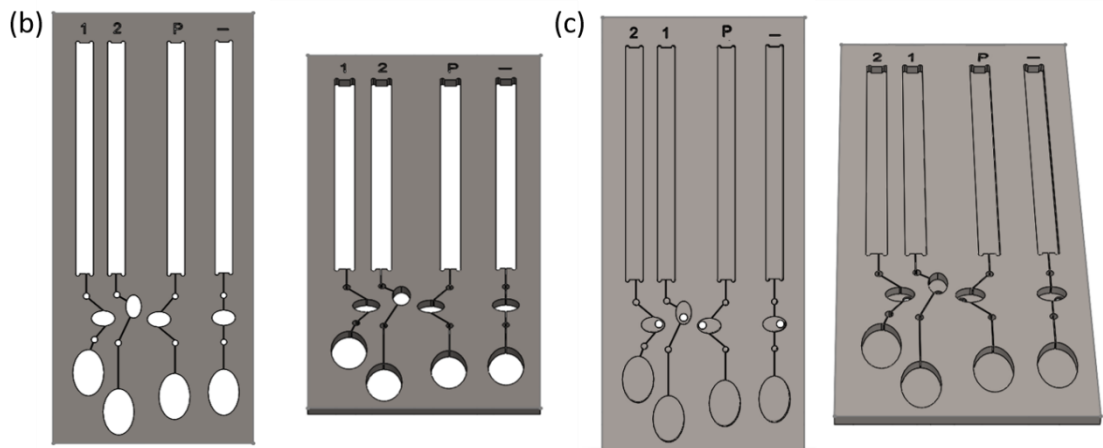
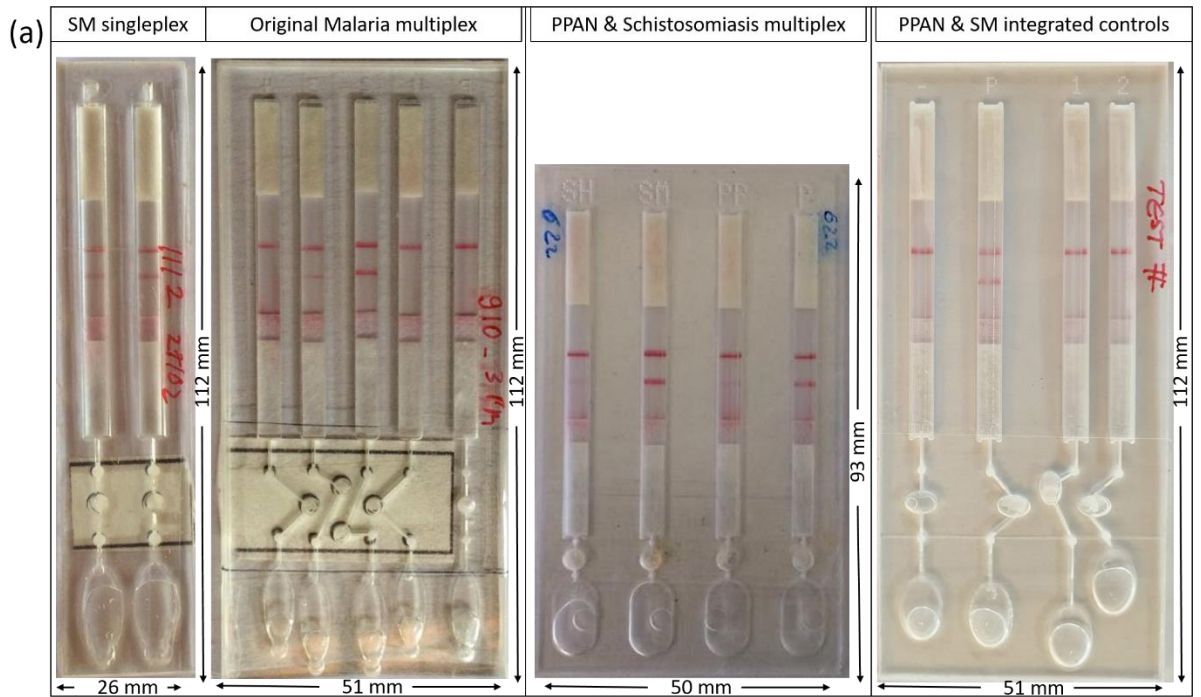


Figure 2-16: The progression of cassette design. (a) Examples of the diagnostic cassette designed and used in successive field trials. (b) The finalised design for manufacturing within the laboratory. The design required two sides of adhesive film for cassette assembly. (c) Finalised design for field trials, incorporates PMMA backing, with inlet holes cut from the amplification chambers.

### 2.2.8 Device Assembly

Construction of the Paper Device is described in Figure 2-18. The assembly instructions were created for training purposes. The process remains the same for devices manufactured for field trials, omitting steps 3 & 4. Additionally, a template of the diagnostic cassette was used to punch the holes in the Wash Chamber in step 2. In the following method, N refers to the number of devices being made, N was dependent on the experiment or trial. Changes made to protocols to facilitate up-scaling procedures in preparation for fieldwork will be further discussed in Section 2.2.9.

Prior to assembly, the plastic cassettes were cleaned with 70% ethanol and subject to sonication for 10 minutes. The cassettes were rinsed with Milli-Q® water prior to overnight drying. Before assembly, all materials (excluding the LF strips) were exposed to UV for 20 minutes for disinfection (Meechan and Wilson, 2006).

The adhesive film (Applied Biosystems™ MicroAmp™ Optical Adhesive Film, Fisher Scientific, UK) was cut to size (2N pieces). First the backing sheet of adhesive film was prepared. Placing the film (matt side facing up) under the plastic cassette, 2 mm holes were punched at the top end of each Wash Chamber using a 2 mm diameter biopsy punch (see Figure 2-18). The backing sheet was left to the side until needed. Then to begin assembly, the second (un-punched) sheet of adhesive film was secured to the front of the cassette and inlet holes were punched into the Amplification Chambers (Figure 2-18).

Valves were needed to isolate the molecular reagents in the Amplification Chamber during the amplification process. In preliminary field trials, glass microfiber paper (GF/F, Whatman®) and mineral oil (light oil, Sigma, Dorset, UK) caused high instances of leaks. Hence, Parafilm® was used to temporarily block the channels.

The Parafilm® was cut into small pieces (roughly 7 x 9 mm). A mould was manufactured to facilitate valve production (see Figure 2-17); the circles (2 mm diameter) were laser cut to replicate cassette valves. Fine tipped tweezers were used to push the Parafilm® into the wells of the mould. The Parafilm® was pressed until deformed into a globule, filling the capacity of the well. A scalpel was then used to slice excess Parafilm® from the top of the well. Using the fine tipped tweezers, the Parafilm® globules were pried from the mould and moved to the valve of the diagnostic cassette.

The LF strips were removed from their original packaging with tweezers. They were placed face down in the plastic cassette, with the conjugation pad orientated closest to the Amplification Chamber. The cassettes were sealed using the adhesive film backing sheet and a scalpel was used to remove any excess film from the perimeter of the device. Nuclease free water was pipetted into the Wash Chambers and sealed with adhesive film. An additional piece of film was kept to seal the Amplification Chambers at the time of use.

Small strips of filter paper (GE Healthcare Whatman® Filter paper: Grade 1 Circles, Fisher, UK), were cut and placed in the Amplification Chambers. Finally, the paper based microfluidic device was attached to the back of the diagnostic cassette using double sided tape; the design printed on the placement panel of the strip align with the inlets to the Amplification Chambers.

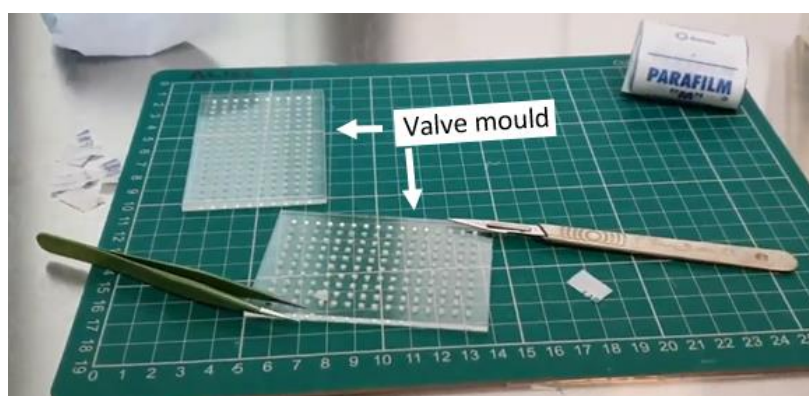


*Figure 2-17: Making the Parafilm® valves using the custom valve mould plate. The tweezers were used to push the Parafilm® globules into the circular wells (mimicking valves) in the plastic valve mould. The scalpel was used to slice the excess Parafilm® from the top of the well. The globules were then removed from the mould and inserted into the diagnostic cassette.*

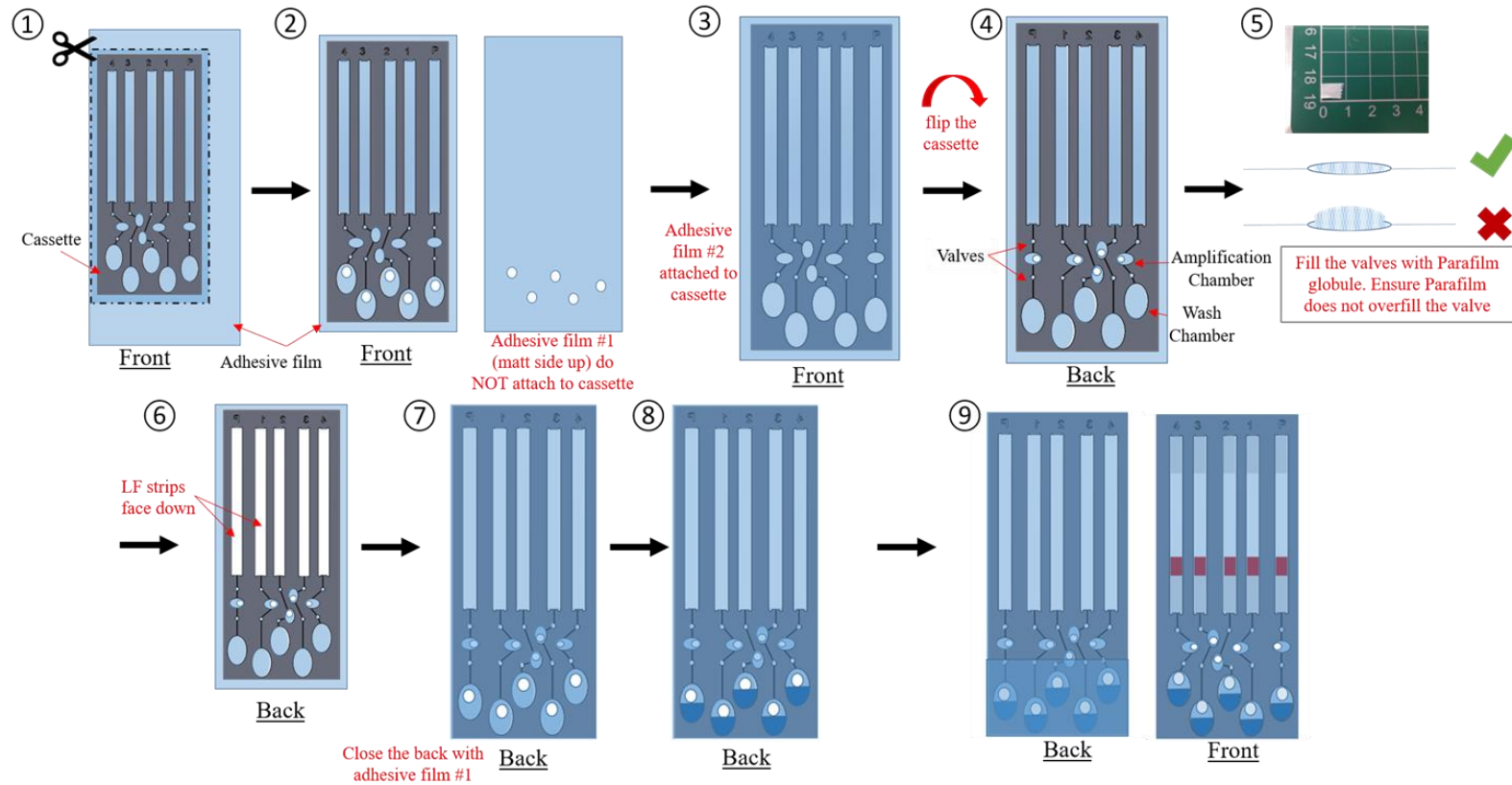
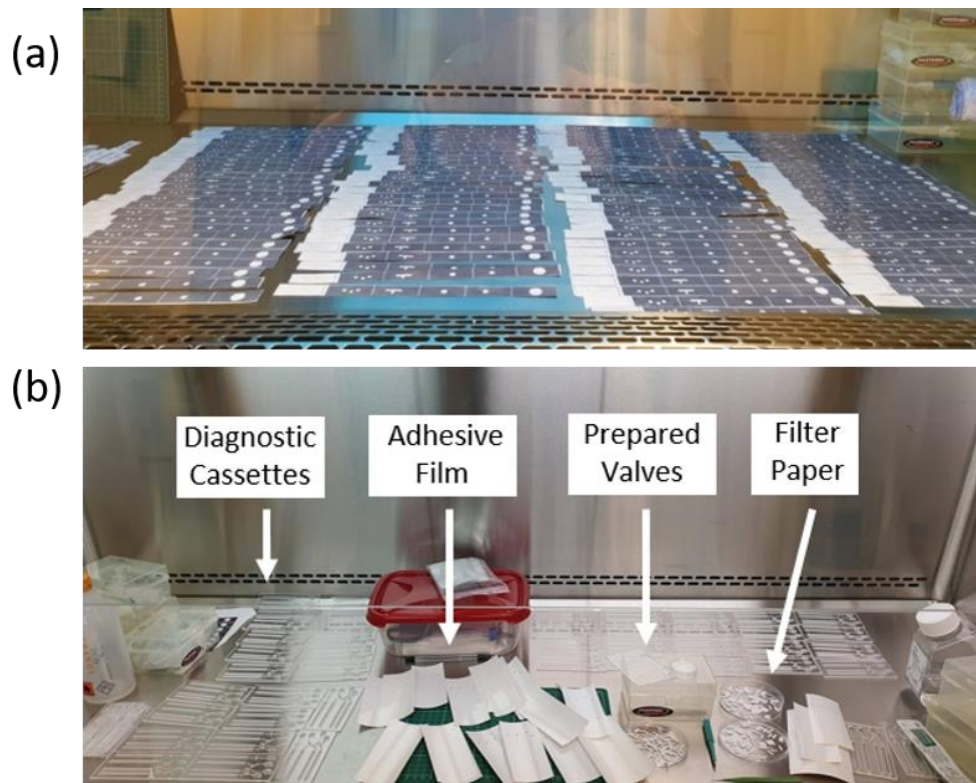


Figure 2-18: Assembly of the diagnostic cassette; diagram modified from materials used for training purposes. Steps ① & ② describe fabrication of the cassette front, the adhesive film was prepared and kept aside until needed. Steps ③ & ④ describe fabrication of the cassette backing (this step is omitted from assembly of field devices). ⑤ & ⑥ Describes creation of Parafilm valves and insertion of LF strips. ⑦ The cassette is closed using the prepared backing film; ⑧ & ⑨ The wash chambers were filled with 80 $\mu$ L nuclease free water and closed using excess adhesive film (omitted from field devices). Step ⑨ shows the finished cassette, an extra piece of adhesive film is needed to close the amplification chamber after processing.

### 2.2.9 Device Assembly for the Field Trials

Bulk manufacturing of the Paper Device for fieldwork required modifications to be made to the assembly protocol, to create a more efficient workflow. Outsourcing the fabrication of the plastic cassettes was the most significant change. However, this caused loss of control as to when the cassette would be manufactured. The average time of assembly per diagnostic cassette was 65 minutes. The preparation of materials reduced the assembly time per device to approximately 10 minutes. Where delivery of equipment was delayed, the change in assembly protocol and preparation of necessary materials expedited device assembly.



*Figure 2-19: Device assembly. (a) The printed paper origami devices exposure to UV in preparation for use in the field. (b) Set-up in preparation for manufacturing of the paper Device for field trials. The cleaned diagnostic cassettes were arranged alongside the pre-cut adhesive film with pre-punched inlets, prepared valves and paper tabs (filter paper). The Diagnostic cassettes were manufactured inside a flow hood to allow exposure of all equipment to UV before use and ensure a clean environment during preparation to decrease risk of contamination from external DNA.*

The adhesive film was cut to size (xN pieces), N refers to the number of devices. Using a laser cut template, the 2 mm diameter inlets were punched in the position of the Wash Chamber. The paper origami devices were printed and heated as per Section 2.2.7.1, double sided tape was applied to the placement panel and the strips were exposed to UV (See Figure 2-19 (a)). Additionally, filter paper pieces used to ‘catch’ the DNA extract, were prepared (10 x 2 mm). All pieces of the adhesive film and paper origami devices were stored in sterile containers until assembly. The remains of the film sheet; used to cover the inlets of the device, were also prepared and stored in sterile bags until time-of-use in the field.

Valves were manufactured using Parafilm® as stated in Section 2.2.8. Filling the plate created valves for 20 devices. Once the plate was filled, the Parafilm® globules were removed from the mould, dipped into a thin layer of mineral oil and stored in a clean Petri dish until the time of assembly.

Assembly of the cassettes follows the stages described in Section 2.2.8. The cassettes were assembled in batches of 20 (set-up depicted in Figure 2-19). The pre-made valves were inserted into the cassettes, any excess oil (for storage purposes) was removed using a cotton bud. The LF strips were inserted into the chambers and for ease of assembly, the small pre-cut pieces filter paper were fitted in the Amplification Chambers before sealing the back of the devices with the prepared backing film. In preliminary trials, air travel caused the water from the Wash Chamber to leak between the chambers of the diagnostic cassette. For this reason, the nuclease free water was aliquoted into 15 mL corning tubes for storage during travel and added to the Wash Chamber at the time of use.



### 2.2.10 Heating

A custom heat block – shown in Figure 2-20 - was designed using SOLIDWORKS 2016 x64 Edition (Figure 2-21). The designs were given to the School of Engineering Mechanical Workshop (University of Glasgow), who manufactured the heat block. To simplify fabrication of the wells, six 15 mm thick aluminium plates were drilled (3 x 53 x 42 mm) to fit the plastic cassette. Each of the six plates were fixed with a bolt to assemble the custom heat block (see Figure 2-20(b)). Manufacturing in this manner also facilitated cleaning and decontamination of the heat block.

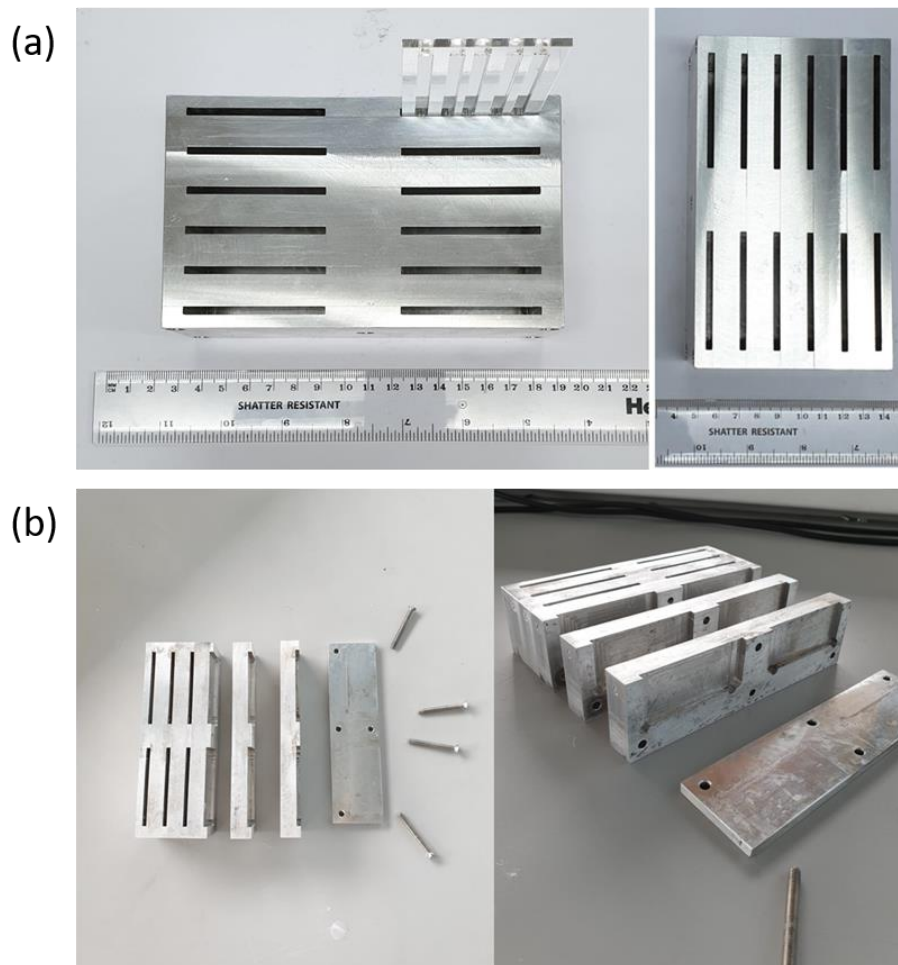


*Figure 2-20: The custom heat block to house the diagnostic cassettes for heating inside the dry heat bath; fabricated by Thomas Dickson and Stephen Monaghan in the school of Engineering Mechanical Engineering Workshop. (a) The custom heat block, placement of diagnostic cassette is demonstrated. (b) Assembly of the heat block. The aluminium plates were fabricated to be assembled and fixed together with bolts. The design enables the block to be disassembled, facilitating disinfection after use.*

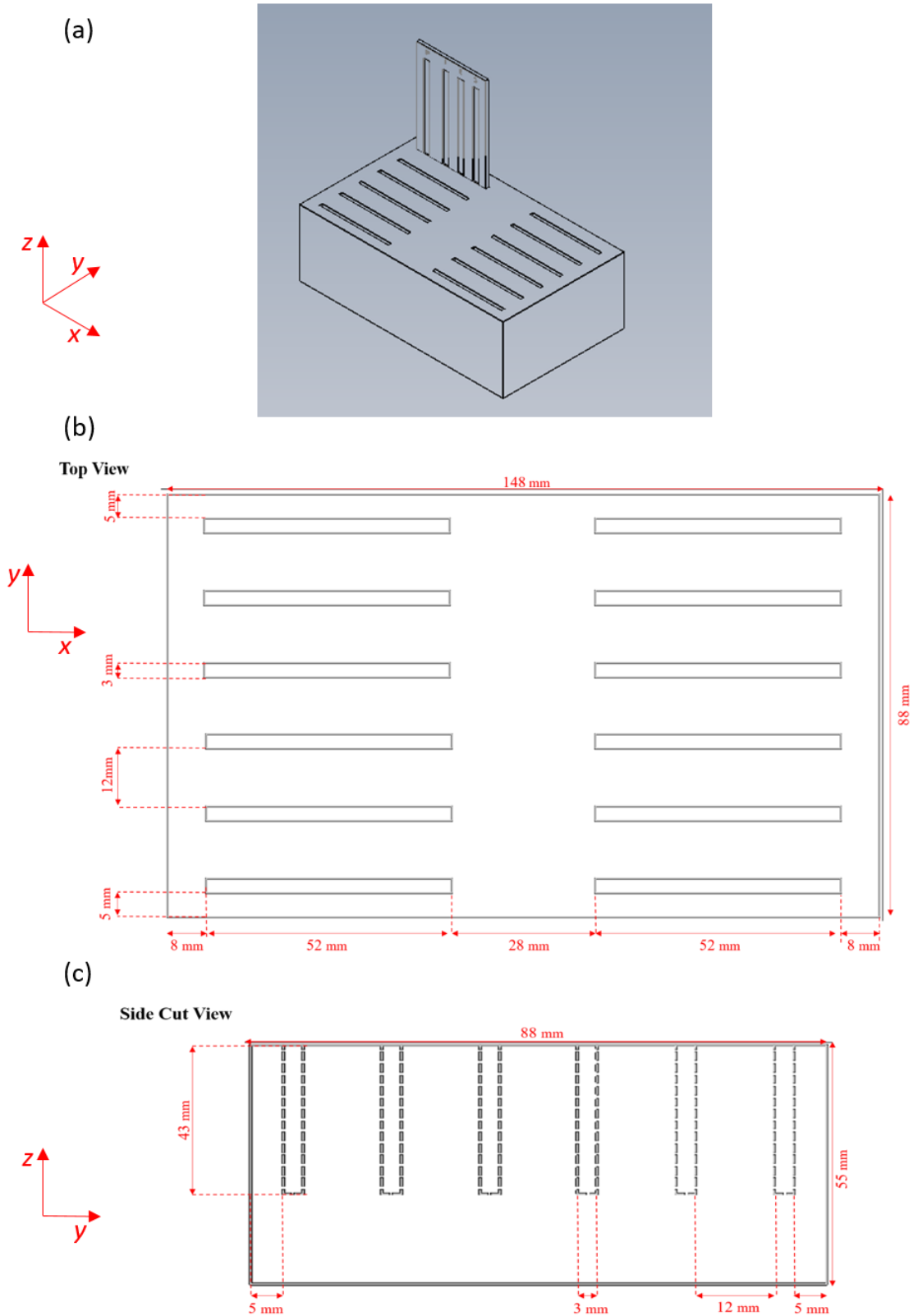


Figure 2-21: Design figure of the custom heat block manufactured to heat the Paper Device diagnostic cassette. (a) 3D design rendered on SOLIDWORKS, the design depicts a diagnostic cassette placed in the heat block. (b) Top view of the heat block design with dimensions. (c) Side cut view of the heat block design with dimensions.

A J type Thermocouple (RS Pro Type J, RS Ltd, Glasgow, UK) was used to assess heating within the plastic cassette. The negative control channel was widened to allow the lead of the thermocouple to be threaded through the channel and placed into the Amplification Chamber. The thermocouple was sealed in the plastic cassette using optical adhesive film. 25  $\mu$ L of TE buffer was pipetted into the Amplification Chamber, engulfing the thermocouple. The Amplification Chamber was sealed once again using adhesive film. Once connected to the PicoLog6 Thermocouple Data Logger (Pico Technologies, St Neots, UK), the diagnostic cassette was placed into the pre-heated block. The set up in the laboratory is as shown in Figure 2-22 (b). Using the custom designed heat block, optimum amplification temperature was achieved within three minutes (Figure 2-22 (a)). Proving that this method of heating is efficient whilst also allowing many tests to be run simultaneously.

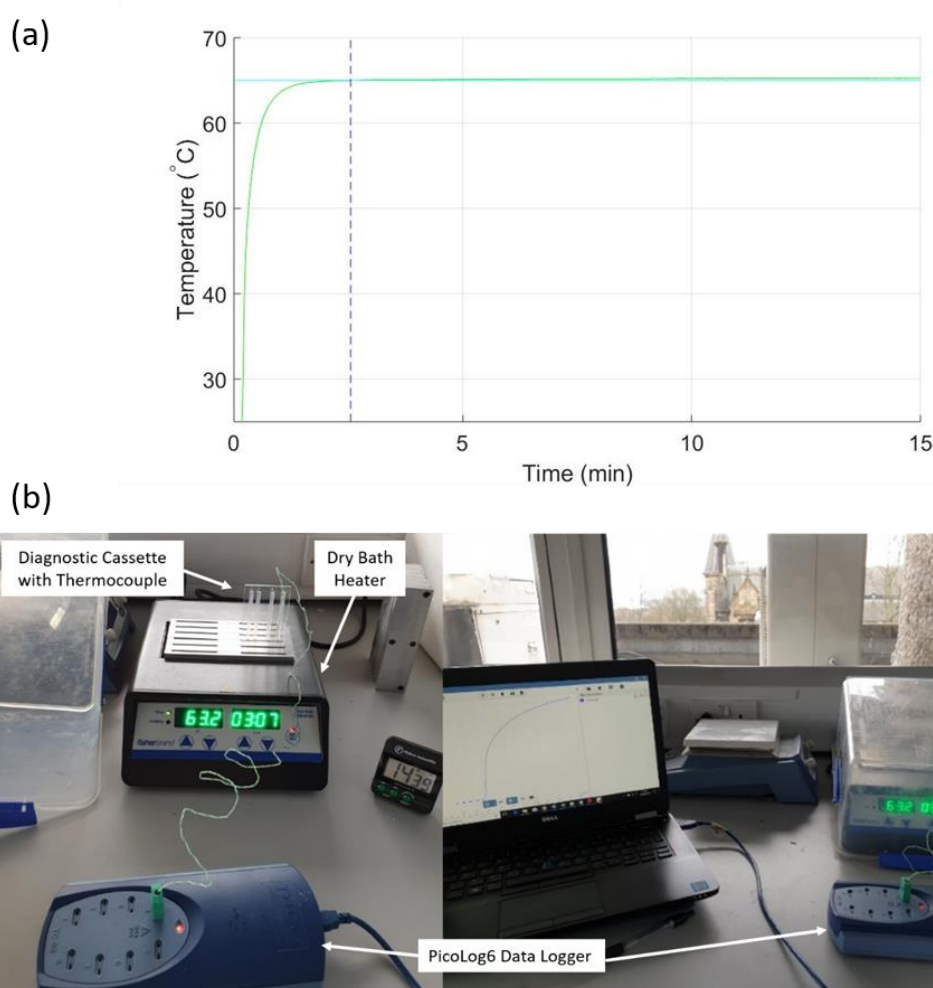


Figure 2-22: The laboratory set up to observe heating of the paper diagnostic cassette. (a) Thermal data collected from the thermocouple placed inside the diagnostic cassette (green line); the optimum temperature required for LAMP (blue horizontal line); time to reach optimum temperature (purple dotted line), 2 min 33 s. (b) The diagnostic cassette was modified to incorporate a thermocouple into the amplification well. Thermal data was collected by the PicoLog6 Thermocouple Data Logger. The box was placed over the heating set-up to mimic working set-up in the field.

## 2.3 Statistical Analysis

Statistical analysis was achieved using Prism 6 Software. Student's t-test were conducted to assess statistical relevance of amplification times for calibration curves (see significance of  $p$  values in Table 2-3). Student's t-tests were used to assess statistical relevance of qPCR Ct values and LAMP Ctt values ( $p < 0.05$  was statistically significant). Gaussian distribution of data was assumed, however, where the variance between data sets was statistically significant (determined by F test), Welch's t-test (unequal variance t-test) was applied to calculate  $p$  values.

*Table 2-3: Symbols for statistical analysis. Ranges of  $p$  values, statistical significance and associated symbols for graphical representation.*

$P$ value	Symbol	Statistically Significant
$p \geq 0.05$	ns	No
$0.05 > p \geq 0.01$	*	Yes
$0.01 > p \geq 0.001$	**	Yes
$0.001 > p \geq 0.0001$	***	Yes
$p < 0.0001$	****	Yes

## 2.4 Summary of the Method Development

This chapter comprises methods used in the research presented in this thesis and the development of methods and processes which were required to carry out research. A summary of the developed methods are listed below.

- The standard MagaZorb<sup>®</sup> procedure for DNA extraction from fresh blood using magnetic beads was modified to process smaller volumes of blood (5  $\mu$ L), and further developed to process blood samples stored on FTA cards. The modified DNA extraction method was then translated onto the paper fluidic for incorporation into the POC Paper Device work flow.
- Standard methods for qPCR and LAMP were defined and carried out on the standard amplification platform, prior to translation into LAMP within the POC Paper Device cassette.
- The interpretation of Paper Device results were defined and the limits of lateral flow strip detection due to amplicon dilution were identified.
- Variants of the Paper Device design were defined, modification in design were made to accommodate for changes in test procedures, and to improve usability and test outcomes in-the field. Additionally the design and monitoring procedure of a heating solution for the POC Paper Device was defined.
- The Paper Device assembly method was defined and modified for upscaling production for field-trials.

## Chapter 3: Development of the *S. mansoni* assay

In this chapter, the motivation for pursuing detection of *S. mansoni* DNA using LAMP and the reported *S. mansoni* genes targeted for molecular diagnosis are discussed. The DNA extraction methods for different *S. mansoni* specimen will be described. Finally, the development of molecular reagents for integration into the POC Paper Device platform to detect *S. mansoni* DNA will be explained.

### 3.1 Introduction

Malaria and intestinal schistosomiasis share similar epidemiological distributions, presenting challenges to public health and socio-economic development in sub-Saharan Africa (Ndeffo Mbah *et al.*, 2014). Surveillance data indicates that co-infections of malaria with NTDs – such as schistosomiasis - are common (Mwangi *et al.*, 2006; Kabatereine *et al.*, 2011), implying that integrated interventions for schistosomiasis and malaria are likely to maximize cost- effectiveness and sustainability of disease control efforts (Kabatereine *et al.*, 2011). Previous iterations of the Paper Device have successfully detected *plasmodium* DNA within patient samples in laboratory trials (Xu, Nolder, *et al.*, 2016). The increased likelihood of individuals presenting with malaria and bilharzia co-infection will enable the detection of *S. mansoni* and *plasmodium* DNA in the same regions, thus, developing molecular reagents to multiplex the detection of *S. mansoni* DNA into the existing POC platform has the potential to expand the diagnostic capability of the Paper Device.

#### 3.1.1 Molecular Assays

Both PCR, qPCR and LAMP have been used to identify *S. mansoni* infections from a variety of human samples, including stool and serum (Ibironke *et al.*, 2011; Fernández-Soto *et al.*, 2014, 2019; Song *et al.*, 2015). Two gene regions have been targeted by the majority of investigators (Pontes *et al.*, 2002; Pontes *et al.*, 2003; Wichmann *et al.*, 2009; Abbasi *et al.*, 2010; Johannes Enk *et al.*, 2012; Lodh *et al.*, 2013; Fernández-Soto *et al.*, 2014, 2019; Song *et al.*, 2015; García-Bernalt Diego *et al.*, 2019). The first is the 121-bp tandem repeat sequence (sm1-7) which was identified in 1990, it is a highly repeated DNA sequence within the schistosome genome (Hamburger *et al.*, 1991) and thus offers interesting opportunities to maximise assay sensitivity. The sm1-7 gene sequence (GenBank Accession No. M61098.1) has been associated as a target sequence to identify *S. mansoni* DNA in infected snail specimens and human plasma, serum, faeces and urine (Pontes *et al.*, 2002; Pontes *et al.*, 2003; Wichmann *et al.*, 2009; Abbasi *et al.*, 2010; Johannes Enk *et al.*, 2012; Lodh *et*

*al.*, 2013; Song *et al.*, 2015). Wichmann *et al.* report detection of human and murine *S. mansoni* infection from serum samples using PCR to target the 121-bp tandem repeat gDNA region, sm1-7 (Wichmann *et al.*, 2009). LAMP primers were later developed by Abbasi *et al.* to provide rapid molecular identification of infected snails (Abbasi *et al.*, 2010). Additionally Song *et al.* report detection of active murine *S. mansoni* infection, using LAMP to detect circulating cell free parasite DNA within serum samples, using a disposable microfluidic cassette (Song *et al.*, 2015).

The second *S. mansoni* region frequently targeted is the mitochondrial minisatellite DNA region, which was identified in the mid-nineties (Pena *et al.*, 1995). The mitochondrial DNA (mtDNA) region (GenBank Accession No. L27240), has been targeted, using LAMP to identify schistosome infections within murine and human specimens (Fernández-Soto *et al.*, 2014, 2019; García-Bernalt Diego *et al.*, 2019). Fernández-Soto *et al.* have reported successful detection of *S. mansoni* from the stool and urine of infected individuals in Brazil, using LAMP which targets mtDNA repeat region of the *S. mansoni* parasite (Fernández-Soto *et al.*, 2014, 2019; Gandasegui *et al.*, 2018). The molecular methods referenced report greater sensitivity than direct parasite observation by KK diagnosis. This suggests that successful integration of molecular reagents to target *S. mansoni* DNA into the POC molecular Paper Device platform, could result in a more sensitive POC diagnostic tool for *S. mansoni*. The referenced studies monitor changes in fluorescence, or visible colour changes to determine amplification results. As a result, modification of the LAMP primers were required to allow LF strip read-out on the Paper Device platform (as described in Section 2.2.3).

### **3.1.2 Target specimen**

The molecular methods referenced in the previous section detect *S. mansoni* DNA within a variety of murine and human specimen. Both of the target genes have been detected in urine, blood and stool specimen, thus, the three specimen were considered for *S. mansoni* DNA detection using the Paper Device. Processing urine for DNA extraction requires a number of centrifugation and drying stages (Sarhan *et al.*, 2015), consequently, stool and blood specimen were chosen for sample processing. With respect to whole blood specimen, the method of DNA extraction to detect *plasmodium* DNA from whole blood will be implemented - refer to Section 2.1.1.1 & 2.2.2 for further details. Stool is a comparably more complicated sample to process than blood, however, there are a range of faecal processing methods which reduce the expense and volume of equipment required and as a result are

better suited for sample preparation in-the-field (Glinz *et al.*, 2010; Becker *et al.*, 2011; Barda *et al.*, 2015).

To increase likelihood of *S. mansoni* DNA identification from a stool specimen a few methods for extracting parasite ovum from faecal specimens were trialled. Common methods of parasite ovum separation from faecal samples include sieving and flotation techniques (Glinz *et al.*, 2010; Barda *et al.*, 2013b). The Mini-FLOTAC method is a flotation technique which enables direct observation of parasites from faecal samples (approx. 2g) and has been tailored for POC use (Maurelli *et al.*, 2016). The method involves specimen homogenisation in an appropriate flotation solution within the Fill-FLOTAC vessel, followed by sample insertion into the Mini-FLOTAC cassette for direct parasite observation using a standard microscope (Barda *et al.*, 2013a). Flotation of parasite ovum within the Mini-FLOTAC cassette results in the floating ova aggregating to the viewing window. The circular Mini-FLOTAC disk facilitates rotation of the viewing window to the viewing platform, and as a result, translation of the parasite ova to the viewing platform, this provides a cleaner sample to facilitate detection of parasite ova using a microscope. A detailed explanation of the Mini-FLOTAC method is referenced in Section 7.7 of the Appendices. The Mini-FLOTAC method requires less manual steps than alternative flotation and sieving techniques (Barda *et al.*, 2013b; Nikolay *et al.*, 2014), thus, was a promising technique to facilitate extraction of *S. mansoni* ova from stool in-the-field.



### 3.2 Chapter Aims & Objectives

The aim of this chapter was to produce a method for the detection of *S. mansoni* DNA on the POC Paper Device, ready to take forward for field trials. This included understanding and optimising the method of recovery of *S. mansoni* DNA from simulated clinical samples; and determining an appropriate molecular assay to transfer onto the Paper Device. To instigate field based detection of *S. mansoni* DNA using the Paper Device, factors such as sample selection, DNA extraction methods and assay design, had to be determined and optimised. The objectives of this Chapter include:

- Determine an appropriate stool substitute for *S. mansoni* ova extraction experiments;
- Design and produce a tool to allow transfer of *S. mansoni* ova from the Mini-FLOTAC device for downstream DNA processing – To enable extraction of *S. mansoni* ova from stool specimen to be processed on the Paper Device.
- Select and optimise DNA extraction methods to recover DNA from *S. mansoni* ova; cercariae stored on FTA cards; and contrived stool specimen.
- Optimisation of published assays targeting different *S. mansoni* gene regions, to allow detection of LAMP amplicons on LF strips – To facilitate the expansion of the Paper Device for POC molecular detection of *S. mansoni* infections.
- Determine amplification of DNA from a variety of *S. mansoni* specimen (genomic parasite, ovum and cercariae DNA) –evidence of detection throughout the schistosome life-cycle, would suggest applicability of detection in an array of samples.

### 3.3 Materials and Methods

#### 3.3.1 *S. mansoni* Gene Targets

The identified target sequences are specific to each primer set used, the published molecular assays target two areas of the schistosome genome, and these include *S. mansoni* mitochondrial (mt) and chromosomal genomic (g) DNA sequences. The industry standard DNA Gene Fragments (gBlocks), were obtained from IDT (Iowa, USA) for assay optimisation. The lyophilized gBlocks were re-suspended following manufacturer's instructions and stored in small aliquots (50 µL of 1 ng/ µL) to minimise freeze-thaw cycles. Serial dilutions (0.1-0.001 ng/ µL) made from the stock gBlocks were stored in a similar manner.

##### 3.3.1.1 *mtDNA target gBlock*

The mtDNA target sequence dsDNA gBlock, was ordered from IDT. The schematic in Figure 3-1 shows the 202 bp mtDNA minisatellite gBlock sequence (GenBank Accession No. L27240) which was used as positive target DNA for amplification using *S. mansoni* mtDNA (SM) assay (described in Section 3.3.5).

```
5' TCGTCTATAGTACGGTAGGTGGGTAAGGTAGAAAATGTTGTTTGTGGATT-  
3' AGCAGATATCATGCCATCCACCCATTCATCTTTTACAACAAACAACTAA-  
  
-CTGTATTTTCGTGCAGATAAGATGTTTGTAGTCTCTACTTGGCAGTGGTAGA-  
-GACATAAAGCACGTCTATTCTACAAACATCAGAGATGAACCGTCACCATCT-  
  
-AGTGTTTAACTTGATGAAGGGGATAGGTGTATGTTCTGTCCTTTGTTTTTTG-  
-TCACAAATTGAACTACTTCCCCATCCACATACAAGACAGGAAACAAAAAC-  
  
-AATAGTGGTTTCGGTTTTGTTTTTTTTTTTTGGTGGGGTTAAAGTATAG3'  
-TTATCACCAAAGCCAAAACAAAAAACCACCCCAATTCATATC5'
```

Figure 3-1: Sequence of *S. mansoni* 202 bp gBlocks Gene Fragment to act as a positive control target for SM primer mix, targeting mtDNA, mitochondrial minisatellite region (GenBank Accession No. L27240).

### 3.3.1.2 gDNA target gBlock

The sm1-7 gDNA target sequence dsDNA gBlock, was ordered from IDT. The schematic in Figure 3-2 shows the 125 bp sequence – sm1-7, the *S. mansoni* gDNA tandem repeat unit (GenBank Accession No. M61098.1) used as a positive target for amplification using *S. mansoni* gDNA (SMchrom) assay.

```
5' ATGATCTGAATCCGACCAACCGTTCTATGAAAATCGTTGTATCTCCGAAA-  
3' TACTAGACTTAGGCTGGTTGGCAAGATACTTTTAGCAACATAGAGGCTTT-  
  
-CCACTGGACGGATTTTTATGATGTTTGTTTTAGATTATTTGCGAGAGCGT-  
-GGTGACCTGCCTAAAAATACTACAAACAAAATCTAATAAACGCTCTCGCA-  
  
-GGGCGTTAATATAAAAACAAGAATGA3'  
-CCCGCAATTATATTTTGTTCCTTACT5'
```

Figure 3-2: Sequence of *S. mansoni* 125 bp gBlocks for SMchrom positive control target, targeting *S. mansoni* gDNA tandem repeat unit, sm1-7 (GenBank Accession No. M61098.1).

### 3.3.2 Stool Substitute



Figure 3-3: Stool substitute. A recipe for faecal substitute was modified from that acquired from NHS virology department, Glasgow. The stool substitute was spiked with beads and *S. mansoni* ova to conduct preliminary extraction trials.

Safety approval was not granted for experiments using stool in the Biological Class II Laboratory within the School of Engineering due to constraints on disposal methods. For this reason, modifications to *S. mansoni* egg extraction protocols from stool samples were carried out using a stool substitute (see Figure 3-3). The faecal substitute recipe obtained from Glasgow NHS virology department consisted of: 2.2 g of Bran Flakes and 3 mL boiling water. The recipe was modified by addition of a ½ tablespoon of refried beans to improve the consistency of the sample.

### **3.3.3 Egg Flotation Cassette**

The Mini-FLOTAC technique has been developed for extraction of *S. mansoni* ova from stool (Barda et al., 2013a) and was designed for observation of parasite eggs in a sealed observation disk. For the purpose of our study, the Mini-FLOTAC method (developed in the University of Naples), was adapted to enable the removal of parasite ova from the flotation disk (Mini-FLOTAC). The egg flotation cassette used in this study was designed to imitate the Mini-FLOTAC method in an open cassette. The PMMA flotation cassette was designed in Solidworks (see Figure 3-4) and manufactured by Epigem Ltd (an image of the device is shown in Figure 3-5).

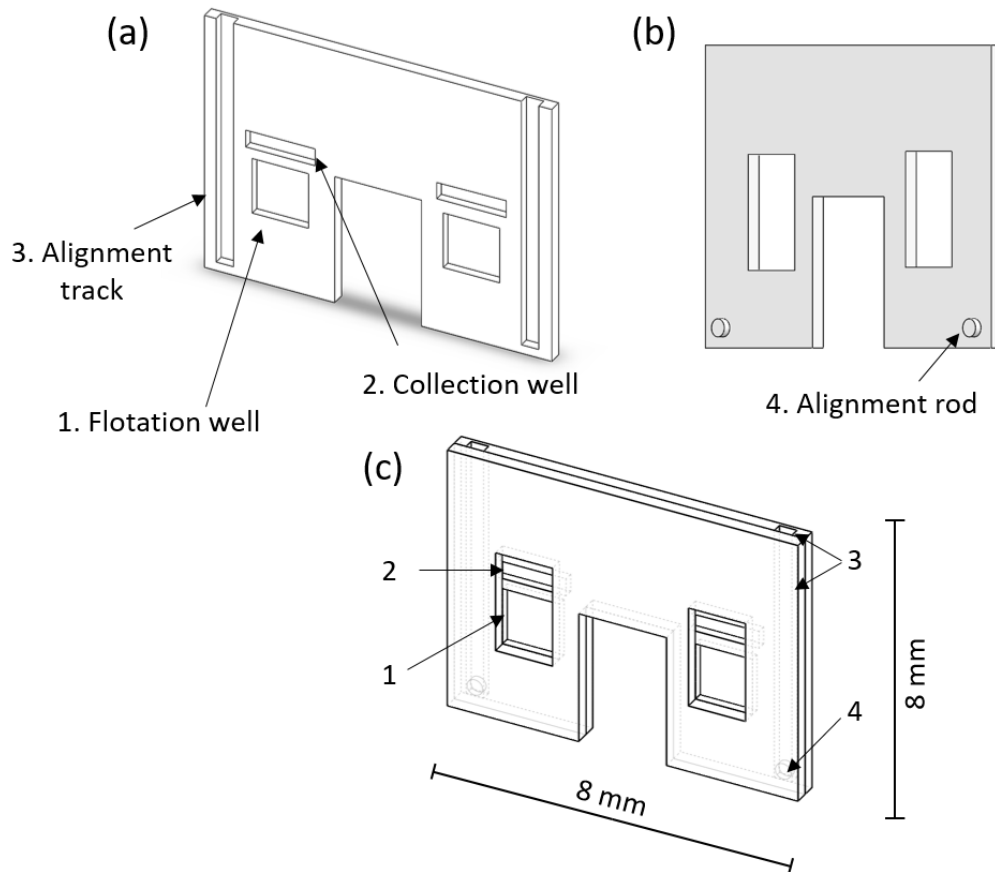


Figure 3-4: Egg flotation cassette design. The cassette was designed on Solidworks to imitate the function of a mini-FLOTAC device. The open design was created to enable floating debris in the flotation well (1) to be transferred to the collection well (2) by sliding motion of the lid. The concentrated solution was then able to be transferred from the collection well for downstream processing. (a) The cassette base, with sample wells and alignment track. (b) The cassette lid with alignment rods to facilitate sliding motion. (c) Design of the assembled cassette.

### 3.3.4 *S. mansoni* DNA extraction

In addition to using dsDNA gBlocks for assay optimisation and sample processing, gDNA was sourced from *S. mansoni* adult worms, and DNA was extracted from *S. mansoni* egg and cercariae samples to test the molecular assays on different stages of the parasite lifecycle.

#### 3.3.4.1 *Schistosome genomic DNA*

Schistosome adult worm gDNA used as a control in downstream experiments was provided by SCHISTO\_PERSIST in the IBAHCM (University of Glasgow). The DNA was extracted from a single adult male *S. mansoni* worm, eluted in nuclease free water. Presence of DNA was confirmed by qPCR before delivery. The schistosome DNA sample was separated into 20  $\mu$ L aliquots and frozen until the time of use to minimise freeze-thaw cycles.

#### **3.3.4.2 DNA extraction from *S. mansoni* ova**

A liver from an *S. mansoni* infected mouse was obtained from the Manchester Collaborative Centre for Inflammation Research (MCCIR) after sacrifice. Following advice from the MCCIR, the liver was sieved through a tea strainer with sterile PBS, stored in 50 mL conical flasks and frozen until the time of use. The PBS solution containing *S. mansoni* ova was thawed and a small volume (~ 5 mL) was poured into a Petri dish and topped up with PBS. The eggs were picked from the PBS solution under 3X magnification of a stereoscopic microscope (Swift Optical Instruments, USA) using a 200  $\mu$ L pipette and stored in 50  $\mu$ L aliquots. The number of eggs stored in an Eppendorf ranged from 1-20 eggs per 50  $\mu$ L. The Eppendorf tubes were labelled with date and the number of eggs present and were refrigerated until the time of need.

DNA extraction from *S. mansoni* ova was carried out using the Promega MagaZorb<sup>®</sup> kit. The manufacturers' protocol for DNA extraction from fresh and frozen tissue was modified to improve yield of DNA from *S. mansoni* ova. The Eppendorf's containing 50  $\mu$ L aliquots of PBS and *S. mansoni* ova were centrifuged at maximum speed (12500 rpm) for one minute using the Gusto mini centrifuge (Fisher Scientific, UK). Following centrifugation, 40  $\mu$ L of the PBS was removed from the Eppendorf tube to concentrate the solution. The sample was then subject to 'heat shock', whereby the samples were placed in a heat block at 98°C for 2 minutes, then left at room temperature to cool for a further 2 minutes and centrifuged once again. The 'heat shock' process was repeated twice more before following the Promega DNA extraction procedure referenced in Section 2.1.1.1, it should be noted that the solution is clear throughout the process due to lack of presence of blood in the sample. The concentration and purity of the extracted DNA sample was assessed using the NanoDrop<sup>™</sup> spectrophotometer (for further details refer to Section 2.1.2). Extracted DNA samples with 260/280 ratios > 1.77 were used in downstream experiments. The extracted DNA was stored on ice (if used later that day) or stored at -20°C until the time of use.

#### **3.3.4.3 DNA extraction from cercariae stored on FTA<sup>®</sup> cards**

An indicating FTA<sup>®</sup> Classic Card storing individual cercaria was donated by Dr Fiona Allan (Natural History Museum, London). The FTA<sup>®</sup> card was stored under manufacturers' recommendations with desiccant until the time of use. The indicating FTA<sup>®</sup> Card turns lighter (almost white) where a sample (individual cercaria), has been deposited.

A 2 mm diameter biopsy punch was used to remove the cercaria from the desired area of card (white area), 5 punches were obtained per spot (per cercaria). Each Eppendorf tube was filled with punches from the card equating to 3 cercariae, before adding 300  $\mu$ L of TE buffer (PH 8.0) and left for half an hour at room temperature prior to processing. After the incubation period at room temperature, 20  $\mu$ L of P.K and 200  $\mu$ L Lysis buffer was added to the Eppendorf tube which was mixed by pulse vortex, and incubated at 65°C for 20 minutes. Following heating, the solution was transferred into a clean Eppendorf tube by squeezing liquid from the pieces of FTA<sup>®</sup> Card and transferred with a pipette into the new Eppendorf tube. The succeeding Binding, Wash and Elution steps follow the method described in Section 2.1.1.1, however, the Elution volume was increased to 100  $\mu$ L. The extracted DNA samples were marked with the date and number of cercariae that the DNA was extracted from and stored on ice (if used that day), or at -20°C until the time of use.

#### **3.3.4.4 Extraction of *S. mansoni* DNA from stool**

The mini-FLOTAC technique was modified for retrieval of *S. mansoni* ova from stool samples for downstream DNA extraction. The sample homogenisation and preparation method remained true to the Mini-FLOTAC technique (Maurelli et al., 2016). The Fill-FLOTAC container – pictured in Figure 3-5, steps 1 to 4 - was used to homogenise the stool samples. Following the Mini-FLOTAC sample preparation method (Refer to Figure 3-5: Steps 1-4), approximately 2 g of stool was inserted into the plunger using a spatula. The appropriate flotation solution, 38 mL of zinc sulphate solution (FLOTAC solution FS7, specific gravity = 1.35) was added to the Fill-FLOTAC. After sufficient homogenization in the Fill-FLOTAC approximately 2 mL of the solution was transferred into the PMMA flotation cassette (referenced in Section 3.3.3) to form a meniscus above the flotation chamber (see Figure 3-5: Step 5). After sufficient time for egg flotation (10 minutes), the lid was slid across, pushing the protruding layer of FS7 solution (containing floating debris) into the collection well (Figure 3-5: Step 6). A 200  $\mu$ L pipette was used to transfer the solution into a 1.5 mL Eppendorf tube. The sample was subject to two cycles of ‘heat shock’ as described in Section 3.3.4.2, and lysis and binding steps described in Section 2.1.1.1. The DNA bound to MZ beads was transferred onto the Paper Device, after which wash and elution steps described in Section 2.2.2 & 2.2.3 were followed to conduct amplification and detection within the Paper Device cassette.

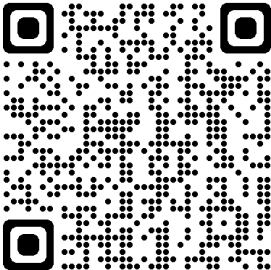
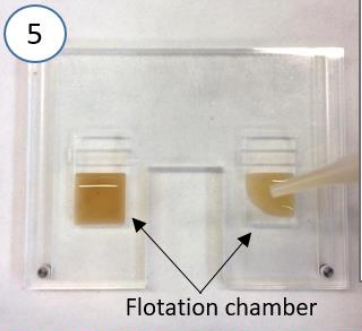
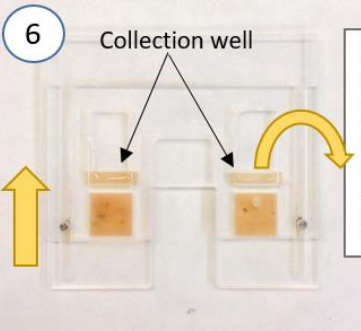
Mini-FLOTAC technique		Mini-FLOTAC technique	
[Images removed from the online document due to copyright restrictions]			
Images show the sample preparation steps 1-3 outlined in the mini-FLOTAC standard operating procedure document. The QR code links to the source document containing sample preparation images.			
			
Flotation Cassette		Flotation Cassette	
<b>5</b>  Flotation chamber	Fill the flotation chambers with homogenized sample. Leave the cassette for 10 minutes to allow flotation of eggs.	<b>6</b>  Collection well	Slide the cassette upward. Transfer the sample from collection wells into 1.5 ml Eppendorf.
<b>▲ CRITICAL STEP</b> it's important to completely fill the well, forming a meniscus above flotation chambers.			

Figure 3-5: The sample preparation for extraction of DNA from stool. Steps 1-4 follow the Mini-FLOTAC technique. The mini-FLOTAC FILL is filled with 38 mL of flotation solution, and the faecal sample is transferred into the plunger with a wooden spatula. Sample preparation is completed by homogenisation of the faecal sample in the flotation solution – the Figure is adapted from that published by Maurelli, Rinaldi and Cringoli. Steps 5 & 6 describe the modified flotation technique using the flotation cassette.



### 3.3.5 Molecular reagents

#### 3.3.5.1 *S. mansoni* Primers

A few primer sets were explored for amplification and detection of *S. mansoni* DNA. The primers and respective references are displayed in Table 3-1. The FITC and Biotin loop primer sets incorporated into the primer mix for LF strip read out were used as referenced, however, un-tagged loop primers were also used during assay optimisation, and as a controls to monitor LAMP amplification on the ABI machine.

The SM primers (Table 3-1(a)) target the minisatellite DNA region (referenced in Section 3.1.1 & 3.3.1.1). In a study carried out by Fernández-Soto *et al.*, isothermal amplification of *S. mansoni* DNA from murine stool specimen was reported using a set of four LAMP primers (Fernández-Soto *et al.*, 2014). The primer sequences published by Fernández-Soto *et al.* were modified (by Dr Gaolian Xu) to enable incorporation of loop primers (LPR5F & LPR5B) in to the target region (Figure 3-6(a)).

The SMchrom primers (Table 3-1(b)) target the sm1-7 gene sequence (GenBank Accession No. M61098.1), references in Section 3.1.1 & 3.3.1.2. The target region has been previously used to amplify *S. mansoni* DNA present within urine, plasma and serum specimens (Wichmann *et al.*, 2009; Song *et al.*, 2015). Additionally, the sm1-7 sequence has been targeted to carry out LAMP for amplification of *S. mansoni* DNA in infected snail species (Abbasi *et al.*, 2010). Due to limitations imposed by the small sequence length, the primers reported by Wichmann *et al.* were modified to incorporate Biotin and FITC tags within the internal primer set (Figure 3-6(b)). Additionally, the primer pairs (SMchrom, Figure 3-6(b)) were modified to allow short fragment (<10 bp) loop primers LPR5F & LPR5B (Table 3-1(c) - designed by Dr. Erin O'Shaughnessy) to be incorporated into the target gDNA tandem repeat unit (Figure 3-6(c)), this modified primer set is referenced as SMchromL throughout this study.

Table 3-1: *S. mansoni* LAMP primer sequences. Sources for respective primer sets are included as references within the table. Where modifications were made to the sequence, the change has been highlighted.

	Gene Target	Amplicon size & Tm	Primer Name	Sequence (5'-3')	Primer Length & Tm	Concentration per run (μM)	Reference
(a)	mtDNA minisatellite sequence GenBank Accession #L27240	202 bp 84.5°C	SMF3	TCG TCT ATA GTA CGG TAG G	19 bp, 61.0°C	0.1	(Fernández-Soto <i>et al.</i> , 2014)
			SMB3	TTA TAC TTT AAC CCC CAC C	19 bp, 60.0°C	0.1	
			SMFIP	TGC CAA GTA GAG ACT ACA AAC ATC T - TG GGT AAG GTA GAA AAT GTT	45 bp, 75.5°C	0.8	
			SMBIP	AGA AGT GTT TAA CTT GAT GAA GGG G- AAA CAA AAC CGA AAC CA	42 bp, 75.5°C	0.8	Dr Gaolian Xu – Unpublished sequence.
			SMLPR5F	[FITC]-GTC CTC TTG TTT TTG AAT	18 bp, <60°C	0.6	
			SMLPF5B	[BIOTIN]-CTG CAC GAA ATA CAG AAT C	19 bp, <60°C	0.6	
(b)	Sm1-7 tandem repeat unit GenBank Accession #M61098.1	105 bp 84.5°C	SMchromF3	GAT CTG AAT CCG ACC AAC CG	20 bp, 64.5°C	0.2	(Abbasi <i>et al.</i> , 2010)
			SMchromB3_2	AAC GCC CAC GCT CTC	14 bp, 64.5°C	0.2	
			SMchromFIP	[FITC]-AAA TCC GTC CAG TGG TTT TTT – TGA AAA TCG TTG TAT CTC CG	41 bp, 74.5°C	1.6	

			SMchromBIP	[BIOTIN]-CCG AAA CCA CTG GAC GGA <u>TTTT</u> TAT -TTT TAA TCT AAA ACA AAC ATC	46 bp, 72.5°C	1.6	
(c)	Sm1-7 tandem repeat unit GenBank Accession #M61098.1	105 bp 84.5°C	SMchromF3	GAT CTG AAT CCG ACC AAC CG	20 bp, 64.5°C	0.16	(Abbasi <i>et al.</i> , 2010)
			SMchromB3_2	AAC GCC CAC GCT CTC	14 bp, 64.5°C	0.16	
			SMchromLFIP	CCG TCC AGT GGT TTT TT – TGA AAA TCG TTG TA	31 bp, 70.5°C	0.8	Modified from Abbasi <i>et al.</i>
			SMchromLBIP	CCA CTG GAC GGA <u>TTTT</u> TAT –TTT TAA TCT AAA ACA AAC AT	39 bp, 68.5°C	0.8	
			SMchromLPR5 F	[FITC]-CATAAAAAT	9 bp, 5.6°C	0.6	Dr Erin O’Shaughnessy – Unpublished sequence.
			SMchromLPF5 B	[BIOTIN]- TCTCCGAAA	9 bp, 22.7°C	0.6	

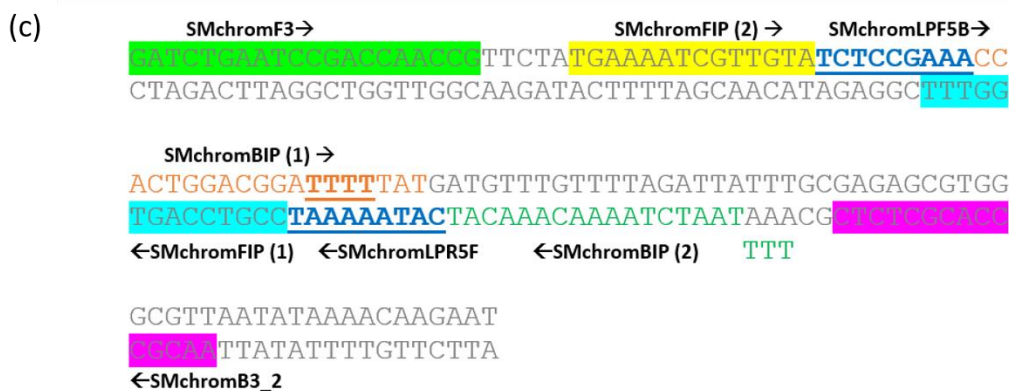
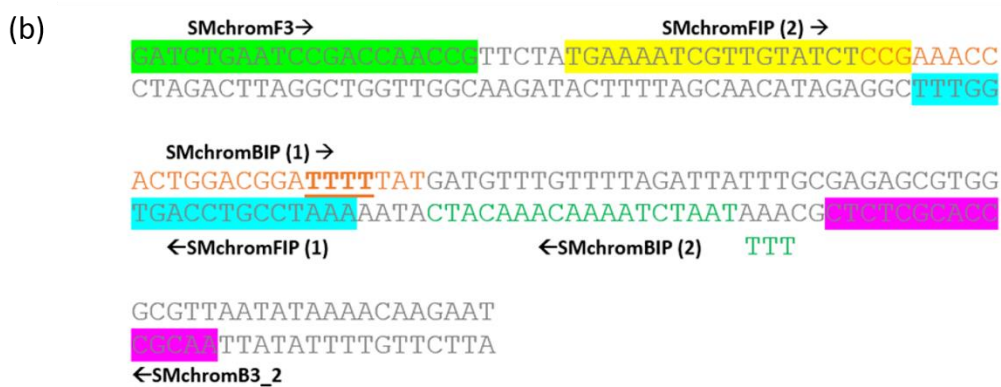
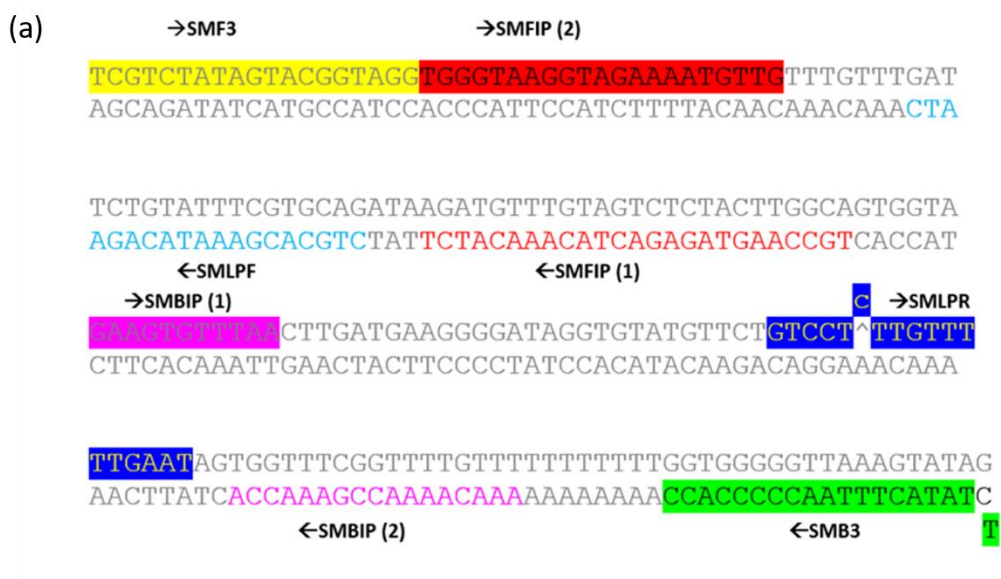


Figure 3-6: Schematics of *S. mansoni* primers within target sequence. (a) SM primer set targeting *S. mansoni* mtDNA. (b) SMchrom primer set targeting *S. mansoni* gDNA sequence, attempts to tag the internal primers (BIP & FIP) with FITC and Biotin were made to enable read-out on the LF strips. (c) SMchromL primer set, to incorporate loop primers into the SMchrom target sequence.

### ***3.3.5.2 Isothermal Mastermix***

The OptiGene Isothermal Mastermix (ISO-004) was used to conduct LAMP on the ABI machine and within the Paper Device.

Temperature trials were carried out with each assay used to amplify schistosome DNA and the optimum temperature for amplification was identified by the temperature which resulted in most efficient time to amplification (consequently the lowest C<sub>tt</sub> value). For the SM primer set the optimum temperature for amplification was 60-63°C, increasing the temperature to 65°C lead to a gradual increase of C<sub>tt</sub> (<5 minutes). The optimum temperature for amplification using the SMchrom primer set was 61°C, the C<sub>tt</sub> increased > 10 minutes when conducting amplification above 63°C. The method used to conduct isothermal amplification remains true to that stated in Section 2.1.3.5.3, however the temperature for amplification was lowered to 63°C on the ABI machine to accommodate optimal amplification conditions for both SM and SMchrom primer sets.

## 3.4 Results

### 3.4.1 qPCR

qPCR was carried out to confirm presence of DNA in extracted samples for downstream LAMP and sample preparation optimisation. Amplification of gBlocks ( $10^{-1}$  &  $10^{-2}$  ng/ $\mu$ L), adult worm (schistosome), egg and cercariae DNA was conducted on the ABI machine following the protocol in Section 2.1.3.2 for 60 cycles – see Figure 3-7(a) for fluorescence data.

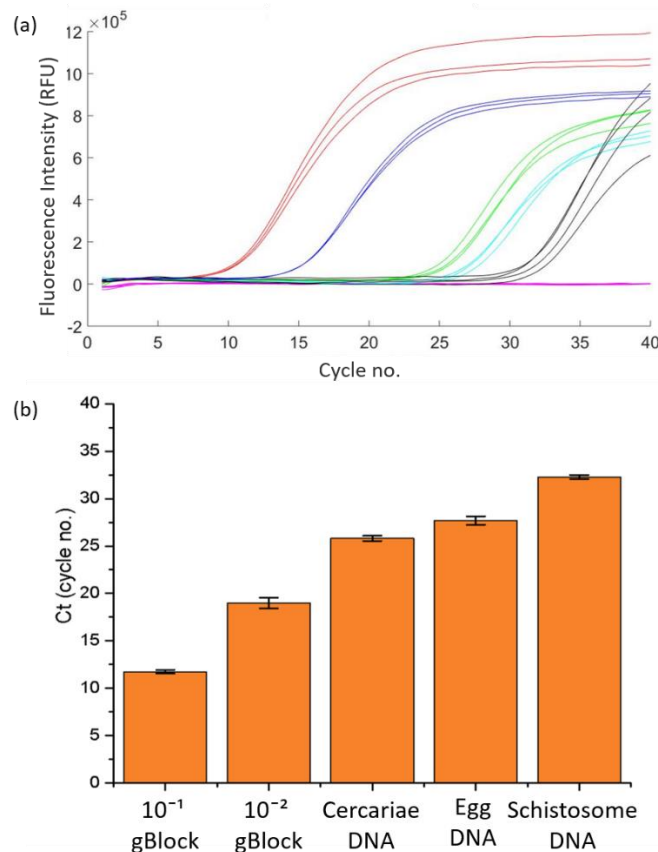
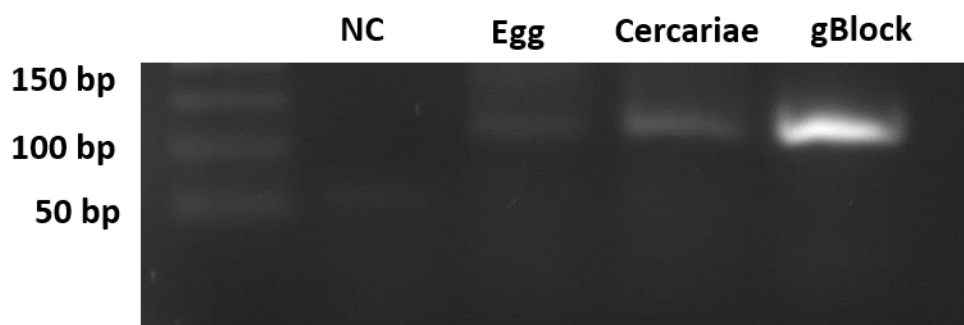


Figure 3-7: (a) The fluorescence curves obtained from conducting qPCR on a range of *S. mansoni* target DNA, serially diluted gBlocks -  $10^{-1}$  &  $10^{-2}$  ng/ $\mu$ L (red & navy blue); and extracted cercariae (green), egg (blue) and adult worm (black) DNA. There was no amplification observed from the NC (pink). (b) The mean Ct values ( $N=5$ ) obtained from conducting qPCR following the methods in Section 2.1.3.2 on a range of *S. mansoni* DNA targets. The error bars are the standard deviation of Ct values obtained for each target.

The gBlock, adult worm, egg and cercariae DNA are plotted in red & navy blue, black, blue and green respectively. To combine the target sample data, the raw fluorescence data was exported from the ABI machine and plotted using the MATLAB<sup>®</sup> code referenced in Section 7.3.1 in the Appendices. Nuclease free water was used as a no target negative control (NC) during the experiment, there was no amplification of the NC (plotted in pink). The threshold value to determine Ct values was set at 100,000  $\Delta$ Rn – to obtain the Ct at the beginning of

the exponential phase of amplification (Ririe, Rasmussen and Wittwer, 1997). The mean Ct values (11.5, 17.7, 25.8, 27.7, 32.3 cycles) for each sample is depicted in Figure 3-7(b).

The number of cycles required for amplification was significantly shorter for the gBlock DNA diluted samples (< 20 cycles), however, all *S. mansoni* DNA produced positive amplification in < 40 cycles. Amplification was confirmed by gel electrophoresis (Figure 3-8). Positive qPCR amplification confirmed that the DNA extraction method recovered a sufficient concentration of DNA for amplification and was suitable for conducting qPCR.



*Figure 3-8: Gel electrophoresis of SMchrom qPCR samples. DNA from a variety of S.mansoni target DNA samples (egg, cercariae, gBlock) sources were amplified by qPCR and gel electrophoresis was carried out to validate amplification. The intensity of the fluorescent band is proportional to the amount of product in the well. The relative intensity of bands between the gBlock and gDNA samples suggest higher concentration of DNA in the gBlock sample, this corresponds with respective Ct values.*

The increase in Ct values between gBlocks and extracted DNA samples was expected due to the high concentration of the target fragment in the synthetic samples. This was also confirmed by gel electrophoresis, where the intensity of the fluorescent band is proportional to the amount of product in the well (Shadle *et al.*, 1997), in Figure 3-8 it is clear that the gBlock sample band exhibits the greatest intensity. The qPCR results confirm that the selected qPCR primers and thus the gene target region is amplified for *S. mansoni* samples throughout the schistosome life cycle. The successful amplification throughout the schistosome life cycle suggests that the target region could be used to confirm presence of *S. mansoni* DNA in a variety of human specimen. Additionally, these results suggest that the extraction method and DNA samples are appropriate for LAMP assay trials.

*The qPCR results confirm that the gDNA gene target region is amplified for S.mansoni samples throughout the schistosome life cycle. This provides a potential to confirm S.mansoni presence in a variety of samples.*

### 3.4.2 Detection of *S. mansoni* DNA by LAMP

Detection of LAMP amplicons on LF strips in the Paper Device provides end-point amplification data. To better understand the assays during optimisation, SM, SMchrom and SMchromL FITC and biotin tagged primer sets were tested by carrying out amplification on the ABI machine to gain real-time data on amplification.

#### 3.4.2.1 SM: mtDNA target sequence

The fluorescence curves resulting from the amplification of a dilution series of gBlock DNA using SM LAMP primers is shown in Figure 3-9(a) & (b). The serial dilution of gBlock DNA was carried out to gain understanding of the lowest detectable concentration of clean gDNA. Nuclease free water was used as a no template negative control target (NC), there was no amplification of the NC – fluorescence data is presented in green in Figure 3-9(a) & (b). The raw fluorescence data was exported from the ABI machine and plotted using the MATLAB® code described in Section 2.1.3.3 and referenced in Section 7.3.1 in the Appendices. The C<sub>tt</sub> (described in Section 2.1.3.5.4) was determined for each amplified sample, the mean C<sub>tt</sub> for respective dilutions is displayed in Figure 3-9(c), as expected, the C<sub>tt</sub> values increased with successive dilutions (Applied Biosystems, 2010).

Following extraction of DNA from *S. mansoni* ova and cercariae samples (refer to Section 3.3.4.2 & 3.3.4.3 for method), isothermal amplification of gBlock, *S. mansoni* adult worm, egg and cercariae DNA was conducted on the ABI machine, following the protocol in Section 2.1.3.5.3 for 40 cycles at 63°C (refer to Figure 7-5 & Figure 7-6 in the Appendices). Amplification of the *S. mansoni* extracted DNA fell within the range of amplification times of gBlock DNA shown in *Figure 3-9*, suggesting that DNA extraction from the samples recovered sufficient DNA for the LAMP reactions.



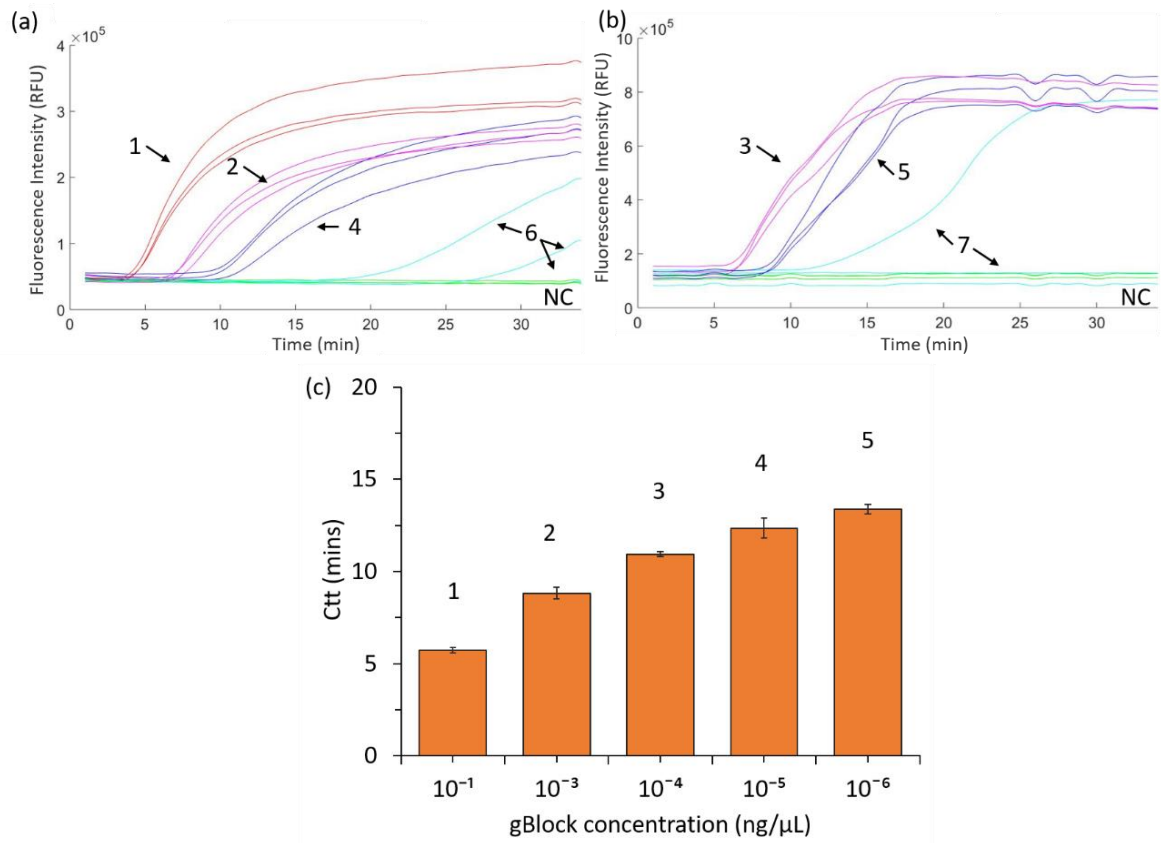


Figure 3-9: LAMP calibration data for SM gBlock dilution series. The gBlock was serially diluted and LAMP was carried out using SM primer mix. (a) & (b) The fluorescence results collected by the ABI machine monitoring real-time LAMP. The dilution concentrations  $10^{-1}$ ,  $10^{-3}$ ,  $10^{-4}$ ,  $10^{-5}$ ,  $10^{-6}$ ,  $10^{-7}$ ,  $10^{-8}$  ng/ $\mu$ L are labelled 1-7 respectively. LAMP was not successful for all sample dilutions 6 & 7, hence the results were not included in the calibration curve. (c) Graphical representation of the average Ctt value for each DNA concentration, the error bars show the standard deviation of the Ctt values obtained for the respective gBlock DNA concentration. The increase of Ctt with decreasing DNA concentration is as expected.

#### ***3.4.2.2 Development of the SMchrom: gDNA target sequence***

The development of the SMchrom primer mix was carried out using a few different B3 oligos, SMchromB3 and SMchromB3\_2, the sequences are referenced in Table 2-1 & Table 3-1 respectively. Preliminary LAMP experiments using SMchromB3 resulted in false positive amplification – refer to Figure 3-10(a), the false amplification was confirmed by melt curve analysis and gel electrophoresis Figure 3-10(b). Failure of the SMchromB3 primers prompt the development of the SMchrom primer mix using the amended SMchromB3\_2 oligo - referenced in *Table 3-1* (b). Due to the short target sequence (< 200 bp) the FITC and biotin molecules were integrated into the internal primers (FIP & BIP oligo set). Amplification was achieved with the untagged oligo sets – refer to Figure 3-10(c), however, no amplification was observed from LAMP carried out using the FITC and biotin tagged SMchrom primer set – refer to Figure 3-10(d). The results suggested that the incorporation of FITC and biotin molecules into the internal primer set inhibit LAMP. The amplified samples were later run on LF strips and both negative and positive target samples resulted in faint test lines – refer to Figure 3-10(e). No amplification was recorded by the ABI machine suggesting that hybridisation of the biotin-FITC tagged primers had occurred. The data presented in Figure 3-10(a), (c) & (d) was exported directly from the ABI software.

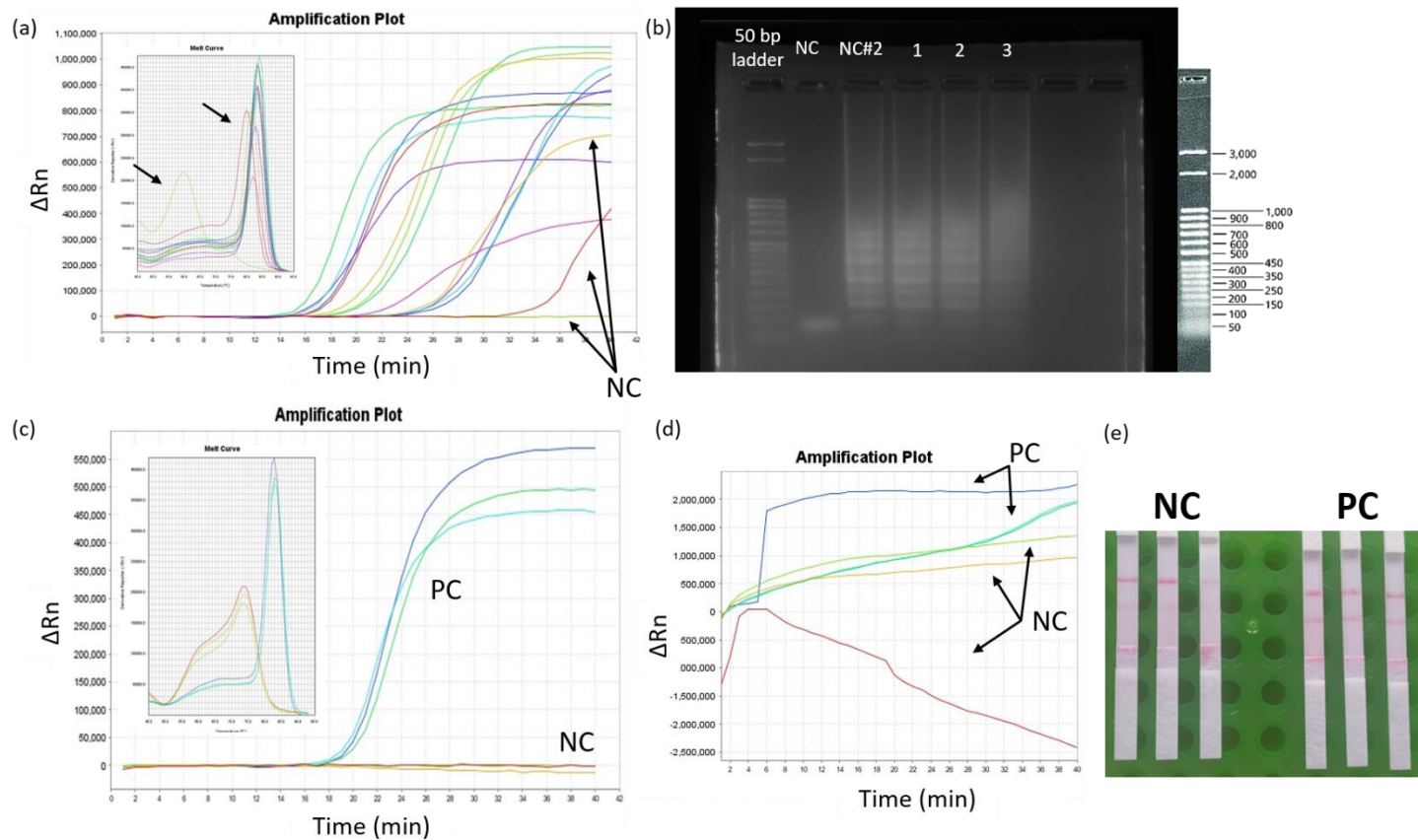


Figure 3-10: The development of SMchrom LAMP assay. (a) Primary LAMP development was undertaken using the qPCR SMchromF3 & SMchromB3 oligo sequences with published internal primer sequences. However, this lead to false amplification of no target negative controls 'NC'. (b) The false amplification of NC samples 'NC#2' was confirmed by gel electrophoresis. (c) Further development was carried out using a modified B3 oligo (SMchromB3\_2), this lead to successful LAMP results, amplification was observed for control target DNA 'PC' and was not present for NC. (d) Integration of FITC and biotin molecules into the SMchrom assay. LAMP carried out with FITC and biotin tagged FIP & BIP primer sets did not produce visible amplification result. (e) The samples were run on LF strips and positive LF read out was determined for both PC & NC.

### 3.4.2.3 Development of the SMchromL & SM primer sets

The SM and SMchromL primer sets described in Table 3-1 were able to amplify gBlock, *S. mansoni* egg and cercariae DNA - Figure 3-12 provides a summary of the results and the fluorescence data is displayed in Figure 7-6 of the Appendices. Amplification of all *S. mansoni* DNA samples was confirmed by gel electrophoresis following the protocol in Section 2.1.4. The bright smears in Figure 3-11 confirm DNA amplification by LAMP using SM (labelled 'SM') and SMchromL (labelled 'SMC') primer sets. The ladder pattern which is characteristic of LAMP amplification was present for positive samples (Zhang *et al.*, 2010; Edwards *et al.*, 2014) and the lower bands appear at the position of the 200-bp and 100-bp ladders for SM and SMchromL amplified samples respectively. The 200-bp and 100-bp sequence lengths are in the range of the expected amplified product for the respective primer sets. The NC for both SM and SMchromL were placed in the final well (8.3  $\mu$ L of each sample), the column is absent of bands. The results obtained for gel analysis confirm the negative results from the ABI machine and suggest correct amplification of the target sample DNA (Edwards *et al.*, 2014).

*The SM LAMP primers (mtDNA gene target) result in amplification of DNA extracted from cercariae and s.mansoni ova, provides potential to confirm s.mansoni infection from a variety of samples.*

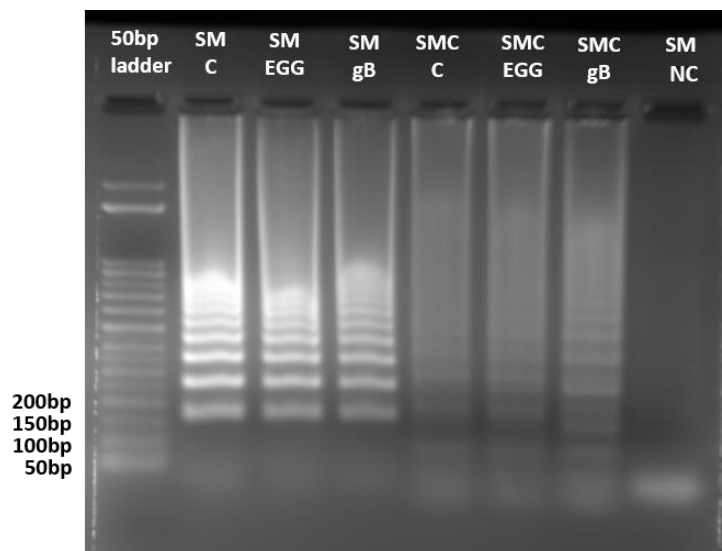


Figure 3-11: Gel electrophoresis for confirmation of isothermal amplification of cercariae (C), egg (EGG) and gBlock DNA sequence (gB) for both SM and SMchromL (SMC) primer sets. Bright bands signify presence of amplified DNA in the sample. The SM and SMchromL bands appear in line with the 200bp and 100bp reference ladder respectively, suggesting correct amplification. No bands were present for the no template control (SM NC), where both SM and SMchromL (SMC) no template controls reactions were combined in the final well of the gel. .

LAMP Primer sets	gBlock DNA	S.mansoni Adult Worm DNA	S.mansoni Egg DNA	Cercariae DNA
Tagged SM	✓	✓	✓	✓
Tagged SMchrom	✗		✗	
Tagged SMchromL	✓		✓	✓

Figure 3-12: Summary of the results of amplification using the mtDNA & gDNA targeting primer sets. SM and SMchromL was able to amplify all extracted DNA samples, however no amplification was achieved using SMchrom primers, suggesting that tagging the internal primers inhibits LAMP.

### 3.4.3 Detection of *S. mansoni* DNA on LF strips

Following LAMP of *S. mansoni* DNA on the ABI machine, 10 µL of the amplified sample was pipetted onto the LF strips, followed by 2 drops of ‘Wash Buffer’ which was supplied by the manufacturer. The LF strips were left for 15 minutes to allow sufficient time for LF and binding before interpreting the LF strip result. The SM LAMP results obtained on the ABI machine correlated with LF strip results, refer to Figure 3-13(a), the amplified gBlock, *S. mansoni* cercariae and egg DNA resulted in a positive LF strip result and the NC produced a negative LF strip result. On the other hand, no positive LF strip results were obtained for the DNA amplified using the SMchromL primer set, refer to Figure 3-13(b). The SMchromL LF strip result contradicts both the fluorescence data collected by the ABI machine (see Figure 7-6 in the Appendices) and the result from gel electrophoresis (Figure 3-11). The LF strip results suggests that one or both of the tagged Loop primers (SMchromLPR5F & SMchromLPP5B) must not be integrating into the sequence during amplification, inhibiting read-out on the LF strip. For this reason, downstream LAMP experiments and studies in-the-field were conducted using the tagged SM primer set, targeting the mtDNA minisatellite region (GenBank Accession No. L27240).

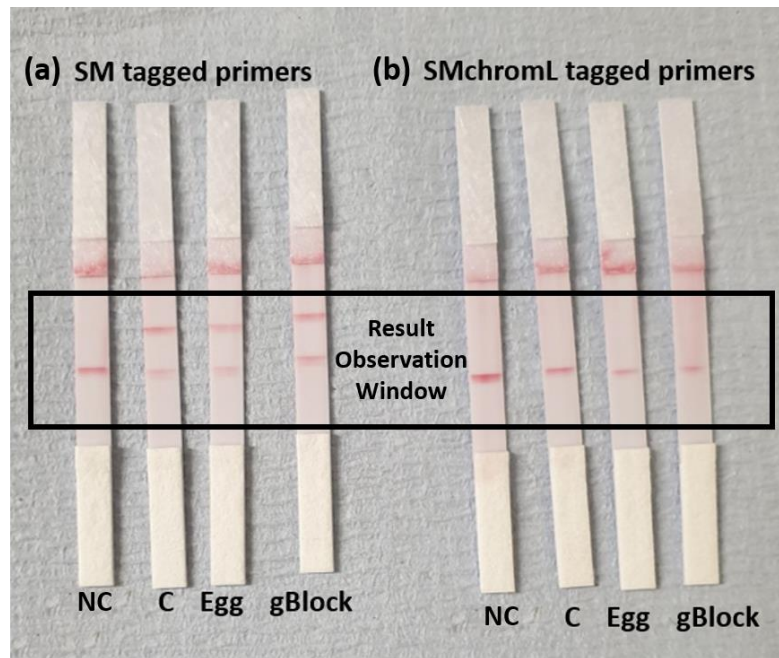


Figure 3-13: Detection of amplified product on LF strips (a) SM amplified *S. mansoni* samples run on the LF strip. Positive results confirmed by presence of two lines within the result observation window, for *S. mansoni* cercariae (C), egg (EGG) and gBlock (gBlock) DNA. (b) SMchromL amplified *S. mansoni* samples run on the LF strip. No positive results suggest failure of one or both of the Loop primers during amplification.

*SMchromL Loop primers (SMchromLPR5F & SMchromLPP5B) not integrating during amplification and therefore inhibits read-out on LF strip. Downstream experiments from patient samples in the field conducted using the tagged SM primer set targeting the mtDNA minisatellite region.*

#### 3.4.4 Investigation into tagged primer sets

The melt curves collated from fluorescence data for LAMP using SM and SMchromL tagged primer sets (Figure 3-14(a)) were analysed against the melt curve data from PPAN tagged and untagged primer sets (Figure 3-14(b)). The derivative reporter melt curves resulting from samples amplified using SM and PPAN tagged primer sets produced a ‘dipped shoulder’ (highlighted in red), around 45°C and 65°C respectively as a result of an increase of fluorescence at the respective temperatures. The ‘dipped shoulder’ was not observed in derivative reporter melt curves for tagged SMchromL or PPAN untagged amplified samples (data plotted in yellow on respective figures). It is thought that the peak may suggest successful integration of the LPR5F during amplification.

In order to explore the assumption that the ‘dipped shoulder’ correlates with integration of FITC-tagged primers, LAMP using PPAN tagged primers was carried out on the ABI machine using Isothermal Mastermix in absence of dsDNA intercalating dye (ISO-004ND). The increase in fluorescence between 45°C and 65°C was observed in PC LAMP samples for both ISO-004 & ISO-004ND Mastermix, which is easily distinguished in the normalised reporter curves – see Figure 3-14(c). The emission wavelength of FITC and the dsDNA intercalating dye are 518 and 520 nm respectively (Liu *et al.*, 2005), as a result, the collective changes in fluorescence would be recorded by Filter 1 of the ABI machine (Applied Biosystems, 2010). The emission intensity of FITC is known to decrease with increased temperature (Liu *et al.*, 2005; Charlot *et al.*, 2017). The decrease in fluorescent signal observed for LAMP using ISO-004ND (plotted in purple in Figure 3-14(c)) is solely the emission recorded from the intercalated FITC. The data suggests that the ‘dipped shoulder’ observed in the derivative melt curve data is due to the FITC-tagged primers, it was only observed in samples containing positive target DNA, suggesting that the increase in fluorescence results from integration of FITC in the amplified product.

It appears that the melt curve analysis may be used to assess the integration of the FITC-tagged Loop primers in LAMP, and as a result, assess development of potential primer sets for LF read-out. The additional background fluorescence due to the integration of FITC-tagged primers within the primer mix results in less pronounced melt curves. During the development of the assay the ability to monitor the fluorescence was paramount, however, it should not be recommend to carry out LAMP using primer mixes containing untagged and FITC-tagged oligos within the same run, as the ABI machine was not able to correct for additional background fluorescence which proved challenging for analysis. However, the amplification can be observed by extracting and analysing the ABI raw fluorescence data. An investigation into the incorporation of alternative tagging molecules - which do not have similar emission spectra to SYBR™ Green or similar dsDNA intercalating dyes - could be beneficial for future studies and avoid the analysis issues described.

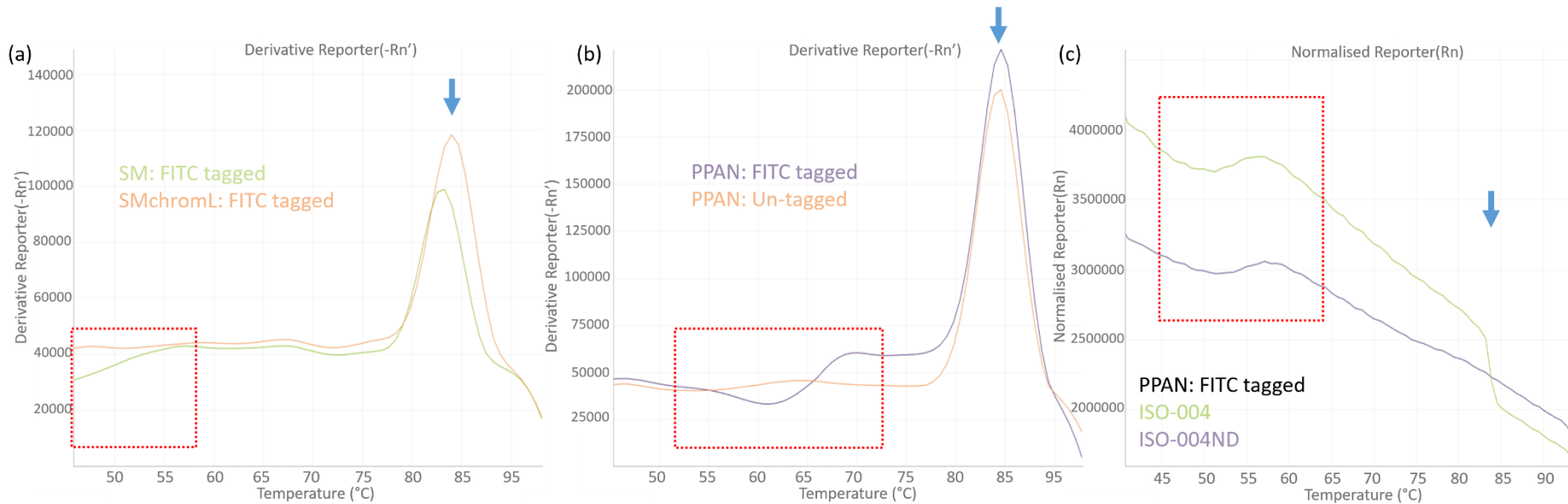


Figure 3-14: Melt curve analysis of FITC and biotin modified primer sets exported directly from ABI software. Melt curve analysis of LAMP carried out using: (a) SM tagged primer set and the developed SMchromL tagged primer set; (b) PPAN tagged primer set; and PPAN untagged primer set. The melt peak is marked with a blue arrow. The 'dipped shoulder' observed for tagged primer sets is marked in red. This is not observed in the tagged SMchromL melt curve, which resembles the profile of the PPAN untagged melt curve (both yellow). (c) The 'dipped shoulder' was confirmed to be caused by FITC primer by analysing melt curves produced by LAMP carried out using tagged PPAN primers with: isothermal Mastermix containing dsDNA binding dye (ISO-004); and isothermal Mastermix which does not include dsDNA binding dye (ISO-004ND). The normalised melt curve data shows the increase in fluorescence (boxed in red) which results in the 'dipped shoulder' observed in the derivative reporter graphical data.



## 3.5 Discussion

### 3.5.1 Biotin and FITC tagged LAMP primers

Primary development of the *S. mansoni* molecular reagents (SMchrom primer set) was carried out using the un-modified loop primers. The primer sequences, concentrations and amplification conditions had been optimised prior to experiments integrating FITC and biotin tagged primers. Unfortunately, amplification was not successful using the tagged SMchrom oligo set. Lack of amplification suggested that the incorporation of FITC and biotin molecules into the internal primer sets (FIP & BIP) had inhibited LAMP amplification. The FIP and BIP primers are fundamental to cycling and elongation phases of LAMP (Hardinge and Murray, 2019), it is possible that the labelled molecules effected these processes, thus hindering amplification. Consequently, the development of an alternate primer sequence was explored (SMchromL). From results of LAMP conducted on the ABI machine, the exponential increase in fluorescence present for SM and SMchromL tagged primers suggested successful integration of modified primers into the gDNA target sequence. Amplification was carried out for a range of *S. mansoni* DNA. Similarly to the SM primer sequence, the SMchromL successfully amplified *S. mansoni* gBlock, eggs and cercariae DNA (see Figure 7-6 in the Appendix). The successful amplification of *S. mansoni* DNA using both SM and SMchromL target sequences throughout the schistosome life cycle suggested that both the target sequences may be applied to detect presence of DNA in a variety of samples (Wichmann *et al.*, 2009; Enk, Oliveira e Silva and Rodrigues, 2012; Song *et al.*, 2015).

### 3.5.2 Detection of *S. mansoni* DNA on LF strips

Detection of SM amplified products was achieved on LF strips. Unfortunately, when conducting experiments trialling detection of the SMchromL amplified samples on LF strips; positive control samples did not produce a positive read-out. SM and SMchromL amplified samples were processed together, therefore failure of detection due to fault in LF strips was highly unlikely. It is believed that one or both of the tagged Loop primers must not be integrating into the sequence during amplification (most likely due to the melt temperature of the primers being too low), inhibiting read-out on the LF strip. Melt curve analysis provided further evidence to believe that the modified tagged primers had not been integrated into the amplified product (see *Figure 3-14*).

The small size of the gDNA tandem repeat unit (GenBank Accession No. M61098.1) posed a limit as to where the Loop primers could be introduced into the sequence, and as a result

limited the primer length and corresponding primer melt temperature. Therefore, as recommended by “A guide to LAMP primer designing” (<https://primerexplorer.jp/e/>), an extended region of the target DNA sequence should be explored in order to integrate larger Loop primers. Primer design softwares for LAMP are limited to sequence designs for regions of > 200-bp. Difficulties faced during assay development make it clear as to why the lower limit of 200-bp was determined. Furthermore, work conducted towards the development of LAMP primers for the gDNA sequence highlighted the complicated nature of assay development.

### 3.6 Conclusion

In summary, the materials and methods section encompassed the materials, methods and developments that suggest the detection of *S. mansoni* DNA on the POC Paper Device will be achieved. A stool substitute was defined and used to develop the sample processing methods to extract *S. mansoni* ova from stool specimen. Additionally, the methods to extract DNA from *S. mansoni* ova and cercariae stored on FTA cards was defined, to provide template DNA for the validation of the *S. mansoni* assays.

Development of previously published *S. mansoni* assay to facilitate expansion of the diagnostic capabilities of the Paper Device was achieved. Unfortunately, the attempts to integrate FITC and biotin molecules into the *S. mansoni* gDNA target region to enable read-out on LF strips were unsuccessful. However, the development of the *S. mansoni* mtDNA target sequence for LF use was achieved. The SM assay exhibited amplification using gBlock, *S. mansoni* adult worm, ova and cercariae DNA, and previous publications have confirmed that the mtDNA minisatellite region has successfully amplified *S. mansoni* DNA from human urine and faecal samples (Fernández-Soto *et al.*, 2014, 2019), which suggests that the target mtDNA can be detected both directly from *S. mansoni* ova and specimen containing circulating DNA (Gandasegui *et al.*, 2018; Fernández-Soto *et al.*, 2019). Thus, the developed SM assay will be integrated into the POC platform to detect *S. mansoni* DNA in stool and blood during trials in-the-field.

### 3.7 Future Work

Further work is required to develop a primer set which will target the Sm1-7 tandem repeat gene region and enable translation of result read-out on LF strips. Wichmann *et al.* report diagnosis of *S. mansoni* from DNA extracted for 1 mL and 10 mL of murine and human plasma, targeting the gDNA region, GenBank Accession No. M61098.1 (Wichmann *et al.*, 2009). The same region was later used for ‘in-chip’ diagnosis from 20 µL of murine serum and whole blood. From data provided by Wichmann’s study this scales up to ~200 µL of human plasma (Song *et al.*, 2015). Thus, further development of biotin and FITC-tagged Loop primers (SMchromL) to target an extended sequence of the gDNA tandem repeat unit (GenBank Accession No. M61098.1) has potential to produce promising results from larger samples of blood. Alternatively, other specimen could be considered to detect *S. mansoni* DNA.

### 3.8 Take home points

- *Extraction and amplification of DNA from a variety of S. mansoni samples was optimised.*
- *Integration of FITC and biotin-tagged loop-primers to target the S. mansoni mtDNA gene region (using the SM primer set) was successful, and enabled the method of detection of LAMP results to be translated into LF strip read-out. As a results, the SM primer set can be integrated into the POC Paper Device platform to conduct field trials to detect S. mansoni DNA.*
- *It was determined that melt curve analysis can be used to assess successful integration of the FITC-tagged Loop primers during LAMP, thus predict whether detection of new assays by LF strip will be successful.*

Previous studies investigating molecular diagnosis of *S. mansoni* were conducted under laboratory conditions, and literature searches reveal that molecular diagnosis of *S. mansoni* had not been conducted in low-resource settings prior to this study. The following work aims to integrate the DNA recovery methods and the assay developed in this chapter, to investigate molecular detection of *S. mansoni* from clinical samples at the POC, which to date has been largely overlooked.

## **Chapter 4: Field studies**

Chapter 4 describes the methods associated with conducting field trials - including preparations, ethical and logistical considerations. In addition to this there is a description of the field settings and detailed methods of reference diagnostics conducted in-the-field for both malaria and schistosomiasis. As detailed in Section 2.2.7.2, there were a few iterations of the Paper Device throughout the duration of this project, the results obtained for the respective cassettes and field trials will be presented and discussed.

### **4.1 Introduction**

LAMP has been reported for the detection of *plasmodium* and *S. mansoni* infections, where investigators highlighted that the LAMP platforms could be appropriate for POC diagnosis and could enable molecular diagnosis in low-resource environments (Connelly et al., 2015). The work described in this chapter was carried out to assess the feasibility of conducting POC molecular investigations in field conditions, within low resource communities in Uganda, where national malaria and bilharzia surveys are routinely carried out. A small number of studies assessing molecular tests have been conducted in established field-based laboratories or in low-tier healthcare settings (Hopkins *et al.*, 2013; Magro et al., 2017a). Although, the environments described in the studies do not match field survey environments, which until now have been largely overlooked. The similar epidemiological distribution of malaria and schistosomiasis in Uganda (Mwangi et al., 2006; Kabatereine *et al.*, 2011), facilitated field trials of the Paper Device for the POC detection of both malaria and *S. mansoni* infections. Preliminary field trials for the multiplexed malaria Paper Device (originally developed by Dr Gaolian Xu) and the singleplex *S. mansoni* cassette - which incorporated the molecular primers developed in the previous chapter - were conducted to gauge the workflow and conditions in low-resource environments. Successive field studies were conducted following necessary amendments to cassette designs, processing and workflow.

## 4.2 Chapter Aims & Objectives

The use of POC molecular tests in low-resource environments and field survey sites has not been widely reported. The aim of this chapter was to gain understanding of the field environment in Uganda, and the influence that the low-resource environment has on the POC molecular test workflow and test outcome. The PAN malaria and *S. mansoni* assays were used to investigate the detection of *plasmodium* and *S. mansoni* DNA on the POC Paper Device from clinical samples in-the-field. A range of methods were developed to assess use of the Paper Device in-the-field; the molecular diagnostic work-flow; source of heating and the sample workflow. Comparative diagnostics were carried out to ascertain POC Paper Device outcomes. The chapter objectives:

- Develop an understanding of the field survey environment;
- Develop a field appropriate molecular diagnostic workflow;
- Assess the POC detection of *S. mansoni* DNA from stool samples;
- Assess the POC detection of *plasmodium* and *S. mansoni* DNA from finger-prick blood samples;
- Investigate factors effecting test outcomes and the workflow in-the-field;
- Develop practical solutions to improve test outcomes, and determine areas for further development and improvement.

### 4.3 Ethics & Logistics

The field studies were conducted with the Vector Control Division (VCD), of the Ministry of Health (MoH) in Kampala, Uganda. The study on neglected tropical diseases was approved by the VCD Research and Ethics Committee, VCDREC/078, and the Uganda National Council for Science and Technology (HS 2193). School children between the ages of 6 and 14 years old were recruited under the supervision of their class teachers and school headmaster. Each child was assigned a unique identification number (ID), their age, sex, name, parents' name (to ascertain consent), school class, height and weight (for treatment purposes) were recorded. Details were computerized and anonymized using the unique ID numbers.

The parents/guardians were informed of the activities by the head teacher at community meetings, and their verbal and written assent for their children's participation was obtained. Where individuals were unable to write, a fingerprint was taken in lieu of a written signature. After testing, those presenting with bilharzia were treated with Praziquantel and all children were given antimalarial therapeutics. The treatment follows guidance in the ethical approval obtained, given that all samples were retested for malaria by qPCR in the United Kingdom, which is a method that is more sensitive than the ones available onsite (Sandeu *et al.*, 2012; Meurs *et al.*, 2015; Berzosa *et al.*, 2018).

## 4.4 Study Settings

The field studies were conducted in rural primary schools in the Mayuge, Apac and Tororo Districts in Uganda. The districts were selected by VCD based on historically surveyed disease burden and the timeline of their national treatment program. The field trips were conducted in late February and early March, at the cusp of the ‘wet season’ in Uganda. Thus, rain and thunder storms were more frequent than the ‘dry’ months, but average temperatures were much cooler, fluctuating from 24°C to 35°C through the day.

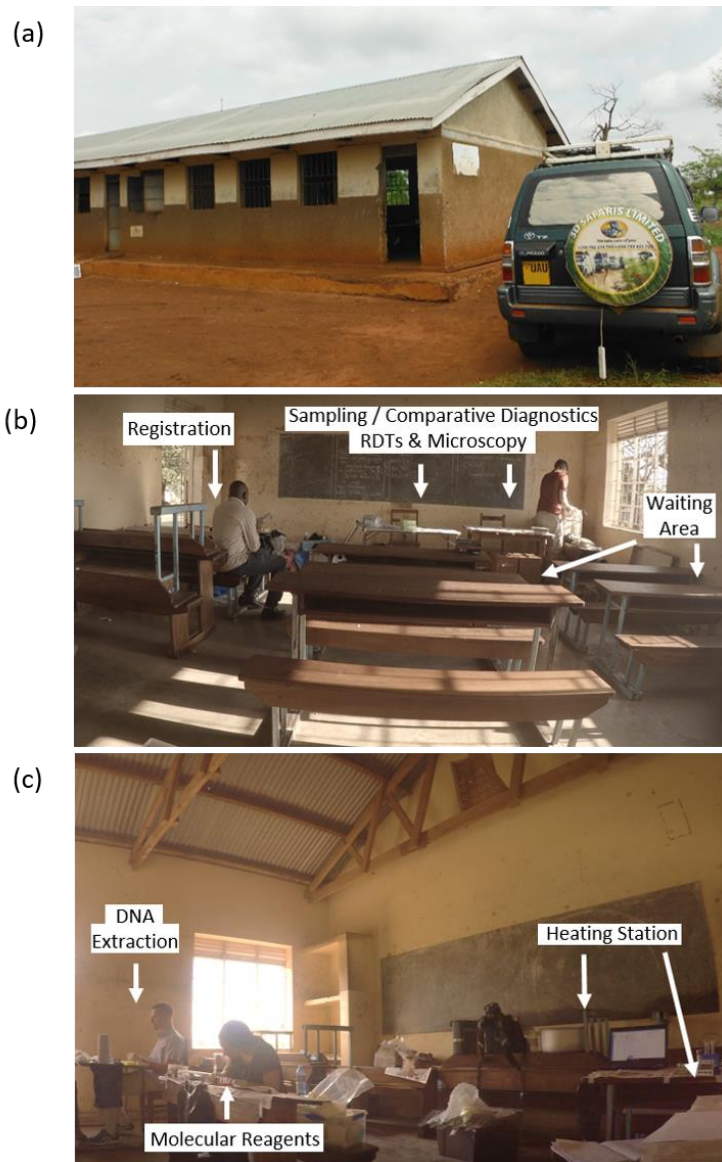


*Figure 4-1: The field site. (a) The classroom used to conduct the second field study in Apache, Apac District, Uganda. (b) The study set-up in the classroom. The participants were registered at the desk by the entrance to the room. The desks in the centre of the room were used as a waiting area. Sampling and comparative diagnostics were conducted at the front of the room. (c) Molecular diagnostic work stations were set-up at the back of the room. Work was conducted linearly across the room: DNA extraction; addition of molecular reagents; heating (LAMP); and diagnostic read-out.*



The field studies were carried out in rural primary schools in selected regions where there was no access to mains electricity or running water. The classrooms resembled that depicted in Figure 4-1(a), a basic building supporting a tin roof and open windows with steel bars to deter theft. The POC testing station was setup in an allocated classroom (Figure 4-1), where the infrastructure resulted in exposure to the wind, dust and on occasion rain through windows and small holes in the roof.

The children were registered at the desk at the entrance to the room by their teacher, under supervision of a VCD technician. After registration, participants were asked to wait at the desks in the centre of the room for finger-prick sampling, Figure 4-1(b). The molecular diagnostic work station (see Figure 4-1(c)), was set-up at the back of the classroom in an attempt to limit the exposure of reagents to sunlight and participant tampering. The three NAAT stages; DNA extraction; addition of molecular reagents; and amplification, were conducted on separate workbenches. The NAAT process was conducted linearly to decrease the risk of contamination to the stock reagents. The workflow and logistics will be further discussed in Section 4.5.2 & 4.5.3 respectively.

## **4.5 Materials, Methods & Development**

This section described the materials, method and development required for carrying out the field-studies in Uganda. This includes preparation and transport of materials; the study workflow, which describes the enrolment, sample and diagnostic workflow; the materials and methods for comparative field diagnostics; heating solutions; and an overview of the field-studies carried out within this project.

### **4.5.1 Fieldwork preparation**

The preparations for field work are described in this section, this includes the storage and transport of reagents and consumables.

#### ***4.5.1.1 Diagnostic Devices***

The Paper diagnostic devices were prepared in the laboratory prior to field trials - for preparation methods refer to Section 2.2.8 & Section 2.2.9 - were stored in sealed foil bags (Fresherpack Ltd, Huddersfield, UK) with silica gel desiccant (Brownell Ltd, London, UK) to limit the exposure to moisture and sunlight. The equipment for microscopic examinations and RDTs were sourced locally in Uganda by the VCD technicians.

#### ***4.5.1.2 Equipment***

Where possible the equipment required for field work was sourced in Glasgow and transported as hold luggage to Uganda, this excludes equipment needed for microscopic examinations, RDTs and drugs for treatment which cannot be brought into the country. All equipment was packed into travel crates appropriate for air travel which were selected to accommodate air transport and travel within Uganda. It was necessary for all equipment, along with personal luggage, to be packed into a 4x4 for travel between districts in Uganda (see Figure 4-2). Poor road conditions for vast stretches of the journey required the equipment (or protective packing) to be able to withstand rough handling and sudden jolts. Where possible the NAAT reagents and other consumables were split between two travel crates to minimise the impact to work in the event of loss or destruction of the crates during travel.



*Figure 4-2: Transportation of equipment. (a) Fieldwork equipment and personal luggage being loaded into the 4x4 in VCD, Kampala. (b) Equipment and luggage packed in and secured on top of the car.*

#### **4.5.1.3 Reagent organisation**

Extraction buffers (Promega) and liquid molecular reagents (Primer Mix) were packed in small aliquots and were stored separately during travel to avoid contamination in the event of spills or leaks. Additionally, Isothermal Mastermix (ISO-DR004) was stored separately and kept in manufacturers packaging, a new bottle of dried Isothermal Mastermix (ISO-DR004) was re-suspended per day of testing. Finally, the DNA templates needed for PC tests were stored in a separate box to limit the risk of contamination of reagents and equipment.

#### **4.5.2 Workflow**

The workflow in the laboratory differed significantly from that in-the-field. During field trials the team enrolled participants, collected samples, organised the running of multiple diagnostic tests in parallel, and finally treating participants, in addition to trialling the POC Paper Device. Whereas in the laboratory, work was limited to trialling the POC Paper Device against LAMP using the ABI machine.

#### 4.5.2.1 Enrolment

The participants were enrolled each day. A single year group was selected by the head teacher, who randomly selected 25 to 26 students (roughly half male and female). The VCD MoH healthcare workers and teacher explained and described what diagnostics were being conducted and the methods for sample collection. In addition to previously acquired consent from parents, verbal consent was received from each child and the teacher. The VCD healthcare workers collected participants personal data such as the name of the child, the name of their head of household (assigned consent), school year, age, height and weight (for treatment purposes). The hard copy and a single electronic copy was kept in a secure file throughout the duration of this project. Each child was given a personal ID number for diagnostic reference. Urine, stool and finger-prick blood sample were collected from each participant. Downstream use of each sample is described in Figure 4-3. During the enrolment process the remaining team members prepared the room, set up equipment, organised and labelled sample collection materials.

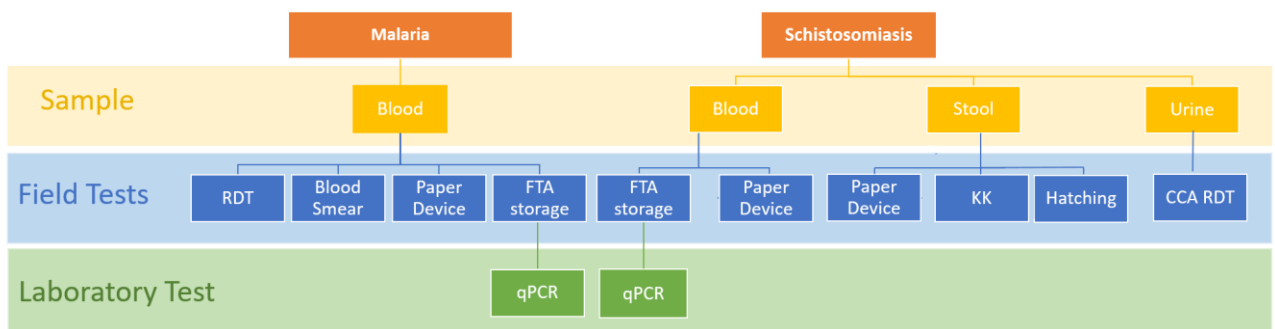


Figure 4-3: Schematic for the sample collection and processing for diagnosis of schistosomiasis and malaria in the field. FTA<sup>®</sup> storage refers to the storage of a finger prick of blood on an FTA<sup>®</sup> card. FTA<sup>®</sup> was used for safe transportation of the sample to the UK for downstream qPCR testing in the laboratory.

#### 4.5.2.2 Sample collection

Each participant was given a urine cup and a plastic sheet to collect urine and stool samples for bilharzia diagnostics. Both containers were labelled with the participants' unique ID number and initials. After returning with both samples the children were instructed to wash their hands and return to the classroom for finger-prick blood-draw. The urine and stool samples were stored in a box away from direct sunlight until use later in the day. Whilst samples were being collected, the negative and positive control DNA templates were tested on the Paper Device following the method in Section 2.2.2.

#### 4.5.2.3 *Sample Processing*

A fingerstick was used to collect blood samples to complete malaria diagnostics. Four separate blood spots were produced from a single finger prick using a sterile lancet. Once a droplet had formed, venous blood was collected with a capillary tube and transferred to the malaria RDT cassette. The second droplet was transferred into an Eppendorf tube, the third was spotted onto an FTA<sup>®</sup> card and finally, the last was smeared onto a clean microscopy slide. The participant's finger was disinfected again and covered with a plaster. Each device was marked with the patient's ID number. The method used to conduct the malaria RDT is further explained in Section 7.7.2 in the Appendices. The blood collected in the Eppendorf tube was processed to conduct the Paper Diagnostic, as described in Section 2.2.2. The microscopy slide was prepared following the procedure in Section 4.5.4.1 for parasite counting. The blood spotted on the FTA<sup>®</sup> card was left to dry and stored following the manufacturer's recommendations. The packet containing dried FTA<sup>®</sup> cards was marked with the date and stored in a folder with desiccant to be returned to the laboratory in Glasgow for confirmatory qPCR.

Both urine and stool samples were used for comparative bilharzia diagnosis. Urine samples were used to diagnose cases of schistosomiasis using the POC-CCA RDT following the protocol stated in Section 4.5.4.4. Stool samples were required for microscopic examination of *S. mansoni* parasite ova in faeces and hatching experiments. A small sample of stool was taken from the centre of the faecal sample; this sample was processed following the method in Section 4.5.4.3 to complete a double Kato-Katz (KK) reading. Where possible the samples which returned negative KK results were processed following the hatching procedure described in Section 4.5.4.5; the samples positive by KK were recorded as positive and were not processed during hatching tests. All waste and consumables (including diagnostic specimens) were incinerated by burning on a bonfire on site. Sharps were transported back to Kampala at the end of the study and discarded by local protocols in the MoH VCD campus.

### 4.5.3 Molecular Diagnostic Workflow

For the Paper Device method, refer to Section 2.2. As Discussed briefly in Section 4.4, the molecular diagnostic work in-the-field was conducted across three work benches (see Figure 4-1 & Figure 4-4). The layout was set-up to minimise risk of contamination of stock reagents. Figure 4-4 shows a diagram of the molecular diagnostic workflow in the laboratory as compared to the workflow in-the-field. In the laboratory the extraction of DNA from blood samples was conducted in Laboratory 1, after which the extracted DNA sample was transferred to the DNA room where molecular reagents were added to the diagnostic cassette. In the laboratory comparative LAMP (carried out on the ABI machine), was run on the same extracted sample. The qPCR tubes and diagnostic cassettes were then sealed in the DNA room and transferred to laboratory 4 and 3 respectively to conduct amplification. After amplification the cassettes were discarded in Laboratory 4 to avoid contamination of equipment with amplified product. In-the-field the DNA extraction, addition of molecular reagents and amplification were conducted on three separate work benches (Figure 4-1 & Figure 4-4) in attempt to mimic the linear laboratory workflow in-the-field.

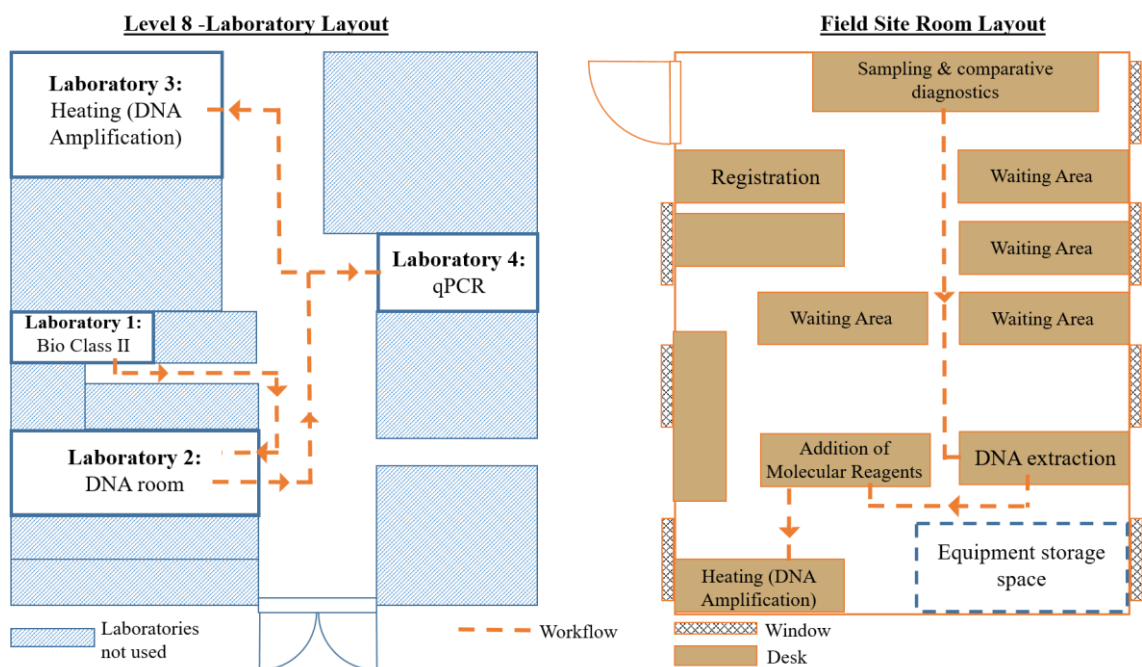


Figure 4-4: Molecular diagnostic workflow in the laboratory as compared to the field site room. Molecular diagnostic work flow was set-up linearly. DNA extraction from blood samples was conducted in Laboratory 1 (on the DNA extraction bench). Extracted DNA samples were transferred to Laboratory 2 (on the DNA bench) for addition of molecular reagents before being moved to the final location to conduct DNA amplification. In-the-field, this process was mimicked by creating a linear work-flow from sampling to DNA amplification, where team members at each bench, avoid moving between sample processing stages conducted on separate benches.

#### **4.5.4 Reference diagnostics**

A brief description of the methods for the reference diagnostics – carried out by the VCD technicians - are included in this section. The reference diagnostic results were not relayed to the Paper Device study team until the end of the field trials to maintain the blind study conditions. More detailed methods associated with the reference diagnostics are included in Section 7.7 of the Appendices.

##### ***4.5.4.1 Malaria Gold Standard: Microscopic examination of a blood smear***

The examination of blood smears was undertaken by the MoH VCD technicians. A few small drops of blood were collected from a finger prick to make up the thick blood smear on a microscope slide. The slides were immersed in Giemsa stain and left to dry before microscopic processing (World Health Organization, 2010). The blood smear was inspected for *plasmodium* parasites using a compound microscope (Model CX21FS1; Olympus Corporation) using a 100X oil immersion objective lens with either electrical or natural light sources (dependent upon availability of electricity). The parasite load was calculated to determine the level of infection for study records and treatment purposes.

##### ***4.5.4.2 Malaria RDT***

The CareStart™ Malaria HRP2/pLDH (Pf/pan) test was used as a reference RDT in-the-field. The RDT was conducted as instructed by the manufacturer (ACCESSBIO, 2020) following WHO guidelines (Harvey and Bell, 2010). A finger prick of venous blood was collected by the MoH nurse and transferred to the RDT cassette using a finger-stick. The results were determined by the VCD technicians' after 10 minutes and noted for study and prevalence records.

#### 4.5.4.3 *Bilharzia* gold standard: Kato-Katz examination

Stool samples for each participant were collected in clean sample collection pots, marked with the participants' unique ID number and initials. The KK technique was conducted by the MoH VCD healthcare workers following WHO guidelines (Genchi *et al.*, 2019). The KK equipment and preparation method is depicted in Figure 4-5(a) and Figure 4-5(b-d) respectively. The slides were examined under a compound microscope (Model CX21FS1; Olympus Corporation) under 10X objective. The *S. mansoni* eggs present on the slide were counted to determine the intensity of infection for study and prevalence (Genchi *et al.*, 2019).



Figure 4-5: KK examination. (a) Equipment to conduct KK test. (b) A small section of the faecal sample being pushed through the fine sieve. (c) The sieved sample collected and transferred into the KK template on top of the microscope slide. After removal of the KK template, a stool pellet remains on the slide. (d) Pre-soaked malachite green cellophane strips applied on top of the stool pellet for staining to aid microscopic examination.



#### **4.5.4.4 *Bilharzia* RDT (POC-CCA)**

Urine samples for each participant were collected in clean sample collection pots, marked with the participants' unique ID number and initials. The POC-CCA tests were run by the VCD technicians following the manufacturer's instructions (Rapid Medical Diagnostics, 2018). The urine was transferred into the cassette using a sample stick (provided by the manufacturer) and results were determined after 10 minutes. The results were recorded for study and prevalence record

#### **4.5.4.5 *Hatching***

The hatching protocol follows the method preciously described by Gower *et al* (Gower *et al.*, 2013). The remainder of the stool sample - left over after completion of KK examinations - was processed for the hatching tests. The stool sample was diluted and passed through a sieve and the hatching set – see Figure 4-6(a) - to collect *S. mansoni* ova. Preparation for the hatching test is depicted in Figure 4-6(b).

The *S. mansoni* ova were left overnight and observed the following afternoon to ensure optimum hatching conditions were maintained (Samuelson *et al.*, 1984; Borges *et al.*, 2013; Gower *et al.*, 2013; Lamberton *et al.*, 2017). Samples where miracidia are observed indicate the presence of bilharzia. In a few cases where the KK examination was negative, miracidia were observed by the hatching test indicating an active *S. mansoni* infection. In such cases, the patient record was amended and KK result was noted as a possible false negative.

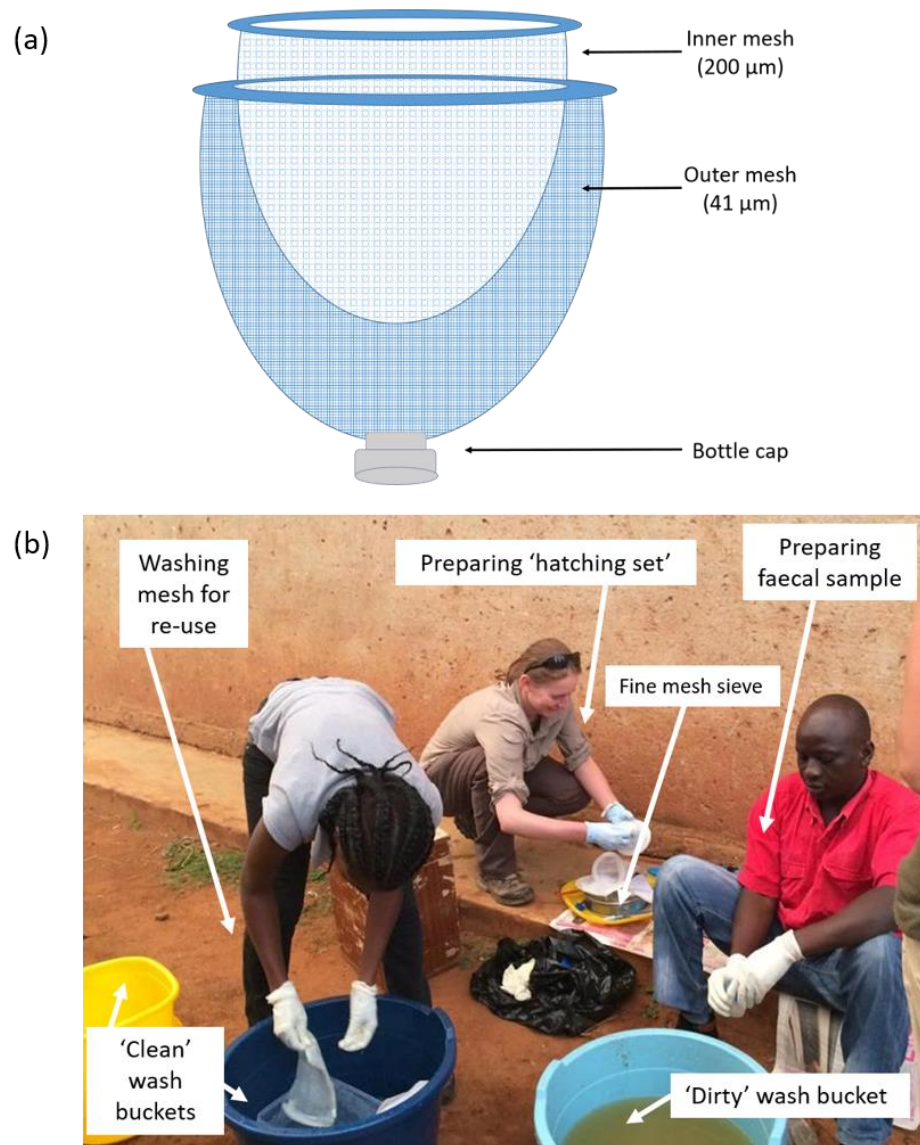
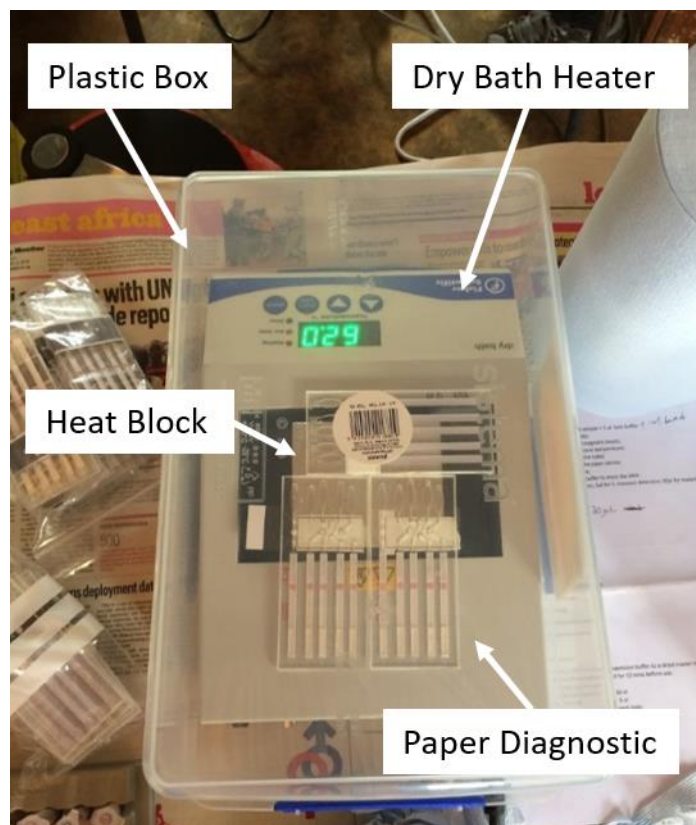


Figure 4-6: Preparation for the hatching test. (a) A diagram of the 'hatching set' made from two nylon nets. The inner mesh (200 µm) and outer mesh (41 µm), fitted with a bottle cap to catch 's.mansoni egg sized debris'. (b) The sample preparation for hatching *s.mansoni* ova from collected stool samples. The faecal sample was prepared: the stool shook in the sample container to break up the sample; sieved through the fine mesh sieve with a toothbrush; and passed through the 'hatching set'. Debris expelled from the hatching set was collected in the dirty wash bucket. After collection of 'egg sized debris' in sample containers, the hatching set was washed in the 'clean wash buckets' to be re-used.

#### 4.5.5 Heating for LAMP

Stable heating is fundamental to the LAMP process. In preliminary field trials the plastic cassette was balanced on top of a standard heat block to heat the Paper Device cassette and induce amplification, the setup is presented in Figure 4-7. The method of heating was limited and only enabled three cassettes to be heated simultaneously. Consequently, testing was limited to a small number (N=10) per day. For this reason, a custom heat block was manufactured (Refer to Figure 2-20), which allowed more tests to be run simultaneously, leading to an increase in the average number of samples processed per day (N=21).



*Figure 4-7: Heating set-up to conduct point-of-care LAMP during the preliminary field trials. The paper diagnostic cassettes were balanced on a standard 1.5 ml tube heat block within the dry heat bath. A plastic box was placed over the heater in attempt to retain heat and deter insects.*

#### 4.5.6 An overview of the field trials

Throughout the duration of this study, three field trials were conducted in rural primary schools within Uganda. The first field trial was instrumental in gaining an understanding of the field environment, and successive field trials aimed to improve on test outcomes from insight and experience gained in preceding trials. An overview of the tests and methods carried out in each field trial are presented in Table 4-1. For further details on the design of the POC Paper Device iterations, see Figure 2-16 in Chapter 2. The BRCA-1 assay was used as a positive control in all iterations of the POC Paper Device, the assay was used as an extraction control, and the PC reaction was spiked with gBlock template, for more details on the assays used, see Table 2-2 . The disease prevalence was calculated from the VCD survey microscopy data, which included a larger participant cohort.

*Table 4-1: An overview of the field trials described in this chapter. The details of the cassette iteration; LAMP assay and sample specimen; and comparative tests, carried out in each trial are stated.*

#	Location	Iteration of POC Paper Device	LAMP assay	Sample specimen	Comparative tests	Disease prevalence	Heating method
1	Mayuge District	Original Malaria multiplex	PAN	Blood	✓ Microscopy ✓ RDT ✓ qPCR	> 90 %	Standard heat block
		SM singleplex	SM	Stool	✓ Microscopy ✓ Hatching ✗ RDT ✗ qPCR	> 90 %	Standard heat block
2	Apac District	PPAN & Schistosomiasis multiplex	PAN	Blood	✓ Microscopy ✓ RDT ✓ qPCR	28 %	Custom heat block & frugal gas stove
			SM	Blood	✓ Microscopy ✗ Hatching ✓ RDT ✗ qPCR	40 %	
			SH *Used as a NC in analysis	Blood	✓ Microscopy ✗ Hatching ✓ RDT ✗ qPCR	N/A	
3	Tororo District	PPAN & SM integrated controls	PAN	Blood	✓ Microscopy ✓ RDT ✓ qPCR	53 %	Custom heat block & mobile heaters
			SM	Blood	✓ Microscopy ✗ Hatching ✓ RDT ✗ qPCR	51 %	

## 4.6 Results

### 4.6.1 Preliminary assessment of the field environment

The first field trip was paramount for understanding the field environment and the changes that were needed in the experimental workflow and to diagnostic procedure. POC LAMP using the multiplex malaria cassette (originally developed by Dr Gaolian Xu) was carried out to assess feasibility in-the-field. Additionally, the singleplex *S. mansoni* cassette was trialled in-the-field to assess the process of *S. mansoni* DNA detection from faecal samples on the POC platform.

#### 4.6.1.1 Multiplex malaria cassette

The multiplex malaria cassette was trialled in the Mayuge District (Uganda); a malaria endemic region, the microscopy results from our study records suggested 81% prevalence of malaria in the study cohort (N=59). The experimental design provided the potential to distinguish DNA from three plasmodium species - *falciparum*, *ovale* and *malariae* (Reboud *et al.*, 2018). Although the three plasmodium species are prevalent throughout sub-Saharan Africa (The Malaria Atlas Project, 2017), RDT diagnosis suggested less than 25% of the study cohort had non-*falciparum* malaria infections; and, those who did, also presented with *P. falciparum* co-infection ( see Section 7.8 of the Appendices for the results). The VCD highlighted that a cassette able to differentiate *plasmodium* species would be useful for surveillance and epidemiological studies (Reboud *et al.*, 2018); but noted that due to the low prevalence of non-*falciparum* malaria in the region, a diagnostic tool that can diagnose *P. falciparum* or pan-malaria (all non-*falciparum plasmodium* species) would be sufficient for further studies.

#### 4.6.1.2 Singleplex *S. mansoni* cassette

The singleplex *S. mansoni* cassette was designed to enable detection of *S. mansoni* DNA from stool samples. The prevalence of bilharzia in the Mayuge district was extremely high (> 90% prevalence recorded by microscopy surveillance data) as a result, the VCD technicians were responsible for choosing samples to process for the Paper Device trial. The selection method was chosen in an attempt to maintain the ‘blinded’ nature of the study for the Paper Device team, whilst ensuring some negative samples were included in the study sample set. The *S. mansoni* ova were retrieved from stool samples using the modified FLOTAC technique – described in Section 3.3.4.4, prior to processing on the Paper Device. The method of downstream DNA extraction is also referenced in detail in Section 3.3.4.4. The preparation of the stool samples for DNA extraction was a lengthy process and resources

for testing were limited, for this reason, the testing of the multiplexed malaria cassette was prioritised, resulting in a smaller test cohort for the *S. mansoni* study. The results are summarised in Figure 4-8 .

In total, 17 samples – from 17 individuals - were processed on the *S. mansoni* cassette throughout the trial. 11 cassettes were included in the analysis, the tests removed from analysis are further discussed in Section 4.6.1.3. The results obtained from the small study cohort were promising. There were 9 cassettes which identified presence of *S. mansoni* DNA and 2 which were negative. Only 2 of the 11 cassettes did not agree with the corresponding microscopy result. The conflicting results were negative by KK and positive on the Paper Device, however, one of the two stool samples which was negative by KK was confirmed as positive by the hatching protocol. Overall the preliminary trial resulted in 8 confirmed true-positive results; 2 confirmed true-negative results; and a single false-positive reported by the Paper Device. Unfortunately the POC-CCA purchased for the trial were faulty – there were no control lines visible - hence the comparison to POC-CCA results was not possible.

The prevalence of both malaria and *S. mansoni* in-the-field was extremely high. Due to the small study cohort and lack of negative cases (2 out of 11); the analysis of the sensitivity and specificity of the cassette was not possible (Bujang and Adnan, 2016).

N=11 stool samples processed on the Paper Device		
<b><i>S. mansoni</i></b>		
N=11 samples for analysis against the KK		
	<b><u>Kato-Katz</u></b>	
	Positive	Negative
<b><u>Paper Device</u></b>		
Positive	8	1*
Negative	0	2

*Figure 4-8: Summary of the results obtained for processing stool samples to detect S. mansoni DNA using the Paper Device in-the-field. POC LAMP results were analysed against comparative diagnostics in the field (Kato-Katz and hatching tests). The preliminary trial resulted in 8 confirmed true-positive results; 2 confirmed true-negative results; and a single false-positive reported by the Paper Device \* one of the negative KK results was a false-negative, the sample was determined as positive in the confirmatory hatching test.*

The pilot study using POC molecular methods to detect *S. mansoni* in stool returned promising results. Thus confirming amplification of the mtDNA target region (GenBank Accession No. L27240) from fresh human stool in-the-field. The small study follows data presented by Fernández-Soto *et al.*; whom detected *S. mansoni* infections from frozen stool samples collected from infected mice (Fernández-Soto *et al.*, 2014). More recently, Gandasegui *et al.* published a large field survey using the mtDNA LAMP primers for the detection of *S. mansoni* infections from human faecal samples (Gandasegui *et al.*, 2018). Although Gandasegui's survey collected stool samples in-the-field, LAMP was conducted in a reference laboratory and presence of infection was determined by a visual colour change of the solution in the qPCR tube. Our study provides preliminary data suggesting that LAMP to detect *S. mansoni* DNA in human stool can be performed as a point-of-care tool in low-resource settings with LF strip visual read-out.

#### **4.6.1.3 Factors effecting the Paper Device in-the-field**

The factors effecting analysis during field trials include leaks from the cassette or between amplification wells; failure of the PC; and lack of a control line on the LF strips. Issues with the design of the malaria multiplex cassette were discussed in Section 2.2.7.2; 16 of the cassettes processed were excluded from analysis due to leaks. Failure of the positive control (N=19) and LF strip control lines (N=6) corresponded to the loss of a further 25 tests. For the *S. mansoni* singleplex cassette, 3 devices were excluded due to failure of the positive control and 3 cassettes leaked during the processing.

#### **4.6.1.4 Considerations for future trials**

As discussed in Section 4.6.1.2 the processing of stool samples was lengthy and required more equipment than a standard KK test. The lengthy stool processing technique, along with various heating steps to complete DNA extraction, introduced an additional strain on already limited-resources in-the-field. After discussion with the VCD it was decided that a cassette which was able to multiplex the detection of malaria and *S. mansoni* DNA could be useful for disease surveillance. As a result, further development was directed towards the detection of *S. mansoni* DNA in blood samples. Due to the high prevalence of *P. falciparum* in Uganda, it was also decided that a *pan plasmodium* (PAN) assay would be sufficient for preliminary trials. Heating on the standard heat block posed an additional strain on the workflow, the cassettes were balanced on top of a standard heat block (see Figure 4-7) thus limiting heating capacity to 3 cassettes at one time. Hence, a customised heat block – presented in Figure 2-20 & Figure 2-21 - was designed for successive trials.

During processing in-the-field large volumes of buffers and solutions were lost due to spills, evaporation and contamination. To evade the effects of this, it was decided that multiple aliquots of solutions should be made for use each day. Additionally, some equipment and cassettes were damaged during transport to the field site, prompting more durable equipment to be sourced for future trials.

#### 4.6.2 Multiplex cassette and frugal heating

The field trial for the first malaria and schistosome combined diagnostic cassette was conducted in the Apac District (Uganda) prior to the ‘wet’ season. VCD’s surveillance data suggested that the district – which is located in the northern region - had lower prevalence of both malaria and *S. mansoni* than Mayuge as surveillance records suggested 28% and 44% infection prevalence respectively. Historically the region was endemic of urinary schistosomiasis - *S. haematobium* (SH). Thus the SH assay (previously developed outside the scope of this study) was integrated in to the testing in an attempt to differentiate the DNA of both schistosome species, refer to Table 2-2 in the Section 2.1.3.5.2 for details of the SH assay.

Unfortunately, during the trial, the heater (and back-up heater) were irreplaceably damaged due to power surges from the generator. In replacement of the damaged heaters, a portable gas stove and saucepan (Figure 4-9) were purchased in Apac town and used as a frugal heating source throughout the trial.

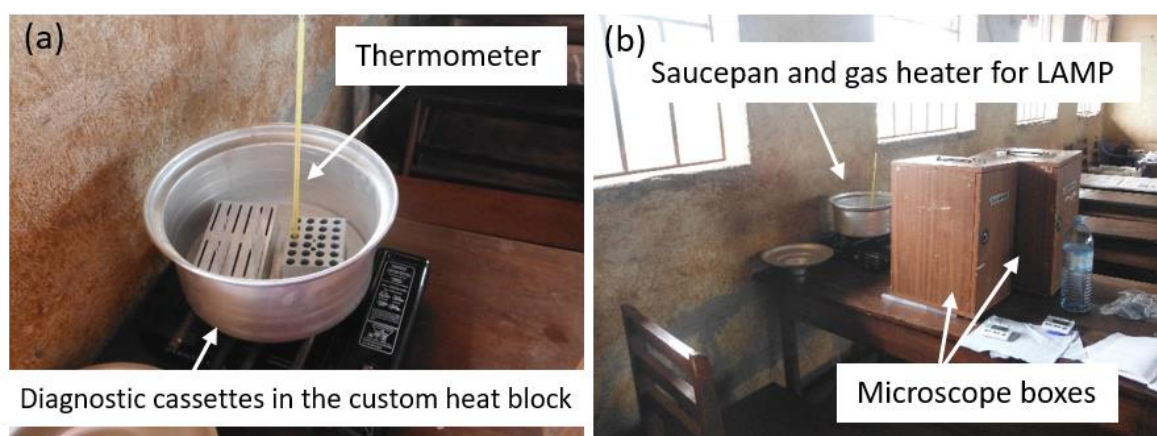


Figure 4-9: Frugal testing using a local cooking stove. (a) LAMP amplification conducted in a saucepan on a gas heater purchased in the field. A thermometer was used to control the temperature visually around  $63^{\circ}\text{C} \pm 4^{\circ}\text{C}$ . (b) Set-up of gas heater used for amplification. Microscope boxes were used to shield the heater from wind to limit heat fluctuation.



Although the VCD had data linking cases of SH to the Apac region, discussions with the school headmaster confirmed that SH had not been reported in many years. Historically when an individual in the community presented with haematuria, the symptoms were reported to the headmaster, who would contact the local health authority for treatment when required. The headmaster believed that by educating the children and their families; and initiating a community surveillance effort, they had eliminated SH cases from their small community. Throughout the study, there were no positive cases of SH recorded by microscopy or comparative dipstick test (the SH RDT), confirming lack of prevalence within our study cohort.

#### ***4.6.2.1 Multiplex malaria and schistosomiasis cassette***

Due to the lack of SH within the community, the results from the Paper Device SH channel were used as a negative control during analysis to monitor possible amplicon contamination events. As a result of the control, only the samples which produced positive results for SH were eliminated from analysis (5 of 33 tests). In the previous trial all of the samples processed between successive external controls were eliminated from the analysis. The inclusion of the SH channel highlighted the importance of including a NC within each diagnostic cassette. Unfortunately the BRCA-1 target DNA - used as a PC- degraded during the field trial. Where possible the *plasmodium* PAN and *S. mansoni* gBlock DNA were used as a PC template, however, target *plasmodium* PAN & *S. mansoni* gBlock DNA was limited. In cases where no PC was included and no positive amplification was observed throughout the cassette, the result was removed from the study analysis (N =7).

In total 33 cassettes were processed and 17 were included in analysis. Of the 33 samples processed, 16 cassettes were removed due to; leaks (N=1); failure of controls (N=10); and contamination events (N=5). Some cassettes exhibited more than one of the described failures. For the malaria results, 6 true-positive tests (PP); and a single true-negative (NN) were recorded (as compared to microscopy). Additionally, there were 4 false-negative (PN); and 6 false-positive (NP) test results. The false-negative results are likely due to heating fluctuations caused whilst conducting LAMP on the gas stove. The malaria RDT results for the 17 samples included in analysis agreed with microscopy results.

Double blinded confirmatory qPCR was carried out on return to the laboratory in the UK, refer to Section 2.1.1.3 & 2.1.3.2 for the methods. TaqMan qPCR results were obtained for 12 of the 17 samples. Due to a miscommunication in the laboratory, the 5 unaccounted samples were processed during a laboratory training session and as a result they were

excluded from the confirmatory qPCR results. 4 of 6 PP results; and the single NN result were confirmed by qPCR. Furthermore, 5 of the 6 NP results were confirmed to be true-positive by qPCR; and 2 of the 4 PN results were confirmed to be false-negative. The results are summarised in Figure 4-10.

For the *S. mansoni* assay there were 14 analysed results, due to lack of a control line on the SM LF strips which prohibited the analysis of 3 tests. The *S. mansoni* results were PP = 1, NN=1, PN=3 and NP=9, as compared to KK examination (see Figure 4-10). As a result of a POC-CCA supply shortage, the POC-CCA RDTs were only carried out on 7 of the 14 samples. The outcome of the Paper Device results as compared to the POC-CCA results were as follows PP=1, NN=1, PN=3, NP=2.

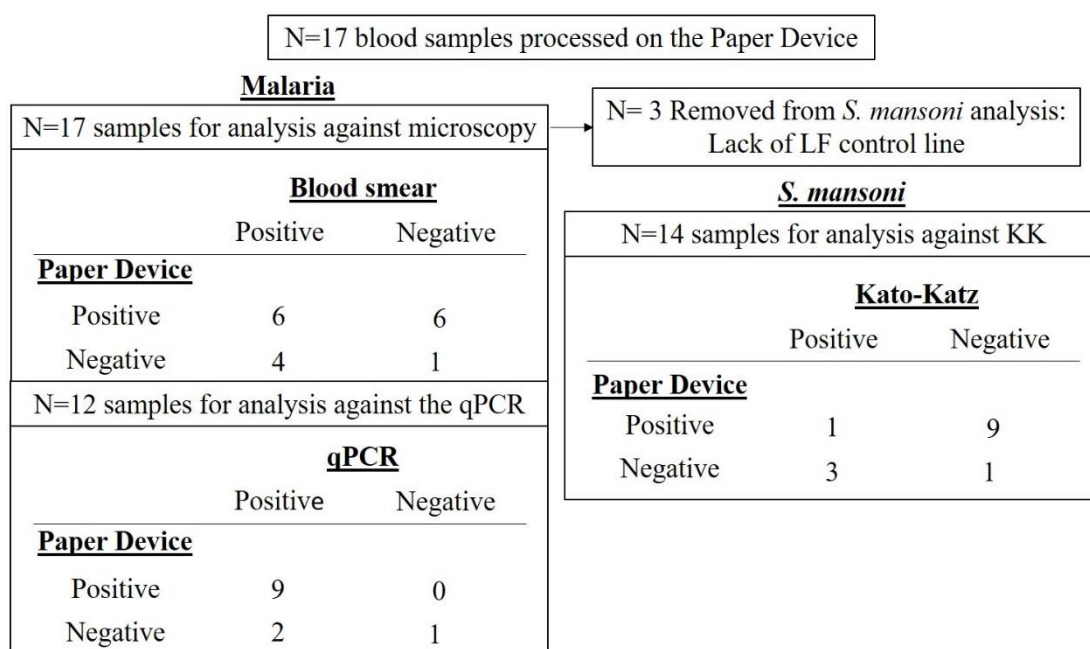


Figure 4-10: A summary of the result obtained for the multiplex malaria and schistosome cassette. The detection of plasmodium and *S. mansoni* DNA in a 5 µL whole blood sample in-the-field. Amplification was carried out using a portable gas stove. Point-of-care LAMP results were analysed against comparative diagnostics in the field (blood smear or Kato-Katz) and malaria results were analysed against comparative qPCR conducted in the laboratory on return to the U.K.

#### 4.6.2.2 Factors effecting the malaria and schistosome Paper Device in-the-field

There was a significant loss of cassettes during the field trial due to leaks which presented from valves and in-between layers of adhesive film, failure of the PC and LF strip controls. Some of the cassettes exhibited multiple of the described failures, contributing to the loss of 16 out of the 33 samples from analysis.

#### **4.6.2.2.1 Heating**

There was a significant loss of testing time due to the failure of heaters, however, the ability to source a field-appropriate replacement heater from Apac town enabled testing to continue. Amplification using the frugal heating technique was subject to temperature fluctuation ( $63 \pm 4$  °C) as the temperature was monitored visually using a thermometer placed in the well of a metal heat block. Up to 30% of the cassettes processed were removed from analysis due to failure of the PC, which was likely due to the fluctuation in temperature (Singleton *et al.*, 2014) caused by user errors.

#### **4.6.2.2.2 Comparative diagnostic tests**

Limited availability of POC-CCA RDTs prior to the national *S. mansoni* surveys for the MDA programs in Uganda resulted in a limited portion of POC-CCA RDTs being carried out in-the-field. Unfortunately, this resulted in lack of confirmatory diagnosis for *S. mansoni* in-the-field for half of the processed *S. mansoni* samples.

#### **4.6.2.3 Considerations for future trials**

Due to the lack of *S. haematobium* in the Northern and Eastern regions of Uganda the SH reagents were to be removed from the Paper Device platform for successive trials. It was decided that a NC should be integrated into future designs to identify contamination events. Changes made to the design of the cassette were discussed in Section 2.2.7.2. The ability to conduct ‘controlled’ LAMP amplification in-the-field is beneficial for understanding whether the occurrence of false negative results are due to conditions in-the-field, or the Paper Device method itself, this was considered for future trials.

### **4.6.3 Integration of controls into the multiplex malaria and *S. mansoni* cassette**

The third field trial took place in the Tororo District in the Eastern Region of Uganda. VCD surveillance data suggested that malaria prevalence in Tororo was lower than in the Mayuge District. The microscopy data collected in-the-field suggested there was 53% prevalence of malaria infection among the participants. Additionally, historic VCD surveillance data suggested a lower prevalence of *S. mansoni* in the region. Microscopy results from the study suggested there was 51% prevalence of *S. mansoni* infection within the study cohort. Surveillance and MDA for bilharzia had not been conducted in the region for over 10 years and the VCD team believed that the likelihood of re-emergence in the region was high, prompting VCD to choose Tororo for testing.

Following the failure of heaters in the previous trial, portable heaters were designed by Dr Arslan Khalid for use in-the-field. Furthermore, a NC was integrated into each cassette to monitor potential contamination events, and a mini-PCR™ thermal cycler was purchased to enable PCR and LAMP to be carried out in-the-field.

#### **4.6.3.1 Multiplex malaria and *S. mansoni* cassette**

A total of 61 samples were processed on the Paper Device, due to processing faults and amplification failures 30 cassettes were included in analysis. 9 of the 61 cassettes processed exhibited blocked valves, this was due to delay in processing after removal from the heat block. 12 of the cassettes were removed from analysis as a consequence of contamination events, and a further 10 due to the failure of the PC. The results for malaria obtained on the Paper Device as compared to gold-standard microscopy were PP = 9; NN = 11; PN = 10. TaqMan qPCR analysis carried out in the laboratory agreed with both the PP and NN results, however, 6 of the 10 PN results which were negative by LAMP in-the-field were confirmed as false-negative by qPCR. The inhibition of LAMP amplification of these samples could be due to a number of factors, for example heating and poor DNA recovery. The heating of the cassettes was monitored throughout the process and is therefore unlikely to have affected the NAAT. It was noted that the majority of the failed samples had relatively low parasite count (< 160 parasites per mL whole blood), thus the low parasite density may have affected the DNA recovery on paper and consequently the LAMP result (Yang *et al.*, 2018), some data for DNA recovery on paper is provided in Section 7.5 in the Appendices. The 4 samples which were positive by microscopy were not detected by qPCR or LAMP, these samples also had a low parasite count, thus, the sampling and the extraction of DNA may also have effected these results.

The results for *S. mansoni*, as compared to microscopy were as follows, PP = 2; NN = 11; PN = 13; NP = 2. A further 2 samples were removed from analysis due to blocked channels. The POC-CCA RDT results suggest 26 of the 28 samples were positive for *S. mansoni* infection; the 2 POC-CCA RDT negative results corresponded to LAMP and microscopy negative results. However, POC-CCA RDTs are reported to overestimate prevalence of *S. mansoni* in-the-field (Fuss *et al.*, 2018). There did not appear to be any correlation between the intensity of *S. mansoni* infection and respective PN results, however, the daily variation in schistosome egg excretion and the overdispersal of egg output result in a high day-to-day variability in KK test results (Weerakoon *et al.*, 2015). As such, the KK result from an individual stool sample may not be representative of true parasite load.

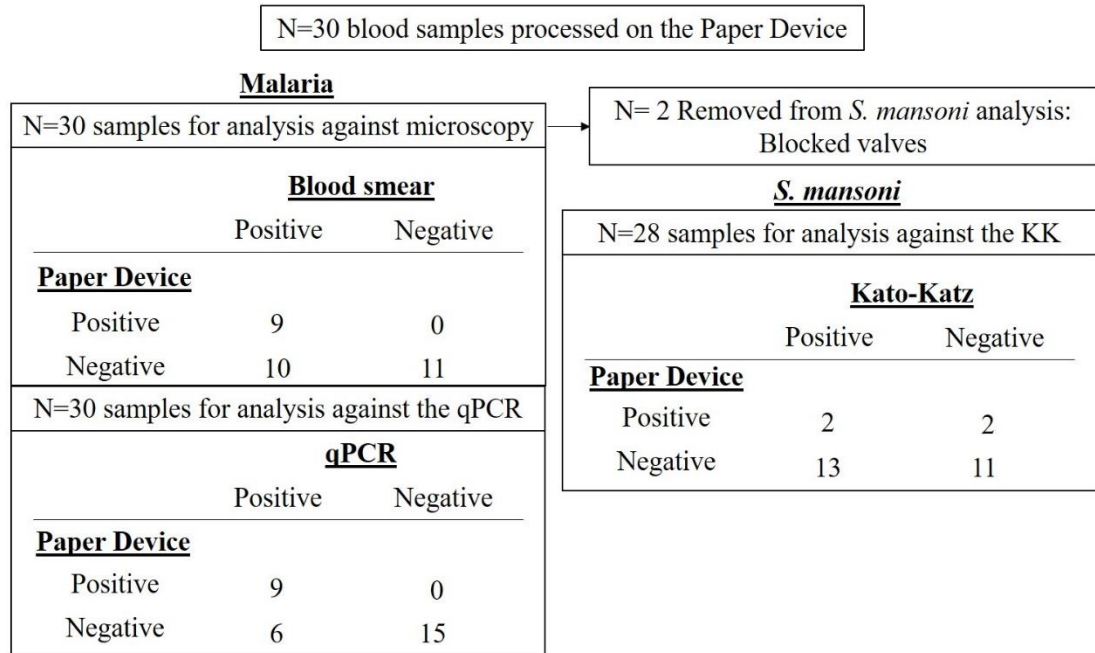


Figure 4-11: A summary of the result obtained for the multiplex malaria and *S. mansoni* cassette. The detection of plasmodium and *S. mansoni* DNA in a 5 µL whole blood sample in-the-field. Point-of-care LAMP results were analysed against comparative diagnostics in the field (blood smear or Kato-Katz) and malaria results were analysed against comparative qPCR conducted in the laboratory on return to the U.K.

#### 4.6.3.2 Mini-LAMP

The miniPCR™ thermal cycler was taken to the field to carry out controlled LAMP (referred to as mini-LAMP) and confirmatory PCR in the field. Following the DNA extraction – following the method described in Section 0, LAMP was carried out using the miniPCR™ thermocycler, following the method described in Section 2.1.3.2 and results were read visually on LF strips.

Mini-LAMP was carried out on 5 samples in parallel to the Paper Device. The investigators were blinded to the associated microscopy results, resulting in the selection of 1 negative and 4 positive samples. Mini-LAMP produced results indicating the presence of *plasmodium* DNA in all blood samples, one of which was negative by both microscopy and confirmatory qPCR (conducted in the laboratory in Glasgow). The same samples processed on the Paper Device produced two negative and two positive results - one sample was excluded from analysis due to lack of amplification of the positive control within the cassette. The positive and a single negative result agreed with microscopy data, however, the second negative result - which did not agree with microscopy or mini-LAMP data - was also negative by confirmatory qPCR in the laboratory in Glasgow.

The respective *S. mansoni* microscopy results indicated that of the 5 samples, 2 were positive and 3 were negative. Mini-LAMP results suggested only 1 of the samples contained *S. mansoni* DNA and the corresponding Paper Device results were all negative. The false-negative results obtained by mini-LAMP suggest that a 5 µL sample of whole blood may not be an appropriate clinical sample to determine an *S. mansoni* infection and may have resulted in lower sensitivity for the detection of *S. mansoni* DNA.

#### 4.6.3.3 MiniPCR™

During the trial PCR was carried out on a single sample using miniPCR™ thermal cycler, see Figure 4-12(a), the method followed the protocol stated in Section 2.1.3.2. The EZ PCR 5X Master Mix, Load Ready™ (miniPCR™, Cambridge, MA) was used to conduct PCR. The Master Mix was designed for field use and is stable at room temperature for up to one month.

A 10 µL fraction of the amplified products were run on the BlueGel™ electrophoresis system, see Figure 4-12(b), the resultant bands (Figure 4-12(c)) were compared against a DNA ladder, the Load Ready™ 100 bp DNA ladder (Cambio Ltd, Cambridge, UK). Both NC and PC along with the DNA extracted from a single patient blood sample were detected. The wells (labelled 1-9) display the DNA ladder; NC for SM, PPAN and BRCA-1; the DNA extracted from a whole blood sample, SM, PPAN, BRCA-1; and PC for SM and PPAN respectively. Wells labelled 2-5 indicate no amplification of target DNA. Whereas wells 6-9 indicate positive amplification of target DNA. The bands appear in line with the expected DNA ladder suggesting correct amplification. The miniPCR™ suggest the sample was positive for *plasmodium* and BRCA-1 DNA. Microscopy results showed the sample was positive for *S. mansoni* infection but negative for *plasmodium* infection. However, both the malaria RDT and confirmatory qPCR (carried out in the laboratory in Glasgow) agreed with the miniPCR™ result. The negative SM result by miniPCR™, suggests that detection of *S. mansoni* DNA in 5 µL of a clinical sample, using the selected molecular reagents may not be reliable.

PCR is recognised as being more sensitive than microscopy (Berzosa *et al.*, 2018). The application of PCR in-the-field is rare due to the cost of reagents and equipment; the need for an uninterrupted power supply for prolonged periods; cold-chain logistics for reagents; and highly skilled technicians to conduct the test (Utzinger *et al.*, 2015). The miniPCR™ is cheaper than a conventional PCR machine, however, the other complications associated with

conducting PCR in-the-field including the preparation time were still an issue. The agarose powder and water solutions to prepare gels were pre-aliquoted and low melt agarose was used to eliminate the need for a heat plate, however, the man-power and time required to process samples for amplification and run the gels remained too high (Table 4-2). Additionally, the portable power bank needed to be solar charged after each complete PCR and gel run. For this reason we did not conduct further PCR tests in the field.

*Table 4-2: Table of the basic equipment and consumables used for PCR, LAMP and POC-LAMP in the field. Y= used, -= not in use, Y/N = used where appropriate.*

<b>Equipment</b>	<b>PCR</b>	<b>LAMP</b>	<b>POC-LAMP</b>
• Power bank	Y	Y	Y/N
• Thermocycler (miniPCR™)	Y	Y	-
• Heater & heat block	-	-	Y
• Laptop	Y	Y	-
• Mastermix	Y	Y	Y
• Primers	x2	x6	x6
• Pipettes	Y	Y	Y
• Gel dock (BlueGel™)	Y	-	-
• LF strips	-	Y	Y
<b>Consumables</b>			
• Pipette tips	Y	Y	Y
• Eppendorf's	Y	Y	Y
• 8-Strip tubes	Y	Y	-
• POC-cassettes	-	-	Y
• Agarose powder	Y	-	-
• TAE	Y	-	-
<b>Time to Amplification (minutes)</b>	90	30	40
<b>Time to result</b>	120	40	50

A finger-prick blood sample for each of the participants was stored on FTA® cards and transported back to the UK for confirmatory qPCR analysis. Confirmatory qPCR for malaria was successfully completed using DNA extracted from the blood spots stored on FTA® cards. It was concluded that the small volume of whole blood (< 20 µL) was not able to provide a concentration of cell-free circulating *S. mansoni* DNA that was large enough to detect *S. mansoni* DNA by qPCR (refer to data in Section 7.6.1 of the Appendices).

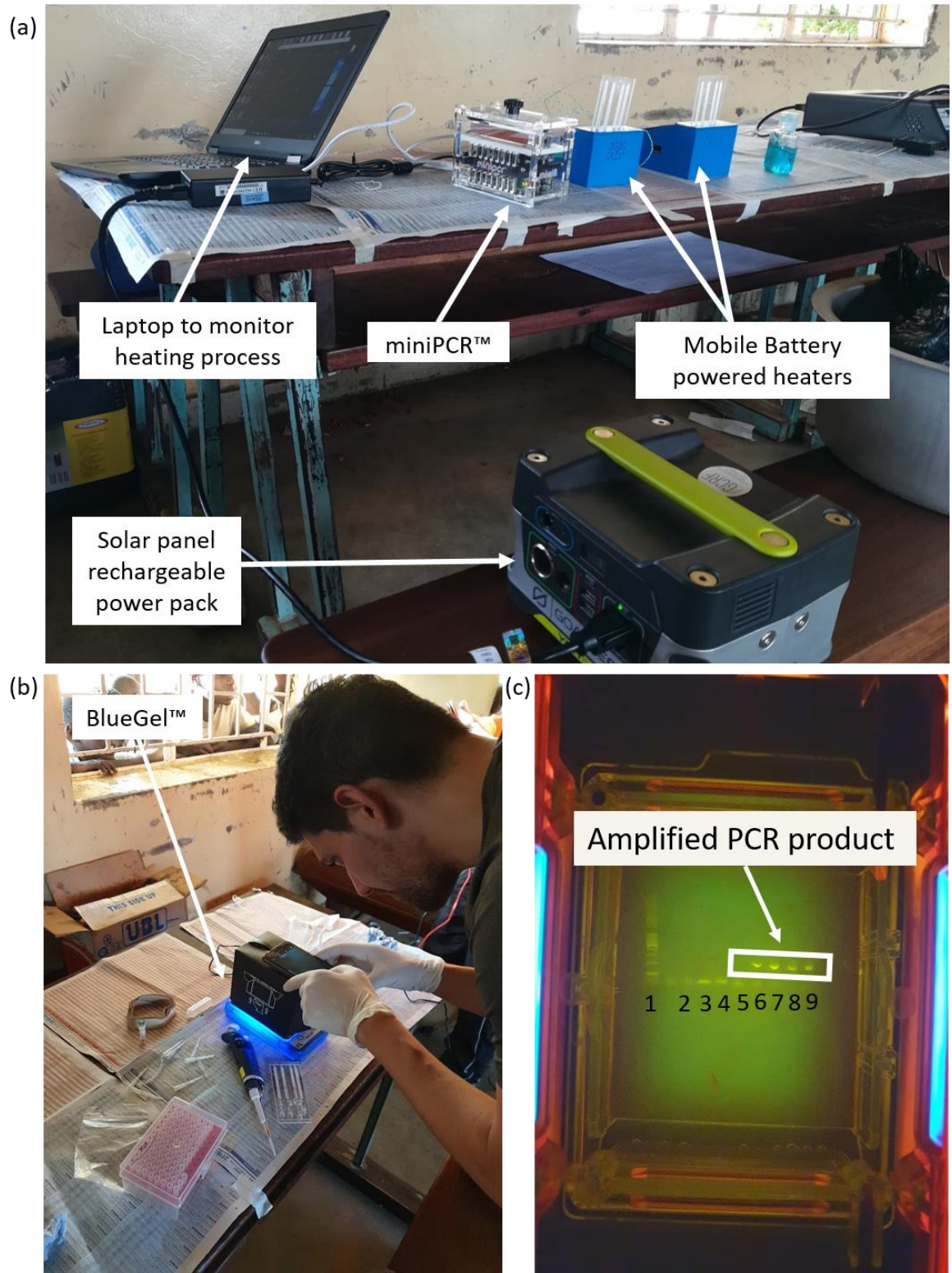


Figure 4-12: miniPCR™ and gel electrophoresis in the field. (a) PCR was carried out using the miniPCR™ thermal cycler in the field. The miniPCR™ was powered by a rechargeable battery pack and temperature cycling was monitored on the laptop. (b) Elías Kabbas-Piñango capturing an image of the gel electrophoresis bands using the BlueGel™ electrophoresis system. (c) Image of the bands produced from Amplified PCR product from control DNA templates and a whole blood sample following DNA extraction. The bands highlighted in the image 6-9 (~150 bp) are amplified PCR product from the positive control DNA template and PPAN and BRCA1 DNA in the whole blood sample.



#### **4.6.3.4 Factors effecting the multiplex malaria and *S. mansoni* Paper Device in-the-field**

##### **4.6.3.4.1 Molecular reagents**

A large portion of the cassettes processed in field trials were excluded from analysis. In the preliminary trials the physical limitations of the cassette (discussed in Chapter 2), such as leaks and heating issues were the major cause of exclusion from analysis, these issues occurred in up to 34 % of the cassettes processed. The re-design of the multiplex malaria and *S. mansoni* cassette eliminated leaks and reduced physical failures of the cassette to 14 %. The heating was monitored using a thermocouple during the final field trial, however, throughout the trials the percentage of false negative positive controls in cassettes remained almost constant (17 to 20%). The data suggests that the molecular reagents may be compromised in-the-field. As a result, further investigation of the effect of storage conditions on molecular reagents used in the field was carried out (detailed in the following chapter).

##### **4.6.3.4.2 Amplicon contamination**

Eliminating the repetitive use of reagents will reduce the frequency of contamination events, which effected up to 20 % of the cassettes processed in-the-field. Integrating pre-stored molecular reagents within the cassette will reduce manual steps within the process, thus reducing the risk of contamination, however, environmental factors in-the-field may still introduce risk of contamination. A linear workflow should be adhered, to assure that the samples and the cassettes housing molecular reagents, are not exposed to LAMP amplicons prior to processing.

##### **4.6.3.4.3 Detection of *S. mansoni* DNA in blood**

Potential to detect *S. mansoni* DNA in whole blood as demonstrated by Song *et al.*, (Song *et al.*, 2015), resulted in the integration of the *S. mansoni* reagents into the pre-existing malaria diagnostic cassette. The combination of *plasmodium* and *S. mansoni* assays into a single cassette decreased sample processing time and as a result, the number of cassettes processed in-the-field per day was increased. The use of the SM mtDNA target region (GenBank Accession No. L27240) to amplify *S. mansoni* circulating DNA in urine has been reported (Fernández-Soto *et al.*, 2019). Thus, it was thought that the same target region may be detected in whole blood samples. The results obtained from the field study (discussed in Section 4.6.3.1) suggest that the target mtDNA sequence (GenBank Accession No. L27240) may not appropriate for detecting presence of *S. mansoni* infection from a fingerpick blood sample, the method may benefit from using larger sample volumes.

Amplification time in the field was increased up to 60 minutes. Fernández-Soto *et al.* report that increasing the amplification time to 120 minutes results in increased sensitivity, allowing detection of *S. mansoni* DNA in clinical urine samples (Fernández-Soto *et al.*, 2019). Increasing the LAMP amplification time to 90 minutes in-the-field produced false amplification of malaria controls. At present, it appears that the two molecular assays are not compatible for use in a single cassette, although increasing the volume of blood used for detection may provide a better platform for *S. mansoni* DNA detection (Wichmann *et al.*, 2009).

Prevalence data for the study cohort collected from KK and POC-CCA test was very different (56.1% and 85.7% respectively). POC-CCA RDTs have been reported to overestimate *S. mansoni* positive infections in locations where prevalence of infection is low (Foo *et al.*, 2015). However, more studies highlight limitations of the KK method in low burden infections (Fuss *et al.*, 2018). The data from this study adds to the growing number of study's highlighting inconsistencies in POC diagnosis of *S. mansoni* infections and the need for a more sensitive field applicable gold-standard test (Legesse and Erko, 2007; Cavalcanti *et al.*, 2013; Colley *et al.*, 2013; Lodh *et al.*, 2013; Foo *et al.*, 2015; Beltrame *et al.*, 2017).

*The field results suggest that the target mtDNA sequence is not appropriate for detecting presence of s.mansoni infection by LAMP from a fingerpick blood sample.*

## **4.7 Discussion**

In this section a range of outcomes and insights gained from carrying out preliminary field trials will be discussed. Attention will be brought to the logistics and lessons drawn from conducting field trials during development of a molecular POC diagnostic tool. The reference diagnostics and respective methods will also be discussed. Finally, the collaboration between the VCD, selection of field sites and potential associated implications will be highlighted.

### **4.7.1 Logistical problems**

The following describes a few of the logistical issues which had not been predicted before the field trials began.

#### **4.7.1.1 Consent**

Confirming assigned consent of the children was the primary hurdle in-the-field. In many cases, the child's name (as recorded in VCD assigned consent data) did not correlate to the name the child used in school which had been listed by the teachers in the study records, and often names were also misspelled. Following assigned consent, the child's name and the name of their parent/head of house was recorded by the teachers and shared with the MoH VCD health care workers. It later became apparent that participant names recorded by the teachers had been spelled phonetically, therefore, recurring names had various spellings throughout the study records. The inconsistencies in the spelling of names required the study team to match phonetically similar names in the study records to the assigned consent data.

#### **4.7.1.2 Variation of samples**

The study required multiple tests to confirm the presence of infection in each participant. Due to the samples being collected for multiple test processing routes there were occasional sample mix-ups, for example, where blood was added to the wrong tubes or slide/RDT for processing. Blood was collected by the MoH nurse, therefore, the sample mix-ups were easily monitored and corrected. On a few occasions it was discovered that participants were sharing stool samples, or handing in collection containers filled with dirt or mud. Similar scenarios have been reported in other studies requiring patient stool specimen, and where sample collection is not directly observed (Shane *et al.*, 2011). Where identified, the invalid stool sample results were omitted from our records.

#### **4.7.1.3 Heating**

Logistical issues more specific to the Paper Device arose during heating. After the extraction of DNA and addition of molecular reagents, the Paper Device cassette had to be heated at 65°C for 40 minutes to carry out LAMP. In some cases the generator used to power the heaters failed and heating ceased for lengthy periods. The custom aluminium heat block was able to retain sufficient heat for roughly ten minutes, in scenarios where the heaters failed, cassettes nearing the end of their heating period (< 10 minutes) were left in the custom heat block to complete LAMP— any heating faults were noted in the study records. There were also timer faults during heating, resulting in the wrong test cassette being removed and results were read too early or late. When such scenarios occurred, the respective results were recorded, however, the fault was noted in the study records and subsequent results were omitted from analysis.

#### ***4.7.1.4 Molecular controls***

The method for DNA extraction was optimised in a lab setting. Firstly the DNA extraction method was trialled in ‘DNA clean’ conditions in our biological laboratory facilities, and after this in a general lab space - areas where no DNA amplification had been previously conducted. Working conditions in-the-field are not comparable to a laboratory environment, therefore, PC and NC were conducted in the cassettes to monitor possible environmental contaminants - for example dust or surface amplicon contamination. In initial field trials the controls were run on designated ‘control cassettes’ at various points in the day, in later iterations of the study, both a PC and NC was integrated within the diagnostic cassette.

A 5 µL sample of nuclease free water (the NC) was added to the NC chamber of each cassette. In instances where the NC returned a positive LF strip result, the cassette results were recorded, and work was ceased until the successive diagnostic cassettes had completed heating. Results of consecutive tests were also noted in study records. In most cases, the NC strips in succession also returned a false-positive LF result. After such an event the working stock primer mix and Isothermal Mastermix were discarded and surfaces were cleaned. After resuming controls with new aliquots of molecular reagents, false-positive results ceased suggesting that contamination of working stock reagents had occurred. The cassettes containing false-positive LF strip results for the NC LF strip were included in the study records but omitted from the study analysis.

LF strips contain a ‘control’ line which is a procedure control to confirm the strips flow function (Rapid Medical Diagnostics, 2018). In molecular laboratory experiments it is routine to include a NC and PC in each run (Viana and Wallis, 2011). Inclusion of the NC strip within the cassette was a ‘field solution’ to mimic standard molecular laboratory protocol, and to allow better understanding of the Paper Device and the potential environmental effects on performance in-the field (Connelly et al., 2015; Trinh and Lee, 2019). Contamination of working stock reagents during field trials was most likely due to handling errors (Viana and Wallis, 2011; Public Health England, 2018), the development of diagnostic cassettes with pre-loaded molecular reagents would eliminate reagent handling and simplify diagnostic preparations.

*Integration of negative and positive controls are vital to monitor molecular amplification out-with laboratory conditions.*

#### 4.7.2 Reference diagnostics

The process of evaluating new and more sensitive diagnostic tests in low resource settings against the current comparative standard reference tests is a common problem (Cavalcanti *et al.*, 2013; Al-Shehri *et al.*, 2018; Fuss *et al.*, 2018). Although RDTs are commonly used for diagnosis of malaria and schistosomiasis in clinics throughout sub-Saharan Africa, microscopy (despite low sensitivity) is still currently the gold standard diagnostic for both diseases (Doenhoff *et al.*, 2004; Rougemont *et al.*, 2004). Both microscopy and RDTs have associated advantages, limitations and logistical issues (Fuss *et al.*, 2018). These alongside complications of conducting comparative analysis of diagnostic tests, will be discussed further in this section.

##### 4.7.2.1 Microscopy

The preparation of slides for both KK and blood smears was timely (>1hr for each) and the requirement for staining and drying slides introduced risk of sample loss or destruction. The microscopy slide preparation was conducted at the back of the classroom to limit risk of tampering by the participants and eliminating trip hazards, which would cause spills or destruction of slides. Blood smears for diagnosing malaria were prepared and read first. The *plasmodium* parasite morphology becomes altered with time after blood collection, rendering diagnosis more difficult after longer periods of time (UCLHS NHS, 2020). Whereas the storage of stool samples for a few hours does not affect diagnostic accuracy of KK to detect *S. mansoni* infection (Fuss *et al.*, 2018). Additionally, preparation of stool samples for KK examination was lengthier than blood smears and required more manual labour, all of which support the decision to conduct malaria diagnosis prior to double KK examinations.

Two technicians were employed to conduct the microscopic examinations. This significantly decreased the time needed to complete sample preparation and slide reading, enabling time to screen 25 patients microscopically alongside conducting RDTs each day. It must be noted however, that increasing the number of technicians also increases cost and the volume of necessary resources. This is a privilege we were able to accommodate in our study, but which may not be a financially viable option for clinics with limited-resources. Additionally, we were not investigating samples to conclude a patient diagnosis; we were conducting mass screening for two specific diseases. Our study allowed batch processing of samples and microscopy readings to quantify burden of two specific parasite infections, this also decreased slide examination time. In clinics there is likely to be a larger array of necessary

examinations and staggered patient sample intake, all of which contribute to increasing diagnostic preparation and examination time.

#### **4.7.2.2 Malaria RDT**

During field trials, preparation of malaria RDTs was very simple. After insertion of the blood sample, running buffer was applied to the sample pad, before result read-out. The instructions for use are shown in Section 7.7.2. For the purpose of our study, all participants had to be treated as malaria positive, as PCR – of higher sensitivity (Berzosa *et al.*, 2018), was conducted on return to the laboratory in the UK. However, in clinical settings, the decision to treat individuals who are malaria negative by RDT can be driven by perceptions of treatment failure, or undetectable malaria in patients who have taken antimalarial medication prior to testing. There are varied reports of sensitivity of RDTs for malaria when tests are conducted in the field and low transmission areas (Tseroni *et al.*, 2015; Diallo *et al.*, 2017), however from our study (conducted in an endemic area) it appears that overall, CareStart™ pf/pan RDT was able to provide a result with sensitivity which was comparable to microscopy. Additionally, the RDT was a much easier test to conduct and provided results more quickly.

#### **4.7.2.3 S. mansoni RDT**

The CCA antigen is detected in unprocessed urine, making sample collection and preparation much simpler than for KK examination. Additionally, stigmas of providing a stool sample are avoided by availability of a diagnosis from urine (Shane *et al.*, 2011). Logistical issues that arose during stool collection, mentioned in Section 4.7.1.2 such as sample sharing, swapping and substitution with dirt, is less likely to occur whilst collecting urine. Furthermore, the variability of egg distribution which occurs when conducting microscopic examinations of stool is avoided by testing urine for presence of CCA (Shane *et al.*, 2011). Ease of collection and sample processing as compared to KK examination all adds to the preference of conducting POC-CCA in the field.

From the study conducted in the Tororo district, where *S. mansoni* was reportedly not present, KK tests reported 56% prevalence within our study cohort; and, results from POC-CCA concluded that prevalence was 85%. The techniques provided widely different conclusions, which contradicts reports that KK prevalence over 50% returns similar results to POC-CCA (Kittur *et al.*, 2016). It is known that urinary tract infections and haematuria may affect POC-CCA results, particularly in cases of weak positive (or trace) results (Shane

*et al.*, 2011; Ferreira *et al.*, 2017), leading to an overestimation of prevalence (Fuss *et al.*, 2018). There is a risk that this may have affected our study data, where we were conducting trials in a suspected low prevalence area. We would like to assume that the POC-CCA has successfully diagnosed *S. mansoni* infection where microscopy has failed to detect *S. mansoni* ova. However, where a more sensitive technique is not presently validated for field use, the POC-CCA may need to be counted as false positive against the gold standard.

#### **4.7.2.4 *S. mansoni* Hatching Tests**

The hatching test is not traditionally used as a diagnosis for *S. mansoni* infection; the technique is most commonly used to collect miracidia, which provide improved outcomes for genomic analysis as compared to *S. mansoni* ova (Webster, 2009; Van den Broeck *et al.*, 2011; Gower *et al.*, 2013). Hatching was only carried out on samples succeeding a resultant negative KK examination. Where hatching showed presence of miracidia in KK negative individuals, the participant was recorded as positive for *S. mansoni* infection.

During hatching tests there is potential to identify low-burden infections due to increased sample size, although, there are reports that hatching demonstrates poor performance with small numbers of *Schistosoma* eggs in faeces (Borges *et al.*, 2013). Additionally, the technique requires a lot of manual work and consumables. One sample can require up to 3 litres of fresh water, in communities where water is limited and expensive, this is not a viable protocol to diagnose a potential *S. mansoni* infection. The sample preparation method increases likelihood of contact with faecal material, increasing risk of infection to the test examiner. Additionally, there is a need for a trained technician to distinguish the miracidia after hatching. Overall the technique introduces more risk to the user, and failure to provide ambient hatching conditions will hinder correct diagnosis (Borges *et al.*, 2013; Gower *et al.*, 2013).

Where we were fortunate to have available manpower and equipment to conduct the confirmatory hatching protocols, this led to diagnosis of a few *S. mansoni* infected individuals where the technicians had failed to detect *S. mansoni* ova using the KK technique. This provided confirmation for a few POC-CCA positive results obtained in the field, where KK examination had contradicted the result.

### **4.7.3 Development of the Paper Device in-the-field**

Conducting field trials whilst the diagnostic platform was still in early development stages required additional resources and tests to monitor potential changes due to adverse working conditions. There were also associated responsibilities, some of which lie out-with the scope of the study. These will be further discussed in this section.

#### **4.7.3.1 Selection of Participants**

For ethical reasons we required a random selection of participants (half male and female) to be taken from each class. To omit selection bias on behalf of the study team, the school teachers were instructed to conduct the random selection of participants. The teachers were aware that the selected individuals would receive treatment, consequently introducing a high possibility of selection bias, to enable the pupils to access treatment. The potential selection bias could be accountable for the extremely high prevalence of malaria and schistosomiasis recorded during the trials – however in the earlier trials (in the Mayuge District), the high prevalence was most likely cause of extremely high prevalence amongst school children in the community (Adriko *et al.*, 2018).

#### **4.7.3.2 Comparative Diagnostics**

In a laboratory trial format, encompassing comparative diagnostic exams within our workflow would not be necessary. A more controlled environment would have allowed for the infection status to be determined and blinded beforehand. The random selection of participants' in-the-field of unknown infection status required comparative diagnostics to be conducted in parallel to the Paper Device. Adherence to microscopic diagnosis has been discussed throughout Section 4.7.2, therefore RDTs were also conducted in hope that lower burden infections may also be identified (Shane *et al.*, 2011; Fuss *et al.*, 2018). The study format resulted in at least five different tests (per participant) being conducted on site to determine the status of infection.

The VCD technicians are well trained and routinely conduct microscopy and RDTs in-the-field. After many years of use in-the-field their workflow and method of testing has been optimised and as a result appeared seamless in comparison to the Paper Diagnostic tool. Nevertheless, initial field trials were vital in understanding the environments that the Paper Device is aimed to be used in, and to observe the effect that the environment has on processing and test conditions. The experimental process evolved with each study resulting in improved testing efficiency, for example, by changing the workflow and enabling more



devices to be heated at once. Additionally, field trials enabled flaws in the diagnostic design such as reagent storage (discussed in subsequent chapters) to be pinpointed, and highlighted areas for further research and development.

#### **4.7.3.3 Additional Resources**

The process of developing a diagnostic in-the-field introduced the need for additional equipment to monitor and understand the potential changes in diagnostic process, such as the heating and DNA amplification. ‘Mock’ diagnostic devices were modified to encompass a thermocouple which allowed temperature monitoring throughout the heating process. The risk of heating fluctuation was increased due to high chance of power surges from the generator causing heating equipment to fail. In the second field trial when heaters were irreparably damaged, a gas stove was purchased locally and LAMP was conducted in a saucepan, seen in Figure 4-9 (a). The temperature of the saucepan was controlled visually using a thermometer and microscope boxes were arranged as a windshield in attempt to retain stable heating, as seen in Figure 4-9 (b).

When conducting field work it seems that no amount of preparation can eliminate occurrence of practical issues. Malleability in the diagnostic process and the ability to source a logical, simple and ‘field appropriate’ heating solution enabled testing to continue. Subsequently, alternate heating solutions such as mobile battery powered heaters have been explored (depicted in Figure 4-12). As mentioned in Section 4.7.1.4, in attempt to provide a better understanding of the performance of the molecular diagnostic in the field, both a PC and NC were included in the new cassettes. The controls were paramount in determining where amplification had failed and led to false-negative results, as well as contamination events which would lead to potential false-positive results.

*An automated heating system, where source of heating is not reliant on an external electricity source should be explored in future field trials*

#### **4.7.3.4 Study Site Selection**

Potential trial sites and timelines were planned with partners in the MoH VCD. Funding deadlines limited the timescale for conducting trials and securing resources for testing, however, we were cautious to work along with the VCD testing and treatment timelines. Our trials had the potential to disrupt the provision of care that VCD provide to communities in Uganda, as we required testing sites in locations where MDA had not been conducted in the last 6 months. Open communication and planning with the MoH and VCD enabled the trial to be conducted with limited disruption to VCD national treatment programs. Additionally, we had to be cautious not to disrupt various ongoing studies based in rural Uganda, such as longitudinal infection studies on bilharzia (Adriko *et al.*, 2018). The VCD work in collaboration with a number of different research groups, their involvement in which, allowed the risk of impact of our trial on other studies and vice versa to be minimized.

#### **4.7.3.5 Study Impact**

In discussions with the head of the Tororo District Health Authority prior to our study, it was made clear that they did not believe that bilharzia was present in their district. The VCD had historically recorded presence of the disease (> 10 years ago) during surveys in a number of small villages on the outskirts of the district. Our (small) study conducted in a single school concluded that 56% of the participants had active bilharzia infections (data provided by results of the KK examinations). The re-emergence of schistosomiasis in the Tororo District had been expected by the VCD, however, such high prevalence was not (Crellen *et al.*, 2016).

The results were conveyed to the community after discussion with the head teacher. Additionally, the data was compiled and sent to contacts in the MoH, to relay to the Tororo District Health Authority. Recording instances of bilharzia in the Tororo district has the potential to change perception of the disease. At the moment, bilharzia is most widely associated with proximity to large bodies of fresh water (Kabatereine *et al.*, 2011; Utzinger *et al.*, 2015), however, our study found presence of bilharzia in a region much further from the lakes. The VCD technicians collected water and snail specimens from a nearby swamp for additional studies. The finding has potential to influence change in current bilharzia surveillance and treatment programs in Uganda (dependent on local funding and resources). On the other hand, this knowledge can instigate other researchers to work alongside the VCD and conduct surveillance in the district, it could be an interesting area to observe routes of re-infection and provide insight into alternate snail habitats.

## 4.8 Conclusion

Preliminary field trials provided a greater understanding of the settings where the POC diagnostics for malaria and schistosomiasis are needed in Uganda. Conducting the reference diagnostics (microscopy and POC RDT tests) in parallel with the Paper Device resulted in a better understanding of the current methods and processes used in low-resource settings. Overall, detection of *S. mansoni* and *plasmodium* DNA within clinical samples, using the POC Paper Device in-the-field in Uganda was successful. The study is one of very few where a POC NAAT has been carried out in limited-resource settings, and highlighted the challenges associated with developing and implementing new diagnostic technologies, without access to laboratories or infrastructure.

First-hand experience of the constraints that the test conditions have on molecular diagnostic testing enabled important changes to be made to the Paper Device in early development stages, such as, focusing on diagnosis from blood samples to evade sample collection problems associated with faecal specimen (discussed in Section 4.7.1.2). Throughout the study changes in the design of the diagnostic cassette were made (as discussed in Section 2.2); and modifications made to the molecular diagnostic workflow enabled a field appropriate linear workflow to be defined. The field trials also provided the opportunity to gain vital feedback from the VCD technicians (the target end user).

The issues experienced with the heating equipment (highlighted in Section 4.7.3.3) resulted in LAMP being carried out in a saucepan using a gas stove for heating. The frugal solution enabled testing to continue despite failure of the electric heater and generator during the trial. Alternate heating solutions were explored in subsequent trials; the first was a heater run on a mobile phone battery; and the second was a heat block reliant on phase change material to propel heating. Both heating methods eliminate the need for a reliant external electricity supply and provide a more stable heating solution than the portable gas stove.

The integration of both PC and NC for the diagnostic assays (discussed in Section 4.7.1.4) was the most notable change made during the development of the Paper Device. These controls are vital to monitor the tests during development in-the-field. The testing environment introduces high risk of contamination of stock reagents. These controls ensure that any potential contamination events, or failure of amplification, can be monitored during processing. The development of an alternate control reaction could be useful for future applications, for example, a reaction which could be interpreted by a colour change (Trinh and Lee, 2019), and conducted in a separate amplification well. Removal LF strips for read-

out of control reactions would make interpretation of the results simpler and allow the size of diagnostic cassette to be decreased and therefore, make the cassettes easier to transport and handle.

The trials also highlighted the need for integration of a simpler or more automated sample processing method. The number of user steps needs to be minimised to simplify use in-the-field. Upscaling the diagnostic process in-the-field proved that the Paper Device method is very hard to conduct without multiple team members to run each stage of sample preparation for the test. Integration of pre-stored molecular reagents would significantly decrease the time for test preparation. Additionally, an automated heating set-up would remove the need for manual timing and decrease the risk of user error.

The factors discussed in this chapter effected the results obtained during field trials. Where possible the changes were accommodated to improve processes and result outcome throughout the study. The lessons learnt will prove useful to those wishing to develop POC molecular diagnostics aimed for use in low-resource and tropical environments.

## 4.9 Take home points

- *Progressed the development of the Paper Device by the adoption and development of the device to enable integration of a new assay, and to carry out field trials in rural settings, in Uganda.*
- *Early integration in-the-field to assess feasibility in diagnostic settings was vital to gain insight into the field environment, it allowed development of the method throughout the trial, and improved understanding of the effects of the field settings on test outcome.*
- *Plasmodium DNA was detected in positive individuals using the POC Paper Device in-the-field and showed good correspondence to qPCR results obtained from FTA<sup>®</sup> stored blood samples processed in Glasgow. .*
- *Field trials confirmed detection of S. mansoni DNA (SM primer set) in stool using LAMP may be conducted in the field. However, preliminary trials assessing LAMP from blood samples suggests a larger sample volumes should be explored.*
- *Low sample output inhibited analysis of the sensitivity and specificity of the diagnostic tool, hence, larger scale field studies are required to better analyse POC outcomes.*
- *Simpler or more automated sample processing method should be developed for further studies to decrease risk of user error.*
- *Integration of negative and positive controls are vital to monitor molecular amplification out-with laboratory conditions. A large portion of false-negative controls inhibited analysis of cassettes, as a result, an investigation into molecular reagents used in-the-field should be overseen to determine the effect of storage conditions on LAMP outcomes.*

## Chapter 5: Storage of molecular reagents

Following field trials, it was identified that a large proportion of the Paper Device cassettes exhibited failure of the control reactions. As a result of the control failures previously discussed, Chapter 5 describes the investigation into the effects of storage on the LAMP reagents – using the PAN malaria assay as a model. The chapter will also describe the trials investigating storage of the molecular reagents in field-like conditions, conducted prior to field studies, and explore potential LAMP reagent storage solutions.

### 5.1 Introduction

One of the major barriers facing the development of molecular diagnostic for use in NTD-endemic countries is the necessity to maintain cold-chain storage for reagent preservation (García-Bernalt Diego *et al.*, 2019). Drying methods are commonly used in the food and pharmaceutical industries to prolong product lifetime. The methods have since been adapted to enable efficient drying of molecular reagents without damaging them (Klatser *et al.*, 1998; Nail *et al.*, 2002; Das *et al.*, 2006; Kamau *et al.*, 2014).

#### 5.1.1 Storage of molecular reagents

Drying methods such as sterile crystallization, spray-drying and powder filling are commonly used to preserve pharmaceutical products (Nail *et al.*, 2002). However, enzymes used to conduct molecular tests are prone to degradation, therefore, investigators have presented methods for air-drying molecular reagents. Kim *et al.* describe air-drying techniques where the reagents are left under a clean air-flow to dry, and later sealed with paraffin wax to reduce exposure to moisture (Kim *et al.*, 2009). Low-melt agarose gel has also been used to encapsulate reagents for extended storage above freezing (Chen *et al.*, 2017). Additionally, investigators have documented reaction mixtures which are stabilised by the addition of ‘gelifying stabilising agents’ (Sun *et al.*, 2013). The referenced methods have been successful for storage of reagents at 4°C and room temperature (25°C), however, storage at elevated temperatures or in-field conditions were not reported. Due to a reduction in enzyme stability, Chen *et al.* suggest lyophilisation for future storage applications (Chen *et al.*, 2017). Lyophilisation is the most common unit process for manufacturing drug products too unstable to be marketed as solutions (Nail *et al.*, 2002), hence, the technique has been widely adapted for molecular reagent storage applications (Das *et al.*, 2006; Brivio *et al.*, 2007; Chen and Ching, 2017; García-Bernalt Diego *et al.*, 2019).

### 5.1.2 Lyophilisation of molecular reagents for storage

Lyophilisation (also referenced as freeze-drying), is a method of removing water by sublimation of ice crystals from frozen material (Tang and Pikal, 2004; Babonneau *et al.*, 2015; Rey and May, 2016; Nagaraj *et al.*, 2018). Sublimation is achieved by maintaining the frozen product under vacuum, without being allowed to thaw (Rey and May, 2016). Lyophilisation has been utilised for the preservation of materials in healthcare applications and by the pharmaceutical industry since the early 1900's (Rey and May, 2016). The method has since been proven to effectively dry molecular reagents and enable prolonged storage at elevated temperatures (Klatser *et al.*, 1998; Nail *et al.*, 2002; Das *et al.*, 2006; Brivio *et al.*, 2007; Ahlford *et al.*, 2010; Kamau *et al.*, 2014; Carter *et al.*, 2017; Chen and Ching, 2017; García-Bernalt Diego *et al.*, 2019). Each stage of the lyophilisation process is critical and unique to the specific substance, hence, the process of freeze-drying has to be adapted to the individual substance and scenario (Rey and May, 2016).

Methods incorporating preloaded molecular reagents into POC diagnostic tools include freeze-drying of molecular reagents (Brivio *et al.*, 2007). Additionally, recombinase polymerase amplification has been achieved by freeze-drying reagents on to a wax printed paper origami platform (Magro *et al.*, 2017a), although, the 'open' storage of freeze dried molecular reagents may not be an appropriate storage method in-the-field as it may introduce risk of potential contamination and increases risk of exposure to moisture.

## 5.2 Chapter Aims & Objectives

During the field trials in Uganda, a large proportion of tests (discussed in the previous chapter) exhibited false-negative positive control reactions. The aim of this chapter was to assess the effect that field storage had on the molecular reagents, and to explore field storage solutions. The objectives for this chapter were:

- Assess LAMP using liquid primer mix and molecular reagents, stored at elevated temperature conditions in the laboratory, to mimic storage conditions in-the-field;
- Assess LAMP using molecular reagents stored in-the-field in Uganda against control reagents;
- Explore lyophilisation of molecular reagents as a field storage solution; and assess LAMP using dried reagents stored at elevated temperatures.



## 5.3 Materials and Methods

### 5.3.1 LAMP reagents

#### 5.3.1.1 Primers

The LAMP PAN malaria assay (for information on the sequences refer to Table 2-2 in Materials and Methods Chapter 2) was designed by Dr Gaolian Xu based on previously published sequences (Polley *et al.*, 2010). The LAMP primers target the 220 bp region of plasmodium mitochondrial DNA, the schematic of the target sequence is shown in Figure 5-1. The Loop primers were tagged with FITC and biotin to enable visual read-out on the LF strips. The primer mix, Table 5-1, was made up to 5  $\mu$ L with the primers and nuclease free water.

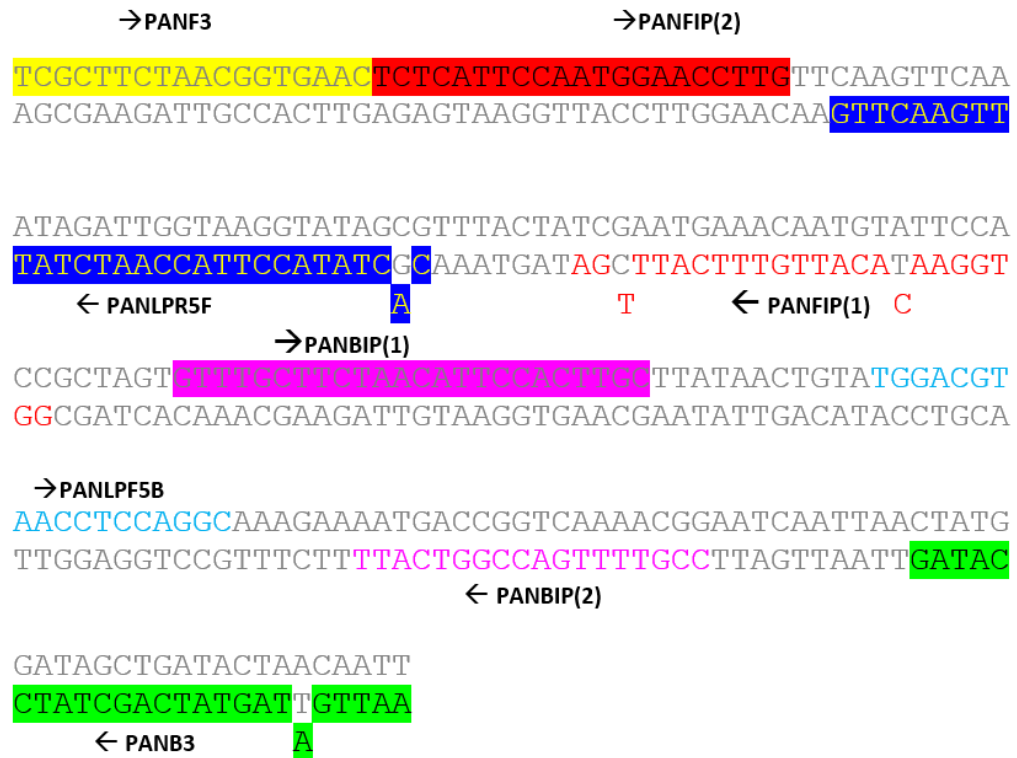


Figure 5-1: Schematic of the plasmodium PAN LAMP primer sequences targeting 220 bp of pan species plasmodium mitochondrial DNA. The arrows depict the direction of polymerisation for each primer sequence.

Table 5-1: Primer concentrations and volumes (per reaction) used to make up plasmodium (PPAN) and 5X pan Primer Mix for LAMP amplification.

Primer Mix- <i>Plasmodium pan</i> (per reaction)			5X pan
Primer Name	Concentration ( $\mu\text{M}$ )	20 $\mu\text{M}$ stock ( $\mu\text{L}$ )	100 $\mu\text{M}$ stock ( $\mu\text{L}$ )
PANF3	0.1	0.125	0.025
PANB3	0.1	0.125	0.025
PANFIP	0.8	1.00	0.2
PANBIP	0.8	1.00	0.2
PANLPR5F	0.6	0.750	0.15
PANLPP5B	0.6	0.750	0.15
dH <sub>2</sub> O		1.25	0.25
Total		5.00	1.00

### 5.3.1.2 Mastermix

ISO-004 Isothermal Mastermix (OptiGene, Horsham, UK) was used to conduct LAMP in the laboratory, following the method in Section 2.1.3.5.3. To maintain reagent stability in-the-field a second mix, freeze dried ISO-DR004 Isothermal Mastermix (OptiGene, Horsham, UK), was used to conduct LAMP during field trials.

### **5.3.2 Storage of molecular reagents**

Storage trials of molecular reagents were carried out by mimicking the field storage conditions in the laboratory and where possible, the reagents were stored in-the-field in Uganda and tested upon return to the laboratory. The molecular reagents and target DNA were pre-aliquoted for use each day to avoid multiple freeze-thaw cycles and temperature cycling; and to ensure that the storage conditions were maintained throughout each study. LAMP was carried out on the ABI machine using the molecular reagents returned from Uganda to evaluate the performance against laboratory 'stock' solutions. The methods used to evaluate the storage of the LAMP reagents will be discussed further in this Chapter.

#### ***5.3.2.1 Molecular reagents stored in-the-field***

Following trials in Uganda, the LAMP reagents stored in-the-field were tested on return to the laboratory in Glasgow. The reagents returned from Uganda were left at laboratory room temperature until the time of use. Freeze-dried Isothermal Mastermix (ISO-DR004) stored in-the-field was re-suspended following the manufacturers protocol at the time of use.

Unless otherwise stated, LAMP was conducted on the ABI machine using 5  $\mu\text{L}$  of  $10^{-5}$  ng/ $\mu\text{L}$  target gBlock DNA, as described in Section 2.1.3.5.3. The field stored LAMP reagents were run with, and compared against 'stock' molecular reagents, which were stored under control conditions ( $-20^{\circ}\text{C}$ ) in the laboratory. Water was used as a NC and a melt curve was run to aid in identifying potential false-positive amplification. Following LAMP, the samples were run on LF strips.

#### ***5.3.2.2 Imitating field storage conditions***

To simulate field storage conditions, the LAMP reagents were stored in a laboratory incubator at  $37^{\circ}\text{C}$ . All storage containers and plates were covered in foil to limit exposure to light throughout the trial. To mimic the travel storage conditions to Uganda, prior to carrying out the controlled storage, the liquid reagents were removed from the  $-20^{\circ}\text{C}$  freezer and stored in travel boxes with cold packs for two days at room temperature.

### 5.3.2.3 *Freeze-drying molecular reagents*

Primary attempts to freeze dry the Isothermal Mastermix (ISO-004 & ISO-DR004) were unsuccessful. OptiGene (the Mastermix manufacturer) agreed to provide pre-lyophilised Mastermix (LYO-004) for incorporation into the device following assignment of a non-disclosure agreement (NDA). Investigators have stated that having a company custom-manufacture lyophilized assay(s), is likely to result in a more optimized and reproducible product (Nagaraj *et al.*, 2018). 15  $\mu\text{L}$  of pre-lyophilised Mastermix solution (LYO-004) was aliquoted into qPCR tube strips. Following recommendation from OptiGene to minimise the volume of the solution subject to lyophilisation, 1  $\mu\text{L}$  of 5X primer mix (see Table 5-1 '5X'), was added to the LYO-004 to complete the preparation of the LAMP reagent. Trehalose acts as an enzyme stabiliser (Lim Chua *et al.*, 2011). The nuclease free water ( $\text{dH}_2\text{O}$ ) in the 5X primer mix was substituted with 10 M trehalose solution (Sigma-Aldrich, UK) in attempt to extend stability of the molecular reagents.

The prepared LAMP reagents were centrifuged and placed into a pre-cooled 0.2 mL aluminium heat block and stored at  $-80^\circ\text{C}$  overnight. Prior to lyophilisation the tube lids were pierced with a 19G needle, to provide an open environment to allow removal of water by sublimation. The lyophilisation process consisted of a pre-freeze and primary and secondary drying stages. The freeze-drying process was completed in 24 hours (in accordance with the NDA between the University of Glasgow and OptiGene Ltd, the exact method of lyophilisation cannot be disclosed in print). The window of the freeze-drier (Labconco FreeZone Triad Bench Top Freeze Drier) was covered with aluminium foil to minimise exposure to light throughout the freeze-drying process. On completion of lyophilisation the tube caps were immediately replaced and sealed to limit exposure of the freeze-dried LAMP reagents to moisture in the environment. The lyophilised LAMP reagents were then stored within a sealed foil bag containing desiccant to minimise exposure to moisture and light.

LAMP using the freeze-dried LAMP pellets was conducted on the ABI machine (following the protocols described in Section 2.1.3.5). 20  $\mu\text{L}$  of resuspension buffer (RB) and 5  $\mu\text{L}$  of target DNA was added to the lyophilised pellet at the time of use. The RB was comprised of 15  $\mu\text{L}$  of resuspension buffer (proprietary composition, supplied by OptiGene) and 5  $\mu\text{L}$  of nuclease free water. Nuclease free water was used in place of target DNA for the NC.

### 5.3.3 An overview of experiments

The table below (Table 5-2), provides an overview of the experiments carried out in this chapter. The experiments were conducted using the PAN malaria assay detailed in Table 2-2 & Table 5-1, and using the LAMP reaction conditions described in Section 2.1.3.5.3.

*Table 5-2: An overview of the experiments carried out in this chapter, a description of the experiment and LAMP reagent storage conditions; the reagents used for the comparative reaction, as a reference control for each experiment; and the target for the assay.*

#	Description of the experiment carried out	Comparative reaction	Target
1	LAMP of a serial dilution of DNA extracted from <i>plasmodium</i> parasites ( <i>plasmodium</i> gDNA), and gBlock DNA, to determine the limitation of the PAN malaria assay.	Cold stored primer mix and ISO-004.	<i>Plasmodium</i> gDNA & PAN gBlock DNA
2	Assessment of the LAMP reagents stored at elevated temperatures in the laboratory, to mimic conditions in-the-field		
2-1	LAMP of liquid primer mix stored in a laboratory incubator (37°C), over a 5 day period. LAMP was conducted each day, all reactions were carried out with control stored Mastermix (ISO-004).	Cold stored primer mix and ISO-004	PAN gBlock DNA
2-2	LAMP of liquid primer mix and re-suspended Mastermix (ISO-DR004) stored at laboratory room temperature (18°C), and in a laboratory incubator (37°C) for t=6 and 24 hours.	Cold stored primer mix and re-suspended ISO-DR004	PAN gBlock DNA
3	Assessment of LAMP using reagents returned from Uganda		
3-1	LAMP using ISO-DR004 stored in-the-field and re-suspended on return to Glasgow, with primer mix stored in Uganda, and cold stored primer mix.	Cold stored primer mix and re-suspended ISO-DR004	PAN gBlock DNA
3-2	LAMP using primer mix and ISO-DR004 stored in-the-field; and primer mix and ISO-DR004 stored in the laboratory incubator (37°C).	Cold stored primer mix and re-suspended ISO-DR004	PAN gBlock DNA
3-3	LAMP using cold stored primer mix and ISO-DR004 stored in-the-field, re-suspended in the laboratory and stored at elevated temperatures for 24 hours.	Cold stored primer mix and ISO-004	PAN gBlock DNA
4	Freeze-drying ISO-DR004 and LYO-004 LAMP reagents with 5X PAN primers; stored at room temperature and in the laboratory incubator (37°C) for one week.	Cold stored primer mix and ISO-004	PAN gBlock DNA

## 5.4 Results

### 5.4.1 Calibration of the detection of *plasmodium* DNA by LAMP

LAMP was conducted on the ABI machine using gBlock and genomic DNA to determine limit of detection for PAN LAMP primers. The fluorescence data for amplification of gBlock DNA:  $10^{-3}$ ,  $10^{-4}$ ,  $10^{-6}$ ,  $10^{-8}$  ng/ $\mu$ L and dH<sub>2</sub>O, collected by the ABI machine is shown in Figure 5-2(a) in red, pink, purple, blue and green respectively. To combine the fluorescence data resulting from amplification of the gBlock DNA, the raw data was extracted from the ABI machine and replotted using the code referenced in Section 7.3.1 of the Appendices. The mean Ctt values for dilutions of gBlock (orange) and genomic (blue) DNA are shown in Figure 5-2(b). The mean Ctt for each sample was calculated from accumulated control data (N=9), Ctt was determined from fluorescence amplification data at 100,000 RFU. The mean Ctt values for gBlock DNA (orange): 6.5, 8.7, 11.7, 14.9 & 18.2 for  $10^{-3}$ ,  $10^{-4}$ ,  $10^{-5}$ ,  $10^{-6}$ ,  $10^{-8}$  ng/ $\mu$ L respectively. The mean Ctt values for dilutions of genomic DNA were 11, 13.5 & 17.1 for 10,  $10^{-2}$ ,  $10^{-3}$  ng/ $\mu$ L respectively. No amplification was observed for the NC or lower dilution concentrations of DNA.

At each dilution of DNA, the mean time to amplification (average Ctt) was statistically significant ( $p < 0.005$ ) as compared to successive dilutions. Amplification of gBlock DNA:  $10^{-8}$  &  $10^{-6}$  ( $p = 0.0013$ );  $10^{-6}$  &  $10^{-5}$  ( $p = 0.0027$ ),  $10^{-5}$  &  $10^{-4}$  ( $p < 0.0005$ );  $10^{-4}$  &  $10^{-3}$  ( $p < 0.0005$ ). Amplification of gDNA:  $10^{-3}$  &  $10^{-2}$  ( $p = 0.0044$ ); and  $10^{-2}$  & 10 ( $p = 0.0024$ ).

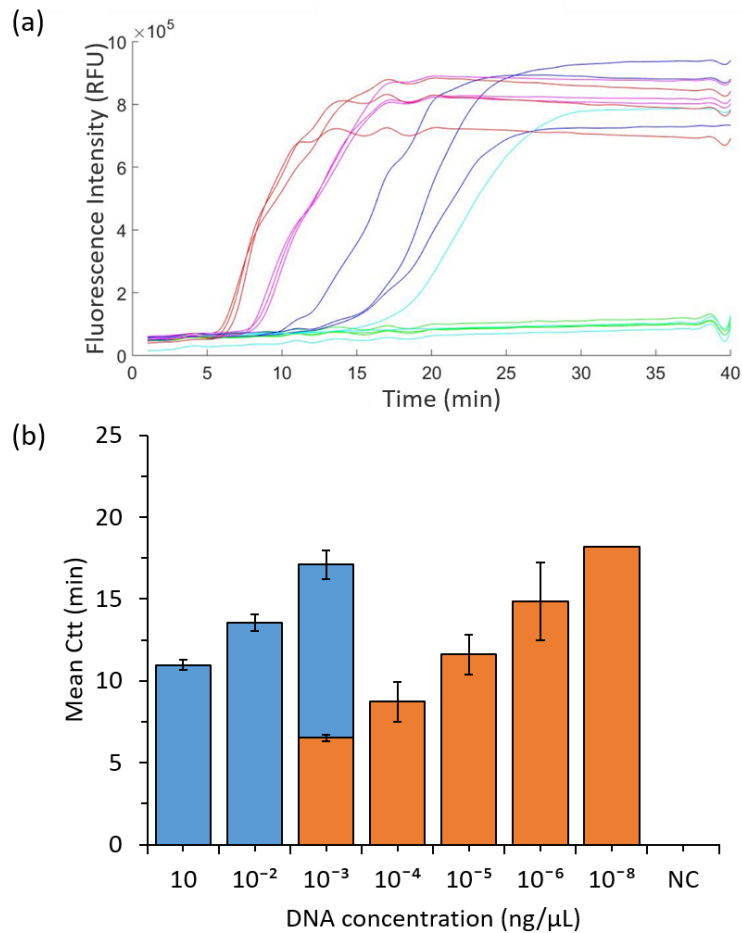


Figure 5-2: *Plasmodium PAN LAMP calibration data.* (a) Fluorescence data collected from ABI machine for LAMP amplification of serially diluted plasmodium gBlock DNA. Data plotted in red, pink, purple, blue and green are  $10^{-3}$ ,  $10^{-4}$ ,  $10^{-6}$ ,  $10^{-8}$  ng/ $\mu$ L gBlock samples and negative control (dH<sub>2</sub>O) respectively. A single  $10^{-8}$  ng/ $\mu$ L gBlock sample amplified, hence, LOD was determined as  $10^{-6}$  ng/ $\mu$ L. (b) Average Ctt Values from LAMP amplification of diluted gDNA (blue) and gBlock DNA (orange). Use of gBlock DNA allows amplification of samples 1000X diluted as compared to gDNA. At concentration of  $10^{-3}$  ng/ $\mu$ L, gBlock DNA (Ctt=6.5) amplifies 10.6 cycles faster than the corresponding gDNA sample (Ctt =17.1).

## 5.4.2 Storage of reagents to mimic storage in-the-field

### 5.4.2.1 Liquid primer storage

Prior to field trials the molecular reagents were stored in ‘field-like’ conditions (described in Section 4.4). The liquid primers were stored over a week and LAMP amplification were carried out each day over a 5 day period to imitate field work structure (see Section 5.3.2.2 for further details). LAMP amplification of the target DNA ( $10^{-6}$  ng/ $\mu$ L *plasmodium* gBlock) was conducted on the ABI machine and the time to amplification (Ctt) was compared to control primers (which were stored at laboratory room temperature and  $-20^{\circ}\text{C}$  throughout the study) the Ctt results are displayed in Figure 5-3. Variation of Ctt for laboratory stored

control primer mix throughout the week was minimal. There was no statistically significant difference between controls 'C' conducted each day ( $p > 0.05$ ), therefore, the Ctt values for control reactions were compiled to provide a larger comparative pool of results (standard deviation = 0.8). The Ctt values for primers stored at room temperature 'RT' also presented with no statistical significance between results each day ( $p > 0.05$ ), results were also compiled in to one bar (standard deviation = 1.1). There was no statistical difference between control and RT stored primer mix ( $p = 0.869$ ). On the other hand, the liquid primers stored in the incubator under simulated field conditions exhibited much larger variation of Ctt values throughout the trial (the data for each day is presented in Figure 5-3). The resultant Ctt values from primer stored at elevated temperatures were not statistically significant for days 1 & 3 ( $p = 0.14$  &  $0.63$  respectively), however, days 2 & 5 were statistically different from control samples ( $p = 0.0048$  &  $< 0.0001$  respectively). A technical failure on day 4 of the study resulted in heating failure which inhibited LAMP, the results were omitted from analysis.

Storage results simulating field conditions (storage at elevated temperature), suggest that conducting LAMP using liquid primer mix stored in-the-field, may increase variation of sample amplification time throughout the week. There appeared to be a general trend of increasing Ctt with prolonged storage at elevated temperatures. However, there was no indication of amplification hindrance or occurrences of false-amplification. It was determined that preliminary field trials may be carried out using liquid LAMP primer mix.



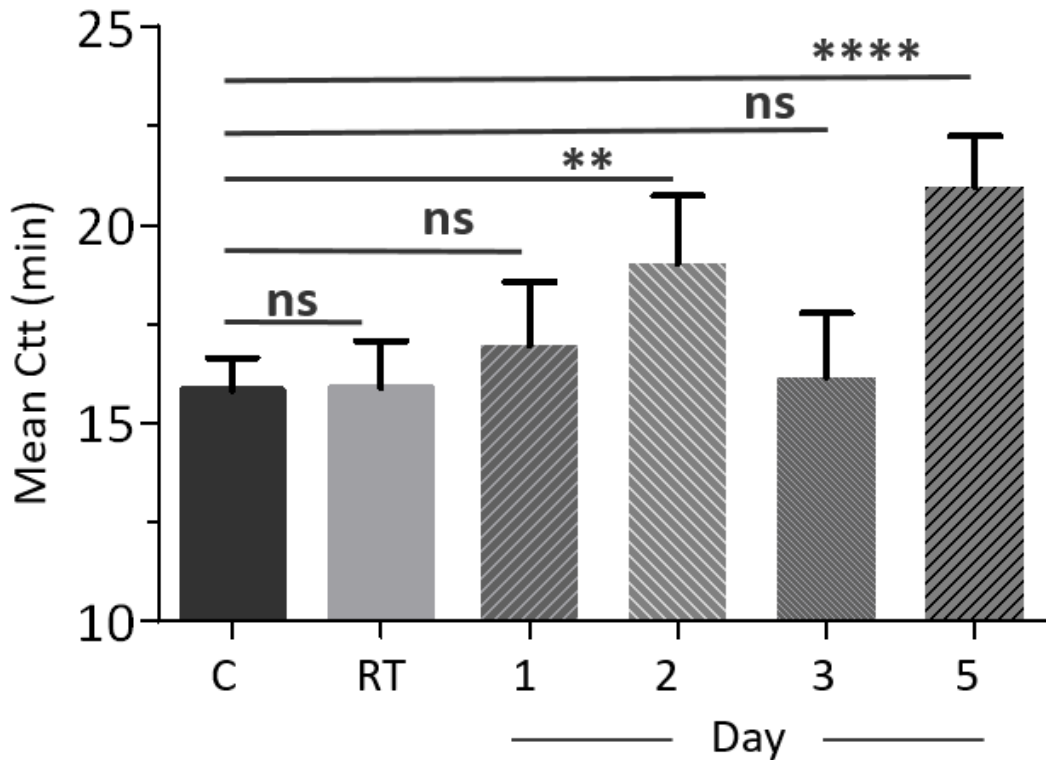


Figure 5-3: Primer Stability. Primer mix was stored in a 37°C incubator (1-5), at room temperature (grey) and as a control at -20°C (black) for 7 days. LAMP amplification of target gBlock DNA ( $10^{-6}$  ng/ $\mu$ L) was conducted in triplicate each day on the ABI machine, Ctt was recorded for each sample. LAMP amplification was carried out over a 5 day period to simulate field work structure. There was no significant difference found between Ctt values of control (C) and room temperature (RT) samples, the results were compiled into a single bar. The experiment was repeated twice. Ctt results were compiled to calculate the mean (15.8, 15.9, 17.0, 19.0, 16.2, 20.9) and standard deviation (0.8, 1.1, 1.4, 1.6, 1.5, 0.2) of amplification times for C, RT and samples stored in the incubator days 1-5 respectively. For each sample, a no template negative control was conducted in triplicate. Statistical analysis: ns represents no statistical significance ( $p \geq 0.05$ );  $0.01 > p \geq 0.001$  is represented by \*\*; and  $p < 0.0001$  is represented by \*\*\*\*.

An aliquot of isothermal Mastermix and target DNA used throughout this study was preserved at -20°C to carry out amplification of primer mix taken to Uganda following field trials for comparative analysis (refer to Section 5.4.3.2 for details).

#### 5.4.2.2 LAMP reagent storage

Both the liquid primer mix and re-suspended Isothermal Mastermix (ISO-DR004) were stored in the laboratory incubator under simulated field conditions for 24 hours. LAMP amplification of target DNA ( $10^{-5}$  ng/ $\mu$ L *plasmodium* gBlock DNA) was carried out on the ABI machine at 6 and 24 hours after Mastermix resuspension. Additionally, reagents were stored at laboratory room temperature and  $-20^{\circ}\text{C}$  for comparative analysis (see Figure 5-4, '-20', 'RT' & '37' refer to molecular reagents stored at  $-20^{\circ}\text{C}$ , laboratory room temperature and simulated field storage conditions respectively). A control reaction was run at time 0 hours with the newly re-suspended Mastermix and stock primer mix. LAMP was also carried out using Isothermal Mastermix stored in field simulated conditions and control primer mix stored at  $-20^{\circ}\text{C}$  (results labelled as '24\*' in Figure 5-4).

There was no statistical difference ( $p > 0.05$ ) between the controls run at  $t = 0, 6$  & 24 hours, therefore, the Ctt results were accumulated to provide a larger comparative data set. The difference between average Ctt values for controls 'C' and stored reagents 'RT' & '37' after 6 hours was not statistically significant ( $p > 0.1$ ), suggesting that the storage of molecular reagents at elevated temperatures up to 6 hours does not have a significant effect on LAMP outcomes. However, after 24 hours there was significant change in LAMP Ctt averages for the liquid reagents stored at room temperature 'RT' and in simulated field conditions '37' as compared to the controls ( $p < 0.0001$ ). Additionally, there was a significant difference in the Ctt averages between reagents stored at RT and  $37^{\circ}\text{C}$  after  $t = 24$  hours ( $p = 0.027$ ) and stored reagents 'RT' & '37' after  $t = 6$  to 24 hours ( $p < 0.0001$ ), suggesting that LAMP is effected after liquid reagents are exposed to storage at elevated temperatures for longer than 6 hours.

The 'control' primer mix and Isothermal Mastermix (stored in field simulated conditions) was used to carry out LAMP after 24 hours of storage (24\*). The average Ctt value was higher than LAMP reagents stored in the incubator ( $\Delta$  average Ctt = 0.8 minutes,  $p = 0.0008$ ), however, the variability of amplification time between repeated samples was lower (standard deviation = 0.08 & 0.33 for '24\*' & '37' respectively). The decreased variation of Ctt values obtained from the mix of 'control' primer mix and Mastermix stored in field simulated conditions agrees with observations made in the previous Section, which concluded that conducting LAMP with primer mix stored at elevated temperatures for prolonged periods of time increases the variation of sample amplification times.

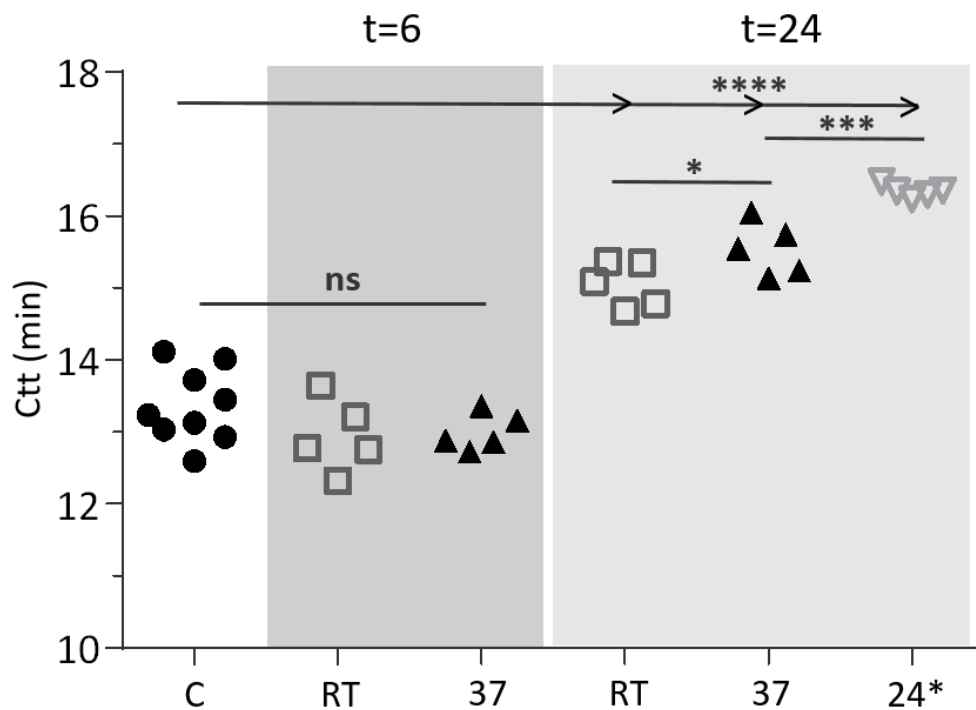


Figure 5-4: Reagent stability. Both Primer mix and re-suspended Mastermix (ISO-DR004) were stored at laboratory room temperature and in a 37°C incubator for 24 hours. LAMP amplification ( $10^{-5}$  ng/ $\mu$ L gBlock DNA) was carried out using the ABI machine after 6 and 24 hours of reagent storage. Control reagents were stored at -20°C. C, RT & 37 refer to results from reagents stored at -20°C, laboratory room temperature and 37°C respectively. Additionally, at 24 hours LAMP was conducted using the Mastermix stored in the incubator with control primer mix (24\*). No amplification was present for no target negative controls. Statistical analysis: ns represents no statistical significance ( $p \geq 0.05$ );  $0.05 > p \geq 0.01$  is represented by \*;  $0.001 > p \geq 0.0001$  is represented by \*\*\*;  $p < 0.0001$  is represented by \*\*\*\*.

Following the storage trials of the molecular reagents in the laboratory, it was concluded that the lyophilised Isothermal Mastermix (ISO-DR004) should be re-suspended daily in-the-field to minimise the effect on amplification time. The re-suspension of new primer mix each day was not feasible during field trials, the results from storage trials of the primer mix conducted in the laboratory suggested that conducting LAMP with liquid primer mix in-the-field may result in more variable amplification times. However, there was no evidence that amplification would be hindered in-the-field. To gauge variation in sample amplification in-the-field, LAMP controls should be conducted daily, prior to sample processing.

### 5.4.3 Storage of molecular reagents in-the-field

Succeeding the field trials, the molecular reagents stored in-the-field were transported back to Glasgow and were used to carry out LAMP on the ABI machine to assess the effects of field storage on LAMP performance. In the lyophilized Isothermal Mastermix (ISO-DR004) was stored in manufacturers packaging - following results of preliminary storage trials in the laboratory (Section 5.4.2.2) - a new bottle of Isothermal Mastermix was re-suspended each day in-the-field. The primer mix was transported to Uganda with cold packs to maintain cold storage until arrival in-the-field, however, there was no access to cold storage after arrival in test locations, thus, liquid primer aliquots and the lyophilized Isothermal Mastermix were exposed to elevated temperatures throughout the duration of the field trials.

#### 5.4.3.1 *Molecular reagents returned from the field*

To assess the effect of storage conditions in-the-field, the LAMP reagents were transported back to Glasgow and LAMP was carried out on the ABI machine against laboratory stored 'control' reagents ( $10^{-6}$  ng/ $\mu$ L *plasmodium* gBlock target DNA was used for amplification). The resultant Ctt values are displayed in Figure 5-5(a), the stock Isothermal Mastermix & stock primer mix, '1' (circle markers); the field stored Isothermal Mastermix & stock primer mix, '2' (square markers); field stored Isothermal Mastermix & field stored primer mix, '3' (triangle markers).

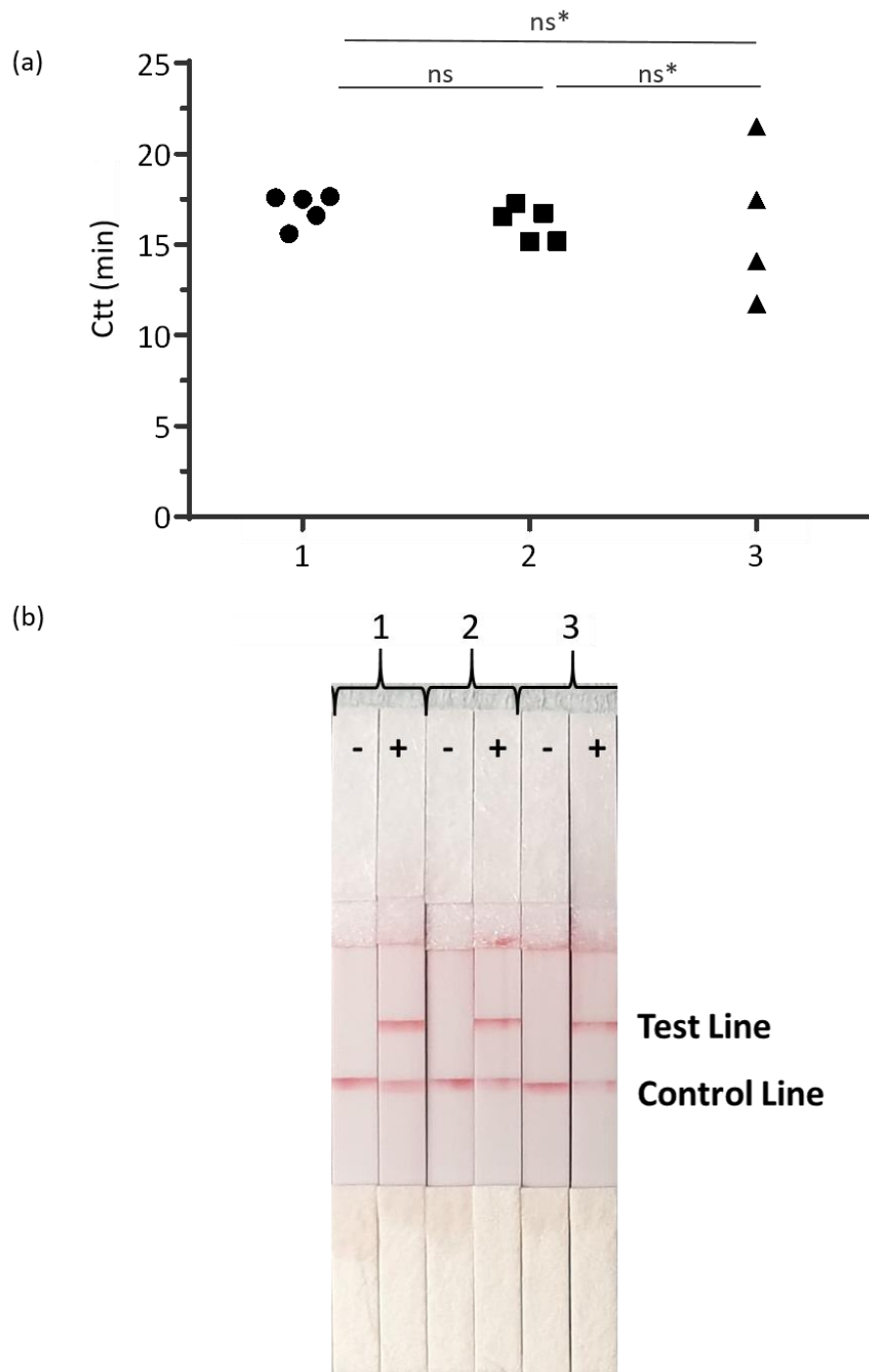


Figure 5-5: Molecular reagents field storage. A bottle of freeze-dried Mastermix (ISO-DR004) and an Eppendorf of primer mix was taken to Uganda and stored in field conditions for 10 days. On return to the U.K, the Mastermix was re-suspended following manufacturers recommendations. (a) LAMP amplification of  $10^{-6}$  ng/ $\mu$ L gBlock DNA was conducted on the ABI machine using field stored reagents and control reagents (Mastermix stored following manufacturers recommendations and primer mix stored at  $-20^{\circ}\text{C}$ ): (1) Control Mastermix and primer mix; (2) Field stored Mastermix and control primer mix; and (3) Both field stored Mastermix and primer mix. No template negative controls were run in triplicate for each sample. (b) Amplified samples were run on LF strips for confirmation. Statistical analysis:  $p \geq 0.05$  is represented by ns; ns\* where  $F$  test was significant.

LAMP carried out using primers and Mastermix stored in-the-field '3' exhibited large variation in amplification times (standard deviation = 4.2 minutes). The Ctt values (average Ctt = 16.9 & 16.2 minutes) collated using the stock and field stored lyophilised Isothermal Mastermix with stock primers (1 & 2 respectively) was non-significant ( $p = 0.10$ ), the variation in amplification times was low (standard deviation = 0.90 & 0.94 minutes) and standard error of the mean = 0.36 & 0.37 respectively. The comparison of LAMP Ctt results from Mastermix stored in-the-field (2) as compared to stock Mastermix (1) suggest that the field stored lyophilized Isothermal Mastermix (ISO-DR004) was not affected by storage conditions in-the-field. The Ctt values resulting from LAMP using both field stored primers and Mastermix (2) support the previous observations that the field storage conditions affect the performance of the primer mix. Although the Ctt results suggest that there is no significant difference ( $p > 0.25$ ) in average Ctt for the control and field stored reagents (average Ctt = 16.9 & 16.2 minutes, '1' & '3' respectively), there was a significant difference in amplification performance (standard error of the mean '3' = 1.8) whilst using both field stored primer mix and isothermal Mastermix to conduct LAMP. Furthermore, LAMP was hindered for one of the samples (N = 5). The LAMP amplified samples were run on LF strips for secondary confirmation, see Figure 5-5(b).

#### ***5.4.3.2 Primer mix returned from the field***

Following preliminary storage trials conducted in the laboratory (see Section 5.4.2.1 for more details) the performance of the liquid primers appeared to be effected by storage at elevated temperatures (Speicher, 2017). The liquid primer mix which was transported back from Uganda to Glasgow was used to assess LAMP performance following field storage. The aliquot of the stock Isothermal Mastermix and target DNA from the preliminary primer storage trials conducted in the laboratory was used for comparative analysis (result discussed in Section 5.4.2.1). The Ctt values obtained from LAMP (see Figure 5-6) using field stored primer mix (Uganda) were compared to results from the preliminary laboratory based storage trials (C & 37) (Section 5.4.2.1) to ascertain simulated field storage conditions.

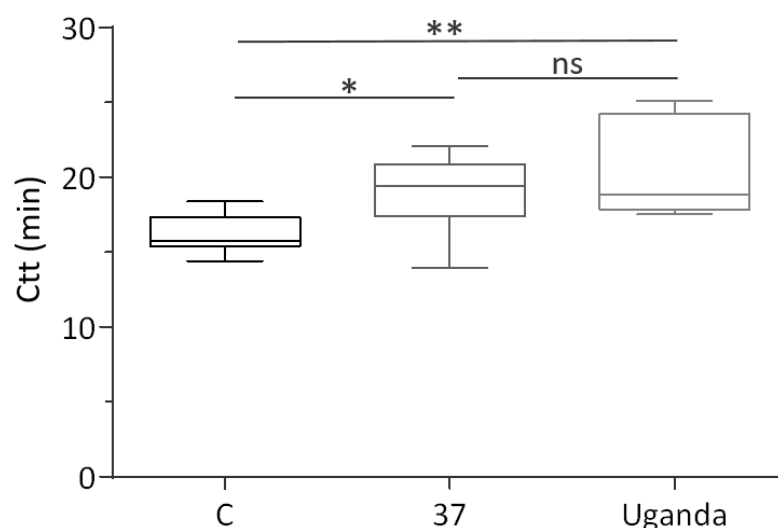


Figure 5-6: Field storage conditions. Primer mix was taken to Uganda and stored in field conditions for 10 days. On return to the U.K, LAMP amplification of  $10^{-6}$  ng/ $\mu$ L gBlock DNA was carried out on the ABI machine using field stored primers and Mastermix stored in the laboratory ( $-20^{\circ}\text{C}$ ). The Ctt values obtained for amplification of field stored primer mix (Uganda) are plotted alongside Ctt values obtained in earlier primer storage experiments (see Section 5.4.2.1, Figure 5-3); primer mix stored at  $37^{\circ}\text{C}$  (37) and  $-20^{\circ}\text{C}$  (C). A no template negative control was run in triplicate, no amplification was observed from the negative sample. Statistical analysis:  $p \geq 0.05$  is represented by ns;  $0.05 > p \geq 0.01$  is represented by \*;  $0.01 \geq p > 0.001$  is represented by \*\*.

The Ctt values for amplification conducted using the primer mix stored in the laboratory incubator (37) and controls (C) in the preliminary laboratory based storage trials (Section 5.4.2.1) were accumulated for comparative analysis. Following the preliminary trials, it was predicted that the Ctt values obtained from conducting LAMP amplification with field stored primers (Uganda) would be greater than the control (C) primer mix. The mean Ctt values for the field stored primer mix (Uganda); primer mix stored under field simulated conditions in the laboratory (37); and controls (C) were 21.1, 19.5 and 16.2 minutes respectively. The large maximum variation shown in the controls was due to two large Ctt values (N=17). There was a statistically significant difference between amplification results of the control and the incubator, and field stored primers ( $p = 0.030$  &  $p = 0.008$ ), suggesting that the primer mix was affected by exposure to elevated temperatures during storage in-the-field (t=10 days). The data obtained following field storage contradicts the manufacturers reports which state that primers will be stable at elevated temperatures up to 6 weeks (Speicher, 2017). The difference in Ctt values obtained from amplification of liquid primer mix stored in the incubator (37) and in-the-field in Uganda were non-significant ( $p = 0.255$ ), suggesting storage within the laboratory incubator ( $37^{\circ}\text{C}$ ) may be used to simulate storage conditions in-the-field.

### 5.4.3.3 Isothermal Mastermix returned from the field

Following the investigation into the storage of lyophilised Isothermal Mastermix (ISO-DR004) in field simulated conditions (described in Section 5.4.2.2), the Isothermal Mastermix (which was stored in the field and re-suspended by manufacturer's instructions on return to the laboratory in Glasgow) was distributed amongst five Eppendorf tubes and subject to storage (in liquid form) at a range of storage conditions for analysis of LAMP outcomes. The re-suspended Mastermix was stored at laboratory room temperature, 30°C, 35°C and 40°C, for 24 hours. The stock Mastermix solution 'L' which had not been taken to Uganda, was used as a control and stored at -20°C overnight. The amplified samples were run on LF strips for visual read-out (see Figure 5-7) at t=0, 'D' refers to the LAMP carried out using the re-suspended Isothermal Mastermix which had been stored in-the-field.

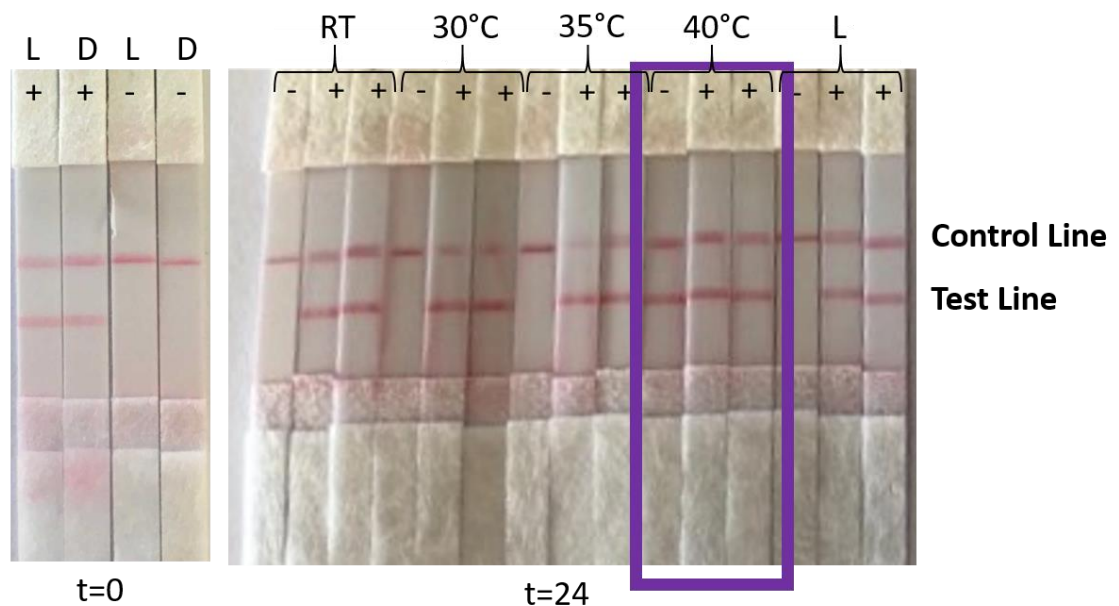


Figure 5-7: Lyophilised isothermal Mastermix stability. A bottle of freeze-dried master mix (ISO-DR004) that was stored in Uganda for 10 days at room temperature, was brought back to the lab and re-suspended following manufacturers recommendations. LAMP was conducted after re-suspension (t=0) and after storage at laboratory room temperature (RT) and various elevated temperatures for 24 hours. The results were interpreted by LF strips, a single no template negative control and duplicate target DNA samples (5 µL of 10<sup>-5</sup> ng/µL gBlock) was amplified on the ABI machine. (L) Refers to the control reaction, where molecular mix was stored at -20°C.



Amplification of the target DNA was successful for re-suspended Mastermix stored up to 35°C after 24 hours, however, at 40°C false amplification of the NC was observed. During the field trials the temperature stayed between 30°C and 34°C throughout the warmest part of the day, and a new Mastermix was re-suspended each morning. The re-suspended solution was kept out of direct sunlight and stored for no longer than 9 hours before being disposed, from the preliminary storage results, it appeared that the storage conditions after re-suspension of the Isothermal Mastermix stored in-the-field should not hinder amplification.

#### 5.4.4 Freeze-drying of LAMP reagents

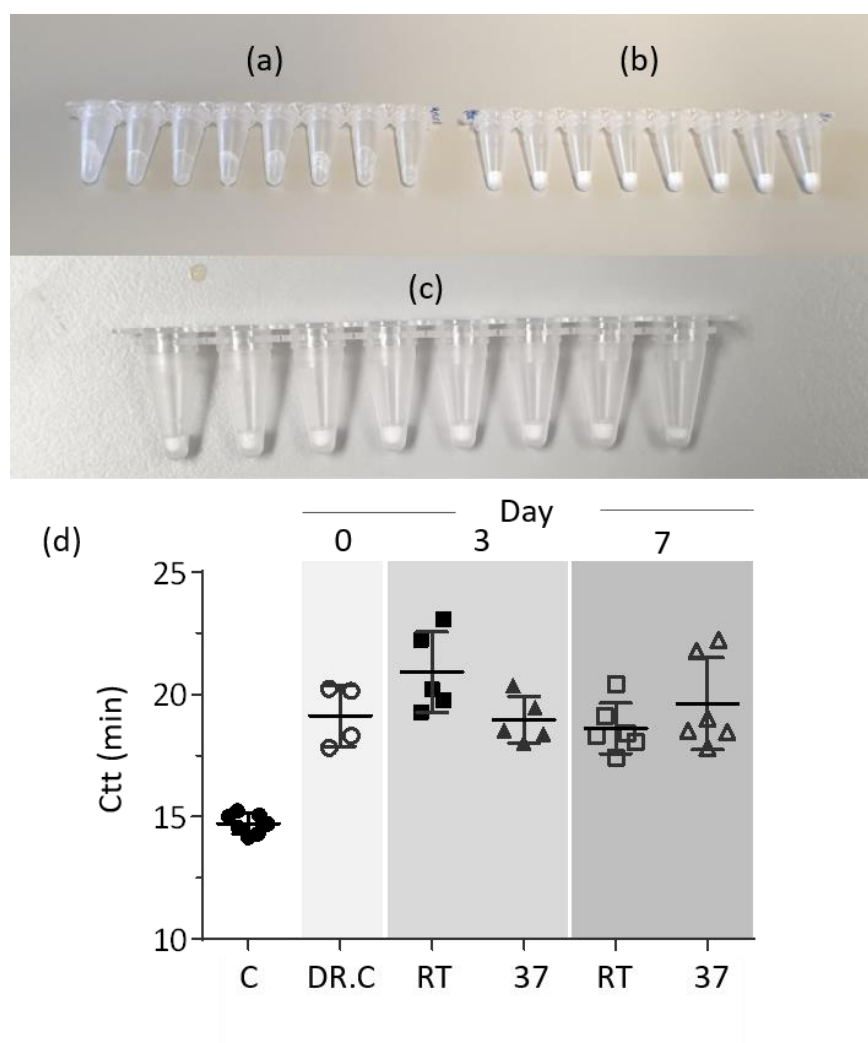


Figure 5-8: Lyophilised molecular reagents. Freeze-drying was tested with a few reagent mixes: (a) ISO-004 Mastermix, unsuccessful; (b) LYO-004 Mastermix and original '5 µL' primer mix; (c) LYO-004 and modified '1 µL' primer mix. (d) The Freeze dried reagent mix with 1 µL of the primer mix was stored for 7 days within a 37°C incubator and at room temperature. The difference in Ctt between control and lyophilised reagents was statistically significant ( $p < 0.0001$ ), however, the variation in Ctt throughout the week was non-significant

The details on the method of lyophilisation were discussed in Section 5.3.2.3. Attempts to lyophilise the original Isothermal Mastermix (ISO-004) were not successful (see Figure 5-8 (a)), it is believed that the components (most likely glycerol) within the Mastermix buffer to protect the enzyme during freeze-thaw cycles also inhibit freeze drying processes. Lyophilisation of Mastermix (LYO-004) with 5  $\mu$ L of primer mix was achieved (Figure 5-8(b)), however, the most reliable lyophilisation results were achieved using the LAMP reagents with the modified '5X' primer mix (referenced in Table 5-1) the LAMP pellets are shown in Figure 5-8(c). Following the optimisation of the lyophilisation process, the freeze-dried molecular reagents (LAMP pellets) were subject to storage at room temperature 'RT' and within a 37°C incubator '37', to assess the feasibility of storage in field-like conditions for 7 days. The resultant Ctt values are displayed in Figure 5-8(d).

A control reaction 'C' was conducted using frozen stock primers and Mastermix. The difference in Ctt values for control reactions were non-significant ( $p = 0.84$ ), thus, the Ctt results were combined for analysis. An ANOVA test determined there was a significant increase in Ctt for lyophilised reagents ( $p < 0.0001$ ). Although the LAMP pellets resulted in delayed amplification ( $\Delta$ Ctt < 6 minutes) as compared to control reagents, other investigators have previously reported longer LAMP amplification times (García-Bernalt Diego *et al.*, 2019; Wan *et al.*, 2020). There was no statistical difference ( $p > 0.05$ ) between Ctt values for LAMP pellets stored at laboratory room temperature as compared to elevated temperatures throughout the week, suggesting a potential solution to improve LAMP reagent stability in-the-field.

## 5.5 Discussion

Manufacturers' conclude that oligonucleotides suspended in water are stable up to 6 weeks at 37°C (Speicher, 2017). The storage of the primers in the laboratory incubator at 37°C resulted in an increase of amplification time, this delay in time to amplification generally correlated to the duration of primer storage at elevated temperatures, contradicting the manufacturer's reports. The amplification time was delayed further as a result of LAMP using both Isothermal Mastermix and primer mix stored at elevated temperatures. The comparison of results using primers stored in-the-field and those stored in the laboratory incubator were non-significant, suggesting that field storage could be imitated in the laboratory, however, this was not the case when amplification was carried out using field stored primers and Mastermix, which exhibited a much larger variation in amplification time (larger Ctt values) after storage in-the-field. Additionally, one of the controls was not amplified (1 of 5), suggesting that LAMP was more significantly affected by the conditions in-the-field, than had been predicted by laboratory trials.

Throughout field trials (described in Chapter 4) there were a large number of cassettes which were removed from analysis due to failed positive controls (~ 20% of the cassettes processed). The experiments carried out in this chapter conclude that the effect of field conditions on molecular reagents likely resulted in the inhibition of LAMP reactions. Furthermore, the variation in amplification activity may have influenced the occurrence of false-negative results in-the-field. Throughout the field trial we had attempted to limit the effect of storage conditions by use of the lyophilised Mastermix (ISO-DR004). Following the analysis of LAMP carried out using field stored reagents, it appears that although the Mastermix may have remained stable, there was a large variation in amplification times (Ctt) when LAMP was carried out using a combination of field stored Mastermix and primer mix.

The lyophilised Isothermal Mastermix (ISO-DR004) did not exhibit significant changes in Ctt after storage in the field and the statistical analysis determined no significance between LAMP carried out using field stored samples as compared to controls (stored under manufacturers' recommendations). As a result, lyophilisation of the LAMP reagents to produce the LAMP pellets was pursued.

Initial drying experiments were explored using 'air-drying' techniques (Kim *et al.*, 2009; Chen *et al.*, 2010). This method appeared appropriate for drying of primer mix, however provided no improvement on storage outcomes from field trials (data not provided).

Fortunately, the Biomedical Engineering Department purchased a freeze dryer (Labconco FreeZone Triad Benchtop Freeze Drier, VWR International Ltd, UK) towards the final months of the project which enabled progress towards the lyophilised reagents to be initiated. The preliminary storage trials of the LAMP pellets have produced promising results and there was no significant change in amplification observed throughout the week of storage at 37°C.

Unfortunately the disruptions caused by COVID-19 meant that the planned pro-longed storage analysis and storage trials of the LAMP pellets in-the-field could not be completed. Investigators have reported that lyophilised PCR reagents were stable after for 3 months at 37°C in the laboratory (Klatser *et al.*, 1998). There is propagation towards the use of molecular POC devices in low-resource environments within tropical regions. Consequently, the ability to store molecular reagents and retain stability in adverse conditions is vital. However, to the best of my knowledge, there is no reference to assessment of the effect of storage of molecular reagents being conducted at the intended point-of-use (Magro *et al.*, 2017a). If more time had been available, the extended trial of the LAMP pellets would have been completed to conclude feasibility for use in-the-field. However, under the current global circumstances, the pursuit of further studies and validation in-the-field are not possible. Although, the data obtained from the storage of the lyophilised Isothermal Mastermix in-the-field provide a positive outlook for the applicability of the LAMP pellets in-the-field. The lyophilisation process is likely to increase the cost of the molecular assay, currently liquid or “wet” qPCR assays can cost less than one dollar per reaction, whereas lyophilized reagents can increase the cost of qPCR per reaction by more than ten-fold (Nagaraj *et al.*, 2018). It is therefore critical that the benefits of lyophilized molecular assays are assessed against the associated benefits gained, such as the elimination of cold-chain storage which will reduce the cost of transportation; the potential to prolong storage of reagents; and simplification of diagnostic processing, which can reduce the cost of training (Nagaraj *et al.*, 2018).

## 5.6 Conclusions

Although preliminary storage trials in the laboratory suggested that LAMP would not be inhibited by storage in hotter environments, an investigation into the effect of field storage on the LAMP reagents concluded that LAMP was significantly affected by working conditions in Uganda. The experiments carried out following field storage suggest that amplification time may vary and that 1 in 5 LAMP reactions may be inhibited in-the-field. It was concluded that throughout field trials roughly 20% of the cassettes processed were removed from analysis due to failed PC reactions. After analysis of the stored reagents, it is thought that failed PC LAMP outcomes were likely due to the storage of reagents in Uganda. However, it would not be appropriate to state that the storage of the molecular reagents were the sole cause of the false-negative results returned by the Paper Device. Many factors could have affected the false-negative outcomes of the clinical samples processed on the Paper Device in-the-field, for example the intensity of infection; the quantity of DNA present in the blood samples; and the quality and recovery of the extracted DNA.

Successful freeze-drying of the LAMP reagents may provide a solution for storage and use of the molecular reagents in-the-field. The preliminary storage trials carried out in the laboratory had positive outcomes, however, further work is needed to conclude feasibility in low-resource and tropical areas. Additionally, a calibration study conducted throughout storage trials could prove beneficial to gaining a greater understanding of the potential effect of the storage conditions in-the-field on the limit of detection of the molecular assay.

## 5.7 Take home points

- *Assessment of storage conditions at the intended point-of-use and the effect on the test reagents should be considered, especially when considering work in harsh conditions.*
- *Air-dried 'primitive' drying techniques were not successful in field storage.*
- *The lyophilised 'LAMP pellets' produced desirable outcomes after short-term storage in field-like conditions. Successful storage of the lyophilised Mastermix in-the-field suggests that the lyophilised 'LAMP pellets' may be an appropriate solution for molecular reagent storage.*
- *Further trials monitoring the effect of storage on the molecular reagents should be conducted at, or after prolonged storage at the point-of-use to gain insight into the effect on amplification outcomes.*

## Chapter 6: Conclusions and Future work

Molecular diagnostic tests are widely accepted as gold standard since they provide high sensitivity and specificity and are capable of distinguishing between various pathogen species (Song *et al.*, 2015). There has been an abundance of research dedicated to the identification and development of molecular probes to detect and distinguish different pathogens. The development of new molecular assays facilitates the adaptation of molecular tests to detect a larger range of pathogens; this has been highlighted by the work presented in this study, whereby the assays to detect *S. mansoni* DNA were adapted for integration into the Paper Device platform to multiplex the detection of *plasmodium* and *S. mansoni* DNA.

Investigators who have presented POC molecular platforms imply that the respective technologies and methods could be deployed to low-resource POC environments (Song *et al.*, 2015). Prior to this study, trials of POC molecular platforms in low-resource field environments have been largely overlooked. The Paper Device platform has now detected *plasmodium* and *S. mansoni* parasite DNA within clinical specimen at the point-of-care in a simple cassette with reduced reliance on expensive laboratory equipment. The method reduces traditional equipment and consumables, resulting in simplified sample processing and flow control with simple LF result read-out.

### 6.1 The *S. mansoni* singleplex cassette

The development of the *S. mansoni* LAMP assay within this study (addressed in Chapter 3), facilitated the expansion of the Paper Device capabilities to detect *S. mansoni* DNA from a variety of *S. mansoni* specimen. Following data which presented amplification of mtDNA from murine stool and urine; and human faecal specimen collected in endemic settings (Fernández-Soto *et al.*, 2014; Gandasegui *et al.*, 2016; Gandasegui *et al.*, 2018), our small study confirmed that amplification of mtDNA target region (GenBank Accession No. L27240) from fresh human stool is achievable using a POC LAMP platform in-the-field. As a result of low sample throughput, the sensitivity of the method could not be assessed, however, Kato-Katz positive (n=8) and negative (n=2) samples were identified by using the Paper Device platform. The preliminary trials also highlighted the difficulty of processing faecal samples in-the-field; the need for a more suitable heating methods in-the-field; and necessary amendments to the cassette design and workflow for future field trials.

## **6.2 The multiplex malaria and schistosome cassette with frugal heating**

As a result of the complications which arose during the processing stool samples in the preliminary field trial, subsequent field trials focused on detecting target *S. mansoni* circulating DNA in blood specimen, which enabled processing to detect *S. mansoni* and plasmodium DNA to be combined into a single cassette. The successful amplification of *S. mansoni* DNA from an array of *S. mansoni* specimen also suggested that the SM primer set would also amplify DNA from *S. mansoni* ova and circulating DNA present in blood samples (Lodh *et al.*, 2013; Anderson *et al.*, 2015; Kato-Hayashi *et al.*, 2015; Ruiz-Villalba *et al.*, 2017; Fernández-Soto *et al.*, 2019).

Failed heating equipment led to LAMP being carried out on the POC cassette using a gas stove. *Plasmodium* DNA was detected in 9 of the 11 samples which were confirmed positive by qPCR. However, there were a large number of false-negative *S. mansoni* results which may have resulted from poor temperature control, or, low concentrations of *S. mansoni* circulating DNA in the blood samples (García-Bernalt Diego *et al.*, 2019). Further studies into the detection of circulating *S. mansoni* DNA in blood samples and the development of alternate *S. mansoni* assay targeting the Sm1-7 gene to allow LF read-out would be beneficial for future trials. Although LAMP was achieved using the frugal heat source, continuous monitoring of the heating set up resulted in additional strain to the process and on resources, as a result, alternate heating platforms were sourced for successive trials.

### **6.3 The multiplexed malaria and *S. mansoni* cassette with integrated controls**

The integration of both PC and NC channels into the POC cassette allowed closer analysis of potential contamination events and LAMP failure. Unfortunately the additional control strips can complicate the interpretation of the cassette results, use of mobile phone applications with image analysis and algorithms may prove useful and simplify result analysis (Capitán-Vallvey *et al.*, 2015). Furthermore, the development of ‘control chambers’ where the results of control reactions do not rely on LF strip read-out – for example using colorimetric read out - would make interpretation of the test results simpler and reduce the size of the cassette, for easier transportation and handling.

Despite controlled temperature monitoring and the elimination of leaks from the POC multiplex malaria and *S. mansoni* cassettes, there were a large occurrence of false-negative results (n=10 and 13 for detection of *plasmodium* and *S. mansoni* DNA respectively). The increase in false-negative results could have been due to the lower prevalence of infection within the community, however, an additional 10 cassettes exhibited failed PC, prompting an investigation into the effect of storage conditions on the molecular reagents.

### **6.4 Overall assessment of the field trials**

It is important to note that field trials provided a unique understanding of the settings where the POC diagnostics for malaria and schistosomiasis are needed in Uganda. First-hand experience of the constraints that the site conditions have on molecular diagnostic testing allowed changes to be made to the Paper Device in early development stages. This is often overlooked in the development of POC devices and should be investigated further for all envisaged devices (including other modalities than LAMP as used here). Additionally, fieldwork provided the opportunity to gain vital feedback from the VCD technicians (the target end user).

Issues that were experienced with heating equipment highlighted the necessity of a heat source which eliminates the reliance on external electricity supplies and provides more stable heating than a portable gas stove. Solar panels are readily available throughout Uganda, thus, new heating solutions to conduct LAMP in-the-field should focus on solar-powered or solar-chargeable solutions (Jiang *et al.*, 2014; Gumus *et al.*, 2016; Dacey, 2020). During processing in-the-field a team member was required to track the cassettes during heating, an automated heating system would reduce strain on the user and reduce risk of heating errors.



Inclusion of an automated heating system was discussed with the VCD technicians and also suggested in feedback during a Paper Diagnostic workshop held at the Ugandan Bioengineering Conference 2019.

The Paper Device has simplified molecular processing and exhibited POC molecular tests in low-resource and rural communities in Uganda. However, the complexity of molecular diagnosis should not be underestimated, the sample processing prior to DNA amplification and detection is a major barrier to simplification of the technique. The integration of magnetic particles into the paper origami platform reduced the volume and cost of comparative laboratory DNA processing, however, was not able to reduce sample processing steps. Unlike current RDTs, sample processing methods required for NAAT are complex and as a consequence, in its current state the POC Paper Device should be handled by experienced and trained technicians. Training is relatively simple and can be supported by printed visual instructions and video protocols, throughout the scope of this study various training sessions were run to translate testing to identify other diseases, such as hepatitis-C, leptospirosis and brucellosis in humans and cattle, as such, shows promise for application in the wider tropical medicine community (Faust *et al.*, 2020).

Upscaling the diagnostic process in-the-field highlighted the difficulty of conducting POC molecular testing. In reality, the process requires a mobile laboratory, this was achieved by packing the necessary equipment, reagents and cassettes into 2 large travel crates (423mm x 400mm x 600mm). The linear workflow was necessary to reduce contamination events, however, this required a few team members to run successive test stages. Integration of pre-stored molecular reagents would significantly decrease the time for test preparation and with both pre-stored LAMP reagents and automated heating the test process could be carried out by a single user.

In addition to the selection of appropriate molecular reagents, primer sequences and target DNA sequences, there are several factors which can affect the outcome of molecular amplification. PCR requires thermal cycling to achieve amplification of the target DNA. The accuracy of heating temperature and the speed at which the sample is cycled between temperatures steps affect the outcome of amplification (Neuzil *et al.*, 2006). The need for accurate and efficient thermal cycling equipment to provide the correct heating temperatures and appropriate temperature ramping, requires more complex heating systems. There are a number of developed PCR chips reported (Neuzil *et al.*, 2006; Jangam *et al.*, 2013; Manage *et al.*, 2013), however cost of fabrication is not reported and it is unclear whether these have

been tested out with the laboratory environment. Although there are cheaper (\$600-800), portable PCR systems commercially available (for example the miniPCR™), heating is limited to a smaller number of reactions (typically 8-16). Additionally, the systems require a laptop or tablet to program the cycles and external electricity supply, all of which may not be available in low resource or remote clinics. NAAT using LAMP for molecular detection eliminates the need for expensive thermal cycling equipment, which has enabled the introduction of frugal heating techniques. Cost analysis of LAMP and qPCR procedures for the diagnosis of TB in peripheral laboratories, concluded that LAMP can reduce costs by up-to \$12 per-test when used as a routine diagnostic (World Health Organization, 2016).

The purity of the DNA extracted from the chosen sample will also affect the outcome of molecular amplification (Barbosa *et al.*, 2015). DNA extraction methods can be very labour and equipment intensive (Barbosa *et al.*, 2015). Advances in DNA extraction methods have extended implementation in POC molecular diagnostics (Ali *et al.*, 2017). Incorporation of magnetic beads, silica and cellulose matrices into portable devices and microfluidic chips, enables DNA extraction to be conducted with less laboratory equipment (Ali *et al.*, 2017). However, at the time of writing, it is unclear if these methods have been tested out-with the laboratory environment. RNA extraction for veterinary surveillance has been conducted in the field for genomic sequencing (Brunker *et al.*, 2020). The ‘lab-in-a-suitcase’ approach facilitated extraction and processing of samples in both low-resource laboratories and field sites.

## 6.5 Storage of molecular reagents

Requirements for cold-chain storage is a major barrier for many tests deployed in sub-Saharan Africa (Pai *et al.*, 2012). Many commercially available reagents and molecular test kits supply liquid reagents, and therefore require cold-chain transport and storage, and as a result limit applications of molecular tests to locations where the appropriate transport and storage conditions are available. It appeared that LAMP outcomes were significantly affected by the storage conditions in Uganda, as a result, around 20% of the cassettes processed during field trials were removed from study analysis due to failed PC reactions. The lyophilised LAMP pellets, developed in the final chapter, are a promising solution for storage and use of molecular reagents in-the-field (Babonneau *et al.*, 2015). Preliminary storage trials carried out in the laboratory had positive outcomes, however, further studies are needed to conclude feasibility in low-resource, tropical areas. Additionally, the use of pre-stored LAMP pellets would reduce the test processing steps. Simplifying the POC test procedure by reducing manual processing stages will consequently reduce the risk of contamination events, leading to improved test outcomes.

## 6.6 Future work

Further investments in technological innovation are being driven by successive global health emergencies including SARS, MERS CoV, Ebola virus, Zika and COVID-19 virus. The WHO has called for the development of open platform technologies to accelerate the development, validation and production of vaccines, therapeutics, diagnostics and reagents for infectious diseases of epidemic potential as part of the WHO Blue Print for R&D preparedness (Peeling *et al.*, 2017). The Paper Device is a platform that simplifies sample processing and has enabled NAAT to be carried out in-the-field, however, in its current state it appears unlikely that it is feasible diagnostic platform for large scale surveillance applications in low-resource environments. The major obstacles being a large number of processing steps and reagent storage. Literature searches reveal that POC molecular platforms tend to address one but not both of these points (Song *et al.*, 2015). Conducting direct LAMP – eliminating nucleic acid extraction steps - would minimise sample preparation steps, however, consequently reduces the sensitivity of the test (Abdulmawjood *et al.*, 2014; Gadkar *et al.*, 2018; Fowler *et al.*, 2020). LAMP has been suggested for specific applications for example screening for COVID-19, antimalarial drug efficacy trials and resistance monitoring programs, vaccine trials, and evaluations of other diagnostic tools (Cook *et al.*, 2015; Vallejo *et al.*, 2015; Fowler *et al.*, 2020). Advances in DNA origami and

enzyme free systems could further propel the application of molecular diagnosis in low-resource settings (Wang *et al.*, 2017).

In addition to simplifying the test procedure by reducing manual processing stages and introducing an automated heating system, further field studies should be carried out to assess appropriate use in healthcare settings. It is how tests are deployed or implemented in a health system that defines the success of POC testing (Pai *et al.*, 2012; Pai *et al.*, 2015; Sharma *et al.*, 2015). A pilot study assessing the use of the Paper Device in different settings can reveal who benefits most from this technology. Additional aspects to consider during pilot studies would be supply chains, storage and safe disposal of the POC devices. Waste management is a particular concern in rural communities, where medical waste retrieval may be scarce or non-existent. The paper origami platform can be safely incinerated on a fire (Reboud *et al.*, 2018), however, the Paper Device cassette may benefit from a waste retrieval plan which enables the PMMA cassettes to be sterilised and re-used; or incorporating a cassette made from biodegradable material.

The work presented in this study highlights the malleability in the NAAT diagnostic process, similar platforms could aid in driving the diagnostic sector towards ‘personalised diagnosis’ with a diagnostic platform or tool which can be tailored to the needs of specific geographical locations. Once fully developed, POC paper molecular detection platforms - such as the Paper Device - could be an extremely useful tool for epidemiological monitoring in endemic settings, where sensitivity, cost and convenience are paramount (Connelly *et al.*, 2015; Song *et al.*, 2015).

## Chapter 7: Appendices

### 7.1 Description of Mastermix

Table 7-1: The names, manufacturers and descriptions of Mastermix used for isothermal amplification (LAMP), PCR and qPCR throughout the scope of this project.

Mastermix	Description	Manufacturer
(q)PCR Mastermix		
Brilliant Multiplex QPCR Master Mix	The qPCR Master Mix used throughout laboratory trials. The Master Mix contains dsDNA binding dye, is supplied in liquid format and stored at -20°C.	Agilent, Stockport, UK
EZ PCR 5X Master Mix, Load Ready™	The PCR Master Mix used in the field trial. Contains integrated DNA binding dye for gel visualisation. The Master Mix was supplied in liquid format and stored at -20°C. However, the Mastermix is room temperature stable for up to one month.	MiniPCR, Cambridge, MA
Isothermal Mastermix		
ISO-004	The 'original' isothermal Mastermix which contains dsDNA binding dye, is supplied in liquid state and stored at -20°C.	OptiGene, Horsham, UK.
ISO-004ND	Isothermal Mastermix which does not contain dsDNA binding dye, is supplied in liquid state and stored at -20°C.	
ISO-DR004	The lyophilised isothermal Mastermix which contains dsDNA binding dye. The Mastermix was supplied in the dried format with re-suspension buffer and stored at room temperature/in the fridge. Used throughout field trials.	
LYO-004	The pre-lyophilised Mastermix solution which contains dsDNA binding dye. The Mastermix solution was supplied in liquid format and stored in the fridge. The Mastermix solution was used to create the dried LAMP pellet for development of molecular reagent storage protocols.	

## 7.2 DNA conversion table

The parasite DNA obtained from collaborators and gBlock DNA was measured on the NanoDrop and quantified in ng/μL, as a result, the DNA used in NAATs throughout this study was reported in ng/μL. The gBlock DNA weight detected can be converted to the corresponding copy number using the equation below, where X is the amount of amplicon (the weight of the gBlock in ng); A is Avogadro's number; N is the length of the target DNA (bp); and 660 (g/mole) is the average mass of 1 bp of dsDNA. The copy number corresponding to the weight of the gBlock DNA was calculated using the equation below and is displayed in Table 7-2. Using this information, a standard dilution of the gBlock DNA was used to calculate the corresponding copies of the *plasmodium* gDNA for both qPCR and LAMP NAATs. The qPCR and LAMP assays are design for different target regions, hence, will result in different copy numbers per reaction.

*Equation 1: Equation for the conversion of the amount of target gBlock dsDNA (ng) to copy number.*

$$\text{Copies} = \frac{X \times A}{N \times 660 \times (1 \times 10^9)}$$

*Table 7-2: The DNA conversion table. The conversions from ng/μL of DNA used in the NAATs to copies per reaction. The qPCR and LAMP reactions comprise of 2μL and 5μL of target DNA respectively.*

Target DNA	Concentration of DNA (ng/μL)	Copies in qPCR reaction	Copies in LAMP reaction
<i>S. mansoni</i> gBlock	10 <sup>-1</sup>	1.7x10 <sup>9</sup>	2.3x10 <sup>9</sup>
	10 <sup>-2</sup>	1.7x10 <sup>8</sup>	2.3x10 <sup>8</sup>
	10 <sup>-4</sup>	1.7x10 <sup>6</sup>	2.3x10 <sup>6</sup>
	10 <sup>-6</sup>	1.7x10 <sup>4</sup>	2.3x10 <sup>4</sup>
<i>Plasmodium</i> gBlock	10 <sup>-1</sup>	1.2x10 <sup>9</sup>	2.0x10 <sup>9</sup>
	10 <sup>-2</sup>	1.2x10 <sup>8</sup>	2.0x10 <sup>8</sup>
	10 <sup>-4</sup>	1.2x10 <sup>6</sup>	2.0x10 <sup>7</sup>
	10 <sup>-6</sup>	1.2x10 <sup>4</sup>	2.0x10 <sup>6</sup>
<i>Plasmodium</i> gDNA	10	8.0x10 <sup>10</sup>	3.2x10 <sup>5</sup>
	10 <sup>-1</sup>	8.0x10 <sup>8</sup>	3.0x10 <sup>4</sup>
	10 <sup>-2</sup>	8.0x10 <sup>7</sup>	-
	10 <sup>-3</sup>	8.0x10 <sup>6</sup>	1.0x10 <sup>3</sup>

## **7.3 ABI fluorescence data**

### **7.3.1 Code to plot the LAMP data**

The raw fluorescence data was required to compare fluorescence data collected in different runs. The raw data was extracted and plotted using MATLAB® software (code presented on the following page). The raw data was extracted from the ABI file (data compiled for Filter 1) and reshaped to arrange fluorescence data for each well into chronological order. The data for each well is normalised using the average fluorescence values determined for data within the user defined baseline. The user can select which wells are plotted by entering the number associated with the corresponding well – for example A1= 1, A12=12, B1=13 and E1=49.

```

clear all
close all
clc
filename = 'Enter File Name';
RawData = xlsread(filename,'Raw Data');
%Finding the number of cycles
nb_cycle=max(RawData(:,1));
%defining the sample size (96 for the 96 well plate)
nb_sample=size(RawData,1)/nb_cycle;
nb_test=size(RawData,2)-1;
L=['A' 'B' 'C' 'D' 'E' 'F' 'G' 'H'];
n_compt=1;
for j=1:8
    for i=1:12
        sample_name(n_compt)= strcat(L(j),num2str(i));
        n_compt=n_compt+1;
    end
end
PC.data=RawData(:,2);
%compiles all the fluorescence values from 'column 2 (filter 1) of the raw
data. %re-shape to get all values for A1, A2 etc. grouped together
%*Z is all the RFU values for each well, time sequential
Z=reshape(PC.data, [nb_sample nb_cycle]);
%give a definition for time (cycle number)
time=1:1:nb_cycle;
timeq=1:0.1:nb_cycle;
i=1;
start=zeros([nb_sample 1]);
K=zeros([nb_sample 10]);
%Maximum=max(Z(:));
o=1;
jj=1;
%this for loop calculates the change in flourescence for each well (works out
the base line) so that the values can be normalised
for jj=1:nb_sample
    for o=2:4
        K(jj,o)=Z(jj,o);
        o=o+1;
    end
    start(jj,1)=mean(K(jj,:));
    jj=jj+1;
end
end

%x:user enter the well 'numbers' (1-96) which have been filled
%x = inputdlg('Enter the number(s) associated with the wells which are filled
(1-96): ','Sample Wells');
%wells = [1 37 73 14 50 86 4 40 76 17 53 89];
%n:the total number of wells filled (number of samples tested)
%n=numel(wells);
%ColorSet makes sure each sample has a different colour graph
ColorSet=varycolor(6);
legend on
set(gca,'ColorOrder',ColorSet);
hold all;
ll={'magenta','black','blue','red','magenta','black','blue','red','magenta','
black','blue','red'};
m=1;
for i=wellss2; %only the well numbers entered by the user will be plotted on
the graph for i
    Value (i,:)=Z(i,:)-(start(i)*1.05);
    Valueq(i,:)=spline(time,Value(i,:),timeq);
    %plot(time,Value(i,:))
    %hold on
    plot(timeq,Valueq(i,:));
    %hold on
    hTitle=title('Enter the Title');
    hXLabel=xlabel('Enter the x axis label');
    hYLabel=ylabel('Enter the y axis label');
    %hold on
    r=1;
    for g=wellss;
        legendInfo(r)=[sample_name(g)];
        r=r+1;
    end
    hLegend=legend([legendInfo],'Location','eastoutside');
    set([hLegend],'FontSize',12);
    %ylim([-10^5 10^5])
    xlim([0 34])
    set(gca,'fontsize',20)
    %this will repeat for all wells (data for A1-H12) to give full graph
    %hold on
    %m=m+1;
end
end

```



### 7.3.2 ABI filter spectrum

The ABI filter spectrum determines which filter the fluorescence data is collected from, the spectrum in Figure 7-1 is provided by the manufacturer. The dsDNA binding dye and SYBR™ Green 518 emission spectrums of 520 nm (Liu *et al.*, 2005), hence, the raw data was extracted from data collected by ABI filter 1.

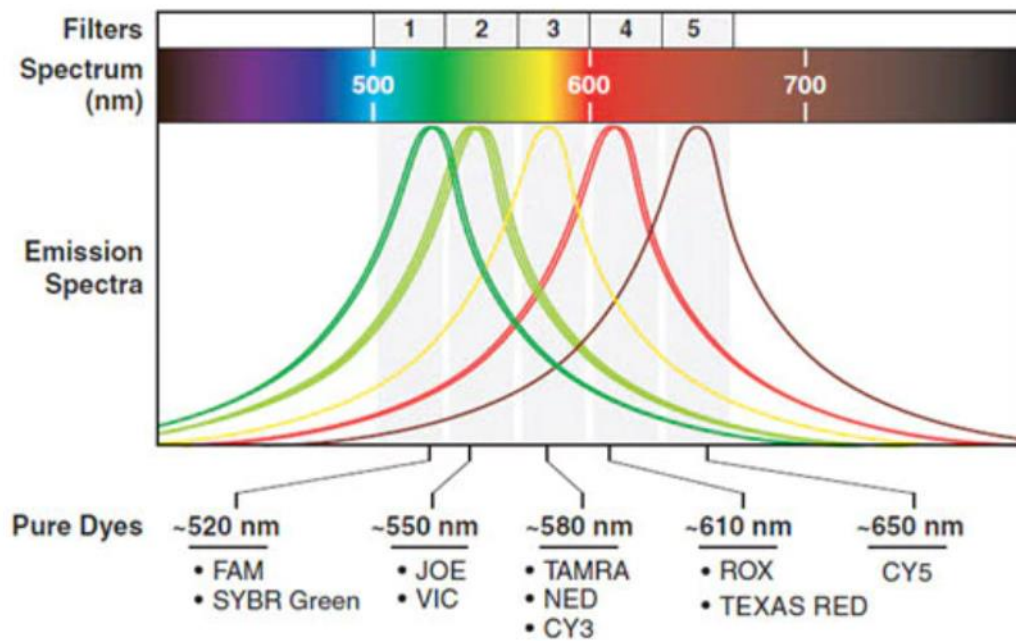


Figure 7-1: The ABI FAST 7500 qPCR machine spectrum filter information as provided by the manufacturer. The dsDNA binding dye and FITC produce emission spectrum ~520 nm, thus the fluorescence resulting from LAMP is recorded by Filter 1.

## 7.4 Melt temperature data

Umelt software (<https://dna-utah.org/umelt/umelt.html>) was used to calculate the predicted melt temperature of the desired target products. The theoretical melt temperatures calculated by Umelt and the melt temperatures recorded experimentally are displayed in Table 7-3.

*Table 7-3: The theoretical and experimental melt temperatures for the respective target samples. The experimental values display the range of melt temperatures returned from three separate LAMP runs.*

Target Name	Umelt temperature (°C)	Observed melt temperature (°C)
BRCA1	87.0	85.3 - 86.0
PPAN	85.5	84.0 - 84.6
SM	84.5	83.0 -83.7
SMchrom	84.5	83.3 - 84.3

## 7.5 DNA extraction trials

Prior to conducting field trials, sensitivity of the LAMP assay was confirmed in the laboratory using serial dilution of WHO international standard *plasmodium* DNA (Reboud *et al.*, 2018). Furthermore, 20 negative patient samples were processed on the paper origami device by Dr Gaolian Xu to affirm specificity of the diagnostic tool (Reboud *et al.*, 2018); additional samples were spiked with WHO international standard plasmodium DNA as a positive control.

Further investigation into the extraction of DNA was conducted using the paper origami device, amplification was conducted within the diagnostic cassette and ABI machine following protocols in Section 2.2. Monitoring of the real-time LAMP data on the ABI machine allowed fluorescence data to determine amplification C<sub>tt</sub> values and time required for amplification of extracted DNA samples. The DNA captured by the paper tabs during extraction using the paper origami device (refer to Section 2.2.2 for method details) was transferred into qPCR tubes by centrifugation, the paper tabs were trapped in the cap of 0.2 mL qPCR tube and centrifuged to collect the eluate.

Whole blood (Cambridge Bioscience, UK) spiked with gBlock DNA ( $10^{-2}$  ng/ $\mu$ L) was used to assess extraction and confirm that artefacts in whole blood did not hinder amplification or cause false-positive results. The experiment was repeated using genomic plasmodium gDNA spiked into PBS (10 ng/ $\mu$ L) solution to allow experiments to be conducted on an open laboratory bench outside of class II biosafety confinements.

Extraction of gDNA a gBlock DNA from spiked human whole blood and PBS confirm the validity of the extraction technique and amplification, See Figure 7-2. In both experiments the DNA extracted on the paper origami device produced amplification with C<sub>tt</sub> values associated with considerably lower DNA concentrations. Amplification was observed between 6 -8 minutes and 13-14 minutes for DNA extracted from whole blood spiked with gBlock DNA (  $10^{-2}$  ng/ $\mu$ L), and gDNA extracted from PBS (10 ng/ $\mu$ L ) respectively, see Figure 7-2(a,c). The percentage recovery was estimated as 22-35% and 19-24% for gBlock and gDNA experiments (Figure 7-2(b,d)). The percentage recovery was calculated under the assumption that the C<sub>tt</sub> correlated to the mean experimental data (bold line).

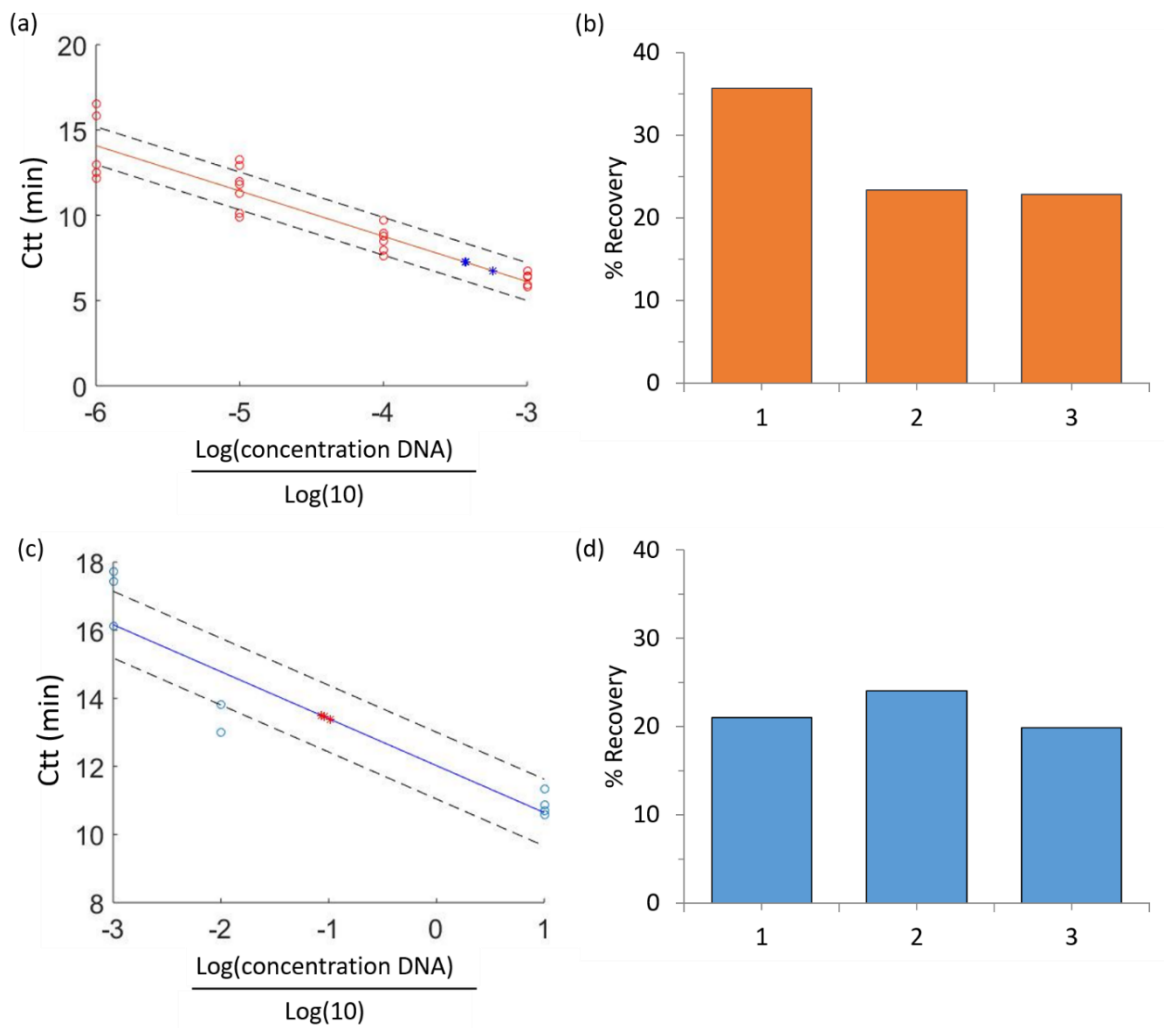
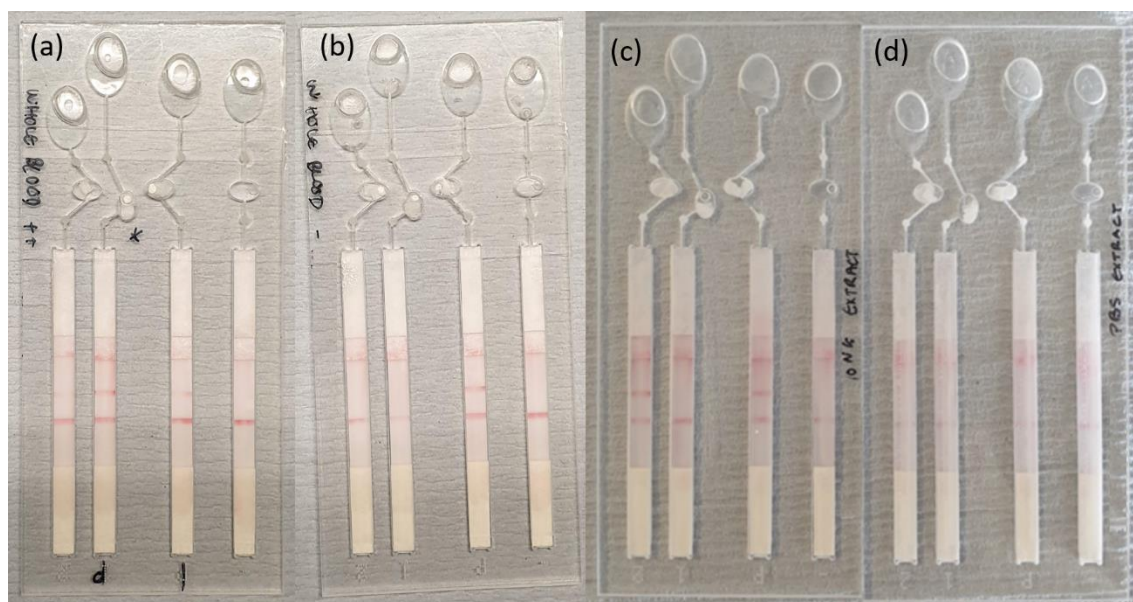


Figure 7-2: DNA extraction processed on the Paper Device. (a) DNA extraction from whole blood spiked with plasmidium gBlock DNA to  $10^{-2}$  ng/ $\mu$ L, whole blood, WB-, was used as a negative control for extraction. (a) Paper tabs were centrifuged to collect eluted DNA for LAMP amplification on the ABI machine. Ctt values for gDNA extraction were 6.7, 7.2, 7.3 cycles (blue star); and associated controls ( $10^{-4}$  &  $10^{-5}$  ng/ $\mu$ L) were 10.0 and 12.9 cycles, which coincided with calibration data (red line). There was no amplification from the no target control, NC, or negative whole blood sample, WB-. (b) % recovery of gBlock DNA extracted from whole blood using the Paper Device method, the extraction was repeated three times; % recovery 35.7,23.3,22.8% is displayed for each repeat 1,2,3 respectively. (c) DNA extraction of genomic plasmidium DNA (50 ng), PBS was used as a negative control for extraction. The graph displays the Ctt values for extracted gDNA (red star) as compared to calibration Ctt data (blue line). There was no amplification from the no target control, 'NC' or the negative PBS samples. (d) % recovery of gDNA extracted from PBS using the Paper Device method, the extraction was repeated three times; % recovery is displayed 21.0, 24.1 and 19.9% for each repeat 1,2,3 respectively.

Additionally, extraction and amplification of DNA carried out in the diagnostic cassette (refer to Figure 7-3), confirmed amplification results from the ABI machine. The engravings on the diagnostic cassette ‘-, P, 1 & 2’ refer to the NC, PC and samples results respectively and molecular reagents to detect *plasmodium* DNA were used for both sample chambers. Results of the DNA extraction & amplification are displayed in Figure 7-3. The engravings on the diagnostic cassette ‘-, P, 1 & 2’ refer to the NC, PC and samples results respectively. Figure 7-3(a) WB+ cassette depicts a positive result (see Figure 2-14 for more details), 1 & P were inverted as indicated in black marker on the cassette. Figure 7-3(b) WB- depicts a negative results. Figure 7-3(c&d) depict the results of DNA extraction from spiked PBS & amplification carried out within the diagnostic cassette with visual read out on LF strips. Figure 7-3(c) shows the cassettes which processed PBS spiked with 50 ng plasmodium gDNA, the cassette depicts a positive result. Figure 7-3(d) cassette processed PBS and the cassette depicts a negative results.



*Figure 7-3: The results from the extraction of plasmodium DNA spiked into whole blood and PBS processed on the Paper Device. The results of amplification were determined by LF read-out. The engravings on the diagnostic cassette ‘2’, ‘1’, ‘P’, ‘-’, where ‘2’ & ‘1’ refer to the sample result, ‘P’ & ‘-’ refer to the PC and NC respectively. (a) WB++, cassette depicts a positive result (see Figure 2-14 for details on identification of results), 1 & P were inverted as indicated in black marker on the cassette. (b) WB-, depicts a negative results. (c&d) Results of dDNA extraction from PBS. (c) 50 ng plasmodium gDNA, cassette depicts a positive result. (d) PBS, cassette depicts a negative result.*

To assess the effect of removal of DNA from paper strips, 50 ng gDNA in 30  $\mu$ L elution buffer was spiked onto paper strips and centrifuged to collect eluate for amplification on the ABI machine. The technique resulted in extremely variable results with percentage recovery ranging from 25-67%. The increased C<sub>tt</sub> suggests large losses in DNA in both the DNA

extraction process ( $\Delta C_{tt} = 2.9$  minutes); and in isolating DNA from the paper itself ( $\Delta C_{tt} = 1.3$  minutes). Extraction and amplification of *plasmodium* gDNA in the diagnostic cassette confirmed results obtained by amplification on the ABI machine, see Figure 7-3. The engravings on the diagnostic cassette ‘-, P, 1 & 2’ refer to the NC, PC, BRCA and *plasmodium* PAN respectively. BRCA-1 primer set (see Figure 7-3) was used as an additional control within the cassette to ensure there was no contamination of human DNA in the extraction process.

The resulting percentage recovery was in agreement with other published studies on recovery of small concentrations of DNA (Katevatis, Fan and Klapperich, 2017). However, the varying recovery of control gDNA from paper tabs suggests that the centrifugation elution technique may not provide a true representation of DNA recovery using the Paper Device method. Additionally, the  $C_{tt}$  may be associated with a range of DNA concentrations. Using a 95% confidence interval (dotted line), the  $C_{tt}$  values correlate to concentrations resulting in percentage recovery between 9-57% and 1-41%.

## 7.6 The development of SM Primers

### 7.6.1 SM qPCR data

The SMchrom qPCR reagents were successful in amplifying DNA obtained throughout the schistosome life cycle (data provided in Section 3.4.1). Originally it had been intended that qPCR would be used as a comparative diagnostic on return to the laboratory in Glasgow (as with the malaria study), however, amplification was not achieved from DNA extracted from the blood spots stored on FTA cards.

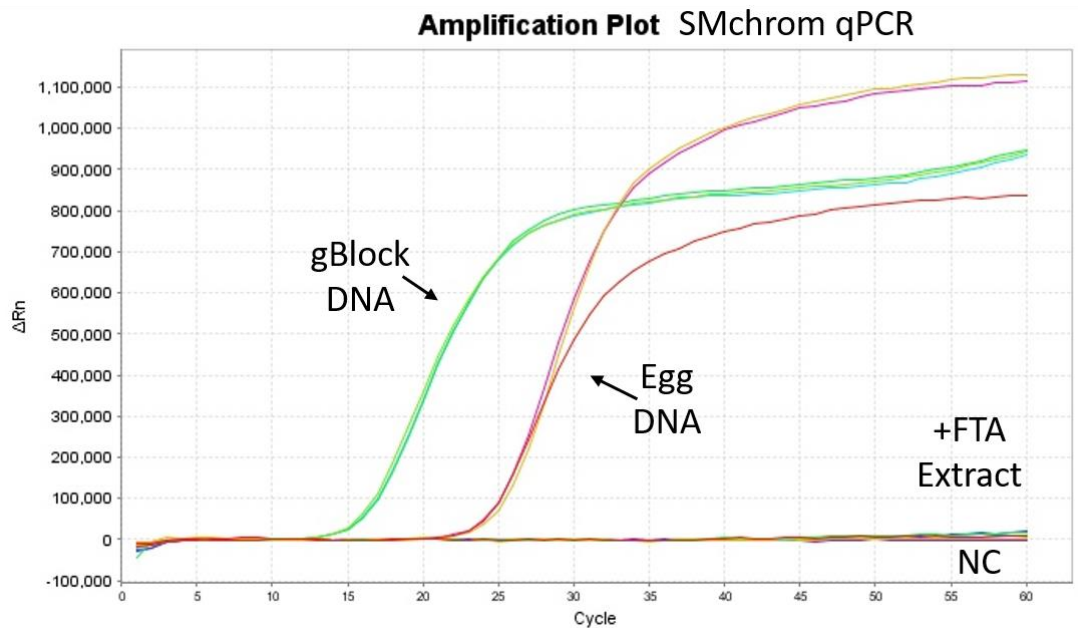


Figure 7-4: The SMchrom qPCR fluorescence curves. TaqMan qPCR was carried out using gBlock, *S. mansoni* egg DNA and extracted DNA from positive blood samples stored on FTA cards (+FTA Extract). Amplification was conducted for 60 samples, however, no amplification was observed from +FTA Extract.

### 7.6.2 SM LAMP primers

During the development of the schistosome primer sets a variety of schistosome DNA samples were used as target DNA in the LAMP reaction to confirm amplification throughout the schistosome life cycle. Multiple targets were trialled to assess feasibility of DNA detection from a variety of samples, for example, successful amplification of DNA extracted from *S. mansoni* ova would suggest that the assay is appropriate for the detection of *S. mansoni* in a stool sample. Figure 7-5 shows the fluorescence data exported from the ABI machine demonstrating the amplification of gDNA (adult worm DNA obtained from SCHISTO\_PERSIST), *S. mansoni* ova and adult worm DNA extracted using the Promega MagaZorb kit. The low DNA yield obtained using the Promega MagaZorb extraction kit (due to the large elution volume) consequently lead to a late amplification time, thus, the DNA was not used for further downstream experiments.

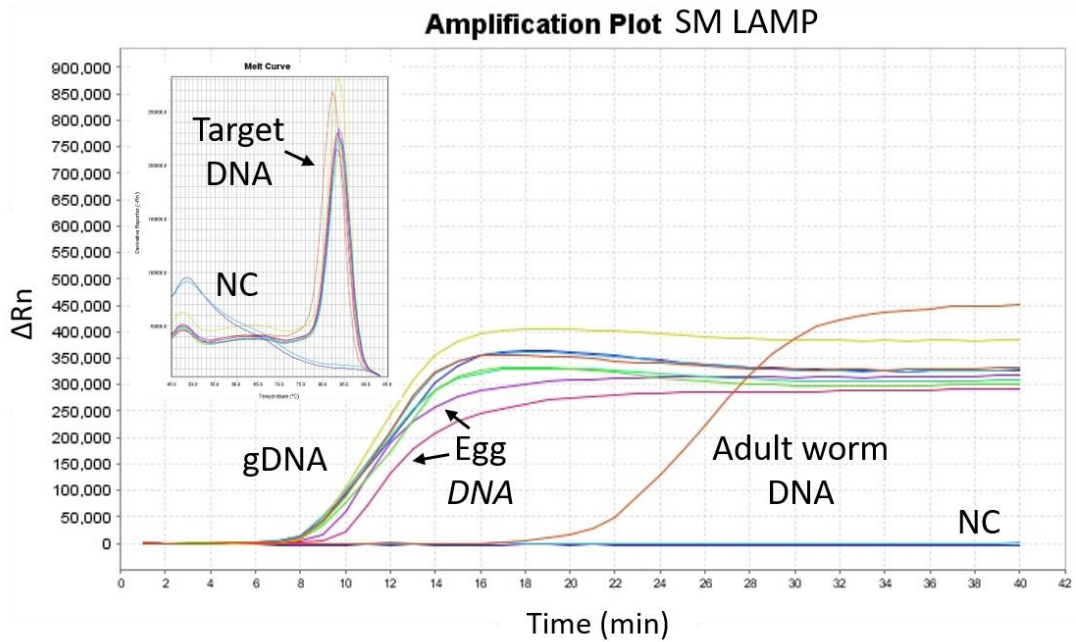


Figure 7-5: Fluorescence data collated for SM LAMP of a variety of target schistosome DNA samples. LAMP was carried out with gDNA (schistosome DNA provided by SCHISTO\_PERSIST), *S. mansoni* ova and adult worm DNA extracted using the Promega MagaZorb kit. There was no amplification observed from the NC.



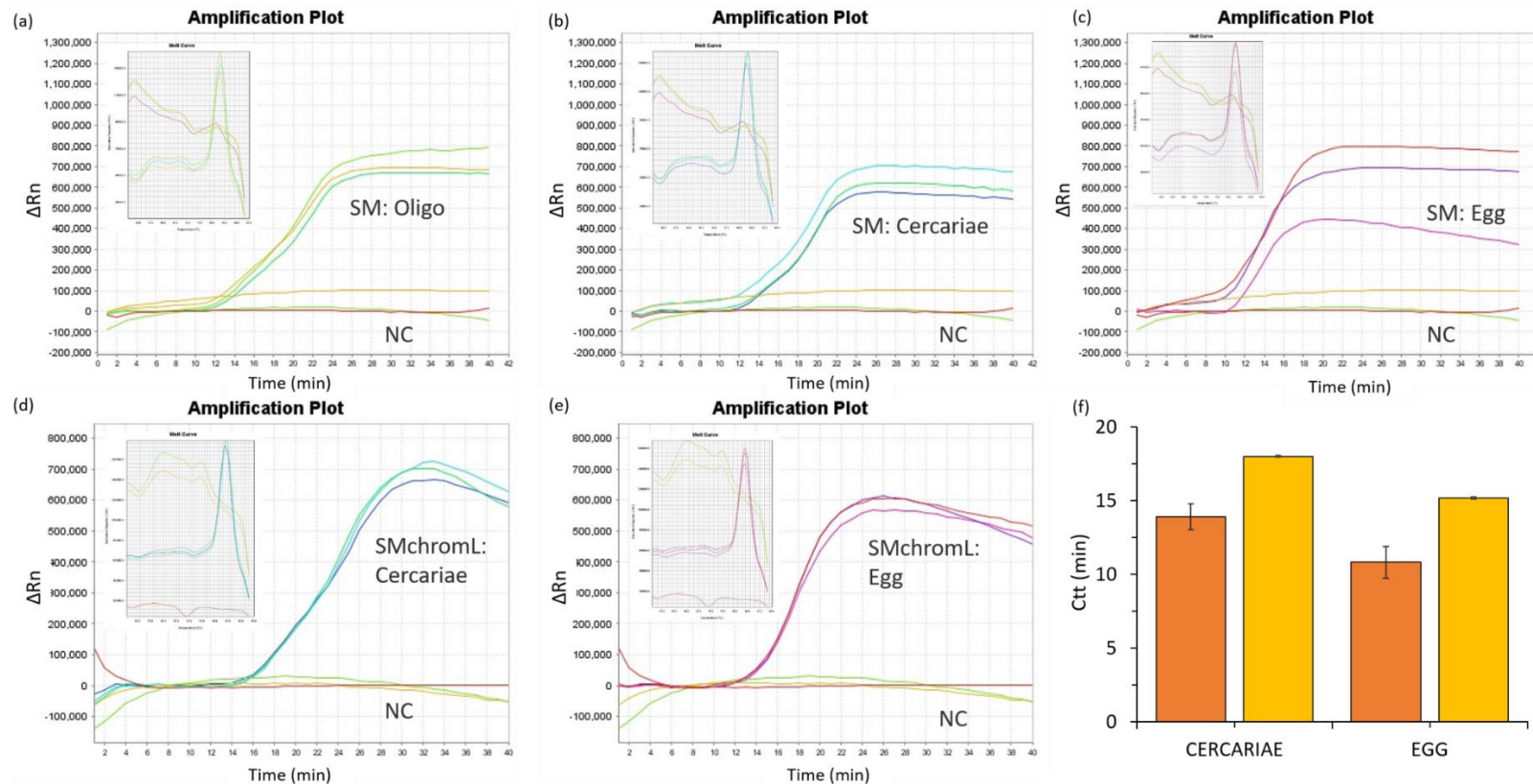


Figure 7-6: Fluorescence data collated for SM and SMchromL LAMP of a variety of target schistosome DNA samples. LAMP was carried out with gBlocks, and extracted *S. mansoni* ova and cercariae DNA. Amplification was confirmed by melt curve analysis. There was no amplification observed for NC samples. Amplification of (a) the SM gBlock using the SM primer set. (b) Extracted *S. mansoni* cercariae DNA using the SM primer set. (c) Extracted *S. mansoni* ova DNA using the SM primer set. (d) Extracted *S. mansoni* cercariae DNA using the SMchromL primer set. (e) Extracted *S. mansoni* ova DNA using the SMchromL primer set. (f) Mean Ct values obtained for amplification of extracted *S. mansoni* ova and cercariae DNA using the SM (orange) and SMchromL (yellow) primer sets, the SM primer set resulted in quicker amplification as compared to the SMchromL primer set.

## 7.7 Reference Diagnostic test methods

### 7.7.1 Blood smear for microscopic diagnosis of malaria

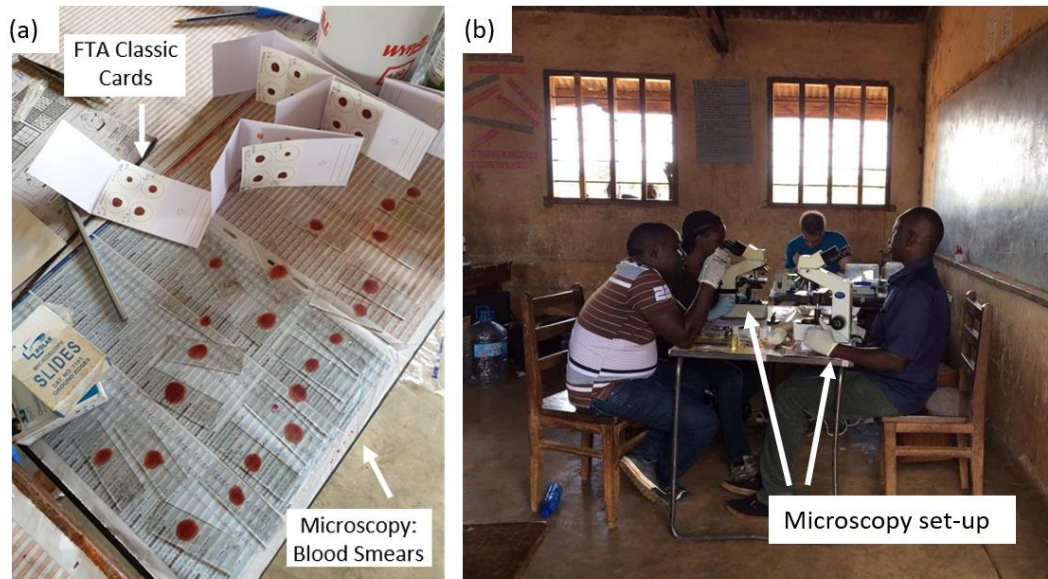
The method of the microscopic diagnostic examination varies slightly during large scale testing as compared to a single patient diagnosis. The following describes the method for microscopic testing used in-the-field (World Health Organization, 2010). The examination requires gloves; cleaned microscopy slides and a slide box; sterile lancets and a sharps container; 70% ethanol; cotton wool and lint-free cotton cloths; a spreader; Giemsa stain; buffered water (PH 7.2); and a microscope (World Health Organization, 2010). Additionally, a pencil, a pen and a results form was needed to complete diagnostic records.

A few small drops of blood were required to make up the thick blood smear. The participants' ring finger was cleaned with alcohol, and pierced with a sterile lancet. The droplets of blood were expressed on to the middle of the slide by gently applying pressure to the finger. The spreader was used to join the drops of blood together to create a film of roughly 1 cm in diameter (see the prepared slide in Figure 7-7(a)). The participants' ID number and initials were marked on the slide in pencil and the slides were left in the slide box to dry, the storage box was used to protect the samples from dust, sunlight and flies. A three percent Giemsa solution was prepared (using locally sourced bottled water) in a basin to stain the slides. The dried microscope slides were arranged in a holding rack and placed into the basin of Giemsa solution. After an hour, clean water was poured into the basin and the slides were transferred from the basin to the drying rack.

Following the slide preparation, the blood smear was inspected using a compound microscope (made in Philippines; Model CX21FS1; Olympus Corporation) using a 100X oil immersion objective lens, with either electrical or natural light sources (dependent upon availability of electricity) the set-up in-the-field is shown in Figure 7-7(b). *Plasmodium* parasites as observed by blood smear microscopy are depicted in Figure 7-7(c). The parasites present in the blood smear were counted against the number of leukocytes (WBC) and recorded as the number of parasites per 200 WBC. The intensity of infection is calculated as the number of parasites per microliter of blood using Equation 2. Additionally, different life stages of the *plasmodium* parasites can be distinguished by microscopic examination (see Figure 7-7(c)). Time to examine the blood smears varied dependent on the parasite load and the examining technician, however, on average each slide was examined within 10 minutes.

Equation 2: Calculation of the number of plasmodium parasites per microliter of blood based on the parasite count against 200 WBC.

$$\text{Parasites per } \mu\text{L} = \frac{\text{no. parasites} \times 8000}{\text{no. WBC}} = \text{no. parasites} \times 40$$



(c) [Image removed due to copyright restrictions]

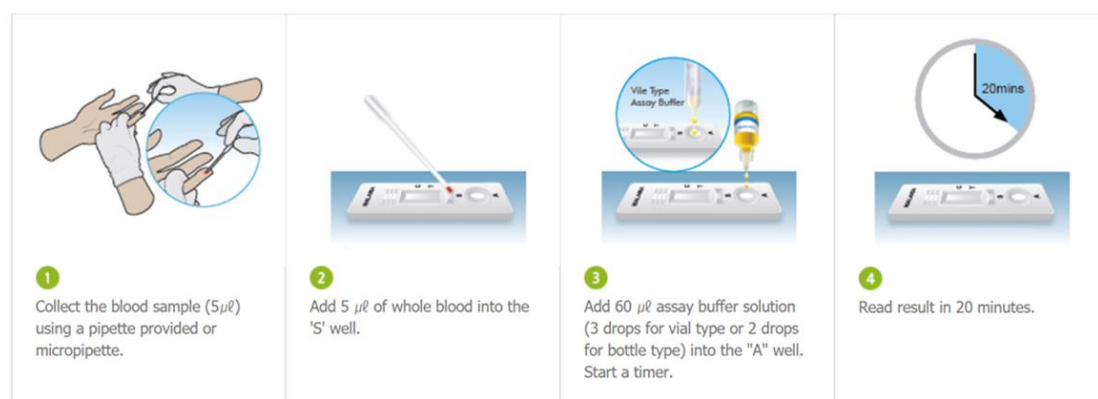
The QR code links to the source image.



Figure 7-7: Malaria gold standard, microscopy. (a) FTA® storage cards left to dry alongside the collection of dried blood smears on microscopy slides prior to Giemsa staining. (b) VCD technicians conducting microscopic examination for plasmodium parasites in blood smear. (c) Illustrations of different plasmodium species and life stages as expected to be observed by microscopy.

## 7.7.2 Malaria HRP2/pLDH (Pf/pan) RDT

### (a) Test Procedure (ACCESSBIO, 2020)



### (b)

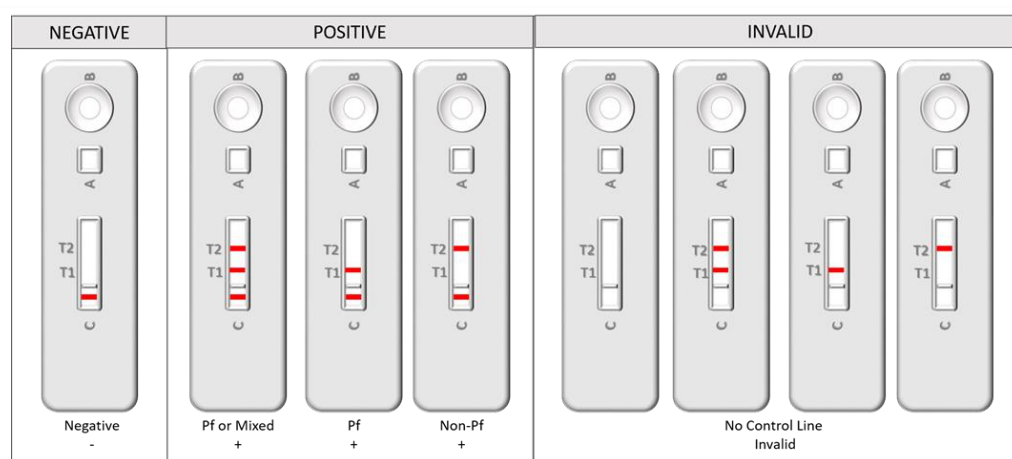


Figure 7-8: Carestart™ Malaria HRP2/pLDH (Pf/pan) RDT. (a) Instructions for the Malaria RDT test procedure as provided by the manufacturer. (b) Review of the different possible test results. A band must be present in the control window 'C' for the test to be valid. All tests which do not present with a band in the control window 'C' should be noted as invalid. No bands suggests a negative result. A band present in the 'T1' window suggests the patient does have falciparum malaria (Pf). A band present in the 'T2' window suggests that the patient has non-falciparum malaria.

The malaria RDT kit provides the diagnostic cassette, sample transfer utensil and assay buffer. Additional equipment needed to carry out the RDT include alcohol swabs; a sterile lancet for blood draw; gloves for the examiner; a timer or watch to keep time for the result read-out; a pen for marking RDT cassettes; a sharps disposal box and non-sharps bin; and results sheets.

The malaria RDT was conducted as instructed by the manufacturer, Figure 7-8(a) (ACCESSBIO, 2020) following WHO guidelines (Harvey and Bell, 2010). The RDT was removed from the packet and labelled with the patients ID and initials. Following standard procedure for extracting a blood sample by finger prick the sample transfer pipette was used to collect the blood sample from the puncture site and deposited into the square sample window 'A', ensuring that the sample was absorbed by the sample pad. The buffer (6

droplets) was then added to the circular buffer window 'B'. The LF devices were left for 15 minutes before determining the results. Refer to Figure 7-8(b) for a diagram of the interpretation of test the results. In order to provide a diagnosis there must be a visible line in the control compartment 'C', where this was not the case the test was marked as invalid and repeated. In addition to the control line a visible line in the 'T1' window suggest presence of *plasmodium falciparum* and 'T2' suggest a non-*falciparum* malaria infection. A test with a visible control line and no lines present in the test window indicates no *plasmodium* infection and the patient was recorded as negative for malaria infection by RDT.

### **7.7.3 The Kato-Katz method for detection of intestinal helminths**

The thick smear KK method requires stool collection pots; a nylon screen/ sieve (425 µm mesh); a flat spatula or wooden tongue depressor to conduct the faecal smear; a KK template which is a plastic template with 6 mm diameter hole; hydrophobic cellophane strips pre-soaked in malachite green solution; tweezers; microscope slides; and a microscope (Tankeshwar, 2016). Additionally, markers, pens and results forms were required for recording results. Scrap paper and newspaper was used to cover benchtops and work surfaces.

The KK technique was conducted by the MoH VCD healthcare workers following WHO guidelines (Genchi *et al.*, 2019). The KK equipment and method is depicted in Figure 4-5(a) and Figure 4-5(b-d) respectively. Microscope slides were arranged on the table and labelled with the sample numbers. A small portion from the faecal specimen was pushed through a fine sieve (Figure 4-5(b)). The KK template was placed on the centre of the microscope slide and the sieved sample was collected and transferred into the KK template using the wooden tongue depressor to produce the stool pellet (depicted in Figure 4-5(c)) of approximately 41.7 mg on the microscope slide (Genchi *et al.*, 2019). A second slide was made for each sample to allow double KK readings. This process was repeated with successive stool samples until the surface of the sieve was full after which it was washed and re-used. Meanwhile, the pre-soaked cellophane strips were removed from the malachite green solution and placed on top on the stool pellet (Figure 4-5(d)). The top of the cellophane strip was pressed to spread the faeces using a clean microscope slide to create a thin film on the microscope slide. The slides were left with the cellophane face-up for an hour to allow the liquid to evaporate and glycerol to clear the faeces.

The KK slides were examined under a compound microscope (made in Philippines; Model CX21FS1; Olympus Corporation) under 10X objective. The malachite green stain causes *S.*

*mansoni* eggs to appear slightly pink under the microscope (aiding distinguishing *S. mansoni* eggs within the stool sample). The *S. mansoni* eggs observed are counted to inform the intensity of *S. mansoni* infection, which is determined by the number of eggs present per gram of faecal matter (EPG). The egg count ‘EC’ was multiplied by 24 (see Equation 3 below) to provide a quantitative diagnosis (Genchi *et al.*, 2019). Additionally the technicians took note of other cross infections for district survey and treatment purposes, being out of the scope of our study this was not saved in our study records.

*Equation 3: Calculation to quantify intensity of helminth infection (X EPG) from egg count resulting from KK examination.*

$$\frac{\text{Egg Count}}{41.7 \text{ mg}} \cdot 24 = \frac{X}{1 \text{ g}}$$

#### **7.7.4 POC-CCA to detect *S. mansoni***

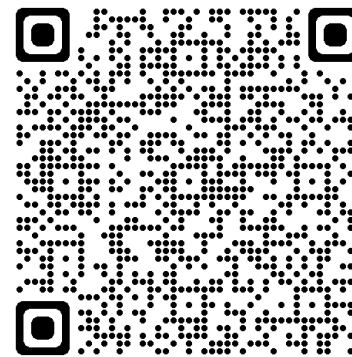
The POC-CCA test kit provides a pipette bulb to transfer the sample; the diagnostic cassette; and running buffer. Additional equipment required include a timer; gloves for the examiner; urine collection pots; and a pen and paper to mark samples pots, diagnostic cassettes and collect results.

The POC-CCA tests were run following the manufacturer’s instructions shown in Figure 7-9(a) (Rapid Medical Diagnostics, 2018). Urine samples were collected in clean sample collection pots, marked with unique ID number and initials. After the collection of samples the RDT cassette package was opened and marked with the corresponding sample number and initials. Using the pipette bulb provided in the kit, one drop of urine was transferred from the sample pot into the marked circular sample well on the cassette (see Figure 7-9). After the sample had absorbed entirely into the specimen pad a single drop of buffer was added to the well. The POC-CCA tests were left for 20 minutes before reading the results (Figure 7-9(c)). The results were interpreted using the manufacturer’s instructions in Figure 7-9(b). Two pink lines in the marked test ‘T’ and control ‘C’ sites suggest the presence of CCA in urine and therefore indicate presence of a schistosome infection (positive test result). Whereas a single red line in the control site ‘C’ indicates lack of CCA in the sample, indicating a negative test result. POC-CCA RDTs with a lack of visible line or a blue line in the control site ‘C’ are invalid (Rapid Medical Diagnostics, 2018) in these instances the cassette was discarded and the sample was re-run.

(a) ASSAY PROCEDURE:

(b) POSITIVE

[Images removed due to copyright restrictions]. The QR code links to the image sources.



- Read the result at **20 minutes**.
- Any results read after **25 minutes** should be considered **invalid** and must be repeated.

(Rapid Medical Diagnostics, 2018)



Figure 7-9: Bilharzia POC-CCA in the field. (a) The assay procedure, as supplied by the manufacturer. (b) Interpretation of results from the POC CCA cassette as published by the manufacturer (Rapid Medical Diagnostics, Pretoria, RSA). (c) Diagnostic cassettes after addition of urine samples; the cassettes were marked with patient unique ID number.

### 7.7.5 The *S. mansoni* hatching test

The hatching protocol follows the method precisely described by (Gower *et al.*, 2013). The materials required include sample pots; a fine mesh nylon screen/ sieve (425 µm mesh) to prepare the faecal sample; the ‘hatching set’ depicted in Figure 4-6(a) in Section 4.5.4.5 - two nylon nets with the mesh diameter of 200 µm and 41 µm (sourced from PlastOk, Merseyside, UK); multiple wash buckets; and a large quantity of locally sourced bottled water.

The left over stool sample (collected in the morning) was placed in a sample container. In the late afternoon the container was filled approximately to half way with locally sourced bottled water and shook to break up the faecal sample. The diluted faecal sample was sieved through a fine mesh sieve (425 µm) using a toothbrush prior to transfer into the hatching set. The sieved faecal sample was added into the inner hatching net. The inner mesh (see Figure 4-6(a)) was then filled with bottled water and shook to disperse the sample. Liquid expelled from the mesh was collected in the ‘dirty’ wash bucket (Figure 4-6(b)). The inner mesh collects any large debris (>200 µm) and the outer mesh collects ‘*S. mansoni* egg-sized’ debris. Smaller debris (<41 µm) was expelled from the mesh and collected in the ‘dirty’ bucket. The hatching nets were flushed thoroughly with water ensuring that the ‘*S. mansoni* egg sized debris’ were washed into the cap attached to the outer mesh. The volume of water required to complete the egg collection was dependent on the sample consistency, on average each sample required 2 L of bottled water. The ‘*S. mansoni* egg sized’ debris collected in the cap attached to the outer mesh was transferred into a clean sample container, and topped up approximately half way with bottled water. The hatching sieves were then washed in the ‘clean’ wash buckets to be re-used.

The containers containing ‘*S. mansoni* egg sized’ debris were left overnight with lids ajar and transferred into a petri dish the following morning. The petri dish were placed in direct sunlight for the morning to provide optimum hatching conditions (exposure to sunlight and warmth) (Gower *et al.*, 2013). Hatching of the *S. mansoni* ova generally began early in the afternoon. The miracidia were observed under a compound microscope (made in Philippines; Model CX21FS1; Olympus Corporation) samples which contain miracidia indicate the presence of a schistosome infection. In a few cases where KK returned a negative result, miracidia were observed by the hatching protocol, in such cases the patient record was amended and KK result was noted as a possible false-negative.



## 7.8 The multiplex malaria preliminary field trial

The preliminary field trial of the multiplex malaria cassette (originally developed by Dr Gaolian Xu) was undertaken in the Mayuge District (Uganda). The Paper Device was used to detect *plasmodium* DNA within a finger prick of patients' blood and differentiate between *plasmodium falciparum* and non-*falciparum* infections (Reboud *et al.*, 2018). The results from the preliminary multiplex malaria field trial (*plasmodium pan*) are displayed in Figure 7-10. Out of the total 59 samples, microscopy results suggested that 48 of the patients had malaria, however, the Paper Device suggested that 56 of the patients' blood samples contained plasmodium DNA. The confirmatory qPCR conducted on return to the laboratory in Glasgow agreed with the POC LAMP results. The sensitivity and specificity were calculated as described in Section 1.4.2 against the qPCR results.

N=59 blood samples processed on the Paper Device

### ***Plasmodium (Pan)***

N=59 samples for analysis against microscopy		
Paper Device	Microscopy	
	Positive	Negative
Positive	47	9
Negative	1	2

N=59 samples for analysis against qPCR		
Paper Device	qPCR	
	Positive	Negative
Positive	55	1
Negative	1	2

Sensitivity = 98 %, CI: 96.2-99.8  
Coincidence rate = 96 %, CI: 93.4-98.6

Figure 7-10: The results collected from the preliminary field trial for P.PAN reagents (Reboud *et al.*, 2018).

## Bibliography

- Abbasi, I. *et al.* (2010) 'Detection of *Schistosoma mansoni* and *Schistosoma haematobium* DNA by loop-mediated isothermal amplification: identification of infected snails from early prepatency.', *The American journal of tropical medicine and hygiene*. 83(2), pp. 427–32. doi: 10.4269/ajtmh.2010.09-0764.
- Abdulmawjood, A. *et al.* (2014) 'Development of Loop-Mediated Isothermal Amplification (LAMP) Assay for Rapid and Sensitive Identification of Ostrich Meat', *PLoS ONE*. 9(6), p. e100717. doi: 10.1371/journal.pone.0100717.
- ACCESSBIO (2020) *Products: Malaria CareStart (pf/pan)*. Available at: [http://www.accessbio.net/eng/products/products01\\_02.asp#this](http://www.accessbio.net/eng/products/products01_02.asp#this) (Accessed: 20 February 2020).
- Achee, N. L. *et al.* (2012) 'Spatial repellents: from discovery and development to evidence-based validation', *Malaria Journal*, 11(164), pp. 1–9. doi: 10.1186/1475-2875-11-164.
- Adriko, M. *et al.* (2014) 'Evaluation of circulating cathodic antigen (CCA) urine-cassette assay as a survey tool for *Schistosoma mansoni* in different transmission settings within Bugiri District, Uganda', *Acta Tropica*. 136(1), pp. 50–57. doi: 10.1016/j.actatropica.2014.04.001.
- Adriko, M. *et al.* (2018) 'Low Praziquantel Treatment Coverage for *Schistosoma mansoni* in Mayuge District, Uganda, Due to the Absence of Treatment Opportunities, Rather Than Systematic Non-Compliance', *Tropical Medicine and Infectious Disease*. 3(4), p. 111. doi: 10.3390/tropicalmed3040111.
- Ahlford, A. *et al.* (2010) 'Dried reagents for multiplex genotyping by tag-array minisequencing to be used in microfluidic devices †', *Analyst*, 135, pp. 2377–2385. doi: 10.1039/c0an00321b.
- Ahmed, H. A. *et al.* (2011) 'The best practice for preparation of samples from FTA® cards for diagnosis of blood borne infections using African trypanosomes as a model system', *Parasites & Vectors*. 4(1), p. 68. doi: 10.1186/1756-3305-4-68.
- Ahrberg, C. D. *et al.* (2016) 'Handheld Real-Time PCR Device', *Lab Chip*, 16(3), pp. 586–592. doi: 10.1039/c5lc01415h.

Ajibola, O. *et al.* (2018) 'Tools for Detection of Schistosomiasis in Resource Limited Settings', *Medical Sciences*. 6(2), p. 39. doi: 10.3390/medsci6020039.

Al-Shehri, H. *et al.* (2018) 'Surveillance of intestinal schistosomiasis during control: a comparison of four diagnostic tests across five Ugandan primary schools in the Lake Albert region', *Parasitology*, 1–8. doi: 10.1017/S003118201800029X.

Al-Soud, W. A. and Rådström, P. (2001) 'Purification and characterization of PCR-inhibitory components in blood cells.', *Journal of clinical microbiology*. 39(2), pp. 485–93. doi: 10.1128/JCM.39.2.485-493.2001.

Alemayehu, S. *et al.* (2013) 'Comparative evaluation of published real-time PCR assays for the detection of malaria following MIQE guidelines', *Malaria Journal*, 12(1), pp. 1–8. doi: 10.1186/1475-2875-12-277.

Alere (2016) *SD BIOLINE Malaria Ag RDT Series : Portfolio of SD Malaria RDTs for Detection of Malaria Antigens*.

Ali, N. *et al.* (2017) 'Current Nucleic Acid Extraction Methods and Their Implications to Point-of-Care Diagnostics.', *BioMed research international*. 2017, p. 9306564. doi: 10.1155/2017/9306564.

Altaras, R. *et al.* (2016) 'Why do health workers give anti-malarials to patients with negative rapid test results? A qualitative study at rural health facilities in western Uganda.', *Malaria Journal*. 15, pp. 1–14. doi: 10.1186/s12936-015-1020-9.

Anderson, L. *et al.* (2015) 'Schistosoma mansoni Egg, Adult Male and Female Comparative Gene Expression Analysis and Identification of Novel Genes by RNA-Seq', *PLoS Neglected Tropical Diseases*, 9(12), pp. 1–26. doi: 10.1371/journal.pntd.0004334.

Applied Biosystems (2010) *7500/7500 Fast Real-Time PCR System Relative Standard Curve and Comparative C T Experiments Getting Started Guide*. Available at: <https://assets.thermofisher.com/TFS-Assets/LSG/manuals/4387783c.pdf> (Accessed: 13 March 2020).

Applied Biosystems (2011) *Real-time PCR: Understanding Ct*. Available at: [http://www3.appliedbiosystems.com/cms/groups/mcb\\_marketing/documents/generaldocuments/cms\\_053906.pdf](http://www3.appliedbiosystems.com/cms/groups/mcb_marketing/documents/generaldocuments/cms_053906.pdf) (Accessed: 11 May 2018).

- Ashley, E. A., Pyae Phyo, A. and Woodrow, C. J. (2018) 'Malaria', *The Lancet*. pp. 1608–1621. doi: 10.1016/S0140-6736(18)30324-6.
- Babonneau, J. *et al.* (2015) 'Development of a dry-reagent-based qPCR to facilitate the diagnosis of *Mycobacterium ulcerans* infection in endemic countries.', *PLoS neglected tropical diseases*. 9(4), p. e0003606. doi: 10.1371/journal.pntd.0003606.
- Barbosa, C. *et al.* (2015) *DNA extraction: Finding the most suitable method, Molecular Microbial Diagnostic Methods: Pathways to Implementation for the Food and Water Industries*. doi: 10.1016/B978-0-12-416999-9.00007-1.
- Barda, B. *et al.* (2013) 'Mini-FLOTAC and Kato-Katz: helminth eggs watching on the shore of Lake Victoria.', *Parasites & vectors*, 6(1), p. 220. doi: 10.1186/1756-3305-6-220.
- Barda, B. *et al.* (2015) 'How Long Can Stool Samples Be Fixed for an Accurate Diagnosis of Soil-Transmitted Helminth Infection Using Mini-FLOTAC?', *PLoS Neglected Tropical Diseases*, 9(4), pp. 1–13. doi: 10.1371/journal.pntd.0003698.
- Barda, B. D. *et al.* (2013) 'Mini-FLOTAC, an Innovative Direct Diagnostic Technique for Intestinal Parasitic Infections: Experience from the Field', *PLoS Neglected Tropical Diseases*, 7(8). doi: 10.1371/journal.pntd.0002344.
- Becker, S. *et al.* (2004) 'Real-time PCR for detection of *Trypanosoma brucei* in human blood samples', *Diagnostic Microbiology and Infectious Disease*, 50, pp. 193–199. doi: 10.1016/j.diagmicrobio.2004.07.001.
- Becker, S. L. *et al.* (2011) 'Comparison of the Flotac-400 dual technique and the formalin-ether concentration technique for diagnosis of human intestinal protozoan infection', *Journal of Clinical Microbiology*, 49(6), pp. 2183–2190. doi: 10.1128/JCM.01035-10.
- Bell, D., Wongsrichanalai, C. and Barnwell, J. W. (2006) 'Ensuring quality and access for malaria diagnosis: how can it be achieved?', *Nature Reviews*, pp. 7–20. doi: 10.1038/nrmicro1525.
- Beltrame, A. *et al.* (2017) 'Accuracy of parasitological and immunological tests for the screening of human schistosomiasis in immigrants and refugees from African countries: An approach with Latent Class Analysis', *PLOS Neglected Tropical Diseases*. 11(6), pp. 1–15. doi: 10.1371/journal.pntd.0005593.

Berensmeier, S. (2006) 'Magnetic particles for the separation and purification of nucleic acids', *Applied Microbiology and Biotechnology*. pp. 495–504. doi: 10.1007/s00253-006-0675-0.

Bergquist, R., Utzinger, J. and Keiser, J. (2017) 'Controlling schistosomiasis with praziquantel: How much longer without a viable alternative?', *Infectious Diseases of Poverty*, 74(6). doi: 10.1186/s40249-017-0286-2.

Berzosa, P. *et al.* (2018) 'Comparison of three diagnostic methods (microscopy, RDT, and PCR) for the detection of malaria parasites in representative samples from Equatorial Guinea 11 Medical and Health Sciences 1108 Medical Microbiology', *Malaria Journal*. 17(1). doi: 10.1186/s12936-018-2481-4.

Biassoni, R. and Raso, A. (2020) *Quantitative Real-Time PCR Methods and Protocols*. 2nd edn. Edited by R. Biassoni and A. Raso. Springer Nature. Available at: <http://www.springer.com/series/7651> (Accessed: 30 March 2020).

Bogoch, I. I. *et al.* (2017) 'Evaluation of a mobile phone-based microscope for screening of *Schistosoma haematobium* infection in rural Ghana', *American Journal of Tropical Medicine and Hygiene*, 96(6), pp. 1468–1471. doi: 10.4269/ajtmh.16-0912.

Borges, D. S. *et al.* (2013) 'Seeding experiments demonstrate poor performance of the hatching test for detecting small numbers of *Schistosoma mansoni* eggs in feces', *Parasitology International*. 62(6), pp. 543–547. doi: 10.1016/j.parint.2013.08.002.

Boyce, M. R. and O'meara, W. P. (2017) 'Use of malaria RDTs in various health contexts across sub-Saharan Africa: a systematic review', *BMC Public Health*, 17(470). doi: 10.1186/s12889-017-4398-1.

Brivio, M. *et al.* (2007) 'A simple and efficient method for on-chip storage of reagents: Towards lab-on-a-chip systems for point-of-care DNA diagnostics', *11th International Conference on Miniaturized Systems for Chemistry and Life Sciences 2007, MicroTAS 2007*, pp. 59–61.

Van den Broeck, F. *et al.* (2011) 'Optimal sample storage and extraction protocols for reliable multilocus genotyping of the human parasite *Schistosoma mansoni*', *Infection, Genetics and Evolution*. 11(6), pp. 1413–1418. doi: 10.1016/j.meegid.2011.05.006.

Brunker, K. *et al.* (2020) ‘Rapid in-country sequencing of whole virus genomes to inform rabies elimination programmes.’ Wellcome Open Research. 2020; 5: 3. doi: 10.12688/wellcomeopenres.15518.1.

Bujang, M. A. and Adnan, T. H. (2016) ‘Requirements for Minimum Sample Size for Sensitivity and Specificity Analysis’, *Journal of Clinical and Diagnostic Research*. 10(10), pp. 1–6. doi: 10.7860/JCDR/2016/18129.8744

Caliendo, A. M. *et al.* (2013) ‘Better tests, better care: improved diagnostics for infectious diseases.’, *Clinical infectious diseases*, 57(S3), pp. 139–170. doi: 10.1093/cid/cit578.

Capitán-Vallvey, L. F. *et al.* (2015) ‘Recent developments in computer vision-based analytical chemistry: A tutorial review’, *Analytica Chimica Acta*. 899 pp. 23–56. doi: 10.1016/j.aca.2015.10.009.

Carter, C. *et al.* (2017) ‘Lyophilized visually readable loop-mediated isothermal reverse transcriptase nucleic acid amplification test for detection Ebola Zaire RNA’, *Journal of Virological Methods*. 244, pp. 32–38. doi: 10.1016/j.jviromet.2017.02.013.

Carter, M. and Shieh, J. C. (2010) ‘Molecular Cloning and Recombinant DNA Technology’, in *Guide to Research Techniques in Neuroscience*. pp. 207–227. doi: 10.1016/b978-0-12-374849-2.00009-4.

Cavalcanti, M. G. *et al.* (2013) ‘Schistosomiasis in areas of low endemicity: A new era in diagnosis.’, *Trends in Parasitology*. 29 (2), pp. 75-82. doi: 10.1016/j.pt.2012.11.003.

CDC (2019a) *About Malaria - Disease*. Available at: <https://www.cdc.gov/malaria/about/disease.html> (Accessed: 4 May 2020).

CDC (2019b) *CDC - Schistosomiasis - Biology*. Available at: <https://www.cdc.gov/parasites/schistosomiasis/biology.html> (Accessed: 5 May 2020).

CDC (2019c) *Treatment of Malaria (Guidelines for Clinicians)*. Available at: <http://www.cdc.gov/malaria/resources/pdf/treatmenttable.pdf> (Accessed: 13 May 2020).

CDC (2020) *Malaria’s Impact Worldwide*. Available at: [https://www.cdc.gov/malaria/malaria\\_worldwide/impact.html](https://www.cdc.gov/malaria/malaria_worldwide/impact.html) (Accessed: 4 May 2020).

Centers for Disease Control and Prevention (2016) *Blood Specimens - Detection of parasite*

*Antigens.* Available at: <https://www.cdc.gov/dpdx/diagnosticprocedures/blood/antigendetection.html> (Accessed: 17 August 2020).

Charlot, B. *et al.* (2017) ‘PLL-FITC fluorescence thermography on dry surfaces’, in *Symposium on Design, Test, Integration and Packaging of MEMS/MOEMS, DTIP 2017*. doi: 10.1109/DTIP.2017.7984505.

Cheever, A. W. and Duvall, R. H. (1974) ‘Single and repeated infections of grivet monkeys with *Schistosoma mansoni*: parasitological and pathological observations over a 31 month period’, *American Journal of Tropical Medicine and Hygiene*. 23(5), pp. 884–894. doi: 10.4269/ajtmh.1974.23.884.

Chen, C. *et al.* (2017) ‘A self-contained microfluidic in-gel loop-mediated isothermal amplification for multiplexed pathogen detection’, *Sensors and Actuators B: Chemical*. 239, pp. 1–8. doi: 10.1016/J.SNB.2016.07.164.

Chen, D. *et al.* (2010) ‘An integrated, self-contained microfluidic cassette for isolation, amplification, and detection of nucleic acids’, *Biomedical Microdevices*. 12(4), pp. 705–719. doi: 10.1007/s10544-010-9423-4.

Chen, H.-W. and Ching, W.-M. (2017) ‘Evaluation of the stability of lyophilized loop-mediated isothermal amplification reagents for the detection of *Coxiella burnetii*’, *Heliyon*, 3, p. 415. doi: 10.1016/j.heliyon.2017.

Choi, J. R. *et al.* (2016) ‘An integrated paper-based sample-to-answer biosensor for nucleic acid testing at the point of care’, *Lab on a Chip*. 16(3), pp. 611–621. doi: 10.1039/C5LC01388G.

Cioli, D. *et al.* (2014) ‘Schistosomiasis control: Praziquantel forever?’, *Molecular and Biochemical Parasitology*. 195(1), pp. 23–29. doi: 10.1016/j.molbiopara.2014.06.002.

Cnops, L. *et al.* (2011) ‘Rapid diagnostic tests as a source of DNA for *Plasmodium* species-specific real-time PCR’, *Malaria Journal*. 10(1), p. 67. doi: 10.1186/1475-2875-10-67.

Colley, D. G. *et al.* (2013) ‘A five-country evaluation of a point-of-care circulating cathodic antigen urine assay for the prevalence of *Schistosoma mansoni*’, *American Journal of Tropical Medicine and Hygiene*, 88(3), pp. 426–432. doi: 10.4269/ajtmh.12-0639.

Connelly, John T., Rolland, J. P. and Whitesides, G. M. (2015) “‘Paper Machine’ for Molecular Diagnostics”, *Analytical Chemistry*. 87(15), pp. 7595–7601. doi: 10.1021/acs.analchem.5b00411.

Cook, J. *et al.* (2015) ‘Loop-mediated isothermal amplification (LAMP) for point-of-care detection of asymptomatic low-density malaria parasite carriers in Zanzibar’, *Malaria Journal*, 14(1), p. 43. doi: 10.1186/s12936-015-0573-y.

Corstjens, P. L. A. M. *et al.* (2014) ‘Tools for diagnosis, monitoring and screening of *Schistosoma* infections utilizing lateral-flow based assays and upconverting phosphor labels.’, *Parasitology*, 141(14), pp. 1841–55. doi: 10.1017/S0031182014000626.

Coulibaly, J. T., Ouattara, M., D’Ambrosio, M. V., *et al.* (2016) ‘Accuracy of Mobile Phone and Handheld Light Microscopy for the Diagnosis of Schistosomiasis and Intestinal Protozoa Infections in Côte d’Ivoire’, *PLoS Neglected Tropical Diseases*, 10(6), pp. 1–10. doi: 10.1371/journal.pntd.0004768.

Coulibaly, J. T., Ouattara, M., Keiser, J., *et al.* (2016) ‘Evaluation of malaria diagnoses using a handheld light microscope in a community-based setting in rural Côte d’Ivoire’, *American Journal of Tropical Medicine and Hygiene*, 95(4), pp. 831–834. doi: 10.4269/ajtmh.16-0328.

Crellen, T. *et al.* (2016) ‘Reduced Efficacy of Praziquantel Against *Schistosoma mansoni* Is Associated With Multiple Rounds of Mass Drug Administration’, *Clinical Infectious Diseases*, p. ciw506. doi: 10.1093/cid/ciw506.

Cringoli, G. *et al.* (2017) ‘The Mini-FLOTAC technique for the diagnosis of helminth and protozoan infections in humans and animals’, *Nature Protocols*. 12(9), pp. 1723–1732. doi: 10.1038/nprot.2017.067.

Crutcher, J. and Hoffman, S. (1996) *Chapter 83: Malaria, Medical Microbiology 4th edition*. Available at: <https://www.ncbi.nlm.nih.gov/books/NBK8584/> (Accessed: 4 May 2020).

Cui, L. *et al.* (2012) ‘Detection of Severe Fever with Thrombocytopenia Syndrome Virus by Reverse Transcription-Cross-Priming Amplification Coupled with Vertical Flow Visualization’. *Journal of Clinical Microbiology*. 50(12), pp. 3881–3885. doi: 10.1128/JCM.01931-12.



Dacey, J. (2020) *Cooking with the Sun*, *Physics World*. Available at: <https://physicsworld.com/a/cooking-with-the-sun/> (Accessed: 6 January 2021).

Das, A. *et al.* (2006) 'Development of an Internal Positive Control for Rapid Diagnosis of Avian Influenza Virus Infections by Real-Time Reverse Transcription-PCR with Lyophilized Reagents', *Journal of Clinical Microbiology*, 44(9), pp. 3065–3073. doi: 10.1128/JCM.00639-06.

Diallo, M. A. *et al.* (2017) 'Evaluation of CareStart™ Malaria HRP2/pLDH (Pf/pan) Combo Test in a malaria low transmission region of Senegal', *Malaria Journal*. 16(1), p. 328. doi: 10.1186/s12936-017-1980-z.

Doenhoff, M. J., Chiodini, P. L. and Hamilton, J. V. (2004) 'Specific and sensitive diagnosis of schistosome infection: Can it be done with antibodies?', *Trends in Parasitology*, 20(1), pp. 35–39. doi: 10.1016/j.pt.2003.10.019.

Drain, P. K. *et al.* (2014) 'Diagnostic point-of-care tests in resource-limited settings.', *The Lancet. Infectious diseases*. 14(3), pp. 239–49. doi: 10.1016/S1473-3099(13)70250-0.

Dwight, Z., Palais, R. and Wittwer, C. T. (2011) 'uMELT: prediction of high-resolution melting curves and dynamic melting profiles of PCR products in a rich web application', *Bioinformatics*. 27(7), pp. 1019–1020. doi: 10.1093/bioinformatics/btr065.

Edwards, T. *et al.* (2014) 'Loop-mediated isothermal amplification test for detection of neisseria gonorrhoeae in urine samples and tolerance of the assay to the presence of urea', *Journal of Clinical Microbiology*. 52(6), pp. 2163–2165. doi: 10.1128/JCM.00314-14.

Engel, N. *et al.* (2016) 'Addressing the challenges of diagnostics demand and supply: insights from an online global health discussion platform', *Global Health*, 1, p. 132. doi: 10.1136/bmjgh-2016-000132.

Enk, M. J., Oliveira e Silva, G. and Rodrigues, N. B. (2012) 'Diagnostic accuracy and applicability of a PCR system for the detection of *Schistosoma mansoni* DNA in human urine samples from an endemic area.', *PloS one*. 7(6), p. e38947. doi: 10.1371/journal.pone.0038947.

Farrar, J. S. and Wittwer, C. T. (2017) 'High-Resolution Melting Curve Analysis for Molecular Diagnostics', in *Molecular Diagnostics: Third Edition*. pp. 79–102. doi:

10.1016/B978-0-12-802971-8.00006-7.

Faust, C. L. *et al.* (2020) 'Harnessing technology and portability to conduct molecular epidemiology of endemic pathogens in resource-limited settings', *Transactions of The Royal Society of Tropical Medicine and Hygiene*. 0, pp. 1–3. doi: 10.1093/trstmh/traa086.

Favero, V. *et al.* (2017) 'Optimization of the Helmintex method for schistosomiasis diagnosis', *Experimental Parasitology*. 177, pp. 28–34. doi: 10.1016/j.exppara.2017.04.001.

Fernández-Soto, P. *et al.* (2014) 'A Loop-Mediated Isothermal Amplification (LAMP) Assay for Early Detection of *Schistosoma mansoni* in Stool Samples: A Diagnostic Approach in a Murine Model', *PLoS Neglected Tropical Diseases*. 8(9), p. e3126. doi: 10.1371/journal.pntd.0003126.

Fernández-Soto, P. *et al.* (2019) 'Detection of *Schistosoma mansoni*-derived DNA in human urine samples by loop-mediated isothermal amplification (LAMP)', *PLOS ONE*. 14(3), p. e0214125. doi: 10.1371/journal.pone.0214125.

Ferreira, F. T. *et al.* (2017) 'Sensitivity and specificity of the circulating cathodic antigen rapid urine test in the diagnosis of schistosomiasis mansoni infection and evaluation of morbidity in a low-endemic area in Brazil', *Revista da Sociedade Brasileira de Medicina Tropical*. 50(3), pp. 358–364. doi: 10.1590/0037-8682-0423-2016.

Fleischer, B. (2004) 'Editorial: 100 years ago: Giemsa's solution for staining of plasmodia', *Tropical Medicine and International Health*. 9(7), pp. 755–756. doi: 10.1111/j.1365-3156.2004.01278.x.

Foo, K. T. *et al.* (2015) 'Evaluation of point-of-contact circulating cathodic antigen assays for the detection of *Schistosoma mansoni* infection in low-, moderate-, and high-prevalence schools in western Kenya', *American Journal of Tropical Medicine and Hygiene*, 92(6), pp. 1227–1232. doi: 10.4269/ajtmh.14-0643.

Fowler, V. L. *et al.* (2020) 'A highly effective reverse-transcription loop-mediated isothermal amplification (RT-LAMP) assay for the rapid detection of SARS-CoV-2 infection', *Journal of Infection*. doi: 10.1016/j.jinf.2020.10.039.

Fuss, A. *et al.* (2018) 'Comparison of sensitivity and specificity of three diagnostic tests to detect *Schistosoma mansoni* infections in school children in Mwanza region, Tanzania',

*PLoS ONE*. 13(8). doi: 10.1371/journal.pone.0202499.

Gadkar, V. J. *et al.* (2018) ‘Real-time Detection and Monitoring of Loop Mediated Amplification (LAMP) Reaction Using Self-quenching and De-quenching Fluorogenic Probes’, *Scientific Reports*. 8(1), pp. 1–10. doi: 10.1038/s41598-018-23930-1.

Gandasegui, J. *et al.* (2016) ‘Biompha-LAMP: A New Rapid Loop-Mediated Isothermal Amplification Assay for Detecting *Schistosoma mansoni* in *Biomphalaria glabrata* Snail Host’, *PLOS Neglected Tropical Diseases*. 10(12), p. e0005225. doi: 10.1371/journal.pntd.0005225.

Gandasegui, J., Fernández-Soto, P., Muro, A., *et al.* (2018) ‘A field survey using LAMP assay for detection of *Schistosoma mansoni* in a low-transmission area of schistosomiasis in Umbuzeiro, Brazil: Assessment in human and snail samples’, *PLOS Neglected Tropical Diseases*. doi: <https://doi.org/10.1371/journal.pntd.0006314>.

Gandasegui, J., Fernández-Soto, P., Dacal, E., *et al.* (2018) ‘Field and laboratory comparative evaluation of a LAMP assay for the diagnosis of urogenital schistosomiasis in Cubal, Central Angola’, *Tropical Medicine & International Health*. 23(9), pp. 992–1001. doi: 10.1111/tmi.13117.

García-Bernalt Diego, J. *et al.* (2019) ‘Progress in loop-mediated isothermal amplification assay for detection of *Schistosoma mansoni* DNA: towards a ready-to-use test’, *Scientific Reports*. 9(1), pp. 1–11. doi: 10.1038/s41598-019-51342-2.

GE Healthcare (2019) *Point of Care Ultrasound*. Available at: <https://www.gehealthcare.com/products/ultrasound/point-of-care-ultrasound> (Accessed: 14 May 2020).

Genchi, M. *et al.* (2019) *Bench aids for the diagnosis of intestinal parasites*. second. World Health Organization.

Glinz, D. *et al.* (2010) ‘Comparing diagnostic accuracy of Kato-Katz, Koga Agar Plate, Ether-Concentration, and FLOTAC for *Schistosoma mansoni* and Soil-transmitted helminths’, *PLoS Neglected Tropical Diseases*, 4(7). doi: 10.1371/journal.pntd.0000754.

González-González, E. *et al.* (2019) ‘Validation of use of the miniPCR thermocycler for Ebola and Zika virus detection’, *PLoS ONE*, 14(5), pp. 13–16. doi:

10.1371/journal.pone.0215642.

Govindarajan, A. V *et al.* (2012) ‘A low cost point-of-care viscous sample preparation device for molecular diagnosis in the developing world; an example of microfluidic origami †’, *Lab Chip*, 12, pp. 174–181. doi: 10.1039/c1lc20622b.

Gower, C. M. *et al.* (2013) ‘Population genetic structure of *Schistosoma mansoni* and *Schistosoma haematobium* from across six sub-Saharan African countries: Implications for epidemiology, evolution and control’, *Acta Tropica*. 128(2), pp. 261–274. doi: 10.1016/j.actatropica.2012.09.014.

Gray, D. J. *et al.* (2011) ‘Diagnosis and management of schistosomiasis’, *BMJ (Clinical research ed.)*, 342(May), p. d2651. doi: 10.1136/bmj.d2651.

Gryseels, B. *et al.* (2006) ‘Human schistosomiasis’, *Lancet*, 368(9541), pp. 1106–1118. doi: 10.1016/S0140-6736(06)69440-3.

Gryseels, B. and Strickland, T. G. (2013) ‘Trematode Infections - Schistosomiasis ’, in *Hunter’s Tropical Medicine and Emerging Infectious Disease*. 9th edn, pp. 867–883.

Gumus, A. *et al.* (2016) ‘Solar-thermal complex sample processing for nucleic acid based diagnostics in limited resource settings.’, *Biomedical optics express*, 7(5), pp. 1974–84. doi: 10.1364/BOE.7.001974.

Hamburger, J. *et al.* (1991) ‘Highly repeated short DNA sequences in the genome of *Schistosoma mansoni* recognized by a species-specific probe’, *Molecular and Biochemical Parasitology*, 44, pp. 73–80. Available at: [https://ac.els-cdn.com/016668519190222R/1-s2.0-016668519190222R-main.pdf?\\_tid=6a40ab31-a7df-4c29-9abc-926990f91624&acdnat=1530803468\\_9b5b7f9381140cc16abb6a604faf6a92](https://ac.els-cdn.com/016668519190222R/1-s2.0-016668519190222R-main.pdf?_tid=6a40ab31-a7df-4c29-9abc-926990f91624&acdnat=1530803468_9b5b7f9381140cc16abb6a604faf6a92) (Accessed: 5 July 2018).

Hardinge, P. and Murray, J. A. H. (2019) ‘Reduced False Positives and Improved Reporting of Loop-Mediated Isothermal Amplification using Quenched Fluorescent Primers’, *Scientific Reports*. 9(1), pp. 1–13. doi: 10.1038/s41598-019-43817-z.

Harvey, S. A. and Bell, D. (2010) *How To Use A Rapid Diagnostic Test*. 1.2. doi: 10.1136/adc.61.1.11.

Heid, C. A. *et al.* (1996) 'Real time quantitative PCR', *Genome Research*. 6(10), pp. 986–994. doi: 10.1101/gr.6.10.986.

Higuchi, R. *et al.* (1993) *Kinetic PCR Analysis: Real-time Monitoring of DNA Amplification Reactions*. Available at: <http://www.nature.com/naturebiotechnology> (Accessed: 30 March 2020).

Hopkins, H. *et al.* (2013) 'Highly Sensitive Detection of Malaria Parasitemia in a Malaria-Endemic Setting: Performance of a New Loop-Mediated Isothermal Amplification Kit in a Remote Clinic in Uganda', *The Journal of Infectious Diseases*, 208, pp. 645–652. doi: 10.1093/infdis/jit184.

Ibironke, O. A. *et al.* (2011) 'Diagnosis of *Schistosoma haematobium* by Detection of Specific DNA Fragments from Filtered Urine Samples', *Am. J. Trop. Med. Hyg.*, 84(6), pp. 998–1001. doi: 10.4269/ajtmh.2011.10-0691.

Jangam, S. R. *et al.* (2013) 'A point-of-care PCR test for HIV-1 detection in resource-limited settings', *Biosensors and Bioelectronics*. 42, pp. 69–75. doi: 10.1016/J.BIOS.2012.10.024.

Jiang, L. *et al.* (2014) 'Solar thermal polymerase chain reaction for smartphone-assisted molecular diagnostics', *Scientific Reports*. 4(1), pp. 1–5. doi: 10.1038/srep04137.

Johannes Enk, M. *et al.* (2012) 'Diagnostic Accuracy and Applicability of a PCR System for the Detection of *Schistosoma mansoni* DNA in Human Urine Samples from an Endemic Area'. *PLoS ONE*. 7(6). doi: 10.1371/journal.pone.0038947.

Kabatereine, N. B. *et al.* (2011) 'Integrated prevalence mapping of schistosomiasis, soil-transmitted helminthiasis and malaria in lakeside and island communities in Lake Victoria, Uganda', *Parasites & Vectors*, 4(232). doi: 10.1186/1756-3305-4-232.

Kamau, E. *et al.* (2014) *Sample-ready multiplex qPCR assay for detection of malaria*. Available at: <http://www.malariajournal.com/content/13/1/158> (Accessed: 2 July 2020).

Kassim, O. and Gibertson, D. E. (1976) 'Hatching of *Schistosoma mansoni* eggs and observations on motility of miracidia ', *J Parasitol* , 62(5), pp. 715–720. Available at: <https://pubmed.ncbi.nlm.nih.gov/988153/> (Accessed: 31 August 2020).

Katevatis, C., Fan, A. and Klapperich, C. M. (2017) 'Low concentration DNA extraction

and recovery using a silica solid phase’, *PLoS ONE*, 12(5), p. e0176848. doi: 10.1371/journal.pone.0176848.

Kato-Hayashi, N. *et al.* (2015) ‘Detection of active schistosome infection by cell-free circulating DNA of *Schistosoma japonicum* in highly endemic areas in Sorsogon Province, the Philippines’, *Acta Tropica*. 141(Part B), pp. 178–183. doi: 10.1016/j.actatropica.2014.05.003.

Kim, J. *et al.* (2009) ‘A disposable, self-contained PCR chip.’, *Lab on a chip*. 9(4), pp. 606–12. doi: 10.1039/b807915c.

Kimani, F. W. *et al.* (2017) ‘Rethinking the Design of Low-Cost Point-of-Care Diagnostic Devices.’, *Micromachines*. 8(11). doi: 10.3390/mi8110317.

Kirunga Tashobya, C., Ssenkooba, F. and Cruz, O. (2006) *Health Systems Reforms in Uganda: Processes and Outputs*. Health Systems Development Programme, London School of Hygiene & Tropical Medicine, UK. ISBN: 0 902657 77 1.

Kittur, N. *et al.* (2016) ‘Comparison of *Schistosoma mansoni* Prevalence and Intensity of Infection, as Determined by the Circulating Cathodic Antigen Urine Assay or by the Kato-Katz Fecal Assay: A Systematic Review’, *Am. J. Trop. Med. Hyg*, 94(3), pp. 605–610. doi: 10.4269/ajtmh.15-0725.

Klatser, P. R. *et al.* (1998) ‘Stabilized, freeze-dried PCR mix for detection of mycobacteria’, *Journal of Clinical Microbiology*, 36(6), pp. 1798–1800.

Koetsier, G., Cantor, E. and New England BioLabs (2019) *A Practical Guide to Analyzing Nucleic Acid Concentration and Purity with Microvolume Spectrophotometers*. Available at: <https://www.bioke.com/support/appnotes/1345/a-practical-guide-to-analyzing-nucleic-acid-concentration-and-purity-with-microvolume-spectrophotometers.html> (Accessed: 2 September 2020).

Lalkhen, A. G. and McCluskey, A. (2008) ‘Clinical tests: Sensitivity and specificity’, *Continuing Education in Anaesthesia, Critical Care and Pain*, 8(6), pp. 221–223. doi: 10.1093/bjaceaccp/mkn041.

Lamberton, P. H. L. *et al.* (2010) ‘In Vitro Praziquantel Test Capable of Detecting Reduced In Vivo Efficacy in *Schistosoma mansoni* Human Infections’, *Am J. Trop. Med. Hyg*. 83(6),

pp. 1340–1347. doi: 10.4269/ajtmh.2010.10-0413.

Lamberton, P. H. L. *et al.* (2014) ‘Sensitivity and Specificity of Multiple Kato-Katz Thick Smears and a Circulating Cathodic Antigen Test for *Schistosoma mansoni* Diagnosis Pre- and Post-repeated- Praziquantel Treatment’, *PLoS Negl Trop Dis*, 8(9). doi: 10.1371/journal.pntd.0003139.

Lamberton, P. H. L. *et al.* (2015) *Modelling the Effects of Mass Drug Administration on the Molecular Epidemiology of Schistosomes*, *Advances in Parasitology*. 87 doi: 10.1016/bs.apar.2014.12.006.

Lamberton, P. H. L., Faust, C. L. and Webster, J. P. (2017) ‘Praziquantel decreases fecundity in *Schistosoma mansoni* adult worms that survive treatment: evidence from a study’, *Infectious Diseases of Poverty*. *Infectious Diseases of Poverty*, 6(110), pp. 1–11. doi: 10.1186/s40249-017-0324-0.

Lee, P. Y. *et al.* (2012) ‘Agarose gel electrophoresis for the separation of DNA fragments’, *Journal of Visualized Experiments*. *Journal of Visualized Experiments*, (62). doi: 10.3791/3923.

Legesse, M. and Erko, B. (2007) ‘Field-based evaluation of a reagent strip test for diagnosis of *Schistosoma mansoni* by detecting circulating cathodic antigen in urine before and after chemotherapy’, *Transactions of the Royal Society of Tropical Medicine and Hygiene*, 101(7), pp. 668–673. doi: 10.1016/j.trstmh.2006.11.009.

Li, H. and Steckl, A. J. (2019) ‘Paper Microfluidics for Point-of-Care Blood-Based Analysis and Diagnostics’, *Analytical Chemistry*, 91(1), pp. 352–371. doi: 10.1021/acs.analchem.8b03636.

Li, S. *et al.* (2016) ‘Loop-mediated isothermal amplification (LAMP): Real-time methods for the detection of the survivin gene in cancer cells’, *Analytical Methods*. 8(33), pp. 6277–6283. doi: 10.1039/c6ay01943a.

Li, Y. *et al.* (2017) ‘Loop-mediated isothermal amplification (LAMP): A novel rapid detection platform for pathogens’, *Microbial Pathogenesis*. 107, pp. 54–61. doi: 10.1016/j.micpath.2017.03.016.

van Lieshout, L. *et al.* (1997) ‘Detection of the circulating antigens CAA and CCA in a

group of Dutch travellers with acute schistosomiasis.’, *Tropical medicine & international health : TM & IH*, 2(june), pp. 551–557. doi: 10.1046/j.1365-3156.1997.d01-324.x.

Lim Chua, A. *et al.* (2011) ‘Development of a dry reagent-based triplex PCR for the detection of toxigenic and non-toxigenic *Vibrio cholerae*’, *Journal of Medical Microbiology*. 60, pp. 481-485. doi: 10.1099/jmm.0.027433-0.

Lim, J. *et al.* (2019) ‘Battery-operated portable PCR system with enhanced stability of Pt RTD’, *PLoS ONE*, 14(6). doi: 10.1371/journal.pone.0218571.

Lindholz, C. G. *et al.* (2018) ‘Study of diagnostic accuracy of Helmintex, Kato-Katz, and POC-CCA methods for diagnosing intestinal schistosomiasis in Candéal, a low intensity transmission area in northeastern Brazil’, *PLoS Neglected Tropical Diseases*, 12(3), pp. 1–16. doi: 10.1371/journal.pntd.0006274.

Liu, W.-T. *et al.* (2005) ‘Emission Characteristics of Fluorescent Labels with Respect to Temperature Changes and Subsequent Effects on DNA Microchip Studies’, *Applied and Environmental Microbiology*, 71(10), pp. 6453–6457. doi: 10.1128/AEM.71.10.6453-6457.2005.

Lodh, N. *et al.* (2013) ‘Diagnosis of *Schistosoma mansoni* without the Stool: Comparison of Three Diagnostic Tests to Detect *Schistosoma mansoni* Infection from Filtered Urine in Zambia’, *Am. J. Trop. Med. Hyg*, 89(1), pp. 46–50. doi: 10.4269/ajtmh.13-0104.

Luchavez, J. *et al.* (2007) ‘An assessment of various blood collection and transfer methods used for malaria rapid diagnostic tests’, *Malaria Journal*, 6(1), p. 149. doi: 10.1186/1475-2875-6-149.

Magro, L., Jacquelin, B., *et al.* (2017) ‘Paper-based RNA detection and multiplexed analysis for Ebola virus diagnostics’, *Scientific Reports*. 7(1), p. 1347. doi: 10.1038/s41598-017-00758-9.

Magro, L., Escadafal, C., *et al.* (2017) ‘Paper microfluidics for nucleic acid amplification testing (NAAT) of infectious diseases’, *Lab on a Chip*. 17(14), pp. 2347–2371. doi: 10.1039/C7LC00013H.

Manage, D. P. *et al.* (2013) ‘An enclosed in-gel PCR amplification cassette with multi-target, multi-sample detection for platform molecular diagnostics’, *Lab on a Chip*, 13, p. 2576. doi:



10.1039/c3lc41419a.

Mark, D. *et al.* (2010) 'Microfluidic lab-on-a-chip platforms: requirements, characteristics and applications', *Chemical Society Reviews*. 39(3), p. 1153. doi: 10.1039/b820557b.

Mauk, M. *et al.* (2015) 'Integrated Microfluidic Nucleic Acid Isolation, Isothermal Amplification, and Amplicon Quantification', *Microarrays*, 4(4), pp. 474–489. doi: 10.3390/microarrays4040474.

Maurelli, M. P., Rinaldi, L. and Cringoli, G. (2016) *Standard operating procedures for Mini-FLOTAC*. Available at :  
[https://www.starworms.org/src/Frontend/Files/userfiles/files/Day%203\\_0915\\_0945.pdf](https://www.starworms.org/src/Frontend/Files/userfiles/files/Day%203_0915_0945.pdf)  
(Accessed: 08 April 2020)

McMorrow, M. L., Aidoo, M. and Kachur, S. P. (2011) 'Malaria rapid diagnostic tests in elimination settings-can they find the last parasite?', *Clinical Microbiology and Infection*. pp. 1624–1631. doi: 10.1111/j.1469-0691.2011.03639.x.

Meechan, P. J. and Wilson, C. (2006) *Use of Ultraviolet Lights in Biological Safety Cabinets: A Contrarian View*. Available at:  
[https://www.ehs.ucsb.edu/files/docs/bs/Meechan\\_and\\_Wilson\\_2006.pdf](https://www.ehs.ucsb.edu/files/docs/bs/Meechan_and_Wilson_2006.pdf) (Accessed: 18 February 2020).

Meng, X. Y. *et al.* (2018) 'Cross-priming amplification-based lateral flow strip as a novel tool for rapid on-site detection of wild-type pseudorabies virus', *Sensors and Actuators, B: Chemical*. 259, pp. 573–579. doi: 10.1016/j.snb.2017.12.087.

Meurs, L. *et al.* (2015) 'Is PCR the next reference standard for the diagnosis of schistosoma in stool? A comparison with microscopy in Senegal and Kenya', *PLoS Neglected Tropical Diseases*, 9(7), pp. 1–16. doi: 10.1371/journal.pntd.0003959.

Mfuh, K. O. *et al.* (2019) 'A comparison of thick-film microscopy, rapid diagnostic test, and polymerase chain reaction for accurate diagnosis of Plasmodium falciparum malaria', *Malaria Journal*, 18(73). doi: 10.1186/s12936-019-2711-4.

Mharakurwa, S. *et al.* (2006) 'PCR detection of Plasmodium falciparum in human urine and saliva samples', *Malaria Journal*, 5(103). doi: 10.1186/1475-2875-5-103.

- Mohamad Azimi, S. *et al.* (2011) 'A magnetic bead-based DNA extraction and purification microfluidic device', *Microfluidic Nanofluid.*, 11, pp. 157–165. doi: 10.1007/s10404-011-0782-9.
- Moody, A. (2002) 'Rapid Diagnostic Tests for Malaria Parasites', *Clinical Microbiology Reviews*, 15(1), pp. 66–78. doi: 10.1128/CMR.15.1.66-78.2002.
- Moonasar, D. *et al.* (2007) 'An exploratory study of factors that affect the performance and usage of rapid diagnostic tests for malaria in the Limpopo Province, South Africa', *Malaria Journal*. 6(1), p. 74. doi: 10.1186/1475-2875-6-74.
- Moonen, B. *et al.* (2010) 'Operational strategies to achieve and maintain malaria elimination', *The Lancet*. pp. 1592–1603. doi: 10.1016/S0140-6736(10)61269-X.
- Morassin, B. *et al.* (2002) 'One year's experience with the polymerase chain reaction as a routine method for the diagnosis of imported malaria', *American Journal of Tropical Medicine and Hygiene*, 66(5), pp. 503–508. doi: 10.4269/ajtmh.2002.66.503.
- Mullis, K. B. and Faloona, F. A. (1987) 'Specific Synthesis of DNA in Vitro via a Polymerase-Catalyzed Chain Reaction', *Methods in Enzymology*. 155(C), pp. 335–350. doi: 10.1016/0076-6879(87)55023-6.
- Mutapi, F. *et al.* (2017) 'Human schistosomiasis in the post mass drug administration era', *The Lancet Infectious Diseases*, 17, pp. e42–e48. doi: 10.1016/S1473-3099(16)30475-3.
- Mwangi, T. W., Bethony, J. M. and Brooker, S. (2006) 'Malaria and helminth interactions in humans: an epidemiological viewpoint', *Annals of Tropical Medicine & Parasitology*, 100(7), pp. 551–570. doi: 10.1179/136485906X118468.
- Nagaraj, S. *et al.* (2018) 'Thermostabilization of indigenous multiplex polymerase chain reaction reagents for detection of enterotoxigenic *Staphylococcus aureus*', *Journal of Microbiology, Immunology and Infection*. 51(2), pp. 191–198. doi: 10.1016/j.jmii.2016.04.004.
- Nail, S. L. *et al.* (2002) 'Fundamentals of Freeze-Drying', In: Nail S.L., Akers M.J. (eds) *Development and Manufacture of Protein Pharmaceuticals*. Pharmaceutical Biotechnology, vol 14. pp. 281–360. doi: 10.1007/978-1-4615-0549-5\_6.

Najafabadi, Z. G. *et al.* (2014) 'Detection of Plasmodium vivax and Plasmodium falciparum DNA in human saliva and urine: Loop-mediated isothermal amplification for malaria diagnosis', *Acta Tropica*, 136, pp. 44–49. doi: 10.1016/j.actatropica.2014.03.029.

Nampala, M. (2018) 'A Critical Evaluation of the National Health System of Uganda', *Biomed J Sci & Tech Res*, 5(5), pp. 4850–4855. doi: 10.26717/BJSTR.2018.05.001266.

Nausch, N. *et al.* (2014) 'Field evaluation of a new antibody-based diagnostic for Schistosoma haematobium and S. mansoni at the point-of-care in northeast Zimbabwe.', *BMC infectious diseases*, 14(1), p. 165. doi: 10.1186/1471-2334-14-165.

Ndeffo Mbah, M. L. *et al.* (2014) 'Impact of Schistosoma mansoni on Malaria Transmission in Sub-Saharan Africa', *PLoS Neglected Tropical Diseases*, 8(10). doi: 10.1371/journal.pntd.0003234.

Ndyomugenyi, R. *et al.* (2016) 'Appropriate targeting of artemisinin-based combination therapy by community health workers using malaria rapid diagnostic tests: findings from randomized trials in two contrasting areas of high and low malaria transmission in southwestern Uganda', *Tropical Medicine and International Health*. 21(9), pp. 1157–1170. doi: 10.1111/tmi.12748.

Neuzil, P. *et al.* (2006) 'Ultra fast miniaturized real-time PCR: 40 cycles in less than six minutes', *Nucleic Acids Research*, 34(11). doi: 10.1093/nar/gkl416.

NHS (2020) *Malaria - Fit for Travel*. Available at: <https://www.fitfortravel.nhs.uk/advice/malaria> (Accessed: 31 August 2020).

NHS Greater Glasgow and Clyde (2019) *NHSGGC: Schistosomiasis*. Available at: <https://www.nhsggc.org.uk/your-health/public-health/public-health-protection-unit-phpu/travel-related-infection/schistosomiasis/> (Accessed: 12 December 2019).

Nikolay, B., Brooker, S. J. and Pullan, R. L. (2014) 'Sensitivity of diagnostic tests for human soil-transmitted helminth infections: A meta-analysis in the absence of a true gold standard', *International Journal for Parasitology*. 44(11), pp. 765–774. doi: 10.1016/j.ijpara.2014.05.009.

Njumkeng, C. *et al.* (2019) 'Coverage and usage of insecticide treated nets (ITNs) within households: associated factors and effect on the prevalence of malaria parasitemia in the

Mount Cameroon area’, *BMC Public Health*, 19(1216), pp. 2–11. doi: 10.1186/s12889-019-7555-x.

Noh, J. Y. *et al.* (2019) ‘Pipetting-based immunoassay for point-of-care testing: Application for detection of the influenza A virus’, *Scientific Reports*. 9(1), pp. 1–9. doi: 10.1038/s41598-019-53083-8.

O’Farrell, B. (2009) ‘Evolution in Lateral Flow–Based Immunoassay Systems’, in *Lateral Flow Immunoassay*. pp. 1–33. doi: 10.1007/978-1-59745-240-3\_1.

Olapaju, B. *et al.* (2018) ‘Age and gender trends in insecticide-treated net use in sub-Saharan Africa: a multi-country analysis’, *Malaria Journal*, 17, p. 423. doi: 10.1186/s12936-018-2575-z.

Pai, M., Ghiasi, M. and Pai, N. P. (2015) ‘Point-of-Care Diagnostic Testing in Global Health: What Is the Point?’, *Microbe*, 10(3), pp. 103–107. Available at: [https://www.ghdonline.org/uploads/Pai\\_et\\_al\\_Microbe\\_2015.pdf](https://www.ghdonline.org/uploads/Pai_et_al_Microbe_2015.pdf) (Accessed: 22 July 2019).

Pai, N. P. *et al.* (2012) ‘Point-of-Care Testing for Infectious Diseases: Diversity, Complexity, and Barriers in Low- And Middle-Income Countries’, 9(9), p. e1001306. doi: 10.1371/journal.pmed.1001306.

Patrinos, G. P., Danielson, P. B. and Ansorge, W. J. (2017) ‘Molecular Diagnostics: Past, Present, and Future’, in *Molecular Diagnostics: Third Edition*. pp. 1–11. doi: 10.1016/B978-0-12-802971-8.00001-8.

Payne, D. (1988) ‘Use and limitations of light microscopy for diagnosing malaria at the primary health care level’, *Bulletin of the World Health Organization*, 66(5), pp. 621–626.

Peeling, R. W., Boeras, D. I. and Nkengasong, J. (2017) ‘Re-imagining the future of diagnosis of Neglected Tropical Diseases’, *Computational and Structural Biotechnology Journal*. pp. 271–274. doi: 10.1016/j.csbj.2017.02.003.

Peeling, R. W. and Mabey, D. (2010) ‘Point-of-care tests for diagnosing infections in the developing world’, *Clinical Microbiology and Infection*. 16(8), pp. 1062–1069. doi: 10.1111/j.1469-0691.2010.03279.x.

Peeling, R. W. and McNerney, R. (2014) ‘Emerging technologies in point-of-care molecular

diagnostics for resource-limited settings’, *Expert Review of Molecular Diagnostics*. 14(5), pp. 525–534. doi: 10.1586/14737159.2014.915748.

Pellegrino, J. and Coelho, P. M. Z. (1978) ‘Schistosoma mansoni: Wandering capacity of a worm couple’, *Journal of Parasitology*, 64(1), pp. 181–182. doi: 10.2307/3279647.

Pena, H. B. *et al.* (1995) ‘Intracellular promiscuity in Schistosoma mansoni: Nuclear transcribed DNA sequences are part of a mitochondrial minisatellite region’, *Proceedings of the National Academy of Sciences of the United States of America*, 92(3), pp. 915–919. doi: 10.1073/pnas.92.3.915.

Pendley, B. D. and Lindner, E. (2017) ‘Medical Sensors for the Diagnosis and Management of Disease: The Physician Perspective’, *ACS Sensors*, 7b00642. doi: 10.1021/acssensors.7b00642.

Polley, S. D. *et al.* (2010) ‘Mitochondrial DNA targets increase sensitivity of malaria detection using loop-mediated isothermal amplification.’, *Journal of clinical microbiology*. 48(8), pp. 2866–71. doi: 10.1128/JCM.00355-10.

Pontes, L. A. *et al.* (2003) *Comparison of a polymerase chain reaction and the kato-katza technique for diagnosing infection with Schistosoma mansoni*. Available at: <http://www.ajtmh.org/docserver/fulltext/14761645/68/6/0680652.pdf?expires=1553613855&id=id&accname=guest&checksum=36545698002EA1023383ADE531B0C492> (Accessed: 26 March 2019).

Pontes, L. A., Dias-Neto, E. and Rabello, A. (2002) ‘Detection by polymerase chain reaction of Schistosoma mansoni DNA in human serum and feces.’, *The American journal of tropical medicine and hygiene*, 66(2), pp. 157–162.

PrimerExplorer (2019) ‘A Guide to LAMP primer designing’, *LAMP primer designing software PrimerExplorer*. Available at: <https://primerexplorer.jp/e/> (Accessed: 5 September 2020).

Public Health England (2018) *UK Standards for Microbiology Investigations- Good practice when performing molecular amplification assays*. Available at: [https://assets.publishing.service.gov.uk/government/uploads/system/uploads/attachment\\_data/file/682533/Q4i5.pdf](https://assets.publishing.service.gov.uk/government/uploads/system/uploads/attachment_data/file/682533/Q4i5.pdf) (Accessed: 25 March 2020).

Rajchgot, J. *et al.* (2017) ‘Mobile-phone and handheld microscopy for neglected tropical diseases’, *PLoS Neglected Tropical Diseases*, 11(7), pp. 4–7. doi: 10.1371/journal.pntd.0005550.

Rapid Medical Diagnostics (2018) *Schisto POC-CCA*® *Rapid test for qualitative detection of: Bilharzia (Schistosomiasis)*. Available at: [http://www.rapid-diagnostics.com/updates\\_15\\_09\\_2019/RMD\\_Pamphlet\\_13\\_12\\_2018\\_Colourweb.pdf](http://www.rapid-diagnostics.com/updates_15_09_2019/RMD_Pamphlet_13_12_2018_Colourweb.pdf) (Accessed: 11 November 2019).

Reboud, J. *et al.* (2012) ‘Shaping acoustic fields as a toolset for microfluidic manipulations in diagnostic technologies’, *PNAS*, 109(38), pp. 15162–15167. doi: 10.1073/pnas.1206055109/-/DCSupplemental.

Reboud, J. *et al.* (2018) ‘Paper-based microfluidics for DNA diagnostics of malaria in low resource underserved rural communities’, *PNAS*, 116(11), pp. 4834–4842. doi: 10.5525/gla.researchdata.722.

Rey, L. and May, J. C. (2016) *Freeze-drying/lyophilization of pharmaceutical and biological products: Third edition, Freeze-Drying/Lyophilization of Pharmaceutical and Biological Products: Third Edition*.

Ririe, K. M., Rasmussen, R. P. and Wittwer, C. T. (1997) ‘Product differentiation by analysis of DNA melting curves during the polymerase chain reaction’, *Analytical Biochemistry*. 245(2), pp. 154–160. doi: 10.1006/abio.1996.9916.

Rodriguez, N. M. *et al.* (2016) ‘A fully integrated paperfluidic molecular diagnostic chip for the extraction, amplification, and detection of nucleic acids from clinical samples †’, *Lab on a Chip*, 16, p. 753. doi: 10.1039/c5lc01392e.

Rollinson, D. *et al.* (2013) ‘Time to set the agenda for schistosomiasis elimination’, *Acta Tropica*. 128(2), pp. 423–440. doi: 10.1016/j.actatropica.2012.04.013.

Rougemont, M. *et al.* (2004) ‘Detection of four Plasmodium species in blood from humans by 18S rRNA gene subunit-based and species-specific real-time PCR assays’, *Journal of Clinical Microbiology*, 42(12), pp. 5636–5643. doi: 10.1128/JCM.42.12.5636-5643.2004.

Ruiz-Villalba, A. *et al.* (2017) ‘Amplification of nonspecific products in quantitative polymerase chain reactions (qPCR)’, *Biomolecular Detection and Quantification*, 14, pp. 7–

18. doi: 10.1016/j.bdq.2017.10.001.

Saiki, R. K. *et al.* (1985) 'Enzymatic amplification of  $\beta$ -globin genomic sequences and restriction site analysis for diagnosis of sickle cell anemia', *Science*. 230(4732), pp. 1350–1354. doi: 10.1126/science.2999980.

Salant, H., Abbasi, I. and Hamburger, J. (2012) 'The development of a loop-mediated isothermal amplification method (LAMP) for Echinococcus granulosus Coprodetection.', *The American journal of tropical medicine and hygiene*. 87(5), pp. 883–7. doi: 10.4269/ajtmh.2012.12-0184.

Samuelson, J. C., Quinn, J. J. and Caulfield, J. P. (1984) 'Hatching, Chemokinesis and Transformation of Miricidia of Schistosoma mansoni', *The Journal of Parasitology*, 70(3), pp. 321–331. doi: 10.1287/mksc.1090.0490.

Sandeu, M. M. *et al.* (2012) 'Optimized Pan-species and Speciation Duplex Real-time PCR Assays for Plasmodium Parasites Detection in Malaria Vectors', *PLoS ONE*. 7(12), p. e52719. doi: 10.1371/journal.pone.0052719.

Sarhan, R. M. *et al.* (2015) 'Evaluation of three extraction methods for molecular detection of Schistosoma mansoni infection in human urine and serum samples', *Journal of Parasitic Diseases*. 39(3), pp. 499–507. doi: 10.1007/s12639-013-0385-3.

Shadle, S. E. *et al.* (1997) 'Quantitative analysis of electrophoresis data: novel curve fitting methodology and its application to the determination of a protein-DNA binding constant', *Nucleic Acids Research*. 25(4), pp. 850–860.

Shane, H. L. *et al.* (2011) 'Evaluation of urine CCA assays for detection of Schistosoma mansoni infection in Western Kenya', *PLoS Neglected Tropical Diseases*, 5(1), pp. 1–7. doi: 10.1371/journal.pntd.0000951.

Sharma, S. *et al.* (2015) 'Point-of-Care Diagnostics in Low Resource Settings: Present Status and Future Role of Microfluidics', *Biosensors*, 5, pp. 577–601. doi: 10.3390/bios5030577.

Sin, M. L. Y. *et al.* (2014) 'Advances and challenges in biosensor-based diagnosis of infectious diseases', *Expert Reviews Molecular Diagnostics*, 14(2), pp. 225–244. doi: 10.1586/14737159.2014.888313.Advances.

- Singleton, J. *et al.* (2014) 'Electricity-Free Amplification and Detection for Molecular Point-of-Care Diagnosis of HIV-1', *PLoS ONE*, 9(11), p. e113693. doi: 10.1371/journal.pone.0113693.
- Smith, L. M. and Burgoyne, L. A. (2004) 'Collecting, archiving and processing DNA from wildlife samples using FTA databasing paper.', *BMC Ecology*, 4, p. 4. doi: 10.1186/1472-6785-4-4.
- Song, J. *et al.* (2015) 'Molecular Detection of Schistosome Infections with a Disposable Microfluidic Cassette', *PLoS Neglected Tropical Diseases*, 9(12), pp. 1–18. doi: 10.1371/journal.pntd.0004318.
- Southern, E. M. (1975) 'Detection of Specific Sequences Among DNA Fragments Separated by Gel Electrophoresis', *J. Mol. Biol.*, 98, pp. 503–517.
- Speicher, N. (2017) *Storing oligos: 7 things you should know*, IDT. Available at: <https://eu.idtdna.com/pages/education/decoded/article/storing-oligos-7-things-you-should-know> (Accessed: 8 April 2020).
- Spencer, H. C. *et al.* (1979) 'The enzyme linked immunosorbent assay (ELISA) for malaria. I. The use of in vitro-cultured Plasmodium falciparum as antigen', *American Journal of Tropical Medicine and Hygiene*, 28(6), pp. 927–932. doi: 10.4269/ajtmh.1979.28.927.
- Spiess, A.-N., Feig, C. and Ritz, C. (2008) 'Highly accurate sigmoidal fitting of real-time PCR data by introducing a parameter for asymmetry', *BMC Bioinformatics*, 9(221). doi: 10.1186/1471-2105-9-221.
- St John, A. and Price, C. P. (2014) 'Existing and Emerging Technologies for Point-of-Care Testing', *Clinical Biochemical Reviews*, 35(3), pp. 155–167. Available at: <https://www.ncbi.nlm.nih.gov/pmc/articles/PMC4204237/pdf/cbr-35-155.pdf> (Accessed: 26 March 2019).
- Stellwagen, N. C. (2009) 'Electrophoresis of DNA in agarose gels, polyacrylamide gels and in free solution', *Electrophoresis*, 30(1). doi: 10.1002/elps.200900052.
- Stothard, J. R. *et al.* (2006) 'Use of circulating cathodic antigen (CCA) dipsticks for detection of intestinal and urinary schistosomiasis', *Acta Tropica*, 97(2), pp. 219–228. doi: 10.1016/j.actatropica.2005.11.004.



- Sulzer, A. J. and Wilson, M. (1969) 'Indirect fluorescent- antibody tests for parasitic diseases. V. An evaluation of a thick-smear antigen in the IFA test for malaria antibodies', *Am J Trop Med Hyg*, 18, pp. 199–205.
- Sun, Y. *et al.* (2013) 'Pre-storage of gelified reagents in a lab-on-a-foil system for rapid nucleic acid analysis', *Lab on a Chip*, 13, p. 1509. doi: 10.1039/c2lc41386h.
- Tang, X. and Pikal, M. J. (2004) 'Design of Freeze-Drying Processes for Pharmaceuticals: Practical Advice', *Pharmaceutical Research*, (2), pp. 191–200. doi: 10.1023/b:pham.0000016234.73023.75.
- Tang, Y. *et al.* (2020) 'Laboratory Diagnosis of COVID-19: Current Issues and Challenges', *Journal of Clinical Microbiology*, 58(6), pp. 1–9. doi: 10.1128/JCM.00512-20
- Tangena, J.-A. A. *et al.* (2020) 'Indoor residual spraying for malaria control in sub-Saharan Africa 1997 to 2017: an adjusted retrospective analysis', *Malaria Journal*, 19(150), pp. 1–15. doi: 10.1186/s12936-020-03216-6.
- Tangpukdee, N. *et al.* (2009) 'Malaria Diagnosis : A Brief Review', *Korean J Parasitol*, 47(2), pp. 93–102. doi: 10.3347/kjp.2009.47.2.93.
- Tankeshwar, A. (2016) *Kato katz technique: Principle, Procedure and Results - Learn Microbiology Online*. Available at: <https://microbeonline.com/kato-katz-technique-principle-procedure-results/> (Accessed: 24 February 2020).
- Tanner, N. A. and Evans, T. C. (2014) 'Loop-mediated isothermal amplification for detection of nucleic acids.', *Curr. Protoc. Mol. Biol.*, 105(January), pp. 15.14.1--15.14.14. doi: 10.1002/0471142727.mb1514s105.
- Tchuem Tchuenté, L. A. *et al.* (2017) 'Moving from control to elimination of schistosomiasis in sub-Saharan Africa: Time to change and adapt strategies', *Infectious Diseases of Poverty*. *Infectious Diseases of Poverty*, 6(1), pp. 1–14. doi: 10.1186/s40249-017-0256-8.
- Teixeira, C. F. *et al.* (2007) 'Detection of *Shistosoma mansoni* eggs in feces through their interaction with paramagnetic beads in a magnetic field', *PLoS Neglected Tropical Diseases*, 1(2), pp. 1–5. doi: 10.1371/journal.pntd.0000073.
- The Malaria Atlas Project (2017) *Trends in Global Malaria Burden*. Available at:

<https://malariaatlas.org/trends/region/MAP/SSA> (Accessed: 11 May 2020).

Thermo Scientific (2012) ‘NanoDrop Lite: Interpretation of Nucleic Acid 260/280 Ratios’, *Technical Bulletin*, p. 1. Available at: <http://tools.thermofisher.com/content/sfs/brochures/T123-NanoDrop-Lite-Interpretation-of-Nucleic-Acid-260-280-Ratios.pdf>.

Tizifa, T. A. *et al.* (2018) ‘Prevention Efforts for Malaria’, *Current Tropical Medicine Reports*, pp. 41–50. doi: 10.1007/s40475-018-0133-y.

Trinh, T. N. D. and Lee, N. Y. (2019) ‘A foldable isothermal amplification microdevice for fuchsin-based colorimetric detection of multiple foodborne pathogens’, *Lab on a Chip*. 19(8), pp. 1397–1405. doi: 10.1039/C8LC01389F.

Tseroni, M. *et al.* (2015) ‘Field application of SD bioline malaria Ag Pf/ pan rapid diagnostic test for malaria in Greece’, *PLoS ONE*, 10(3), pp. 1–11. doi: 10.1371/journal.pone.0120367.

UCLHS NHS (2020) *Urgent malaria testing*. Available at: <https://www.uclh.nhs.uk/HP/GPNEWS/Pages/Urgentmalariatesting.aspx> (Accessed: 21 February 2020).

Udugama, B. *et al.* (2020) ‘Diagnosing COVID-19: The Disease and Tools for Detection’, *ACS nano*, 14(4), pp. 3822–3835. doi: 10.1021/acsnano.0c02624.

Unicef (2018) *Malaria*. Available at: <https://data.unicef.org/topic/child-health/malaria/> (Accessed: 4 May 2020).

Utzinger, J. *et al.* (2015) ‘New Diagnostic Tools in Schistosomiasis- A Review’, *Clinical microbiology and infection*. 21(6), pp. 529-542. doi: 10.1016/j.cmi.2015.03.014. doi: 10.1016/j.cmi.2015.03.014.

Uzochukwu, B. S. *et al.* (2009) ‘Cost-effectiveness analysis of rapid diagnostic test, microscopy and syndromic approach in the diagnosis of malaria in Nigeria: implications for scaling-up deployment of ACT’, *Malaria Journal*. 8(1), p. 265. doi: 10.1186/1475-2875-8-265.

Vallejo, A. F. *et al.* (2015) ‘Evaluation of the loop mediated isothermal DNA amplification (LAMP) kit for malaria diagnosis in *P. vivax* endemic settings of Colombia.’, *PLoS*

*neglected tropical diseases*. 9(1), p. e3453. doi: 10.1371/journal.pntd.0003453.

Versi, E. (1992) “‘Gold standard’ is an appropriate term ’, *British Medical Journal*. British 305(6846), p. 187. doi: 10.1136/bmj.305.6846.187-b.

Viana, R. V and Wallis, C. L. (2011) *Good Clinical Laboratory Practice (GCLP) for Molecular Based Tests Used in Diagnostic Laboratories*. South Africa. Available at: <http://www.intechopen.com/books/wide-spectra-of-quality-control> (Accessed: 24 February 2020).

Vogelstein, B. and Gillespie, D. (1979) 'Preparative and analytical purification of DNA from agarose', *Proc. Natl. Acad. Sci.* 76(2), pp. 615-619. doi: 10.1073/pnas.76.2.615.

Walsh, D. I. *et al.* (2017) 'Enabling Microfluidics: from Clean Rooms to Makerspaces', *Trends in Biotechnology*. 35(5), pp. 383–392. doi: 10.1016/j.tibtech.2017.01.001.

Wan, J. *et al.* (2020) 'Development of a test kit for visual loop-mediated isothermal amplification of Salmonella in spiked ready-to-eat fruits and vegetables', *Journal of Microbiological Methods*. 169. doi: 10.1016/j.mimet.2019.105830.

Wang, P. *et al.* (2017) 'The Beauty and Utility of DNA Origami', *Chem.* 2, pp. 359–382. doi: 10.1016/j.chempr.2017.02.009.

Wang, T.-Y., Guo, L. and Zhang, J.-H. (2010) 'Preparation of DNA Labeled Based on Multiplex PCR Technique', *Research Journal of Nucleic Acids*, 2010. doi: 10.4061/2010/421803.

Webster, B. L. (2009) 'Isolation and preservation of schistosome eggs and larvae in RNA later(R) facilitates genetic profiling of individuals.', *Parasites & vectors*, 2(1), p. 50. doi: 10.1186/1756-3305-2-50.

Weerakoon, K. G. A. D. *et al.* (2015) 'Advances in the diagnosis of human schistosomiasis', *Clinical Microbiology Reviews*, 28(4), pp. 939–967. doi: 10.1128/CMR.00137-14.

White, N. J. (2008) 'How antimalarial drug resistance affects post-treatment prophylaxis', *Malaria Journal*, 7(9), pp. 1–7. doi: 10.1186/1475-2875-7-9.

Wichmann, D. *et al.* (2009) 'Diagnosing Schistosomiasis by Detection of Cell-Free Parasite DNA in Human Plasma', *PLoS Neglected Tropical Diseases*. 3(4), p. e422. doi:

10.1371/journal.pntd.0000422.

Wongsrichanalai, C. *et al.* (2007) 'A Review of Malaria Diagnostic Tools: Microscopy and Rapid Diagnostic Test (RDT)', *Am. J. Trop. Med. Hyg.* 77, pp. 119–127. Available at: <https://www.ncbi.nlm.nih.gov/books/NBK1695/> (Accessed: 31 July 2020).

Wooden, J., Kyes, S. and Sibley, C. H. (1993) 'PCR and Strain Identification in *Plasmodium falciparum*', *Parasitology Today*, 8. Available at: [https://ac.els-cdn.com/016947589390131X/1-s2.0-016947589390131X-main.pdf?\\_tid=a5c8f0c2-06e8-4ceb-b43e-ca54adc70c8f&acdnat=1530797751\\_7adcd597d7065500b603dee7018d45e3](https://ac.els-cdn.com/016947589390131X/1-s2.0-016947589390131X-main.pdf?_tid=a5c8f0c2-06e8-4ceb-b43e-ca54adc70c8f&acdnat=1530797751_7adcd597d7065500b603dee7018d45e3) (Accessed: 5 July 2018).

World Health Organization (2010) *Basic malaria microscopy*. 2nd edn, *World Health Organization*.

World Health Organization (2015) *Guidelines for the Treatment of Malaria*. 3rd edn. Available at: [www.who.int](http://www.who.int) (Accessed: 14 May 2020).

World Health Organization (2016) *The use of loop-mediated isothermal amplification (TB-LAMP) for the diagnosis of pulmonary tuberculosis: policy guidance*. Available at: [https://www.ncbi.nlm.nih.gov/books/NBK384520/pdf/Bookshelf\\_NBK384520.pdf](https://www.ncbi.nlm.nih.gov/books/NBK384520/pdf/Bookshelf_NBK384520.pdf) (Accessed: 10 July 2020).

World Health Organization (2017) *Primary Health care systems (PRIMASYS): case study from Uganda, abridged version*. Available at: <http://apps.who.int/bookorders>. (Accessed: 21 July 2020).

World Health Organization (2018a) *World Health Organization Model List of Essential In Vitro Diagnostics First edition (2018)*. Available at: [http://www.who.int/medical\\_devices/diagnostics/Selection\\_in-vitro\\_diagnostics](http://www.who.int/medical_devices/diagnostics/Selection_in-vitro_diagnostics) (Accessed: 3 December 2019).

World Health Organization (2018b) *World Malaria Report 2018*. Available at: [www.who.int/malaria](http://www.who.int/malaria) (Accessed: 4 May 2020).

World Health Organization (2019a) *WHO Malaria Terminology*, *Global Malaria Program*. Available at: [https://apps.who.int/iris/bitstream/handle/10665/208815/WHO\\_HTM\\_GMP\\_2016.6\\_eng.p](https://apps.who.int/iris/bitstream/handle/10665/208815/WHO_HTM_GMP_2016.6_eng.p)

df?sequence=1.

World Health Organization (2019b) *World Malaria Report 2019*. Available at: <https://www.who.int/publications-detail/world-malaria-report-2019>.

World Health Organization (2020a) *Ending the neglect to attain the Sustainable Development Goals A road map for neglected tropical diseases 2021-2030*. Available at: <http://apps.who.int/bookorders>. (Accessed: 18 May 2020).

World Health Organization (2020b) *Malaria*. Available at: <https://www.who.int/news-room/fact-sheets/detail/malaria> (Accessed: 4 May 2020).

World Health Organization (2020c) *Schistosomiasis*. Available at: <http://www.who.int/en/news-room/fact-sheets/detail/schistosomiasis> (Accessed: 11 May 2018).

Xu, G., Zhao, H., *et al.* (2016) ‘A capillary-based multiplexed isothermal nucleic acid-based test for sexually transmitted diseases in patients †’, *Chem. Commun*, 52, p. 12187. doi: 10.1039/c6cc05679b.

Xu, G., Nolder, D., *et al.* (2016) ‘Paper-Origami-Based Multiplexed Malaria Diagnostics from Whole Blood’, *Angew. Chem. Int. Ed*, 55, pp. 1–5. doi: 10.1002/anie.201606060.

Xu, H. *et al.* (2020) ‘An ultraportable and versatile point-of-care DNA testing platform’, *Science Advances*. 6(17), p. eaaz7445. doi: 10.1126/sciadv.aaz7445.

Yang, X. *et al.* (2012) ‘Integrated separation of blood plasma from whole blood for microfluidic paper-based analytical devices’, *Lab on a Chip*, 12, pp. 274–280. doi: 10.1039/c1lc20803a.

Yang, Z. *et al.* (2018) ‘Rapid Veterinary Diagnosis of Bovine Reproductive Infectious Diseases from Semen Using Paper-Origami DNA Microfluidics’, *ACS Sensors*, 3, pp. 403–409. doi: 10.1021/acssensors.7b00825.

Zhai, P. *et al.* (2020) ‘The epidemiology, diagnosis and treatment of COVID-19’, *International Journal of Antimicrobial Agents*. 55(5). doi: 10.1016/j.ijantimicag.2020.105955.

Zhang, J. *et al.* (2019) ‘Loop-mediated isothermal amplification-lateral-flow dipstick

(LAMP-LFD) to detect *Mycoplasma ovipneumoniae*', *World Journal of Microbiology and Biotechnology*, 35(3), p. 31. doi: 10.1007/s11274-019-2601-5.

Zhang, X. *et al.* (2010) 'Development of a loop-mediated isothermal amplification assay for rapid detection of subgroup J avian leukosis virus', *Journal of Clinical Microbiology*, 48(6), pp. 2116–2121. doi: 10.1128/JCM.02530-09.